

PRODUCT YIELD AND EXERGY ANALYSIS OF BISPHOSPHONATE SYNTHESIS
AND MEDICAL DRUG PRODUCTION PROCESSES



by

Fatma Banu Yavuztürk

Submitted to Graduate School of Natural and Applied Sciences
in Partial Fulfillment of the Requirements
for the Degree of Doctor of Philosophy in
Chemical Engineering

Yeditepe University

2018

PRODUCT YIELD AND EXERGY ANALYSIS OF BISPHOSPHONATE SYNTHESIS
AND MEDICAL DRUG PRODUCTION PROCESSES

APPROVED BY:

Prof. Dr. Seyda Malta
(Thesis Supervisor)


.....

Prof. Dr. Hasan Sadıkođlu


.....

Prof. Dr. Mustafa Özilgen


.....

Assist. Prof. Dr. Canan Acar


.....

Assist. Prof. Dr. Cem Levent Altan


.....

DATE OF APPROVAL:/...../2018

ACKNOWLEDGEMENTS

Firstly, I would like to express my sincere thanks to my thesis supervisor, Prof. Seyda Malta Bucak, for her help and guidance, clear sighted suggestions and valuable comments throughout this study. I am grateful to her for her helps and patience. It was an especial experience to persue my thesis under her supervision which broadens my knowledge on this study and my mind.

I also would like to give my sincere thanks to my professor Mustafa Özilgen for his support, encouregements and helps. His valuable contrubitions give more insights to the study. He have been a good accelarator for me and without his support and everything it would not be easy to accomplish the study. Besides his professions his personality teach me a lot, especially the meaning of success and living with a positive perspective.

I am glad to have a change to meet and work with my proessors.

Additionally, I would like to give my thanks to Atabay Pharmaceuticals Inc., Istanbul team, who gave me the chance to work in their laboratories with a valuable team. Especially to Bülent Atabay, the president, for his encauregements, support, knowledge and valuable contrubitions. His open minded attitude and entrepreneurial spirit opened the door of this study. My collegues during this study, Unal Çatal, his supports on synthesis, Caner Arıkan and Fazlı Beyazaslan their analytical contributions helped and encoureged me all the time. I would like to thank to all the team, for their understanding and helps.

I am also thankful for the analytical support of Prof. Hakan Göker, Ankara University and Prof. Tuncel Ozden Gazi University for their analytical knowledge and contributions.

Finally, I would like to thank to my family for their endless support, encouregement and love, which makes everything easier and more pleased.

ABSTRACT

PRODUCT YIELD AND EXERGY ANALYSIS OF BISPHOSPHONATE SYNTHESIS AND MEDICAL DRUG PRODUCTION PROCESSES

Introduction of the waste of the pharmaceutical industry to the biosphere creates unusual potential disease patterns. Achieving the active pharmaceutical ingredient (API) production by utilizing the minimum energy and generating as little waste as possible are among the reasonable cleaner production practices. Zoledronic acid is the API of some bone-disease drugs. It is synthesized via the reaction of 1h-imidazole-1-yl- acetic acid hydrochloride with phosphorous acid and phosphorous halogen at moderate temperatures. The product is later separated by crystallization in water. Since the concentration of API is very low in the finished product, batch amount of API is chosen as 50 g. Chemical processes are generally investigated to determine the most convenient production procedures and equipment. In the studies performed in small scale set up, it is important to foresee an upscale design. Exergy utilization is among the considerations in process design and there is almost no information available in the literature yet, regarding the exergy analysis of the production processes of pharmaceuticals. During the chemical synthesis of zoledronic acid under GMP (good manufacturing practice) conditions, the most energy consuming step was found to be crystallization. On the other hand, the most energy consuming step during sterile finished product manufacturing was filling, followed by sterilization of the primary packaging equipment and the materials, and the operation of the HVAC system. The initial cumulative degree of perfection (CDP) was calculated to be 1.47×10^{-2} per cent for the API synthesis, however exergy efficiency of the synthesis process to 2.29×10^{-2} per cent with increasing the yield through process optimization. The CDP of the finished product was 17 per cent and 75 per cent before and after packaging of the finished product, respectively. Synthesis at the maximum attainable conversion ratio and the highest exergy efficiency assures minimum waste generation.

ÖZET

BISFOSFONAT SENTEZ VE MEDİKAL İLAÇ ÜRETİMİNDE ÜRÜN VERİMİ VE EKSERJİ ANALİZİ

İlaç atıklarının biosfere verilmesi, alışılmadık şablondaki hastalıkların oluşmasını tetiklemekte. aktif farmasötik bileşen (API) üretimini minimum enerji harcayarak ve az atık üretecek şekilde yapmak da, makul olan daha temiz üretim uygulamalarından. Zoledronik asit, kemik hastalıklarında uygulanan ilaçların aktif farmasötik birleşenidir. 1h-imidazol-1-yl- acetik asit hidroklorit ile fosforus asitin, fosforus halojen valığında orta dereceli sıcaklıklarda gerçekleşen reaksiyonundan sentezlenmektedir. Ürün reaksiyon solusyonundan, sudaki kristalizasyon ile ayrılır. Aktif farmasötik bileşen miktarının bitmiş ürünlerdeki varlığı düşünüldüğünde, API parti miktarı olarak 50 g seçilmiştir. Kimyasal üretimlerdeki incelemeler, genellikle en uygun üretim metodu ve ekipmanların seçilmesi için yapılır. Bu çalışmalarda, küçük ölçekli bir kurulum, büyük ölçeğe geçerken yapılacak öngörü için önemlidir. Ekserji kullanımı, üretim sürecinin tasarımı için kullanılan hususlardan olup, farmasötik kimyasalların üretimi üzerine yapılmış bir ekserji analizi ile ilgili literatür bilgisine henüz neredeyse hiç rastlanmamaktadır. İyi imalat uygulamaları (GMP) altında gerçekleştirilen, zoledronik asitin kimyasal sentezinde, en fazla enerji kaybı, kristalizasyon adımıyla gerçekleşmektedir. Ayrıca, steril bitmiş ürün üretimine ait en fazla enerji harcayan adımlar, dolum, takibinde birincil ambalaj ekipman ve malzemelerinin sterilizasyonu ve steril alanı oluşturmak için HVAC sisteminin çalışmasıdır. API sentez adımı için birinci kümülatif mükemmellik derecesi (CDP) yüzde 1.47×10^{-2} iken, ekserji verimliliği, işlem optimizasyonu ile artan ürün verimini hesaba katarak, yüzde 2.29×10^{-2} olarak bulunmuştur. Bitmiş ürün için ise, CDP, ambalajlama öncesi yüzde 17 ve ambalajlama sonrası yüzde 75 olarak hesaplanmıştır. Elde edilen en yüksek konversiyon oranı ve ekserji verimi, atık oluşumu için minimum değeri sağlamaktadır.

TABLE OF CONTENTS

ACKNOWLEDGEMENTS	iii
ABSTRACT.....	iv
ÖZET	v
LIST OF FIGURES	xi
LIST OF TABLES	xiii
LIST OF SYMBOLS/ABBREVIATIONS.....	xv
1. INTRODUCTION	1
2. THEORITICAL BACKROUND.....	4
2.1. CHEMISTRY OF BISPHOSPHONATES.....	4
2.2. MECHANISMS OF ACTION	6
2.3. TOXICITY	10
2.3.1. Hypocalcaemia	11
2.3.2. Atrial Fibrillation.....	11
2.3.3. Osteonecrosis of the Jaws.....	12
2.4. BISPHOSPHONATES IN OSTEOPOROSIS AND BONE DISEASES	12
2.5. BISPHOSPHONATES IN CANCER	15
2.6. EXERGY ANALYSES	21
3. MATERIALS AND METHODS.....	24
3.1. MATERIALS	24
3.1.1. Chemicals Used in The Synthesis of Zoledronic Acid.....	24
3.1.2. Chemicals Used in The Production of Zoledronic Acid Injectable.....	24
3.1.3. Buffers and Chemicals for HPLC Applications	25
3.1.4. Glassware Required for The Synthesis and Analyses	25

3.1.5. Laboratory Equipment	25
3.2. METHODS	27
3.2.1. Nuclear Magnetic Resonance Spectrometry	27
3.2.1.1. ¹ H-NMR	27
3.2.1.2. ¹³ C-NMR	28
3.2.2. 2D NMR Methods	29
3.2.2.1. Homonuclear COSY	29
3.2.2.2. Heteronuclear HSQC	30
3.2.2.3. Heteronuclear HMBC	30
3.2.3. Mass Spectrum	30
3.2.4. Fourier Transform Infrared Spectroscopy (FTIR)	32
3.2.5. Water Content Analyses – Karl Fischer	33
3.2.5.1. Volumetric Karl Fisher Analysis	34
3.2.5.2. Calorimetric Karl Fischer Analysis	34
3.2.6. Differential Scanning Calorimetry Thermal Analysis (DSC)	35
3.2.7. High Performance Liquid Chromatography (HPLC)	36
3.2.7.1. HPLC Parts	37
3.2.7.2. HPLC Assay Method for Zoledronic Acid	39
3.2.8. Thermogravimetric Analysis (TGA)	41
3.2.9. Melting Point	43
3.2.10. Exergy Methods	43
4. EXPERIMENTAL STUDIES	45
4.1. SYNTHESIS METHODS	46
4.1.1. Reaction in Chlorobenzene with Phosphoric Acid	47
4.1.1.1. 1 st Experiment	47
4.1.1.2. 2 nd Experiment	47

4.1.1.3. 3 rd Experiment.....	48
4.1.2. Reaction in Methane Sulphonic Acid with Phosphorous Acid	49
4.1.2.1. 4 th Experiment.....	51
4.1.3. Effect of Temperature.....	51
4.1.3.1. 5 th Experiment.....	51
4.1.3.2. 6 th Experiment.....	51
4.1.4. Method of Crystallization	52
4.1.4.1. 7 th Experiment.....	52
4.1.4.2. 8 th Experiment.....	53
4.1.5. Effect of pH	53
4.1.5.1. 10 th and 11 th Experiments.....	53
4.1.6. Excess of Halo Phosphorous Compound.....	53
4.1.6.1. 12 th Experiment.....	53
4.1.7. Excess of Phosphorous Acid	54
4.1.7.1. 9 th Experiment.....	54
4.1.7.2. 13 th Experiment.....	54
4.1.8. Reproducibility	54
4.1.8.1. 14 th , 15 th , 16 th Experiments	54
5. RESULTS AND DISCUSSION	56
5.1. EXPERIMENTAL RESULTS AND DISCUSSION	56
5.1.1. Reaction in Chlorobenzene with Phosphoric Acid.....	56
5.1.1.1. 1 st Experiment	56
5.1.1.2. 2 nd Experiment	56
5.1.1.3. 3 rd Experiment.....	57
5.1.2. Reaction in Methane Sulphonic Acid with Phosphorous Acid	57
5.1.2.1. 4 th Experiment.....	57

5.1.3. Effect of Temperature.....	59
5.1.3.1. 5 th Experiment.....	59
5.1.3.1. 6 th Experiment.....	59
5.1.4. Method of Crystallization.....	66
5.1.4.1. 7 th Experiment.....	66
5.1.4.2. 8 th Experiment.....	76
5.1.5. Effect of pH.....	76
5.1.5.1. 10 th and 11 th Experiments.....	76
5.1.6. Excess of Halo Phosphorous Compound.....	77
5.1.6.1. 12 th Experiment.....	77
5.1.7. Excess of Phosphorous Acid.....	77
5.1.7.1. 9 th Experiment.....	77
5.1.7.2. 13 th Experiment.....	78
5.1.8. Reproducibility.....	78
5.1.8.1. 14 th , 15 th , 16 th Experiments.....	78
5.2. EXERGY RESULTS AND DISCUSSIONS.....	81
5.2.1. Zoledronic acid and Injectable Solution Synthesis.....	82
5.2.2. Production of The Injectable and Parenteral Zoledronic Acid Solution.....	85
5.2.3. Analytical Testing.....	92
5.2.4. Transportation of The Materials.....	93
5.2.5. Renewability of The Process.....	93
6. CONCLUSION AND FUTURE WORK.....	96
REFERENCES.....	99
APPENDIX A.....	127
APPENDIX B.....	196
APPENDIX C.....	210

APPENDIX D..... 256



LIST OF FIGURES

Figure 2.1. Molecular structures of bisphosphonates	5
Figure 2.2. Mechanisms of action of bisphosphonates	7
Figure 2.3. Schematic diagram of mevalonate pathway	9
Figure 2.4. Biomedical applications of bisphosphonates	10
Figure 2.5. Anti-tumor effects of bisphosphonates	19
Figure 2.6. Anti-tumor activity of zoledronic acid	21
Figure 3.1. The compact ProPlus NMR system (Agilent)	29
Figure 3.2. Principle of Mass Spectrometer	31
Figure 3.3. Micromass Quattro Micro Mass Spectrometer	32
Figure 3.4. Shimadzu IR Affinity-1, IR Spectrometer	33
Figure 3.5. Volumetric titration details of a Karl Fischer apparatus	34
Figure 3.6. Metrohm KF system, 841 Titrando	35
Figure 3.7. Differential Scanning Calorimeter (DSC)	36
Figure 3.8. Shimadzu HPLC systems	38
Figure 3.9. Polarity of solvents commonly used to compose mobile phase	38

Figure 3.10. Pyris 1 TGA, PerkinElmer	42
Figure 3.11. Stuart SMP 40 Melting Point Apparatus	43
Figure 4.1. Synthesis reaction of zoledronic acid by phosphorylation	45
Figure 4.2. Flow chart for zoledronic acid synthesis	46
Figure 4.3. Schematic representation of reaction set up	46
Figure 5.1. [1-Hydroxy-2-(1H-imidazole-1-yl)ethan-1,1-di-yl]bis(phosphonic acid)	60
Figure 5.2. TGA and DSC curves of a) standard vs b) 7th experiment CR1	67
Figure 5.3. TGA and DSC curves of a) standard vs b) 7th experiment CR2-1	70
Figure 5.4. TGA and DSC curves of a) standard vs b) 7th experiment CR2-2	71
Figure 5.5. TGA and DSC curves of a) standard vs b) 7th experiment CR3-1	72
Figure 5.6. TGA and DSC curves of a) standard vs b) 7th experiment CR3-2	73
Figure 5.7. TGA and DSC curves of a) standard vs b) 7th experiment CR4	75
Figure 5.8. Schematic description of the steps of the zoledronic acid synthesis, separation and purification steps.....	83
Figure 5.9. Exergy loss in each step of the zoledronic acid production process Step 1.	85
Figure 5.10. Schematic description of the injectable zoledronic acid solution production and its packaging.	86

LIST OF TABLES

Table 2.1. Incidence of bone metastases	16
Table 3.1. Chemicals used in zoledronic acid synthesis.....	24
Table 3.2. Chemicals used in Zoledronic Acid Injectable production.....	24
Table 3.3. Laboratory equipment list.....	25
Table 3.4. IR peaks of zoledronic acid	33
Table 3.5. Different HPLC assay methods for bisphosphonates	41
Table 5.1. IR spectra data of zoledronic acid	57
Table 5.2. ¹ H-NMR results of Zoledronic acid in the literature	61
Table 5.3. ¹³ C-NMR results of Zoledronic acid in the literature	62
Table 5.4. HSQC results of Zoledronic acid	64
Table 5.5. HMBC results of Zoledronic acid	65
Table 5.6. Mass spectrum results of Zoledronic acid in the literature	65
Table 5.7. DSC results of Zoledronic acid in the literature	68
Table 5.8. Summary of results obtained in experiment 7 th	76
Table 5.9. Results obtained for reproducibility	79

Table 5.10. ^1H -NMR results of reproducibility batches	79
Table 5.11. ^{13}C -NMR results of reproducibility batches	80
Table 5.12. Summary of the results	94
Table 6.1. Variation of the yield and the exergetic efficiency under different reaction conditions	97



LIST OF SYMBOLS/ABBREVIATIONS

b	Flow availability of a stream
c_p	Specific heat capacity
CexC	Cumulative exergy
ex	Specific exergy
Ex	Total exergy
h	Specific enthalpy
H	Total enthalpy
i	Species i
k	Number of heat sources
m	Mass
N	Number of moles
MW	Molecular Weight
Q	Heat
P	Pressure
s	Specific entropy
S	Total entropy
T	Temperature
U	Internal energy
W	Work
V	Volume
0	Restricted dead state
Δ	Change in related parameter
η_b	Exergy efficiency
ANT	Adenine nucleotide translocase
API	Active pharmaceutical product
AppCp	Adenosine-5'-[(β , γ)-methylene]triphosphate
ATP	Adenosine triphosphate

BP	Bisphosphonates
CexC	Cumulative exergy
CDP	Cumulative degree of perfection
ch	Chemical
C-NMR	Carbon nuclear magnetic resonance
COSY	Correlation spectroscopy
DSC	Differential scanning calorimetry
FPP	Farnesyl disphosphate
FTIR	Fourier transform infrared
Gen	Generation
GGPP	Genarylgenaryl diphosphate
GMP	Good manufacturing practice
HCM	Hypertrophic cardiomyopathy
HMBC	Heteronuclear Multiple Bond Correlation
HMG-CoA	5-hydroxy-3-methylglutaryl-coenzyme A
H-NMR	Proton nuclear magnetic resonance
HPLC	High-performance liquid chromatography
HSQC	Heteronuclear Single-Quantum Correlation
HVAC	Heating, ventilating and air conditioning
ICH	International conference on harmonization
KF	Karl-Fischer
MVP	Mevolanate pathway
in	Inlet
N-BP	Nitrogene containing bisphosphonates
out	Outlet
PTFE	Polytetrafluoroethylene
PPi	Pyrophosphates
RI	Renewability indicator
TGA	Thermogravimetric analysis
UV	Ultraviolet
WFI	Water for injection

1. INTRODUCTION

Bisphosphonates are being known since 19th century, where the first synthesis was performed in Germany in 1865 [1]. They were initially used in the industry as calcium carbonate precipitation inhibiting agents and preventers of scaling. They can act as sequestering agents for calcium and because of this feature they are called as 'water softeners'. They particularly can inhibit calcium carbonate precipitation, similar to polyphosphates. Water installations benefit this feature to prevent scaling. [2]. First biological activities of these substances were presented in 1968 by Fleisch and coworkers [3]. The studies of Fleisch was inspired from pyrophosphates which were found in plasma and urine. They found that these compounds inhibit calcium phosphate precipitation by binding to hydroxyapatite which is calcium compound existing in bone and teeth structure and so inhibiting its dissolution [4]. However they were destroyed locally by phosphatases and were not stable in the body. Because of this, Fleisch searched analogs compounds that were not destroyed enzymatically [1, 5]. The bisphosphonates was the ones which fulfilled these conditions.

Pyrophosphates and bisphosphonates differ in their structure with the substitution of an oxygen atom by the carbon which connecting two phosphates. Hydroxyapatite which is a mineral form of calcium apatite creating a high affinity for bisphosphonates [6]. The calcium ions in hydroxyapatite chelated by the oxygen atoms of phosphate [7]. This creates an ideal target for treating diseases associated with bones and teeth since hydroxyapatite is unique to these tissues [8].

Zoledronic acid is a bisphosphonate derivative, which is also known as zoledronate, works to decrease the amount of calcium released from the bones into the blood. By this future it increases the bone density (thickness) by slowing down the bone breakdown. Biological usage of bisphosphonates dates back to 1990s [1]. It is used for treating osteoporosis as well as to prevent skeletal fractures in patients with cancers such as multiple myeloma and prostate cancer. It can be helpful for treating pain from bone metastases and used to treat hypercalcemia of malignancy. It is indicated for the treatment of patients with multiple myeloma which is a cancer type of malignant plasma cells and used in conjunction with standard antineoplastic therapy and in patients with bone metastases from solid tumors [9].

Zoledronic acid may be used also to prevent repeated fractures in patients diagnosed hip fracture with its annual dosage [10].

The purpose of the first part of this study is to synthesis zoledronic acid and to produce parenteral preparations as injections ready to be used. In the scope of this study, firstly the molecule will be synthesized and the finished pharmaceutical forms will be developed. From the molecule to the finished product, the process will be defined. The success of this project will result discernible advantages in preventing bone fractures in post-menopausal period of women and in cancer patients and will reduce health expenses by resolving the long and hard treatment periods contributing to government health budget. This part of the study will be carried out in Atabay Pharmaceuticals and Fine Chemicals Inc. Laboratories.

Products of the innovator company Novartis are in the market serving as preventer of bone breakdown caused by oncological or non-oncological reasons. Sales for 2010 reached 2 billion \$ and expected sales will reach 3 billion \$ until 2017. Patents of the company covering different indications for example usage in cancer patients for bone strengthening, in post menopausal osteoporosis and in breast cancer treatment in Europe and USA, have expired in 2013, eliminating patent violation due to production and being in the market. It should be noted that production of such pharmaceuticals economically contributes to our country by preventing the outflow of foreign currency.

Another aspect of the study is, as a chemical process, it is necessary to evaluate energy consumption and savings, for the selection of production process and the equipment used. For this purpose exergy tool is used. Exergy loss during the process is calculated for zoledronic acid synthesis and for finished product manufacturing. Losses are caused by irreversibilities such as, heat transfer at $\Delta T > 0$, mixing, reaction and from other external losses by means of not utilized systems, like wasted cooling and heating streams, exhaust gases etc.

The theoretical background section gives the basic information on the chemistry, mechanisms of action, toxicity and uses of bisphosphonates in different diseases including cancer in general and for zoledronic acid as the bisphosphonates used in this study. Chemicals, equipment and methods used for the analysis of zoledronic acid is given in materials and methods section. Experimental section includes details of each trial for the synthesis of zoledronic acid. In results and discussion part, experimental results and exergy

results are discussed. As a final part, conclusions on zoledronic acid synthesis and finished dosage form production and exergy evaluations are given.



2. THEORETICAL BACKGROUND

Bisphosphonates are synthetic analogs of inorganic pyrophosphate molecules, an endogenous regulator of bone mineralization. When hydroxyapatite on bone surfaces undergoing remodeling, bisphosphonates could bind to these molecules due to their ability to chelate calcium ions [11]. Radioactive labelling studies show that bisphosphonates are present in endocytic vacuoles which are cellular membrane-bound compartments filled with extracellular compounds such as water, inorganic and organic molecules including enzymes [12] and other organelles in osteoclasts [13]. Radioactive labelling in calvarial cells which are belonging to the upper part of the skull, also shows that bisphosphonates could enter to different organelles of bone cells such as cytoplasm and as well as mitochondria [14]. This feature of bisphosphonates is thought to impair the action of osteoclasts. Osteoclasts are cells in charge with resorbing bone by removing bone mineralized matrix and breaking up the organic part. Besides their effects on mature osteoclasts, bisphosphonates are found also effective on osteoclast precursor cells, by preventing the recruitment, differentiation, and fusion of osteoclast precursors [15].

2.1. CHEMISTRY OF BISPHOSPHONATES

Bisphosphonates have two P-C bonds linked to single carbon atoms and are used clinically as medicines for bone diseases. They are stable chemical derivatives of pyrophosphates which are found widely in the nature. The simplest type of pyrophosphates is inorganic pyrophosphate (PPi). This compound has lightened the way of the discovery of bisphosphonates as a circulating endogenous 'water softener' in the body [16]. (Figure 2.1)

The P-C-P part of the structure allows a great number of possible alterations. Physicochemical, biological, therapeutic, and toxicological characteristics could undergo alteration caused by small changes in the structure of the bisphosphonates. Many bisphosphonates have been studied in humans with respect to their effects on bone, and eight of them are commercially available today which are used for treatment of bone diseases [17].

The structural difference of bisphosphonates from pyrophosphate is reasoned by two additional side-chains attached to the central (geminal) carbon atom, represented as R₁ and R₂ in Figure 2.1. The synthesis of wide range compounds of same family with different

properties could be achieved with different numerous substitutions of these side-chains. The feature of calcium affinity of BPs generally related with hydroxyl substitution at R_1 . Nitrogen atom presence in R_2 on the other hand determines mechanisms of action of BPs. They are effective on reducing bone resorption and they have also additional pharmacological properties that makes BPs unique when compared with other medications used in osteoporosis which is a disease that causes bones to become weaker and to easily fracture. The treatment comprised of selective uptake and long-term residence of BPs in the skeleton [9].

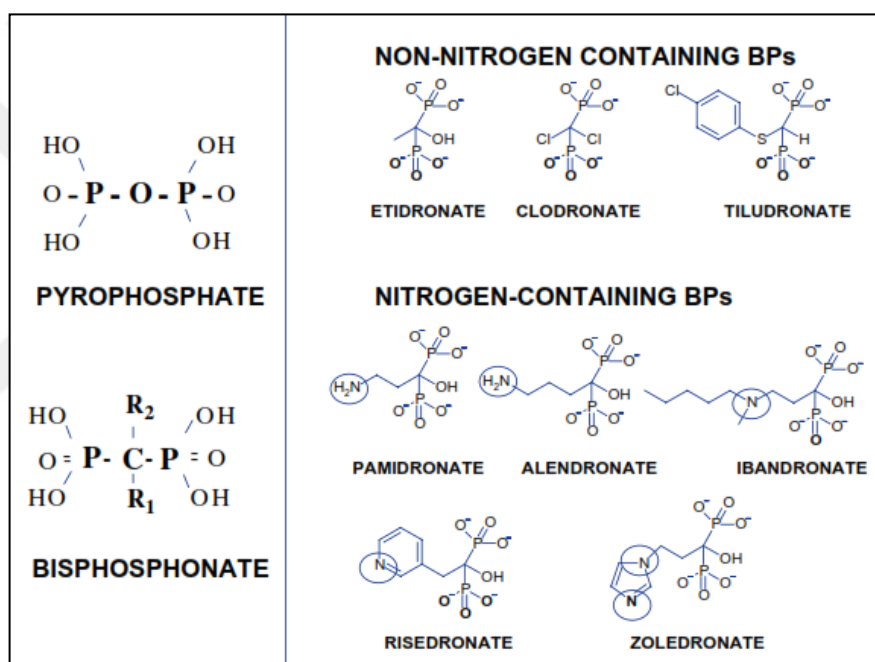


Figure 2.1. Molecular structures of bisphosphonates [9].

To understand their mechanisms firstly BPs behavior in the body is studied. When they administered to the body, they are taken up by the skeleton, mainly at active remodeling sites, and in such a way they can bound to bone mineral strongly. In the studies performed with BPs, mouse bone and human bone particles showed that the presence of an OH substitution in R_1 increases the binding of BPs to bone mineral independently of R_2 structure [18].

The effect of OH substitution is assumed due to the tridentate binding of hydroxyl-substituted bisphosphonates to calcium. Considering this effect clinically effective BPs have mostly an OH substitution in R_1 . However when other substitutions such as Cl or H are participated in

the molecule at R₁ provide bidentate binding to calcium crystals, or lack of R₁ group molecules such as clodronate and tiludronate are found as they have significantly lower binding affinities [6].

In line with previous studies, investigators found that among hydroxyl-substituted BPs, clodronate with the lowest kinetic affinity constant was the weakest inhibitor of hydroxyapatite growth rate. However studies among hydroxyl-substituted bisphosphonates zoledronate was observed like the most potent inhibitors of the growth of hydroxyapatite crystals, with 35% difference in its binding affinity from those of ibandronate and risedronate. Considering these results according to their binding affinities, the bisphosphonates are ranked as follows: zoledronate > alendronate > ibandronate > risedronate > etidronate > clodronate [9].

2.2. MECHANISMS OF ACTION

Bone resorption is the breakdown process of the bones by osteoclast cells. Bisphosphonates, are delivered to osteoclasts by a specific release mechanism after accumulation in bone tissues. The environment of the space between the bone and osteoclasts during resorption has acidic property. This acidic property causes the release of the bound bisphosphonates and in that way they start to accumulate and up taken via fluid-phase endocytosis [13, 19]. A proton pump in the membrane of osteoclast cells which is in charge with bone resorption process is generating this acidic environment [20, 21]. Upon uptake by osteoclasts, inhibitory activity of bisphosphonates comes out through two main mechanisms, which are structure-dependent. (Figure 2.2)

The first-generation bisphosphonates are the ones that do not contain nitrogen atoms in their structure. Some of them such as etidronate and clodronate act as analogs of pyrophosphates. They are metabolized to a cytotoxic analog of ATP, adenosine-5'-(β,γ -dichloromethylene)-triphosphate (AppCp). The mitochondrial adenine nucleotide translocase (ANT) is inhibited by this compound and apoptosis is triggered ultimately [22, 23]. 10–100-folds more potent inhibitors than the first-generation bisphosphonates have a nitrogen atom in an alkyl chain in their structure, some examples are alendronate or pamidronate (Figure 2.1). Their studies prove that their inhibition effect on bone resorption is through the mevalonate pathway (Figure 2.2) [24]. This pathway is used in prenylation, to synthesis proteins such as Rho,

Rac, Ras, or Rab which are important for cytoskeletal organization and cell morphology. Osteoclast cell activity is directly affected by prenylation. If this pathway is disrupted the activity of osteoclasts is decreased and even apoptosis occurs [25].

Pamidronate, risedronate, ibandronate, alendronate and zoledronate are some of nitrogen-containing BPs (N-BPs) which are not metabolised to AppCp-type nucleotides like simple BPs. According to preclinical models, N-BPs are also considerably more potent inhibitors of bone resorption than the simple BPs [26]. The mechanism of action of N-BPs was firstly appeared in 1992. First clues depend on the studies of Amin et al., 1992. In a macrophage study, they have reported that, the N-BPs ibandronate and incadronate have inhibition effects on the squalene synthase and on enzymes in cholesterol biosynthesis pathway (the mevalonate) [27].

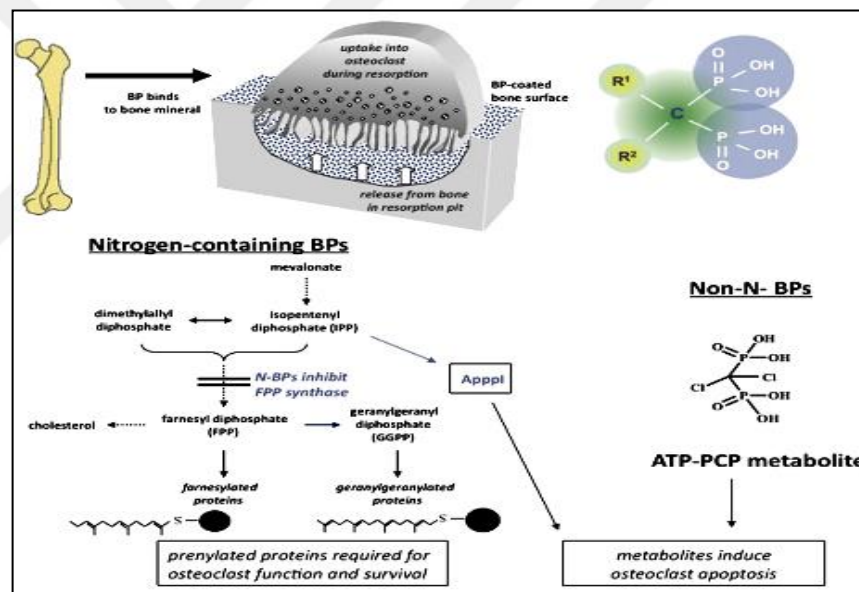


Figure 2.2. Mechanisms of action of bisphosphonates [16]

Mevalonate pathway is primarily in charge with the cholesterol and farnesyl diphosphate (FPP) and geranylgeranyl diphosphate (GGPP) synthesis which are isoprenoid lipids. Such isoprenoid lipids are used as building blocks for the synthesis of a different metabolites, including dolichol and ubiquinone [28]. Isoprenoid lipids are also required for prenylation of proteins (Figure 2.3) [29].

The prenylation process comprise of combination of isoprenoid groups, which are comprised of 15-carbon chain for FPP and 20-carbon chain for GGPP, with carboxy-terminal motifs of

targeted protein from its cysteine residue [30]. The farnesylated and modified proteins obtained with geranylgeranyl group [11] contains up to 2% of mammalian proteins. They are part of predominantly small GTPase signaling proteins and nuclear lamins phosphodiesterase subunits. For these proteins to function correctly, prenylation is needed because with this process membrane anchor sides are generated to allow the proteins participated in cell membranes, and this process is also part of their interactions with such proteins like regulatory GAPs and GDIs [30]. These GTPases are like molecular switches when they have prenylated, because of that their activity are important and should be strictly controlled. Unprenylated small GTPases are accumulated in their active (GTP-bound) state after N-BPs exposure to the cells according to recent studies. This accumulation causes activation of downstream signaling kinases in an inappropriate way [32]. The process of prenylation in cultured cells are studied by measuring FPP, GGPP or the radiolabeled mevalonate incorporation with both farnesylated and geranylgeranylated proteins (Figure 3) [11].

Farnesyl diphosphate (FPP) and geranylgeranyl diphosphate (GGPP) are needed for prenylation of proteins which are fundamentals for osteoclast cell survival and function. Nitrogen-containing bisphosphonates are inhibiting prenylation of FPP synthase, thereby preventing the synthesis of FPP and GGPP [11].

There are numerous studies confirming that in vitro proving that N-BPs (10 μ M zoledronate or 100 μ M risedronate or alendronate) inhibit the incorporation of mevalonate into prenylated small GTPase proteins in purified osteoclasts [33, 34] and in vivo prevent protein prenylation in osteoclasts [22, 34, 35]. Besides in vitro studies, Fisher et al., shown in vivo that N-BPs have effects on the mevalonate pathway of osteoclast cells. In a rat study in which animals are treated with N-BPs showed HMG-CoA reductase are in suppressed levels in osteoclasts, assumed because of the feedback regulation in the mevalonate pathway [36].

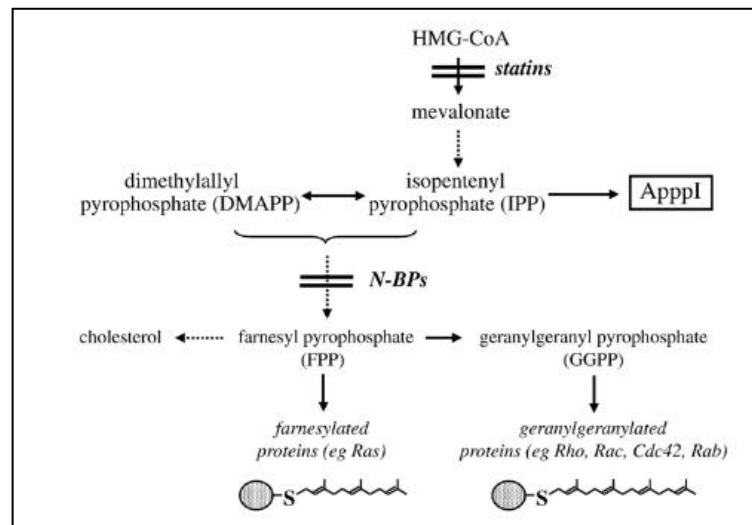


Figure 2.3. Mevalonate pathway representation[11]

The prenylation of small GTPases could be indirectly blocked with the inhibition of the synthesis of FPP and GGPP by interfering proximal enzymes of mevalonate pathway for example N-BPs induced HMG-CoA reductase inhibition or FPP synthase inhibition [30]. Benford et al. aiming N-BP actions using J774 macrophages, concluded with the simple BPs (i.e. clodronate and etidronate) has no effects on mevalonate pathway whereas used N-BPs prevent the mevalonate incorporation into both farnesylated and geranylgeranylated proteins [26].

Some important signaling proteins such as families of those the Ras, Rho, Rac, Cdc42 and Rab are prenylated small GTPases. These proteins regulate different cell processes which are responsible for function in osteoclast cells [31]. The effects of N-BPs on osteoclasts are proved that they have inhibition effect on the mevalonate pathway [25], achieving this effect by the loss of prenylated proteins (and loss of downstream signaling) and/or accumulation of unprenylated proteins (and downstream signaling pathways caused by inappropriate activation). For example, in vitro or in vivo studies show the relate absence of in ruffled border in osteoclasts treated with BPs with the inhibition of prenylation of Rho, Rac or Cdc42 [37]. Since cytoskeletal organization in osteoclasts needs Rho, Rac and Cdc42 [31], with the loss of prenylation as a characteristic result of BP treatment of these small GTPases. For vesicular trafficking, Rab GTPases are essential regulators. Several of these molecules are known to be needed for osteoclast function [38, 39, 40]. Lack of these proteins prenylation would therefore affect formation of the ruffled border in osteoclasts, trafficking of lysosomal enzymes and transcytosis of degraded bone matrix [41]. When subjected to

high concentrations of N-BP (G), apoptosis in osteoclast cells occur with the disruption of downstream signaling. This disruption occurs with the loss of prenylation of small GTPases such as Rac in the pathways which promote cell survival [42].

Bisphosphonates are widely used and found clinically effective in different bone diseases due to their inhibitory effect on bone resorption [43] (Fig 2.4). Bisphosphonates are also used as bone targeting agents to deliver other drugs [44, 45, 46]. Their liposomal formulations are found to inhibit macrophage growth which in turn inhibits of restenosis and induces apoptosis in tumor-associated macrophages and monocytes [47, 48]. Bisphosphonates are also used to coat and stabilize nanoparticles [49, 8] and as linkers between a delivery system and different targeting moieties [50, 51]. They can also be used as bone coating agents since they enhance bone formation around implants [52, 53].

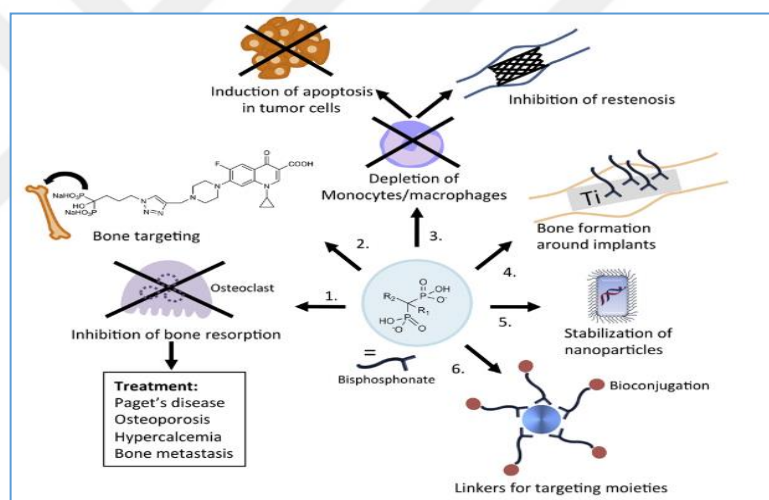


Figure 2.4. Biomedical applications of bisphosphonates [43].

2.3. TOXICITY

For the patients suffering severe renal insufficiencies, recommended dose for zoledronic acid could not be proper and dose modifications could be required, since the molecule has been associated with deterioration of renal function. For minimizing the side effects of osteoclast inhibitors some considerations could be taken into account such as, giving attention to dental health of the patient selected, supplementation with calcium and vitamin D, and monitoring of laboratory values effectively [54].

Studies performed for cardiovascular effects of BPs show that they have no significant effects. For example, an electrocardiography study by Camm, (2010) is performed on zoledronic acid administrated patient group versus placebo. No significant differences are observed between two patient groups after third year of the administration. There were not significant differences between the groups in terms of cardiovascular deaths, stroke, and other non-arrhythmia cardiovascular adverse events. However arrhythmia was observed as more common in the zoledronic acid group than in the placebo group (6.9% vs 5.3%; P= 0.003) [55].

2.3.1. Hypocalcaemia

Hypocalcaemia is the event of presence of low serum calcium levels in the blood. Amino group containing bisphosphonates are used as potent inhibitors of bone resorption. So, amino BPs can stimulate the decrease in calcium levels in circulation, particularly at sudden high concentrations resulted from intravenous administrations. This feature caused symptomatic hypocalcaemia frequently encountered in patients treated with intravenous zoledronate, particularly for the indications and doses for oncology [56]. This adverse effect is more common in patients having some risk factors such as hypoparathyroidism occurred before, kidney failure and vitamin D deficiency. Administrations in such patients should be in controlled manner with post-infusion controls and precautions should be taken. For oral administration hypocalcaemia was encountered weeks after the start of treatment but rarely [57].

2.3.2. Atrial Fibrillation

Atrial fibrillation is heart rhythm disorder. This unexpected adverse effect firstly observed during the results evaluation from a clinical trial performed with intravenously administered zoledronate, for osteoporosis treatment-the HORIZON study with frequency of once a year. Atrial fibrillation is seen in the patients treated with the pharmaceutical as defined “serious” in higher ratio than the placebo group (absolute risk: 1.3% against 0.5%; P<.001), but results were not different between the two groups when overall incidence of atrial fibrillation is considered [58]. The timing of serious adverse events did not correspond with drug

administration or the pharmacokinetic profile of the drug. Preclinical and other clinical trials of zoledronic acid for the treatment of osteoporosis or other indications did not identify an effect on atrial fibrillation adverse effects [55].

2.3.3. Osteonecrosis of the Jaws

Osteonecrosis of the jaw, commonly called ONJ, occurs when the jaw bone is exposed and begins with starving of bone because of insufficient blood supplied. In osteonecrosis (osteo meaning bone and necrosis meaning death), the bone begins to weaken and die, and this process not always causes pain however usually it is a painful phenomenon. ONJ is associated with cancer treatments (including radiation), infection, steroid use, or potent antiresorptive therapies that help prevent the loss of bone mass [59].

Osteonecrosis on the jaw as a bone disease encountered in patients diagnosed with cancer and treated with ABPs in 2002. After the FDA notices with this failure various articles published in medical journals [60, 61, 62, 63] and also in general newspapers [57].

After zoledronate treatment in dogs, non-viable osteocytes accumulation and suppressed cortical remodeling have been observed, in the jaws with areas of necrosis of the matrix. These results could help to understand the delays in healing and infections observed after the tooth extractions [64].

Considering that millions of patients have been prescribed bisphosphonates for the treatment of osteoporosis, the relative prevalence of osteonecrosis on the jaw in these patients was low. Old age more than 60 years, female sex, and previous invasive dental treatment were the most common characteristics of patients who developed osteonecrosis on the jaw [65].

2.4. BISPHOSPHONATES IN OSTEOPOROSIS AND BONE DISEASES

Zoledronic acid is administered to the patients intravenously (4 mg in 100 ml 0.9% saline over 15 min), of which plasma peak is cleared from the circulation after a few hours [66]. Plasma concentration levels could be detectable within a week after administration, however fall to less than 1% of the concentration at the end of the infusion within a 24 hours [67].

The half-life in bone however, could be measurable in years with ongoing biological activity after a single dose for at least 3 years [68].

Bisphosphonates are known as well-recognized inhibitors of osteoclastic activity and because of that they are preferred therapeutic options for various systemic metabolic bone diseases [43]. Current main indications of bisphosphonates include Paget's disease, hypercalcemia of malignancy and post-menopausal osteoporosis [69, 70, 71]. Bisphosphonates are being investigated for the treatment of fibrous dysplasia [72], osteoarthritis [73] and rheumatoid arthritis [74].

Considering their effects on bone tissue, oral bisphosphonate therapy became the key element of pharmacological management for patients with osteoporosis for last 15 years. According to the studies performed as randomized controlled trials, bisphosphonates can decrease fracture incidence by 16 to 47% depending the fracture site and the chosen agent [75]. For example alendronate as a generic has been the initial treatment offered for bone diseases in UK similar to other countries of which usage also supported by National Institute for Health and Clinical Excellence (NICE) technical appraisals. In a recent meta-analysis, Wilkes et al. showed that in medicated patients as followed up in large scale observational cohorts a decrease in fracture incidence is achieved when compared to that resulted in randomized controlled trials. [76].

Bisphosphonates were studied on human bone marrow stromal cells (BMSC) for their proliferation and osteogenic differentiation. BMSC support the function of bone marrow cells which are the flexible tissue placed in the interior of bones. In a study, BMS cells are collected from patients complaining end-stage degenerative joint disease and because of that went through primary total hip arthroplasty. Collected cells were investigated as two groups one of the cell group is treated with a bisphosphonate (alendronate, risedronate, or zoledronate) and other group is remained as control group. Both groups are analyzed over 21 days of culture. Direct cell counting is used to detect cell proliferation. Osteogenic differentiation of BMSC was assessed with alkaline phosphatase bioassay and gene expression was analyzed. Bisphosphonate treated group results showed an enhanced proliferation of BMSC after 7 and 14 days of culture. Steady-state mRNA levels of key genes were generally increased by bisphosphonate treatment in a type and time dependent manner. Gene expression levels varied according to differences in donors. This study states that using

a clinically relevant *in vitro* model bisphosphonates is found to enhance proliferation of BMSC and initiate osteoblastic differentiation [77].

In another study the efficacy of bisphosphonates with postmenopausal women osteoporosis are evaluated for the prevention of vertebral, hip, and nonvertebral-nonhip fractures. In this study eight randomized placebo controlled group the effects of zoledronic acid (1 study), alendronate (3), ibandronate (1), risedronate (2), and etidronate (1) are studied in terms of bone fractures with a systematic literature search through a follow-up of 3 years (or 2 years if used for registration purposes). The study concludes that among the available bisphosphonates for osteoporosis, zoledronic acid has the highest probability of offering the best overall fracture protection [78].

A nonclinical study is performed to investigate the effects of bisphosphonates on osteoblast viability and function was performed *in vivo*. For proliferation and cell control the enzyme activities and cell numbers of osteoblast cells are measured with enzyme linked assays in 24, 48, and 72 hours. It is found that cell viability is decreased as drug concentration is increased revealing the cytotoxicity of these molecules in high concentrations. However in lower concentrations they have therapeutic benefits without the cytotoxic effects which may result in osteonecrosis, proving increase in transforming growth factor of osteoblast cells [79].

Increasing evidences are showing zoledronic acid, a nitrogen-containing bisphosphonate (N-BP), can inhibit tumor cells by blocking the enzyme farnesyl pyrophosphate synthase in the mevalonate pathway (MVP). It is believed that resulted accumulation of unprenylated proteins caused by the cytotoxic effects of zoledronic acid. FPPS inhibition cause also accumulation of isopentenyl pyrophosphate and the apoptotic ATP analog, nevertheless the role of this mechanism as a cytotoxic action of bisphosphonates is not so clear. It is because the treatment with mevalonate pathway intermediates has been shown that via rescuing protein prenylation they could overcome N-BP-induced apoptosis [80].

Although BPs have been used clinically for many years before their mechanism of action was known entirely, it is now well studied. Bisphosphonates are directly binding to mineralized bone surfaces. So since they deposit in the bone, they could be cleared rapidly from the bloodstream and from the body by renal filtration [81]. The intracellular concentration of BPs in most tissues is very low because these agents do not readily cross the plasma membrane. BPs are taken into the cell by fluid-phase endocytosis. Such cells use

these intracellular actions are osteoclasts, macrophages [82, 19], and monocytes [83]. Since then bisphosphonate accumulation are seen in those cells. In such a way bisphosphonates are targeting bone remodeling. BPs have been shown to be internalized by several human cancer cell lines, including breast, prostate, and myeloma since they use fluid-phase endocytosis. The rate of BP uptake by cancer cells varies widely between the cell lines tested since now [84]. Additionally, the effects of BPs also varies depending on their mechanism of action, in which their biochemical structure has the key role.

Different studies showing that N-BPs have inhibitory effects on human myeloma cell lines and multiple myeloma cells, by inhibiting cellular growth via inhibition of the mevalonate pathway and create apoptosis. The dose of the drug has also role on this affect [85, 86, 87, 88]. For example, in a study performed with newly diagnosed multiple myeloma patients with pamidronate (90 mg), there was a significant increase in the proportion of apoptotic plasma cells after a single infusion which are detected in bone marrow [87]. In another study, zoledronic acid (50 mM) in a dexamethasone combined medication shown having antiproliferative effects on myeloma cell lines [89, 90, 91].

The data performed through early studies suggesting zoledronic acid as administrated annually has therapeutic effects in women with osteoporosis. A randomized, double-blind study, is performed to compare the effects of zoledronic acid with alendronate. In 24-week time, it is found that the first attack of action of a single infusion of zoledronic acid 5 mg compared with weekly oral alendronate 70 mg in postmenopausal women with low bone mineral density, reduces bone resorption markers more rapidly than alendronate [92].

2.5. BISPHOSPHONATES IN CANCER

In tumor disease, bone metastases are very commonly seen. Indeed, any malignant tumor is capable of metastasizing to the skeleton, however few types resulted frequently metastases in bone. Among different cancer types, breast cancer be in the lead most frequent cause of bone metastases, it is followed by prostate, lung cancers, thyroid carcinoma, and renal cell carcinoma is the (Table 2.1).

Table 2.1. Incidence of bone metastases [94]

Primary Tumor	Median	Range
Breast	73 %	47-85%
Prostate	68%	33-85%
Thyroid	42%	28-60%
Kidney	35%	33-40%
Bronchus	36%	30-55%

These five tumor entities given in Table 2.1 are found the reason for more than 80% of skeletal metastases [93]. Bone metastases are seen at autopsy in about 65%-80% of all women who die of breast cancer. According to the studies a forecast of every fourth newly diagnosed patient will develop bone metastasis. This corresponds an incidence of 180,000 cases (women) per year in the USA and estimated incidence 48,000-50,000 cases per year (women) in Germany. Considering survival time, an average is estimated as 2.5 years, although there is a wide range variation margin [94].

In the patients having the solid tumors generally arising from lung, kidney, breast, thyroid and prostate, bone metastasis could be encountered. It is found that around 70% of patients with advanced prostate cancer or breast cancer, and up to 40% of patients with other advanced solid tumors will develop bone metastases. Additionally it is clinically observed that in more than 50% of men with advanced prostate cancer and around 20% of women with advanced breast cancer, bone metastases are observed in the skeleton [95]. Metastatic bone disease disrupts the normal homeostasis of bone, and the resulting in imbalanced bone metabolism which damages bone integrity, resulting in skeletal defects including bone pain, pathological fractures. In those cases in order to prevent or repair major structural damage, spinal cord and/or nerve root compression, and hypercalcaemia of malignancy, orthopedic surgeries became a requirement. Nowadays osteoclast activation is accepted as the key step in the establishment and growth of bone metastases of such cancer types [96].

Studies for patients having breast cancer show that vertebral fractures are encountered a 4–5 times higher rate than an age matched group of well women. This fractures are most likely related to chemotherapy induced menopause. Bone metastase is also common in patients having prostate cancer. Prostate cancer is observed as having different bone lesions than encountered in breast cancer. Instead of the tendency for bone lesions to be either osteolytic

or mixed osteolytic and osteoblastic, in the prostate cancer metastases appear as osteoblastic lesions on X-ray. New bone structures near the prostate cancer cells are laid down by osteoblasts, probable effects of direct stimulation of DNA synthesis and proliferation of the osteoblasts and fibroblasts assumed by prostatic osteoblastic factors [97, 98].

As explained in section mechanisms of actions, N-BPs has found as directly affecting the cholesterol synthesis, via the mevalonate pathway. This pathway is essential for any cell type since the proteins synthesized are used in many essential cell functions. Anti-tumor activity of different BPs has been demonstrated mainly in breast, prostate and myeloma cell lines. In vitro studies show that, particularly zoledronic acid, reveals inhibitory effects on tumor cell adhesion, invasion, and tumor cell proliferation [99, 100, 101, 102].

Zoledronic acid-induced tumor cell apoptosis has been demonstrated to result in activation of the caspase pathway, caspase molecules play important roles in apoptosis pathway [102, 103, 104, 105]. In support of the inhibition of the mevalonate pathway, to inhibit the suppression of protein prenylation reasoned by zoledronic acid intake, the caspase pathway is activated and apoptosis in human breast cancer cell lines occurs [105, 106, 107].

BPs as bone resorption inhibitors, have effects on the release of bone-derived cytokines and growth factors, especially they have role on bone making them less attractive to tumor cells in terms of colonization, tumor migration, invasion, adhesion, proliferation and survival [108].

Investigations performed for bisphosphonates as clinical trials in the preventative degree have shown that's besides delaying the occurrence of bone metastases in the cancer, bisphosphonates also found delaying the lesions of non-osseous parts of the body in a study, and survival was prolonged [109]. Other trials however have shown the opposite [110, 111, 112, 113]. Likewise, animal studies for cancer and metastases, obtained results have been conflicting. In vitro works which has purposed bisphosphonates effects on tumor cells and activities has found a variety of antitumor effects such as apoptosis induction, inhibition of cell growth [114, 26, 102, 105, 115], inhibition of invasive behavior [116, 117] and inhibition of angiogenic factors [104, 105]. Bisphosphonates are further found that they have the potential to enhance anti-tumor activity of cytotoxic drugs which are toxic to the body. Besides direct effects on tumor cells, bisphosphonates effect on osteoclasts creates a strong

rationale for the use of these drugs as a supporter in patients having malignancies and more preferably having metastasis to bone [118].

The tumor growth and metastatic spread is a multistep process. For a tumor to metastasize it must grow at its primary site, migrate, adhere and invade basement membrane and extracellular matrix proteins, escapes from immune system destruction, spread to distant sites, where must again proliferate and survive the local environment. Potential effects of bisphosphonates biologically were studied in *in vitro* and this is advantageous for addressing the steps of cancer cell progression and survival separately. (Figure 2.5) [118].

At the times when only inhibitory effect on osteoclasts are known or revealed, a study in 1996 by van der Pluijm et. al. showed that bisphosphonates are also able to reduce tumor burden in bone, potentially. In a way that they inhibit cell adhesion. This study was known with revealing inhibitory effects bisphosphonates in tumor seeding in bone as an unknown role of these molecules [119].

Bone metastases are found most common in patients with breast cancer [120]. Bone disease causes significant morbidity, resulting in major skeletal events such as fracture, hypercalcemia, or spinal cord compression. Another common and frustrating complication of metastatic bone disease is bone pain [121, 122, 123].

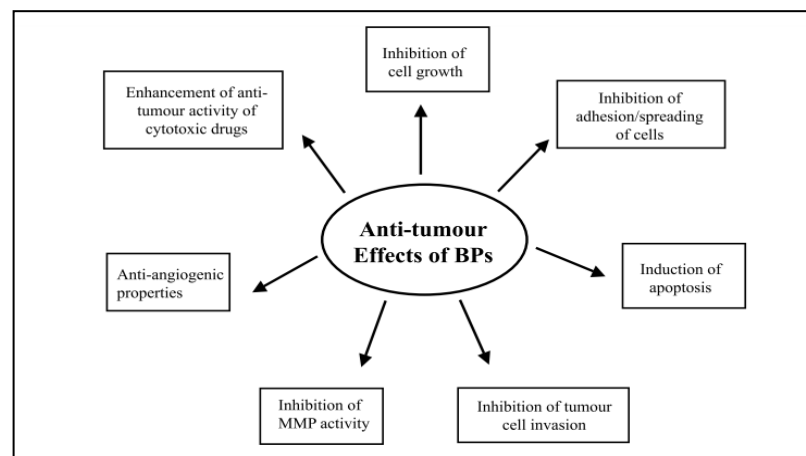


Figure 2.5. Anti-tumor effects of bisphosphonates [118]

In another study, bisphosphonates anti adhesion effect on tumor cells are revealed proving their anti-tumor effects. When the breast and prostate cancer cells were pre-treated with bisphosphonates, inhibition of adhesion of tumor cells to bone was observed as dose-

dependent. This anti-adhesion effect was not due to cytotoxicity. This effect was due to their inhibition capability on adhesion of tumor cells at determined doses. It is also found that, the bisphosphonates found having no effect on adhesion of normal cells (fibroblasts) to bone matrix [124].

Pamidronate (at 100 μM) and zoledronate (at 50 μM) when assessed with DNA fragmentation assay were also found having directly inducing effect on apoptosis of the breast cancer cells [102].

In a study six bisphosphonates including zoledronic acid were administered to three breast cancer cell lines. Apoptosis was observed through flow cytometry of a DNA fragmentation assay during cell proliferation measurements. In the studies performed for different breast cancer cell lines, bisphosphonates are found to have direct effects on cell proliferation and apoptosis. Zoledronate found to be the most potent among this six bisphosphonates, in which their very effects having different magnitude are observed. This study showed promising anti-tumor potential of BPs [103].

In a 2-year follow-up study, carried out for zoledronic acid and pamidronate, pre-planned multiple-events analysis showed that zoledronic acid 4 mg reduced the risk of a skeletal complication (including HCM) by 20% more than pamidronate 90 mg. Breast cancer patients with skeletal-related effects (not including HCM) results were comparable between treatment groups after 24 months (49% with pamidronate and 46 % with zoledronic acid) [125].

A study performed with patients with metastatic bone disease often having severe bone pain and debilitating skeletal complications. Zoledronic acid is investigated in patients with genitourinary malignancies, including prostate cancer, renal cell carcinoma, and bladder cancer complaining with secondary bone metastasis to these complications. This study is presented an evidence in patients in randomized, placebo-controlled trials, monthly zoledronic acid at 4 mg significantly reduced the proportion of patients with skeletal-related events. Its effects include delaying of the onset of bone complications compared with placebo [126].

Pivotal trials are performed as prospective, randomized controlled to support efficacy and safety of zoledronic acid covering more than 3000 subjects. Involving a broad tumor types, zoledronic acid administrated intravenously every 3–4 weeks resulted besides decreasing

skeletal-related events frequency, first skeletal-related event is delayed. Comparing with pamidronate, zoledronic acid is found more effective in breast cancer and the only bisphosphonate approved as effective for metastatic prostate cancer, lung cancer, and renal cancer [127].

Summary studies through Medline search also performed to show current evidence for clinical, anti-tumor, and survival benefits from zoledronic acid in patients with genitourinary cancers. These studies revealed that among patients with bone metastases from prostate cancer or renal cell carcinoma, compared with placebo zoledronic acid significantly delayed the onset and reduced the incidence of skeletal complications. Zoledronic acid is only bisphosphonate which showed as supporting the cell survival and delaying progression of bone lesions in patients having urologic malignancies. Additionally, zoledronic acid proved as reducing the occurrence of skeletal-related pathologic fractures which could be caused by the reduced survival. Bisphosphonates are approved in preclinical studies for their direct anti-tumor effects, besides their remarkable palliative benefits [128].

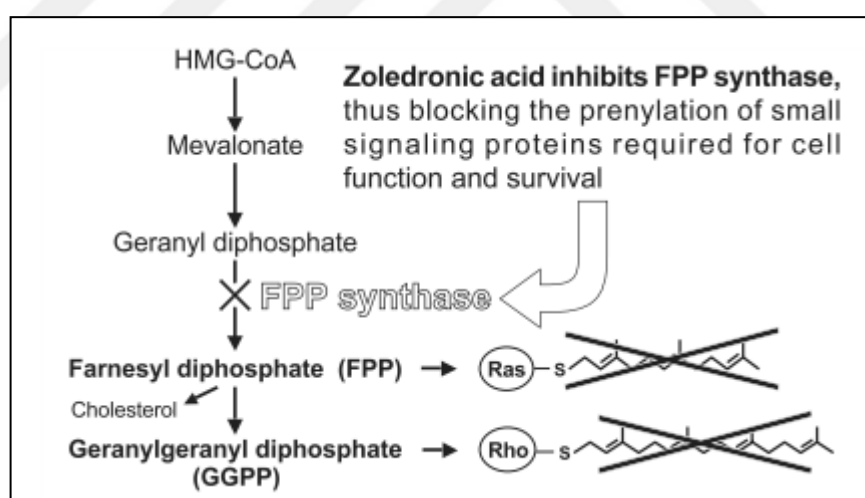


Figure 2.6. Anti-tumor activity of zoledronic acid [129]

The effects of bisphosphonates on tumor cell are summarized as not only by inhibit proliferation and induce apoptosis, but they also interfere the adhesion of cancer cells to the bone matrix and they can inhibit tumor cell migration and invasion. Anticancer drugs like taxoids, doxorubicin or imatinib are known to potentiate their anti-tumor effects [129].

2.6. EXERGY ANALYSES

Production of the pharmaceuticals demands more energy than the production of the other chemicals because of the need for a sterile environment. Maintenance of a clean environment, including the manpower, sterilization of the equipment, raw materials and the operating plant and the product itself is achieved at the expense of energy utilization. Exergy is defined as the maximum amount of work which can be produced by a quantity or flow of matter, heat or work as it comes to equilibrium with a reference environment [130]. Unlike energy, exergy is not conserved, but may be destroyed due to irreversibilities in any real process and entropy is generated. Principles of conservation of mass and energy are used together with the second law of thermodynamics in exergy analysis in design of the processes, to improve energy and exergy efficiency. During the recent years, exergy analysis has got a great importance as they increasingly applied for evaluation and optimization the efficiency of various manufacturing processes and become very popular for evaluating sustainability of various energy-intensive systems.

Dinçer (2011), discussed that obtaining reductions in energy consumption, increasing sustainability of a process and environmental emissions via exergy analysis. Exergy analysis provides a more realistic and meaningful assessments than energy analysis since it is usually destroyed and may be lost in a process as demonstrated with drying [131] and industrial yogurt production processes [132]. Engineers and scientists has a consensus on that the thermodynamic performance of a process is best evaluated by performing an exergy analysis in combination with of conventional energy analysis. They suggested exergy give more insights to the efficiency improvement efforts of a process than just energy analysis.

Further discussions of exergy analysis for many processes and systems are given elsewhere [133, 134, 135, 136]. The recent examples of process analysis via exergy method include those of Degerli et al. (2015) [137], where energy and exergy efficiencies are compared in farm to fork grain cultivation and bread making processes in Turkey and Germany; Jokandan et al. (2015) [132], where comprehensive exergy analysis of an industrial-scale yogurt production plant was carried out; Genc and Hepbasli (2015) [138] who studied the performance assessment of a potato crisp frying process; Pelvan and Özilgen (2017) [139], where exergy efficiency of the black loose tea production process was assessed; Nasiri et al. (2017) [140], where exergy analysis of an industrial-scale ultrafiltrated cheese production

plant is carried out and Genç et al. (2017) [141], who performed exergy analysis of wine production process. Numerous chemical processes are also assessed with exergy analysis [142], including cement [143], petrochemicals, separation processes [144], inorganic chemicals etc. [142]. The concept of “sustainable medicine” draw significant attention during the last decade [145], especially after finding out that the active pharmaceutical ingredients enter ecosystems via wastewater after they have metabolized by the human body, or when they are disposed of in unused state. Advanced wastewater treatment should be in place to come up this problem which is counted as a main prohibitive costs. This means active pharmaceutical ingredients are neither completely removed by routine sewage treatment processes nor entirely degraded, and such practices alarm the experts because of the potential changes in disease patterns and pharmaceutical use in response to climate change [146, 147]. This newly recognized kind of contamination is not limited to that of the people, also the animals make a significant contribution. Contamination of rice with antibiotics originating from the urine of cattle reaching to the fields with the underground water is reported by Hawker et al (2013) [148]. The concern should also be extended to cover the waste generation during medical drug generation.

To our knowledge, there is no study in the literature regarding waste minimization during medical drug production or applying exergy analysis to pharmaceuticals industry. In this study, a range of different reaction parameters will be assessed to discover a simpler, high-yield, easily controllable and a cheaper way of zoledronic acid production process with the highest possible exergy efficiency and the highest product to waste ratio. At the start of pharmaceutical product trials, bisphosphonate synthesis was a new area in our country. In this study we aimed to contribute national pharmaceutical industry with an optimized and qualified production.

Presence of the active medical ingredients in the waste water started to draw attention recently. The first study was carried out in Germany in three institutions. A hospital, a psychiatric hospital and a nursing home [149], where the authors draw attention to the lack of data and commented about the importance of carrying out further research on that topic. The present study draws attention to the pollution by the API which may spread to the environment by the waste water from a medical drug manufacturing facility. Since there is no mention of such a pollution in the literature yet. The present study is very important since

it draws attention to an undisclosed form of pollution, but, unfortunately, its results cannot be compared with those of the others, for the very same reason.



3. MATERIALS AND METHODS

3.1. MATERIALS

3.1.1. Chemicals Used in The Synthesis of Zoledronic Acid

Table 3.1. Chemicals used in Zoledronic acid synthesis

Material	CAS number	Formula	Supplier
1 H imidazole 1 yl acetic acid	87266-37-3	$C_5H_7ClN_2O_2$	Wudi Reaction Pharma&Chemicals co., Ltd (Shandong Province, China)
Phosphorous acid	13598-36-2	H_3PO_3	Sigma Aldrich (USA)
Phosphorous trichloride	7719-12-2	PCl_3	Sigma Aldrich (USA)
Methanesulphonic acid	75-75-2	CH_4O_3S	Sigma Aldrich (USA)
Sodium hydroxide	1310-73-2	NaOH	Merck Millipore (Germany)
Ethanol	64-17-5	C_2H_5OH	J.T. Baker, Poland

3.1.2. Chemicals Used in The Production of Zoledronic Acid Injectable

Table 3.2. Chemicals used in Zoledronic Acid Injectable Production

Material	CAS number	Formula	Supplier
Mannitol	69-65-8	$C_6H_{14}O_6$	Rockett, France
Sodium Citrate dihydrate	6132-04-3	$HOC(COONa)(CH_2COONa)_2 \cdot 2H_2O$	Merck, Germany
Water for Injection	7789-20-0	H_2O	Atabay, Turkey

3.1.3. Buffers and Chemicals for HPLC Applications

The standards used for HPLC analyses were purchased from U.S. Pharmacopeial Convention, (US). HPLC grade methanol and other materials i.e. tetra butyl ammonium hydrogen sulphate, potassium dihydrogen phosphate, triethylamine were obtained from Merck Millipore (Germany).

3.1.4. Glassware Required For The Synthesis and Analyses

2 L glass reactors were used to carry reaction medium from Borucam, Turkey, with auxiliary materials, such as mixer paddle, reflux condenser. The mixer was obtained from Senco, China. Other glassware such as volumetric flasks from Zag, Turkey, beakers from Isolab, Germany and Schott, UK and glass pipettes, from Lamtek, UK, were used during the analyses. Studies are performed under hood, from Köttermann, Germany. For filtration Nutsche apparatus from Pyrex USA, filter papers (150 μm) from Sartorius Germany are used.

3.1.5. Laboratory Equipment

Table 3.3. Laboratory Equipment List

Equipment	Model / Supplier
Balances	METTLER AE 260, AJ 100, AX 250 (UK) Sartorius, CPA225D, Germany
pH meter	METTLER TOLEDO S-20, (UK)
Differential scanning calorimetry (DSC)	DSC 131, Setaram Instrumentation (France)
Thermogravimetric analysis (TGA)	Pyris 1 TGA, Perkin Elmer (USA)
Melting point	Stuart SMP 40 (UK)
Karl-Fischer (KF)	Metrohm KF system, 841 Titrando, Dosino 800, Ti stand 803 (Switzerland)
Ultrasonic water bath mixer	Bandelin Sonorex, RK 514 (Germany)

Table 3.3. Continued...

Equipment	Model / Supplier
High Pressure Liquid Chromatography Pump Detector Auto Sampler Column heater Communications bus module Degasser Reservoir tray	SHIMADZU, LC-2030 C (Japan) LC-20AT SPD-M20A SIL-20AC CTO-20A CBM-20A DGU-20A5 -
Proton nuclear magnetic resonance (H-NMR)	AGILENT (Varian) Mercury 400 FT-NMR ¹ H-NMR(400 MHz) (USA)
Carbon nuclear magnetic resonance (C-NMR)	AGILENT (Varian) Mercury 400 FT-NMR, ³ C-NMR (100 MHz) (USA)
Heteronuclear single quantum coherence spectroscopy (HSQC)	AGILENT (Varian) Mercury 400 FT-NMR, (USA)
Heteronuclear Multiple Bond Correlation (HMBC)	AGILENT (Varian) Mercury 400 FT-NMR, (USA)
Correlation Spectroscopy (COSY)	AGILENT (Varian) Mercury 400 FT-NMR, (USA)
Mass Spectroscopy (MS)	Waters Alliance HPLC with Waters Micromass ZQ (USA)
Fourier-transform infrared spectroscopy (FTIR)	IRAffinity-1 SHIMADZU, 8400 S (Japan)
Magnetic stirrer	VELP, ARE (Italy) LAB Companion, Jeio Tech/ TM-14S (US)
Hot plate	Borkim, Mtops MS300HS (Turkey)
Water bath	JeioTech BW-10H (South Korea)
Vacuum Dryer	Memmert, VO 200 (Germany)
Ultrasonic water bath mixer	Bandelin Sonorex, RK 514 (Germany)

3.2. METHODS

3.2.1. Nuclear Magnetic Resonance Spectroscopy

Nuclear magnetic resonance spectroscopy is the technique for determining the structure of organic compounds. It identifies the carbon-hydrogen framework of an organic compound. Entire structure of the molecules could be entirely identified with the data of NMR. Several common nuclei, such as hydrogen (^1H), the ^{13}C isotope of carbon, the ^{19}F isotope of fluorine, and the ^{31}P isotope of phosphorus, have magnetic moments and therefore can be detectible by NMR. H-NMR and C-NMR is most common used techniques to figure out the structure. The principle of the NMR depends on the alignment of charged particles with an external applied magnetic field. The atomic nucleus is a spinning charged particle, and it generates a magnetic field. When an external magnetic field is present, the nuclei align themselves either with or against the field of the external magnet. Without an external applied magnetic field, the nuclear spins are random and spin in random directions [150].

3.2.1.1. ^1H -NMR

H-NMR or proton NMR is used to detect the proton alignment in a molecule. Each group of chemically equivalent protons gives rise to a signal. The protons that are in the same environment, and identical are called chemically equivalent protons. When they exposed to a magnetic field they create overlapping signals on the spectrum. Therefore, the equivalent proton sets in a molecule can be determined by looking at the number of signals in the H-NMR spectrum [151].

Tetramethylsilane (TMS) is usually used as the reference compound because it has kind of symmetry and can easily be removed from the sample by evaporation because it is a volatile compound. TMS is also at a lower frequency than most other compounds because the protons in the methyl group are in a more electron dense environment because of lower electronegativity of silicon compared to carbon atom. The positions of the signals in an NMR spectrum are determined compared to the reference substance. This position of the signals depends on the chemical shift [151].

Chemical shift (δ), is the distance of the proton signal from the reference substance. The proton chemical shifts range from 0 ppm to 15 ppm. The chemical shift for a specific proton is identical for each spectrometer used. The magnetic field was scanned from low to high values, which is from left to right. So, the signals on the right are as upfield or shielded and signals to the left called as downfield or deshielded [152].

For the calculation of chemical shift the chemical shift for base substance methylene, ethylene or methane for alkanes and addition of chemical shift caused by substituents as the adjacent atom effect. For aliphatic (sp^3) C-H proton chemical shifts the Curphy-Morrison table can be used [152].

The intensity of each signal is related with the number of protons that causes the signal. The amount of energy absorbed is proportional to the number of equivalent atoms that rises the signal [151].

The effective magnetic field is also affected by the orientation of neighboring nuclei. The spin-spin coupling effect causes splitting of the signal for each type of nucleus into two or more lines. For the splitting of the signals, N+1 rule is considered. N is the number of equivalent protons which belongs to the adjacent carbon [152].

For the ethylene group in Zoledronic acid when the effect of OH-C group and -N- chemical shifts are added, it could be found that the signal will be introduced around 4.7 [151]. An imidazole ring has doublet for adjacent H atoms around 7.4 and a single peak for the H between two N atoms and shifted more around 8.7 [153].

AGILENT (Varian) Mercury 400 FT-NMR spectrometer is used for H-NMR (400 MHz). The results are recorded with chemical shift values δ (ppm) scale with using D_2O as solvent and 3-(Trimethylsilyl) propionic acid- D_4 sodium salt as internal standard from Merck (Germany) to figure out H positions of the zoledronic acid molecule.

3.2.1.2. ^{13}C -NMR

Fundamentals of H-NMR were applicable for the ^{13}C -NMR with proton NMR spectrum. Less coupling is observed because only 1.1 per cent of naturally occurring carbon is ^{13}C . The ^{13}C NMR is directly related with the carbon skeleton not just the proton attached to it.

Different carbons or set of equivalent carbons are found with the number of signals and the splitting of a signal tells us how many hydrogens are attached to each carbon. N+1 rule is applicable here also. The chemical shift tells us the hybridization (sp^3 , sp^2 , and sp) of each carbon [151].

AGILENT (Varian) Mercury 400 FT-NMR spectrometer is used for ^{13}C -NMR (100 MHz) spectrum. The results are recorded with chemical shift values δ (ppm) scale with using D_2O as solvent and 3-(Trimethylsilyl) propionic acid- D_4 sodium salt as internal standard from Merck (Germany) to figure out H positions of the zoledronic acid molecule.



Figure 3.1. The compact ProPlus NMR system (Agilent) [154]

3.2.2. 2D-NMR Methods

2D-NMR methods performed in the study includes COSY, HSQS and HMBC spectroscopies, to observe the relations within the molecule.

3.2.2.1. *Homonuclear COSY*

Homonuclear COSY gives the mononuclear correlation, in this spectrum the two axes correspond to H-NMR results and gives proton correlation in the molecule and this information gives better understanding of structure [150].

3.2.2.2. *Heteronuclear HSQC*

Heteronuclear HSQC is Heteronuclear Multiple-Quantum Coherence and two axes correspond to 2 different isotopes (usually ^{13}C and ^1H). The interaction gives H's coupling to nuclei [150].

3.2.2.3. *Heteronuclear HMBC*

Heteronuclear Multiple Bond Correlation analysis gives correlations between carbons and protons that are separated from each other in conjugated systems, by two, three, and sometimes four bonds. Direct one-bond correlations are suppressed in these analyses. The output of this analysis is the information on connectivity like a proton-proton COSY analysis [155].

AGILENT (Varian) Mercury 400 FT-NMR spectrometer is used for 2D-NMR spectrums. The results are recorded with chemical shift values δ (ppm) scale with using D_2O as solvent and 3-(Trimethylsilyl) propionic acid-D4 sodium salt as internal standard from Merck (Germany) to figure out H positions of the zoledronic acid molecule.

3.2.3. **Mass Spectrum**

The mass spectrometer gives the molecular weight of a molecule. Usually the highest peak is the molecular ion peak. The mass spectrometer cuts a molecule into fragments, which are going to appear in the spectrum. When sample is submitted to the system an electron beam is supplied and creates a molecular ion. The ion is passed through a magnet which ends up a detector. When an ion passes through a magnet, it moves in a curved direction and hits to the detector in some point. The radius of this point is measured. This curved path is caused by a centripetal force which is the force that makes a body follow a curved path. The magnetic force of the apparatus is equal to this force. By the help of this concept, the radius is given in the below formula.

$$r = \frac{mv}{qB} \quad (3.1.)$$

The equation gives m , mass of the substance, with known values as r the radius of the path, as B the magnetic field, q is the charge and v is the velocity [156].

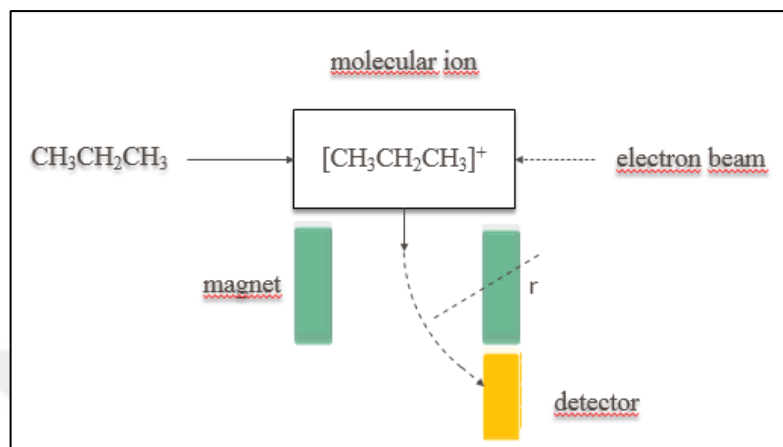


Figure 3.2. Principle of mass spectrometer

The machine gives the spectrum as relative abundance to m/q ratio. Relative abundance is representing the abundance of the charged substance when electron beaming continues. The more the charged substance is abundant, the peak in mass spectrum gets higher. When electron beaming hits to the electrons which are core electrons that is not shared as the bond, the substance gets charged. If electron beaming hits one of the bonding electrons, molecule is cut into charged fragments randomly. Each of these fragments also appears on the spectrum [156].

Waters Alliance HPLC equipment related with Waters Micromass ZQ spectrometer is used for HPLC/MS spectrums. Molecular weight is stated as $[M-H]$ by mass spectrums with negative Electro Spray method. Spectrums are categorized using two different techniques. 1) TIC (Total ion chromatogram) which is a chromatogram created by summing up intensities of all mass spectral peaks belonging to the same scan [157] and 2) SIR (Single ion resolution) (as $M-H=271$ m/z) [158, 159]. The requirement of mass spectrometer parameters are; Capillary voltage: 2.41 kV, cone voltage: 36 V, source temperature: 95°C, desolvation temperature: 350°C. Nitrogen is used as inert gas.

Chemicals used in mobile phase, acetonitrile, formic acid purchased from Merck, Germany.



Figure 3.3. Micromass Quattro Micro Mass Spectrometer [160]

3.2.4. Fourier Transform Infrared Spectroscopy (FTIR)

FTIR is used to identify materials, and assesses purity of the material. The principle of FTIR is that the most molecules absorb light in the infra-red region of the electromagnetic spectrum. This absorption corresponds to the bonds present in the molecule. In this way the information of structure of molecule is obtained. Typical frequency range for the measurement as wave numbers is $4000 - 600 \text{ cm}^{-1}$ [161].

Infrared spectroscopy principle is based on the vibrations of the atoms of a molecule. In an infrared spectroscopy, infrared radiation is passed through a sample and according to the sample nature, some light is absorbed at a particular energy. These absorptions are reflected as peaks on the spectrum. The energy at which any peak on the spectrum appears corresponds to the frequency of a vibration of the sample molecule [162].

According to the owned functional groups, FTIR is useful for identification of some particular molecule groups which have characteristic vibrational frequencies in the infra-red range such as organic groups, side chains and cross-links involved compounds. The sample is compared with the reference. The resultant absorption spectrum from the natural bond vibration frequencies indicates the presence of functional groups and various chemical bonds

presented in the sample. The sameness of the sample with the reference shows the purity of the product [161].

Shimadzu IR Affinity-1 is used during the study to identify the produced sample and the match of the sample to the reference standard.

Table 3.4. IR peaks of zoledronic acid [163]

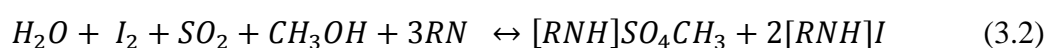
Frequency (cm ⁻¹)	Assignments	Frequency (cm ⁻¹)	Assignments
1642.26	CH=CH Stretching	1193.12	P-O Stretching
1406.52	C-H stretching	1293.62	P=O Stretching
928.41	C-C Stretching	2806.31	-CH ₂ Stretching
1586.02	C-N stretching	3204.74	-OH Stretching
1341.36	Alcohol		



Figure 3.4. Shimadzu IR Affinity-1, IR Spectrometer [164]

3.2.5. Water Content Analyses – Karl Fischer

Karl Fisher is based on the reaction of water with iodine. The reaction occurs in an alcohol medium. Methanol is most common used solvent for Karl Fischer, ethanol is also getting common recently, because it may increase the solubility of hydrocarbons [165]. The reaction is as below;



Where RN is representing a base such as pyridine or imidazole. In Karl Fisher method, as different from the other moisture loss methods, the system measures only water content, since iodine is selectively reacts with water. It is a fast, accurate and price technique. Crystal water could be determined with Karl Fisher [166].

3.2.5.1. Volumetric Karl Fisher Analysis

In volumetric technique, iodine amount added to the sample solution is calculated and volumetric measurement of water content is performed. Solids and liquids with high amounts of water content (100 ppm – 100 per cent) volumetric titrations are useful [167].

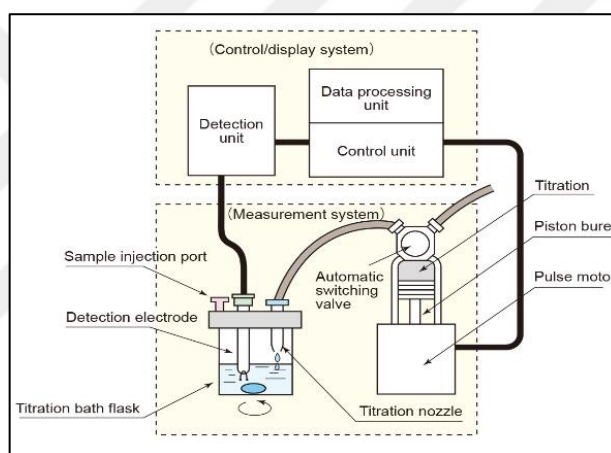


Figure 3.5. Volumetric titration details of a Karl Fischer apparatus [168]

3.2.5.2. Calorimetric Karl Fischer Analysis

Sample is dissolved in the titration cell. The reagent is released by the induction of the electrical current. The electrical current to release enough amount of solvent to react with water in the sample is calculated to find content water. The technique is useful for low amounts of water content (1 ppm to 5 per cent) [166].



Figure 3.6. Metrohm KF system, 841 Titrando [169]

Combi titrant 5; 1 ml \cong ca. 5 mg H₂O Aquastar™, including iodine and imidazole, from Merck is used as the Karl Fisher reagent for titration. Metrohm KF system, 841 Titrando is used in the analyses.

Titration medium is first placed into the cell and titrated dry by means of the titrant. Sample is loaded to the titration vessel from a weighing boat. Since for solids, which may contain water as water of crystallization, for the analysis sample preparation is important. Sample should be completely dissolved for a total water content determination. If this should not be possible in methanol, addition of chloroform, formamide or other solvents may be required [170]. To dissolve the samples, formamide and acetic acid (1:1) (v:v) is used as the solvent medium. Formamide, (Merck lot no. K44330584324), acetic acid (Merck lot no. K45178056348) is used during experiments.

30-40 ml of acetic acid, formamide mixture (1:1) is transferred to the titration vessel, and titrated with the Reagent to the electronic end point to consume any moisture that may be present. Quickly add 300 mg sample, mix for 30 sec. Then, titrated with the Karl Fisher Reagent to the electrometric endpoint.

3.2.6. Differential Scanning Calorimetry Thermal Analysis (DSC)

Differential Scanning Calorimetry (DSC) is used to measure melting temperature of the samples, to characterize the samples that has the same melting point with the reference sample. DSC is an apparatus measures the heat change during the thermal decomposition of

the samples. When we heat or cool a sample, it gives the endothermic (heat absorption) and exothermic (heat out) behavior of the sample, and gives us the quantitative and qualitative data, of which process the sample undergoes [171]. The thermal core of a DSC system consists of two cells, a reference and a sample cell. These the two cells reaches to the same temperature, as they are heated. To perform a DSC measurement, the reference cell is first filled with reference sample and the sample cell with the sample itself and heated. The absorption of heat during melting, sets up a voltage, which is converted into power and gives ΔT (the temperature differential). DSC is widely used in drug discovery and development [172].

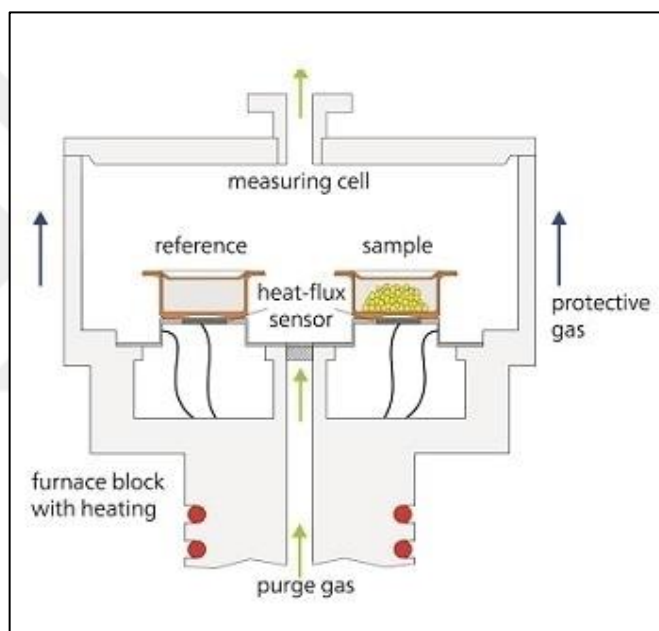


Figure 3.7. Differential Scanning Calorimeter (DSC) [172]

3.2.7. High Performance Liquid Chromatography (HPLC)

HPLC technique is used to identify the sample in a high pressurized liquid to force to sample into a column packed with stationary phase. A typical HPLC system consists of a pump (to obtain consistent flow rate), an injector or autosampler, at least one detector and to control the required system temperature of separation step, a column oven is used. A variety of detector types are available, including UV-VIS, refractive index (RI), photo diode array, and fluorescence [173].

Bisphosphonates are very strong chelators, and they readily interact with metals in the setup of production and analysis. Their affinity effect could be observable also on HPLC systems such as in injection valve or tubing or HPLC columns. Because of this the samples are giving poor peak shape and irreproducible chromatography. In order to overcome the adsorptive character of bisphosphonates, adding tailing suppressors in the mobile phase is a good approach [174, 175]. Another certain way to overcome such interactions on the setup will be use a non-metallic system [176, 177].

Considering all these, the selection of the column packing material is still critical, since the interactions with column packing material is still a case besides the chelation of bisphosphonates with metal ions. The use UV detection as the detection type is difficult for bisphosphonates because in general, most of them lack chromophore groups. But, risedronate sodium instead has a pyridinyl group, which makes it sufficiently sensitive for detection directly by UV detector. Additionally, risedronate sodium is readily ionizable in solution and, so, it can be analyzed by a liquid chromatographic technique using reversed phase conditions and used mobile phase should contain ion-pair reagents. Therefore, the type of liquid chromatography using a non-metallic system or not and detector types should be evaluated to identify different bisphosphonates [178].

For the development of analytical separation methods, several strategies have been followed mainly IEC (ion-exchange chromatography) [177] and reversed-phase liquid chromatography (RPLC) [175] often in combination with an ion-pairing agent.

Optimization of separation conditions of the test mixture of two bisphosphonates was carried out in three stages: (a) choice of the complexing agent concentration; (b) determination of the optimal composition of the mixed mobile phase (organic compound-buffer) and (c) effect of mobile phase pH [179].

3.2.7.1.HPLC Parts

3.2.7.1.1. Mobile Phase

The mobile phase is a liquid that moves through the packed bed of stationary phase in the column under pressure.

It is the mixture of organic and aqueous solvents and is more polar than stationary phase [181].



Figure 3.8. Shimadzu HPLC systems [180]

3.2.7.1.2. Organic carrier

Acetonitrile and methanol are usually used common carriers mixed with other solvents to compose the mobile phase. Acetonitrile has lower viscosity - reduces back pressure and often results in slightly better peak shape and has lower UV cut-off - advantage for UV detection. Methanol is used because it is less expensive, less toxic and is more polar to reduce the risks of solid buffer precipitation [181].

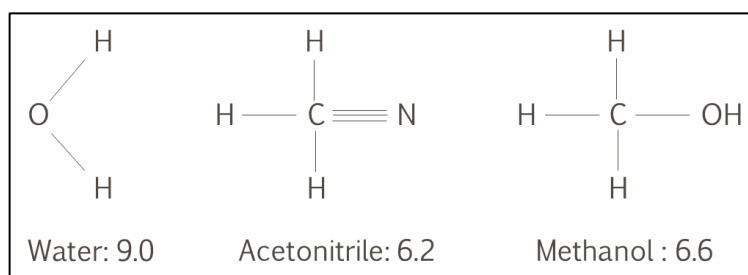


Figure 3.9. Polarity of solvents commonly used to compose mobile phase

Replacement of methanol with acetonitrile led to lower k values and even to shorter analysis time. However when methanol was used the chromatographic peaks could be much more deformed [182, 180].

3.2.7.1.3. *Effect of pH*

Bisphosphonates belonging to quadribasic acids having several pKa values that capable of forming multiply charged ions in solution. Therefore, the pH level of mobile phase is very important parameter in the ion-pair HPLC for analysis of bisphosphonates because of the significant effect on the retention behavior and peak shape. Ionisable species need to employ pH control. The retention factor of test mixture compounds were measured for different eluent pH (5–8.5) at the constant concentration of ion-pairing modifying agents [180].

3.2.7.2. *HPLC Assay Method for Zoledronic Acid*

3.2.7.2.1. *1st HPLC Method*

In the firstly validated method, Shimadzu LC-20AT is used as the apparatus. C18, 250 x 4.6 mm, 5 μ column with 20 °C column temperature and UV, λ : 215 nm detector is used. Flowrate is 1.5 ml/min with injection volume of 10 μ l. Isocratic pump is used. Perchloric acid solution was prepared with 10 ml of 70 per cent perchloric acid and 2 ml ortho-phosphoric acid in water. Buffer solution was prepared as including 50 mM octane sulphonic acid sodium salt solution / 0.1 mM ethylenediamine tetra acetic acid disodium salt (in perchloric acid solution). Mobile phase is 960:40 v/v mixture of buffer:acetonitrile. Mixture is prepared and used after filtered through 0.45 μ m membrane filter.

Zoledronic acid standard solution is prepared as having 0.4 mg/ml zoledronic acid monohydrate reference standard, by weighing the standard and dissolving with mobile phase by the help of magnetic stirrer and injected after filtered through 0.45 μ m syringe filter.

Test Solution is prepared as 0.4 mg/ml zoledronic acid monohydrate sample; by weighing the sample dissolving with mobile phase by the help of magnetic stirrer and injected after filtered through 0.45 μ m syringe filter.

10 μ l sample and standard solutions are injected to the column and the peaks are recorded.

Calculations for assay is made by the help of sample and standard areas;

$$\text{Assay} = ((r_u/r_s) \times (C_s/C_u)) \times 100 \times \text{Potency} \quad (3.2)$$

Where, r_u is the peak area of zoledronic acid monohydrate in test solution, C_s is concentration of standard of zoledronic acid monohydrate, r_s is peak area of zoledronic acid monohydrate in standard solution and C_u is the concentration of sample of zoledronic acid monohydrate. By using this method zoledronic acid is detected around 10.8th minute. Limit is chosen as 98.0-102.0 per cent.

3.2.7.2.2. 2nd HPLC Method

An alternative method is validated to detect any possible impurities. Shimadzu LC-2030C is used as the apparatus. 250 x 4.6 mm, 5 μ m ODS-3V Inertsil column with 30 °C column temperature and UV, λ : 215nm detector is used. Flowrate is 0.7 ml/min with injection volume of 10 μ l. Isocratic pump is used.

Ethylenediamine tetra acetic acid solution is prepared as the mixture of 5 ml of 2 M sodium hydroxide solution is added to 1 M ethylenediamine tetra acetic acid solution. Mobile phase is prepared as; weighing 0.035 moles disodium hydrogen phosphate dehydrate and 0.01 moles tetra-n-butyl ammonium hydrogen sulphate mixing with 900 ml distilled water, 100 ml methanol and 2 ml of ethylenediamine tetra acetic acid solution. pH of the mobile phase is adjusted to 7.9 and the solution is filtered through 0.45 μ m syringe filter. Distilled water is used as the diluent.

Zoledronic acid standard solution is prepared as; weighing approximately 43 mg zoledronic acid monohydrate USP standard (equivalent to 40 mg zoledronic acid) and by transferring to 50 ml volumetric flask and completed to volume with the diluent and injected after filtered through 0.45 μ m syringe filter. (c. 0.8 mg/ml zoledronic acid monohydrate).

Test solution is prepared as; weighing approximately 43 mg zoledronic acid monohydrate sample (equal to 40 mg zoledronic acid) and transferring to 50 ml volumetric flask and completed to volume with the diluent and injected after filtered through 0.45 μ m syringe filter. (c. 0.8 mg/ml zoledronic acid monohydrate).

10 μ l sample and standard solutions are injected to the column and the peaks are recorded.

Calculations for assay is made by the help of sample and standard areas;

$$\text{Assay} = (R_n / R_s) \times (W_s \times P \times 100 / W_n \times (100 - S_n)) \times 100 \quad (3.3)$$

Where, R_n is the peak area from the sample solution, R_s is the peak area from the standard solution, W_s is the weight of zoledronic acid to prepare the standard solution, W_n is the weight of zoledronic acid for sample solution, P is the potency of the standard (as is basis), and S_n is the water content potency of the sample. By using this method zoledronic acid is detected around 16.6th minute. Limit is chosen as 98.0-102.0 per cent. Other methods used in the literature for the assay of zoledronic acid are summarized in Table 3.5.

Table 3.5. Different HPLC Assay Methods for Bisphosphonates

Reference	Column type	Detector, Wavelength, nm	Flowrate, ml/min	Injection Volume, μ L	Column Temp., $^{\circ}$ C	Injection Time, min	Mobile Phase
Prasad et al. [183]	Intersil ODS column (250 x 4.6 mm, 5 μ L)	UV, 215 nm	0.8	5	50 $^{\circ}$ C	15 min	phosphate buffer pH 7.2 \pm 0.005 and methanol 900:100 v/v
Shanmugasundaram et al. [184]	Hypersil silica (C18 250 x 4.6 mm, 5 μ)	UV, 215 nm	1.1	20	30 $^{\circ}$ C	10 min	triethylamine buffer pH 3: acetonitrile (50:50)
Reddy et al. [185]	Chromosil column (250 x 4.6 mm, 5 μ m)	UV, 210 nm	1.0	15	50 $^{\circ}$ C	15 min	phosphate buffer pH 7-7.5 and methanol 900:100 v/v
Mastanamma et al. [186]	ODS reverse phase column (250 x 4.6 mm, 5 μ m)	UV, 210 nm	0.8	20	25 $^{\circ}$ C	15 min	phosphate buffer pH 3 and methanol (60:40)
Aluoch et al. [179]	Zorbax Eclipse XDB C18 150 x 4.6 mm, 3.5 μ m)	UV	1.0	25	22 $^{\circ}$ C	-	buffer and acetonitrile 90: 10 (v/v) pH 7.5
Nandan [187]	Allsep1 anion exchange column, 150 4.6 mm i.d, 7 μ m	UV, 215 nm	0.7	20	60 $^{\circ}$ C	20 min	-
Nandan et al. [188]	Inertsil ODS-3 V, 250 4.6 mm i.d, 5 μ m,	UV, 215 nm	0.8	50	50 $^{\circ}$ C	-	phosphate buffer pH 7.2 and methanol 900:100 v/v

3.2.8. Thermogravimetric Analysis (TGA)

TGA measures the samples weight under heating and controlled environment and gives the variation of weight with changing of temperature. TGA apparatus consists of a sample pan,

with a precision balance. This pan is inserted in a controlled environment and mass change is monitored during the experiment. A sample purge gas controls the sample environment. [189].

The Pyris 1 TGA from PerkinElmer is used during the study. The analysis is used mainly quantify loss of water, loss of solvent, loss of plasticizer, decarboxylation, pyrolysis, oxidation, decomposition, weight per cent filler, amount of metallic catalytic residue remaining on carbon nanotubes, and weight per cent ash [189]. Besides decomposition temperature, TGA analyses purposed to measure the water loss of zoledronic acid as a monohydrate molecule.



Figure 3.10. Pyris 1 TGA, PerkinElmer [190]

3.2.9. Melting Point

The melting point measurements are performed according to European Pharmacopeia 9.0 2.2.14. The capillary method is used to detect the temperature at which the last solid particle of a substance in a compact column passes into the liquid phase.



Figure 3.11. Stuart SMP 40 melting point apparatus [191]

Stuart SMP 40 Melting point apparatus is used during the experiments. The sample is introduced into a capillary tube compactly at about 4 mm to 6 mm in height and inserted into the machine. The temperature of the bath increased at a rate about 1 °C/min and the temperature at which the last particle passes into the liquid phase is recorded [192].

3.2.10. Exergy Methods

In order to calculate the energy and exergy of the reaction, the first and the second laws of thermodynamics are employed. The restricted dead state was chosen as the thermomechanical state of the inlet streams, heat capacity of each species were calculated from the Kopp's rule, and then the mass (1), energy (2) and the exergy (3) balances are formulated as:

$$\sum(N)_{in} - \sum(N)_{out} = 0 \quad (3.4)$$

$$\sum(N_i h_{f,i}^0)_{in} - \sum(N_i (h_{f,i}^0 + c_{p,i}(T - T_0)))_{out} = Q - W \quad (3.5)$$

$$\sum(N_i [e_i^{ch} + (h_{f,i}^0 + c_{p,i}(T - T_0) - T_0 [s_i^0 + c_{p,i} \ln \frac{T}{T_0} - R_u \ln x_i])])_{in} - \sum(N_i [e_i^{ch} + (h_{f,i}^0 + c_{p,i}(T - T_0) - T_0 [s_i^0 + c_{p,i} \ln \frac{T}{T_0} - R_u \ln x_i])])_{out} + Q \left(1 - \frac{T}{T_0}\right) - W = X_{destroyed} \quad (3.6)$$

Chemical exergies as e_i^{ch} , standard molar entropy (kJ/mole K) of each species, s_i^0 , enthalpies of each species as $c_{p,i} \ln \frac{T}{T_0}$, and mole fractions as x_i are employed in equation 5.3. Chemical exergies are calculated from:

$$ex_{ch}^0 = \Delta g_f^0 + \sum_{i=1}^N n_i ex_{chem,i}^0 \quad (3.7)$$

$$ex_{ch}^0 = \sum_{i=1}^N n_{repeating\ units} ex_{chem,repeating\ unit}^0 \quad (3.8)$$

Values of ΔG are calculated using the group contribution method when the data were not available in the literature. Thermodynamic data are presented in Table B.2 and Table B.5, where ex_{ch}^0 represent standard chemical exergy, n is the number of moles and Δg_f^0 is the standard Gibbs free energy of formation.

Each step of the zoledronic acid synthesis (Table B.1 and Table B.2) and the injectable finished solution production process is assessed thermodynamically in Table B.3 and Table B.4. When thermodynamic data were not readily available in the literature, group contribution method was used for its estimation. Energy utilizations of the process equipment were obtained from the data given in the equipment specification sheets.

3.2.10.1. Thermodynamic Analysis

The cumulative degree of perfection (CDP) is calculated to evaluate the efficiency as the ratio of the exergy of the product to exergy of the total input including the exergy of the raw materials and the fuels.

$$\eta_b = \frac{(mb)_{products}}{\Sigma(mb)_{raw\ materials} + \Sigma(mb)_{fuels}} \quad (3.9)$$

where $(mb)_{raw\ materials}$ is the exergy of raw materials supplied to the system, $(mb)_{fuels}$ is the exergy of any fuel (including electricity or natural gas, etc.) supplied to the system and $(mb)_{products}$ is the exergy of the product obtained at the end of the process.

In CDP calculations, the raw materials added to the process are evaluated as chemical exergies and physical exergies. Physical exergies are calculated according to the condition of each stream such as temperature and mole fractions, at which specific material is supplied to the process (Table B.2).

4. EXPERIMENTAL STUDIES

4.1. SYNTHESIS METHOD

In literature there are different methods for bisphosphonate synthesis. BPs have been prepared mainly by reaction of a carboxylic acid with phosphorous acid and halo phosphorus compounds such as phosphorus trichloride (Figure 4.1), phosphorus pentachloride, or phosphorus oxychloride, by alkylation of tetraalkylmethyl bisphosphonate and related compounds [193], by Michael type addition to tetraethylethylidene bisphosphonate [194], by [3+2] cycloaddition [195], and by reaction of an acylphosphonate with a dialkyl phosphite in the presence of a catalytic amount of base [196].

The most expedient method for the preparation of 1-hydroxybisphosphonates, and the method reported for the preparation 4-amino-1-hydroxybutylidene-1,1-bisphosphonic acid, is the reaction of 4-aminobutyric acid (GABA) with phosphorus trichloride and phosphorous acid (Figure 4.1) [197].

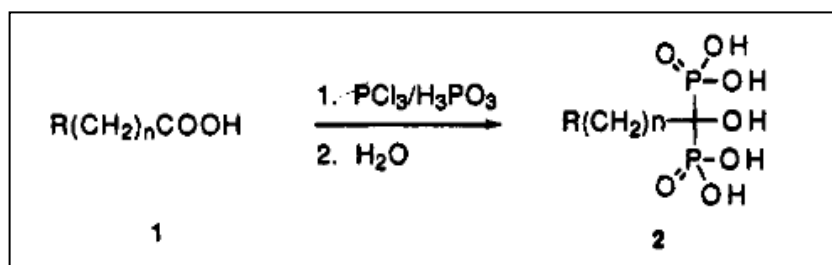


Figure 4.1. Synthesis reaction of zoledronic acid by phosphorylation [197].

1-H-imidazole-1-acetic acid hydrochloride will be phosphorized by phosphoric acid and PCl_3 and crude zoledronic acid will be synthesized. This product will be further purified to obtain the monohydrate form. After the production trials in the lab scale, pilot facility will be established and commercial batches will be produced.

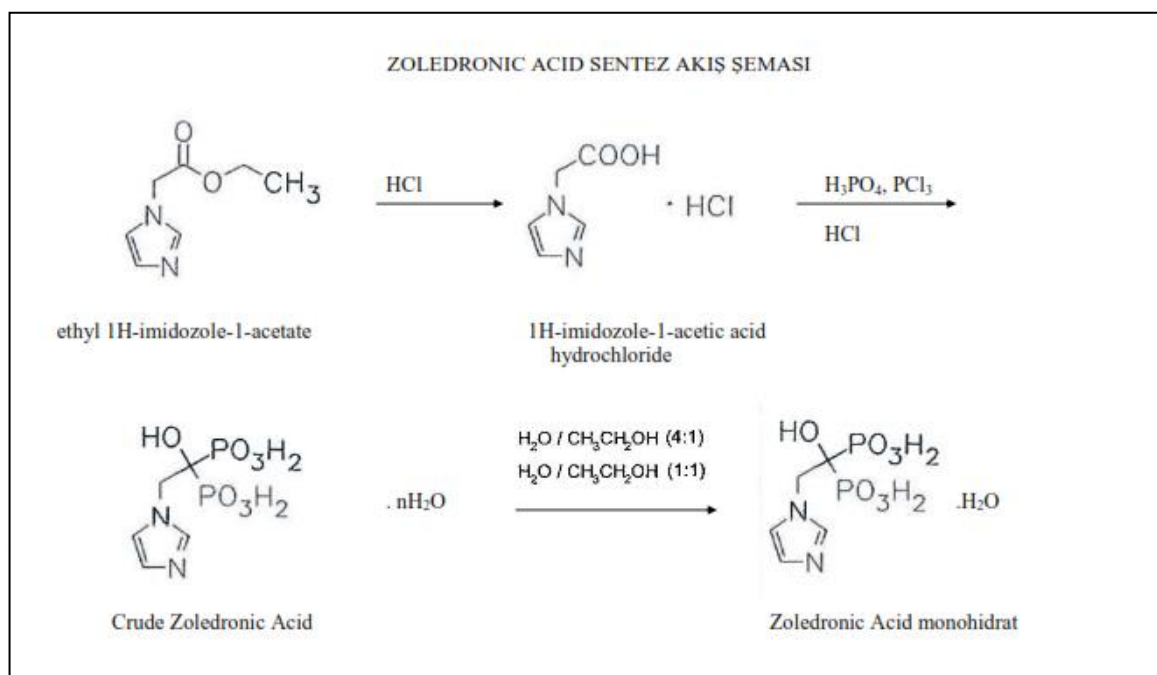


Figure 4.2. Flow chart for zoledronic acid synthesis [198]

Several experiments were carried out to optimize the reaction conducted for the synthesis of zoledronic acid. After each experiment chemical analyses such as determination of melting point, HPLC assay and IR spectra were performed. In this section experiment procedures are presented with the chemical analysis in order to explain why certain strategies are followed.

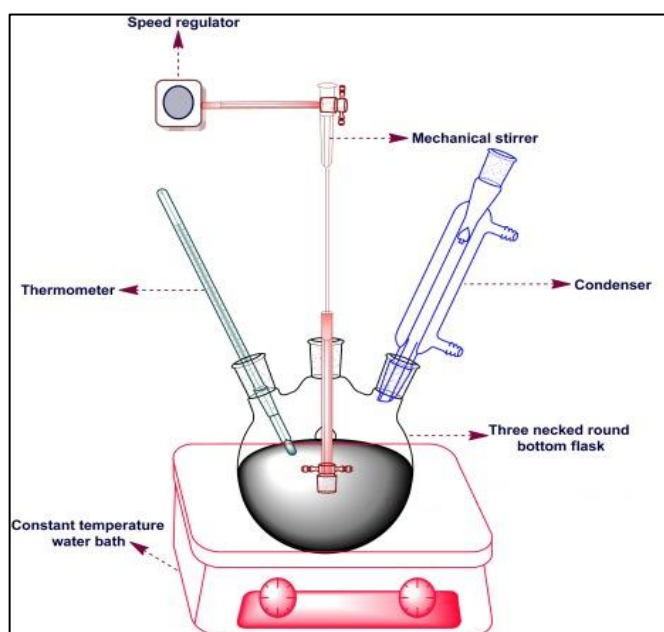


Figure 4.3. Schematic representation of reaction set up [199]

A 2 L three neck round reaction flask, equipped with a thermometer to monitor temperature during synthesis and reflux condenser to control gas output is used. Since the phosphorylation reaction medium is a dense liquid, for 2 L volume flask mechanical stirrer is used for more proper and homogenous stirring. For heating or cooling of reaction medium a water bath is used. To reach high temperatures for example 100 °C a hot plate is used. Schematic representation of reaction set up is given in Figure 4.3. The synthesis reaction was carried out under fume hood, because of some volatile reactants such as PCl_3 and released corrosive gases during the reaction such as HCl.

4.1.1. Reaction in Chlorobenzene with Phosphoric Acid

4.1.1.1. 1st Experiment

17.2 g (0.105 mol) Imidazol 1-yl- Acetic Acid HCl (starting material) and 24.5 mL (0.25 mol) o-Phosphoric Acid (85 per cent) (phosphorylating agent) are weighed and mixed with 50 ml chlorobenzene (solvent) in a three neck volumetric flask. Reaction mixture is heated to 100 °C with hot plate. 27.8 ml (0.319 mole) PCl_3 is dropwise added to the reaction mixture. HCl gas generation and foaming is observed once PCl_3 is added. A viscous mixture is obtained and the color turned yellow. Total PCl_3 addition span a total of 1.5 hours and a viscous precipitate is observed, which stuck to the walls of the flask, therefore the experiment was discontinued with further testing.

4.1.1.2. 2nd Experiment

In order to overcome the issues about handling the viscous reaction mixture, the amounts of all chemicals are doubled. Again, a yellow viscous mixture is obtained after PCl_3 introduction over 1.5 hours, followed by further mixing of another three hours. At the end of the reaction, the viscous precipitate and its upper phase is separated by decantation.

80 ml of 9 N HCl is added to the viscous precipitate and the mixture is stirred mechanically for three more hours. With the addition of HCl, an orange solution is obtained. To remove the impurities, 30 g absorbent is added to the reaction mixture and stirring is continued for 30 more minutes. The solution is filtered using Nutsche and the filtrate is taken. To

precipitate zoledronic acid out of the reaction solution, a solvent in which ZA is insoluble is used as a precipitating agent. Both acetone and ethanol are potential candidates, however in industrial scale, ethanol is safer so for the first trial 140 mL ethanol is used.

Once the filtrate is cooled to 25-30 °C, ethanol is added, however precipitation is not observed. Ethanol is removed from the medium with distillation and acetone is used to precipitate the solid. A white powder is obtained which is filtered through Nutsche, and left to dry in a vacuum oven.

4.1.1.3.3rd Experiment

Initially, 29 ml o-Phosphoric Acid (85 per cent) is mixed with 125 mL chlorobenzene and 30 g Imidazol 1-yl- Acetic Acid HCl is added after which the reaction mixture is heated to 60 °C. 55.6 ml PCl_3 is added dropwise over 2-2.5 hours. Similar to the first trial HCl gas generation is observed but the solution color was remained colorless and so throughout the reaction. In this trial, temperature range of the reaction is reduced to 60-70 °C and PCl_3 addition period is increased to 2 hours. The reaction is further mixed for six hours.

The temperature increased to reflux temperature ($T=100$ °C) upon addition of 160 ml 9 N HCl and the reaction is mixed another five hours. Once the reaction is cooled to 30 °C, upper phase is separated with decantation. Absorbent is added to this upper phase and filtered from Nutsche. Since it is very acidic solution pump speed of Nutsche apparatus kept at lowest degree. A clear solvent is obtained.

For the precipitation of Zoledronic acid acetone (350 ml) is added and the solution is mixed for 2 hours however, precipitation is not observed.

The amount of acetone was doubled (700 ml) and the solution is mixed for one more hour. White solid crystals precipitated out of the solution. Precipitate is filtered from Nutsche and dried in the oven at 40 °C for one hour. 4.40 g of a product is obtained, which was not zoledronic acid as easily dissolved in the water.

As the reaction does not proceed to form the desired product, a more effective phosphorylation agent, phosphorous acid is chosen for the next experiment. Also, methane

sulphonic acid is used as an alternative solvent to overcome the homogeneity problems at low temperatures, to allow the reaction to be carried out at lower temperatures.

The reference, US4621077 [200], which gives method for alendronic acid and neridronic acid synthesis, explains chlorobenzene usage in the synthesis as the solvent similar to US4939130 [201] for zoledronic acid. Using this solvent gives solid and unstirrable masses during the reaction. Some of other patents [200, 202, 203, 204, 205] suggesting the use of chlorobenzene as reaction solvent, however the same drawback described above is again experienced. Because of this drawback US4922007, US5019651 [206, 207] and US5510517 [208], as well as WO 2003093282 [209], suggests the use of methane sulphonic acid as reaction solvent, therefore in the next experiment methane sulphonic acid is used. Considering patent references and low yields obtained with phosphoric acid, phosphorous acid is used as phosphorylating agent for the next experiments. In methane sulphonic acid experiments phosphorous acid is used in the literature [206, 207, 208, 209], so second reactant is chosen as phosphorous acid in the following experiments.

4.1.2. Reaction in Methane Sulphonic Acid with Phosphorous Acid

4.1.1.4.4th Experiment

0.3 moles Imidazol 1-yl-acetic acid HCl and 0.6 moles Phosphorous Acid (98 per cent) are weighed and mixed with 2 moles methane sulphonic acid (99 per cent) (solvent) in a three neck volumetric flask. Reaction mixture is heated to 60 °C in a water bath. 1 mole PCl_3 is added dropwise at 60 °C for 5 hours. Mixing of the solution continued for 15 hours. The solution became a yellow dense liquid and have a unique odor suggesting that phosphorylation took place.

4.1.1.4.1. Filtration

We use water-absorbent mixture to filtrate the solution. The solution is mixed for half an hour and is filtrated from Nutsche. 200 ml NaOH (30 w/w per cent) solution is added gradually, while the temperature is kept at 40 °C in a cold water bath. 245 ml Ethanol (96

per cent) is added to the mixture and crystallization is observed. Upon mixing, the crystals dissolved and mixing is continued for three hours until a clear precipitation of solid is observed. Temperature is lowered to -2 to -7 °C with salted ice bath. The solution is further mixed for three hours to help precipitation. The crystallized solid is collected by filtering from Nutsche.

4.1.1.4.2. Crystallization

For purification of zoledronic acid different methods are encountered in the literature. WO 2004075860 [210] gives water crystallization technique. Similarly, US8193355 [211] explain the crystallization as mixing the precipitated solid with purified water and dissolving the solid at an elevated temperature; cooling the solution for crystallization; and filtering and vacuum drying of the crystallized product.

Crystallization temperature used for the dissolution of zoledronic acid determines the particular polymorphic form of zoledronic acid. In case of the solution heated to higher temperatures to about 90 to 95° C, the crystalline monohydrate is produced. [212]

Time for the recrystallized mass to reach room temperature may range from 1 to 20 hours, depending on the size of the batch being processed. There is no disadvantage to further extending the cooling period, if not resulting in an increase in processing expense, where a suitable time for a batch size can be experimentally determined. The cooling of the solution could be simply achieved by radiation cooling in atmospheric conditions, together with stirring, or controlled cooling mechanisms could be used such as jacket vessels or similar like cold water bath [213].

The crystallization may be performed with stirring at ambient or reduced temperatures such as about 20° C to 25° C or lower until the desired crystal yield has been obtained, in a time range from one hour to about 72 hours. The crystallization step could include cooling or heating the solution furtherly, or inducing precipitation by adding an agent. Recovery of the isolated solid can be performed by filtration, centrifugation, and decanting [212].

According to US20060178439, the obtained compound can be dried furtherly under ambient or reduced pressures. Drying under pressure at a temperature of between 40° C- 80° C, or

even higher. Drying can be performed from about 2 hours to 24 hours until a required residual solvent content has been obtained [212].

In this experiment, in crystallization step, 15 g of zoledronic acid crystals are dissolved in 300 ml water. Crystallization is achieved by mixing the solution for two hours at 90 °C, followed by cooling down to 25-30 °C with a water bath mixing for two hours at this temperature. At 70 °C precipitation is observed. The obtained solid is filtrated from Nutsche and washed with water again. The solid material is obtained at the end of process is approximately 10 g. Crystals are then dried in an oven at 60 °C for 12 hours.

4.1.3. Effect of Temperature

4.1.3.1. 5th Experiment

The same experiment repeated with slightly lower temperature 58 °C. The yield of synthesis was low (around 40 per cent). The low yield temperature below 60 °C suggests that the reaction should be carried out above 60 °C.

However, the reaction temperatures should not exceed 65° C in extreme levels. Since the reaction becomes self-heating above 85° C, and the temperature will increase steadily under adiabatic conditions. [206, 213]

4.1.3.2. 6th Experiment

Based on previous results, the experiment was repeated at 60-65 °C. It is observed that the yield increased to 60 per cent.

4.1.4. Method of Crystallization

4.1.4.1. 7th Experiment

Now the reaction conditions are optimized. The same synthesis method is used with experiment 7th and amounts of reactants are increased to optimize crystallization methods.

Trials were performed to increase the crystallization yield and purity of product.

4.1.4.1.1. First Crystallization Trial

Crystallization is performed with 1:30 (solid : water). Zoledronic acid is dissolved at 90-95 °C with hot plate and mixed for two hours, followed by hot filtration to separate any foreign material. The solution is cooled down to 25-30 °C with water bath and mixed at this temperature for 2 hours. The mixture is filtrated from Nutsche and the precipitate is washed with water and put in a vacuum oven at 50-60 °C.

4.1.4.1.2. Second Crystallization Trial

Crystallization is performed again in 1:30 (solid : solvent) ratio this time solvent being water / ethanol mixture (1: 1). The crystallization solution is heated to 58-62 °C and mixed for two hours. In this trial Zoledronic acid is suspended in the solution, not completely dissolved in this conditions. The solution is separated into two when hot in order to examine the cooling effect on precipitation of the product. The first part is cooled down to 25 °C and filtrated.

The second part is cooled down to 25 °C mixed for two hours and cooled to 0 °C, mixed at this temperature for 2 hours and filtrated. The precipitated ZA samples are dried for 15 hours in vacuum oven.

4.1.4.1.3. Third Crystallization Trial

Crystallization is performed with water, (solid : water ratio 1:15). ZA is dissolved at 90-95 °C and mixed for two hours and filtrated hot from Nutsche to get rid of foreign particles.

When hot, solution was separated into two parts, to examine the effects of addition of ethanol on the precipitation of the product.

Second half is cooled down to 25 °C. 3:1 (water : ethanol) is added and then cooled down to 0 °C within 2 hours, mixed at this temperature for 2 hours and filtrated. Filtrate is dried for 15 hours in oven.

4.1.4.1.4. Fourth Crystallization Trial

Using water : ethanol in 1:1 ratio for crsytallization let to incomplete dissolution of the synthesised product, 4:1 water : ethanol ratio is also tried. This time zoledronic acid is dissolved at 78-80 °C and mixed for two hours and cooled down to 25 °C further mixing for 2 hours. Then, the solution is cooled down to 0 °C and mixed for another 2 hours at this temperature, followed by cold filtration. The precipitate is dried in vacuum oven for 12 hours.

4.1.4.2. 8th Experiment

The experiment is repeated with the established crystallization method, where water is used to dissolve zoledronic acid at 90 °C and ethanol water (1:3) is used for precipitation in cold media.

4.1.5. Effect of pH

4.1.5.1. 10th and 11th Experiments

Effect of change in pH is experimented with parallel experiments. The yield found was lower for lower pH value. The same experiment carried out at pH 1 lead to the precipitation of a product that was not zoledronic acid.

4.1.6. Excess of Halo Phosphorous Compound

4.1.6.1. 12th Experiment

In 12th experiment excess amount of halophosphorus compound, ie. PCl_3 is used where instead of 1: 3 carboxylic acid: halophosphorous ratio, excess PCl_3 is at 1:4.5 ratio is employed [214]. No yield difference is observed, so the ratio 1:3 kept as optimum amount for this reactant.

4.1.7. Excess of Phosphorous Acid

4.1.7.1. 9th Experiment

The experiment is repeated with excess amount of phosphorylation agent (25 per cent excess) where carboxylic acid: phosphorous acid ratio is increased 1:2 to 1:2.5.

4.1.7.2. 13th Experiment

Phosphorylation agent is used with increased excess amount (50 per cent excess) and having molar ratio of 1:3.

4.1.8. Reproducibility

4.1.8.1. 14th, 15th, 16th Experiments

Three production trials are repeated as validation batches. Synthesis yield increased from 30 per cents to 50 per cent at the end of the trials. Analytical tests is performed according to the methods Materials and Methods in Chapter 3. Purity results are found in the range of 98-102 per cent in HPLC. The finally accepted procedure have the details described below.

Reactants are mixed as 0.6 moles 1H imidazole-1-yl-acetic acid HCl and 0.9 moles phosphorous acid, in 4 moles methane sulphonic acid. Heated up to 65 °C. 2 moles of

phosphorous trichloride is added dropwise at this temperature and the reaction occur during 15 hours. Filtrant is given at 75 °C and the solution is filtered hot from Nutsche. Filtrate is cooled to adjust the pH with NaOH (30 per cent NaOH solution) to 0.6-0.8. At 20 °C, 4.1 moles ethanol added to precipitate zoledronic acid as solid. Reaction solution is mixed for about 2 hours at 20 °C and cooled to minus degrees and mixed at this temperature after which the solid is filtrated by the help of Nutsche. Crude zoledronic acid is crystallized in water (1 ZA: 20 water) and precipitated by the effect of ethanol (with water : ethanol ratio of 3:1).



5. RESULTS AND DISCUSSION

5.1. EXPERIMENTAL RESULTS AND DISCUSSION

Experiments for synthesis of zoledronic acid are designed to increase the production yield while keeping the purity level high. For this, reactant amounts, reaction medium and temperature as critical parameters for phosphorylation reactions are modified.

5.1.1. Reaction in Chlorobenzene with Phosphoric Acid

5.1.1.1st Experiment

Using chlorobenzene as the solvent causes a viscous precipitate, which was hard to mix and stuck to the walls of the flask, therefore the experiment was discontinued with further testing.

5.1.1.2. 2nd Experiment

Using double amounts of reactants and the solvent helped dealing with the sticky solution. Acetone and ethanol are used commonly to precipitate the zoledronic acid as solid from the reaction solution. Ethanol is safer and chosen as the first choice but no precipitation is observed. Ethanol is removed from the medium with distillation and acetone is used to precipitate the solid. A white powder is obtained which is filtered through Nutsche, and left to dry in a vacuum oven.

The melting point of the product was found as 210 °C using capillary method according to EP 9.1 - 2.2.14 (Stuart SMP 40), where the MP of the reference material is 244 °C. Zoledronic acid is sparingly soluble in water (25 °C), whereas the synthesized product dissolves easily in water. Based on these results, the reaction conditions were considered unsuitable no further analysis was performed and a modified procedure is employed.

5.1.1.3. 3rd Experiment

With excess PCl_3 and prolonged reaction period (from 3 h to 6 h) and prolonged PCl_3 addition period (2-2.5 hours) temperature range of the reaction is reduced to 60-70 °C a clear solvent is obtained at the end. For the precipitation of zoledronic acid acetone (350 ml) is added and the solution is mixed for 2 hours however, precipitation is not observed.

When the amount of acetone was doubled (700 ml) and the solution is mixed for one more hour solid crystals precipitated out of the solution.

MP of the product is found to be 210 °C, which is lower than that of the desired product.

Table 5.1. IR spectral data of zoledronic acid

Frequency (cm^{-1})	Assignments
1642.26	CH=CH Stretching
1193.12	P-O Stretching
1406.52	C-H Stretching
1293.62	P=O Stretching
928.41	C-C Stretching
2806.31	-CH ₂ Stretching
1586.02	C-N Stretching
3204.74	-OH Stretching

IR analysis performed for that sample. The unique peaks for zoledronic acid are represented in Table 5.1 [163]. The obtained product is found not zoledronic acid observing not similarity to the reference material. HPLC analysis therefore was not performed and this synthesis method was also classified as unsatisfactory.

As the reaction conditions are found hard to deal, challenging crystallization and giving a low yield product, other phosphorylation agents and reaction medium are questioned. Phosphorous acid is also used commonly as phosphorylation agent and which was found more efficient. Methane sulphonic acid is used recently as an alternative solvent to overcome the homogeneity problems at low temperatures, to allow the reaction to be carried out at lower temperatures in bisphosphonate synthesis. The experiments then continued with phosphorous acid as phosphorylation agent and methane sulphonic acid as the solvent.

5.1.2. Reaction in Methane Sulphonic Acid with Phosphorous Acid

5.1.2.1. 4th Experiment

By using methane sulphonic acid, the problems regarding with the sticky reaction mixture is overcome. The reaction also performed moderately lower temperatures (65 °C). Longer period of PCl_3 addition also helped to phosphorylation, because of that addition period is prolonged to 5 hours. An orange-yellow colored dense liquid obtained at the end with a smell unique to phosphorous compounds. Ethanol is used as precipitation agent, and with the addition of ethanol, a white solid starts to precipitate immediately.

Solid material is 26.8 g (a yield of 54 per cent). Obtained solid is tested for melting point and found as 244 °C, which is the same as the reference standard of zoledronic acid.

In this experiment, crystallization in water is experienced. Crystals obtained are zoledronic acid monohydrate with the water content of 7.1 per cent. Crystallization yield is 0.67 per cent. IR results (Figure A.1) shows 0.99 fit with the USP standard. Comparability percentage gives how similar two substances are.

HPLC analyses are performed as explained in the Materials and Methods in Chapter 3. Two runs are performed and a mean result is considered on anhydrous basis (Figure A.2 and Figure A.3). So results in the appendix are corrected with the water content found in Karl-Fischer analysis. In this trial the water content is found to be 7.1 per cent (Figure A.4). The result meets the monohydrate limit. Assay as purity is in total 99 per cent when compared with the USP standard.

Results of analysis for identification and purity for experiment 4th approved that the obtained product is pure zoledronic acid monohydrate.

5.1.3. Effect of Temperature

5.1.3.1. 5th Experiment

The same experiment repeated with slightly lower temperature 58 °C, to show if lower temperature ranges are possible for the reaction. The yield of synthesis was low (around 20 per cent) and that purity was low showing the reaction is not accomplished well. The results at temperature below 60 °C suggests that the reaction should be carried out above 60 °C.

5.1.3.2. 6th Experiment

Based on previous results, the experiment was repeated at 60-65 °C. It is observed that the yield increased to 60 per cent. IR result of 6th experiment suggested 0.99 fit with the reference (Figure A.5). HPLC analyses performed with the alternative method described in the Materials and Methods in Chapter 3. Mean result suggests, 90.59 per cent purity on as is basis considering zoledronic acid in monohydrate molecule (Figure A.6 and Figure A.7). TGA analysis is applied to analyze the water content giving 8.15 per cent weight loss. Considering this result molecule is a monohydrate and assay result gives 98.62 per cent as monohydrate molecule. TGA curve obtained is not a smooth curve. The gradual water loss could be because of the surface water or any remained solvents.

The structural tests are also done for experiment 6th, since the synthesis method is consistently giving the same quality comparable with the reference standard.

5.1.3.2.1. Structural Tests

To validate the structure of zoledronic acid that we get at the end of first trials we made NMR, 2D- Homonuclear COSY Spectrum, 2D-Heteronuclear HSQC Spectrum, 2D-heteronuclear HMBC Spectrum, mass spectrum in Ankara university. We use standard of Zoledronic acid firstly to compare with our synthesized product.

5.1.3.2.1.1. *NMR Analyses*

Nuclear magnetic resonance spectroscopy became the superior technique for determining the structure of organic compounds. For NMR complete analysis and interpretation of the entire spectrum is expected. Using NMR as an analytical tool correctly, it is necessary to understand on which principles the methods are based. NMR and Mass Spectrums were conducted after zoledronic acid was converted to ammonium salt with ammonium hydroxide.

5.1.3.2.1.2. *¹H-Proton NMR Spectrum*

Proton NMR (also Hydrogen-1 NMR, or ¹H NMR) is used to determine the structure the molecules of a substance as an application of nuclear magnetic resonance in NMR spectroscopy with respect to hydrogen nuclei [215].

H atoms in the molecule are found comparing with reference standard and literature references. There are few samples of references which studied zoledronic acid before and their results are given in Table 5.2. Proton numbers are given according to Figure 5.1.

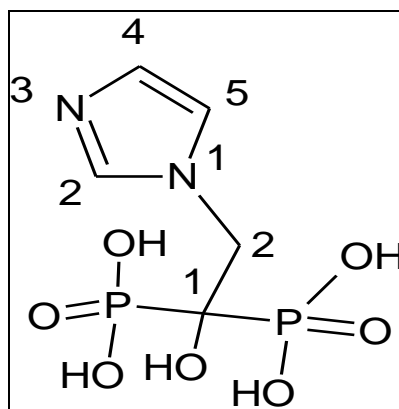


Figure 5.1. [1-Hydroxy-2-(1H-imidazole-1-yl)ethan-1,1-diyl]bis(phosphonic acid)

Table 5.2. ¹H-NMR results of Zoledronic acid in the literature

Reference	Chemical shifts, ppm			
	Ethane 2-CH ₂	Imidazole H-4	Imidazole H-5	Imidazole H-2
Srinivasa Rao <i>et al.</i> [216]	4.63-4.66 (m)	7.34 (s)	7.48 (s)	8.68 (s)
Ratrou <i>et al.</i> [217]	4.21-4.28 (m)	6.62 (s)	6.99 (s)	7.48 (s)
Nmrdb [218]	4.35 (s)	6.98 (s)	7.22 (s)	7.77 (s)
Samsel <i>et al.</i> 2008 [219]	4.46 (m)	6.90 (s)	7.23 (s)	7.75 (s)

In NMR principle when a peak is created a proton is changing its direction against or alignment to the magnetic field. According to the structure of the molecule there are four different hydrogen nuclei. Imidazole ring hydrogens are on carbon 2 and 4, 5 (Figure 5.1.). The hydrogens 4 and 5 are adjacent hydrogens. If there are any adjacent atoms attached to the neighboring carbon, it appears as multiplet (m) according to the n+1 rule and adjacent hydrogens on the neighbor carbon are numbered as n. So considering the n+1 rule, for single adjacent atoms, peaks would be as doublets. However they are observed as singlets (s) having close chemical shifts, because they are close to be symmetric and have shifting effects on each other and they appear as singlet. Hydrogen on carbon numbered 2 is expected to have larger chemical shift because of the electronegativity from the neighboring atoms.

In general distribution of proton chemical shifts associated with different functional groups, aromatic rings are in range of 6-9 ppm [220]. Imidazole part of the molecule is analyzed by H-NMR in the literature and H-2 usually give peak around 7.8 with deuterium as the solvent and H-4 and H-5 around 7.1 [221]. In zoledronic acid these peaks are shifted to the left of the spectrum by the effect of additional groups.

Ethane group attached to imidazole ring has two hydrogen atoms on the same carbon numbered as 2. As they have no adjacent protons, their peaks are expected to be a single peak having higher magnitude than single protons. However with the effect of P atom, the peak is observed to have further splitting [222]. RN-CH hydrogens give peak in 2-3 ppm region [223]. However with other groups attached to the adjacent carbon have shifting effects and their peaks are observed in 4-5 ppm region.

Considering all these, following results are obtained from H-NMR analysis; as deuterium (D_2O) as solvent and chemical shifts (δ) as ppm; 4.678 - 4.726 (t, 2H, $J=9.6$ Hz, Etan 2-CH₂), 7.385 (s, 1H , imidazole H-4), 7.536 (s, 1H, imidazole H-5), 8.735 (s, 1H, imidazole H-2) (δ (ppm) : Proton chemical shift, J (Hz): Coupling constant, t, s: Multiplicity of the 1H resonance). Comparing with literature, the substance is found to be a zoledronic acid molecule. The spectrums are given in Figure A.9, A.10 and A.11. The peak around observed around 4.8 is associated with water could be part of the solvent. For the other H molecules as hydroxyl groups (OH) are not appeared on the spectrum because of the interactions with the solvent.

5.1.3.2.1.3. ^{13}C - NMR Spectrum

Carbon NMR (^{13}C -NMR or sometimes simply referred to as carbon NMR) is used to detect the structure of molecules in a substance. In C-NMR, nuclear magnetic resonance (NMR) is applied with respect to carbon atom. It is analogous to proton NMR (H-NMR) and allows the identification of carbon atoms in an organic molecule just as proton NMR identifies hydrogen atoms. Zoledronic acid C-NMR is analyzed in the literature and some references are given in Table 5.3. Carbon numbers are given according to Figure 5.1.

Table 5.3. ^{13}C -NMR results of Zoledronic acid in the Literature

Reference	Chemical Shifts, ppm				
	Ethane C-2	Ethane C-1	Imidazole C-4	Imidazole C-5	Imidazole C-2
Srinivasa Rao <i>et al.</i> [216]	53.0	73.2	118.5	124.2	136.1
Ratrou <i>et al.</i> [217]	52.1	75.1	122.8	125.8	140.0
Nmrdb [218]	49.3	77.9	129.2	119.3	137.6

The C-NMR spectrum of a compound displays a single sharp signal for each structurally distinct carbon atom in a molecule. In proton NMR spectroscopy, the relative strength of signals are normally proportional to the number of atoms generating each signal, however

in C-NMR the situation is not like this. This makes the number of discrete signals and their chemical shifts important for evidence of a chemical structure. The general distribution of carbon chemical shifts associated with different functional groups are C-H saturated carbons in 0-50 ppm, aromatics 100-170 ppm, C-OH and C-N groups in 50-100 ppm ranges [220]. Carbons in imidazole molecule without any subsequent groups, give peaks as; C-4 and C-5 around 121-122 ppm and C-2 around 135-136 ppm [221].

According to the structure of the molecule given in Figure 5.1, there are five different groups of carbons so five different peaks are expected. The results are as; with deuterium (D_2O) as solvent and chemical shift (δ) as ppm; 55.475 (Ethane C-2), 74.4-77.1 (t, Etan C-1), 121.2 (imidazole C-4), 126.91 (imidazole C-5), 138.8 (imidazole C-2).

According to spectrums obtained (Figure A.12 and Figure A.13) carbon atoms of the ring is expected over 100 ppm which are seen as three peaks between 120-140 ppm. The highest shift is expected as C-2 considering neighboring atoms and the lower two peaks are associated with two adjacent carbon atoms. One of the carbon atoms numbered as C-2 is expected having the lower chemical shift. The other carbon of ethane as C-1 has hydroxyl group expected in 50-100 range. All peaks are expected as singlets however the effects of the magnetic field of P atoms causes further splitting for the peaks close to the P groups [222]. Due to two P atoms the peak is split as a triplet (in magnitude 1:3:1).

Considering all the data obtained, the molecule is found fitting to the data in the literature and identified as zoledronic acid.

5.1.3.2.1.4. 2D- Homonuclear COSY Spectrum

Two-dimensional nuclear magnetic resonance spectroscopy (2D NMR) give the data as plotted in a space which is defined by two frequency axes rather than one. Correlation spectroscopy (COSY) is one of the types of 2D NMR analysis. COSY gives homonuclear proton-proton interactions which give signals of neighboring atoms up to four bonds. Correlations appear when there is spin-spin coupling between protons, but no correlation means no coupling [223].

The diagonal peaks are associated with the molecule itself, and other peaks are cross peaks which are away from the diagonal are related with the neighboring atoms and they are

symmetric to the diagonal. Zoledronic acid has two peaks giving relation with the imidazole 4-H and imidazole 5- H protons which are symmetric to the diagonal (Figure A.14 and Figure A.15).

5.1.3.2.1.5. 2D-Heteronuclear HSQC Spectrum

The 2D HSQC (Heteronuclear Single-Quantum Correlation) is used to obtain a 2D heteronuclear chemical shift correlation between directly-bonded ^1H and X-heteronuclei (commonly, ^{13}C and ^{15}N). It is widely used because it is based on proton-detection, which gives high sensitivity [224].

Table 5.4. HSQC results of Zoledronic acid

	Carbon δ (ppm)	Proton δ (ppm)
Etan C-2 CH_2	55.470	4.678 - 4.726
Imidazole CH-4	121.230	7.385
Imidazole CH-5	126.914	7.536
Imidazole CH-2	138.825	8.735

As seen from the Table 5.4 and the Figures A.16 and A.17, hydrogen atom relation with its directly bonded carbon are observed as peaks on the spectrum. 2D Spectrum is composed as one axis referenced to C-NMR and one axis to H-NMR and peaks are seen as associating hydrogen peaks in H-NMR and related carbon peaks of C-NMR.

5.1.3.2.1.6. 2D-heteronuclear HMBC Spectrum

The HMBC (Heteronuclear Multiple Bond Correlation) experiment gives correlations between carbons and protons that are separated by two, three, and, sometimes in conjugated systems, four bonds. It is used for the correlation map between long-range coupled ^1H and heteronuclei (commonly, ^{13}C). Direct one-bond correlations are mainly not visible since they are suppressed. The intensity of cross peaks depends on the coupling constant. For angles near 90 degrees such as dihedral angles, the coupling is near zero. Thus, the absence of a cross peak does not confirm that carbon-proton pairs are many bonds apart [225].

Table 5.5. HMBC results of Zoledronic acid

	Carbon δ (ppm)	Protons
Imidazole CH-4	121.230	Imidazole H-2 and H-5
Imidazole CH-5	126.914	Imidazole H-2, Ethane 2-CH ₂ and H-4
Imidazole CH-2	138.825	Imidazole H-4, H-5 and Ethane 2-CH ₂

As seen in the Table 5.5 and in Figures A.18 and A.19, correlation between imidazole carbons with neighboring bonds are observable. Imidazole C-2 has three bond correlation with H-4 and H-5 and H-2 on ethane. Imidazole C-5 has two bond correlation with imidazole H-4, three bond correlation with imidazole H-2 and ethane H-2. Imidazole C-4 has two bond correlation with imidazole H-5 and three bond correlation with imidazole H-2. The difference between two bond and three bond correlations could be seen as the density of the peaks.

5.1.3.2.1.7. *Zoledronic Acid Mass Spectrum*

A mass spectrum is an intensity vs. m/z (mass-to-charge ratio) plot and the length of the bar indicates the relative abundance of the ion. The mass spectrum of a sample gives the distribution of the ions of a molecule in terms of their mass (more correctly: mass-to-charge ratio). When a pure sample is considered given to the system the heaviest compound is the molecular ion itself and the lowest masses are ion fragments of the molecule [219]. Zoledronic Acid molecular weight $C_5H_{10}N_2O_7P_2 = 272$ m/z . Waters Alliance HPLC equipment with Waters Micromass ZQ spectrometer is used for HPLC/MS spectrums. Different mass spectrum results are given in Table 5.6.

Table 5.6. Mass spectrum results of Zoledronic acid in the literature

References	Srinivasa Rao et al. [216]	Ratrout et al. [217]
Molecular weight, m/z	271.0	273.0

As the first step in the mass spectrometric analysis is using electron ionization to create gas phase ions of the compound. This molecular ion undergoes fragmentation. Each primary

product ion derived from the molecular ion, undergoes fragmentation, and fragmentation continues. The ions are separated in the mass spectrometer according to their mass-to-charge ratio, and are detected in proportion to their abundance. Ions detected by mass spectrometer provide information about the nature and the structure of their precursor molecule. In the spectrum of a pure compound, the molecular ion, if present, appears at the highest value of m/z (followed by ions containing heavier isotopes) and gives the molecular mass of the compound [227].

Mass Spectrums of zoledronic acid is represented in Figure A.20, highest peak on the spectrum is on 273 m/z . The common molecule is found at 271 m/z . This two weight difference could be caused by the common carbon isotope ^{12}C and ^{13}C [228].

5.1.4. Method of Crystallization

5.1.4.1. 7th Experiment

Now the reaction conditions are optimized. The same synthesis method is used with experiment 7th and amounts of reactants are increased to optimize crystallization methods. Trials were performed to increase the crystallization yield and purity of product.

Besides HPLC for purity (Figure A.21 and Figure A.22 for the 1st trial, Figure A.24 and Figure A.25, Figure A.27, Figure A.28 for 2nd trial, Figure A.30, Figure A.31, Figure A.32 and Figure A.33 for 3rd trial and Figure 36 and Figure 37 for the 4th trial), differential scanning calorimetric (DSC) analyses are also performed to support polymorphic structure. A typical DSC scan of zoledronic acid shows an endothermic peak below about 160-170 °C due mainly to water desorption, and a subsequent endotherm at about 200 °C, concomitant to an exothermal reaction [229]. Thermogravimetric analysis (TGA) analyses also performed to detect the water content of the each crystallization trial. TGA curves are given with DSC results to observe the mass loss associated with water loss in parallel. DSC curve of Zoledronic acid standard gives decomposition at 235.27 °C. In different crystallizations, different results of water content was found this caused some differences in the peak around 100 °C. However all DSC results of different crystallizations gave same melting point proving consistent polymorphic structures.

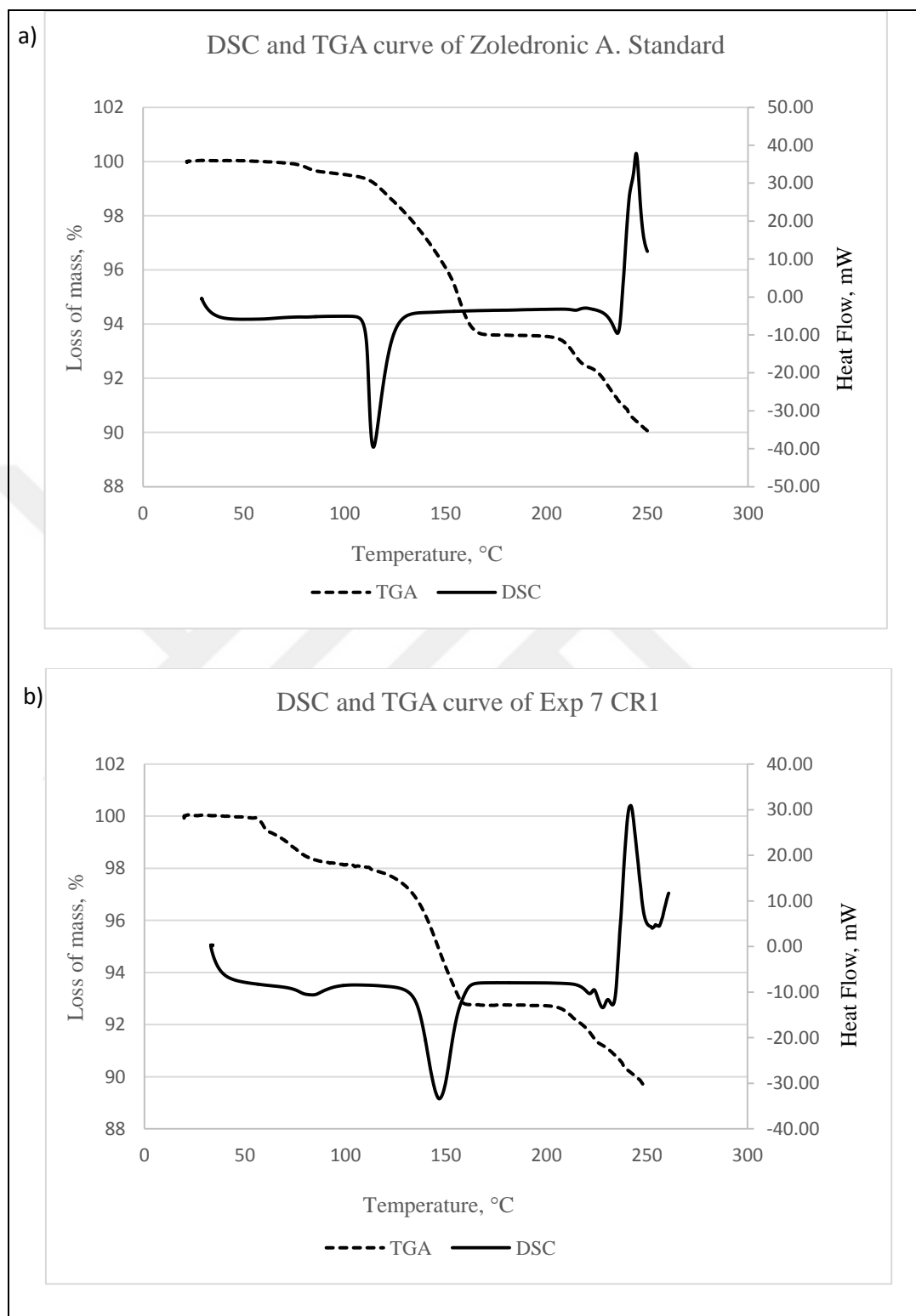


Figure 5.2. TGA and DSC curves of a) standard vs b) 7th experiment CR1

Figure 5.2 shows the DSC curve of zoledronic acid monohydrate standard. Starting from 100 °C and going forward, an endothermic sharp peak occurs at 114 °C. At 235 °C another peak is observed which reveals endothermic features before decomposition. This endothermic peak changes into an exothermic peak. This short peak could show the energy gained by the molecule before decomposition. The interpretation of the DSC curve could be challenging. DSC is used to determine the temperatures at which the sample goes through decomposition and melting. However using DSC curve alone could not give exact interpretation of these temperatures. The peaks observed between 100 °C and 160 °C could not be interpreted as melting but a solvent evaporation. The sample begins to decompose at least in two steps above 196 °C. A decomposition is not observed until around 225 °C. The decomposition products are liquid at this temperature. The thermal behavior of zoledronic acid was further investigated using a TGA analysis (Figure 5.2) [230].

Some different references that worked zoledronic acid DSC results are summarized in Table 5.7.

Table 5.7. DSC results of Zoledronic acid in the literature

References	Mohakhud et al. [212]	Mettler [230]	Labriola et al. [231]
Endotherm for water loss, °C	88	100-160	68-128
Endotherm for decomposition, °C	224	190-211	211-215
Exothermic reaction, °C	234	226	-

5.1.4.1.1. First Crystallization Trial

After water crystallization, the obtained amount is 22.8 g with moisture content of 7.13 per cent is calculated from the thermogravimetric analysis (TGA). TGA curve of trial 1 is represented in Figure 5.2. From the original 30 g the crystal zoledronic acid is 21.85 g which gives the yield of 73 per cent.

In Figure A.23, first crystallization trial decomposition point is 228 and 233 °C. This gradual decomposing could be caused because of the new generated decomposition products. Starting from 100 °Cs onward, a broad endothermic peak is observed which gives at 146 °C a relatively sharp endothermic peak. The endothermic peaks are changing directly into an

exothermic peak which is at 242 °C. The peaks obtained are close to the standard. The broad curve around 150 °C could be explained by a melting process of a component and/or the gradual water loss.

5.1.4.1.2. Second Crystallization Trial

Crystallization in 1:30 (solid : solvent) ratio and solvent as water / ethanol mixture (1: 1) zoledronic acid could not completely dissolved. The suspension solution is separated into two when hot in order to examine the cooling effect on precipitation of the product. The first part is cooled down to 25 °C and filtrated. In Figure A.26 the DSC curve shows a broad endothermic peak from about 130 °C onward, giving peak point at 149 °C. An endothermic peak is observed at 237 °C could be represented as the decomposition temperature. This curve changes directly into an exothermic peak at 243 °C.

The second part is cooled down to 25 °C mixed for two hours and cooled to 0 °C, mixed at this temperature for 2 hours and filtrated. The precipitated ZA samples are dried for 15 hours in vacuum oven.

DSC result shows decomposition at 240.01 °C for the second part (Figure A.29). The DSC curve shows, an endothermic peak at 145 °C and another shorter one at 160 °C. Another endothermic peak is observable at 240 °C interpreted for decomposition. At 245 °C, the observed peak gives an exothermic feature.

The dispersion was arbitrarily separated into two, therefore after drying their total mass is measured. 26 g product with 2.22 per cent moisture, giving a yield of 84 per cent is obtained.

5.1.4.1.3. Third Crystallization Trial

Crystallization performed with water, (solid : water ratio 1:15) and, solution was separated into two parts when hot, having a clear solution. One part is precipitated with ethanol and the effects of ethanol on the precipitation is observed parallel with the sample precipitated without ethanol effect.

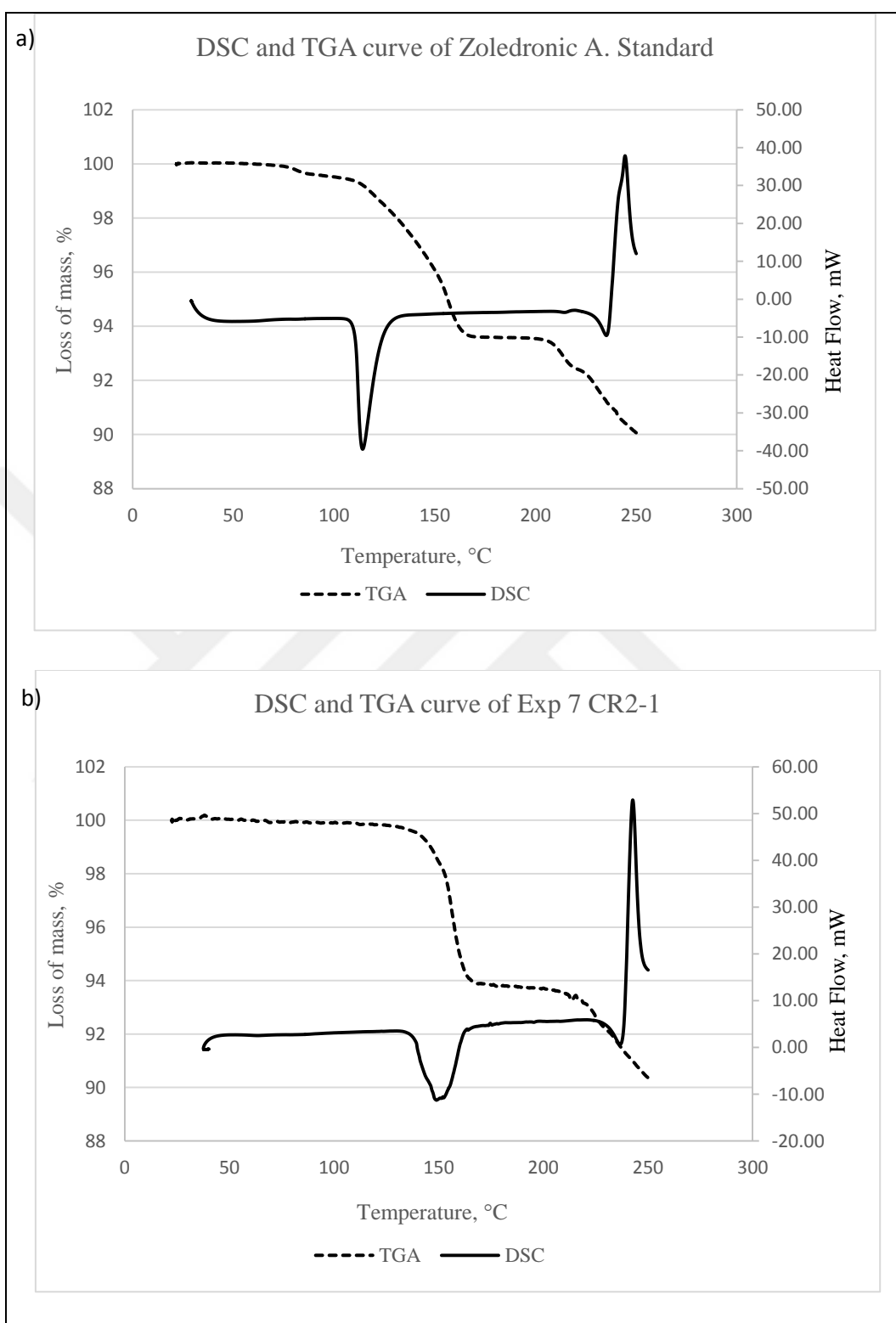


Figure 5.3. TGA and DSC curves of a) standard vs b) 7th experiment CR2-1

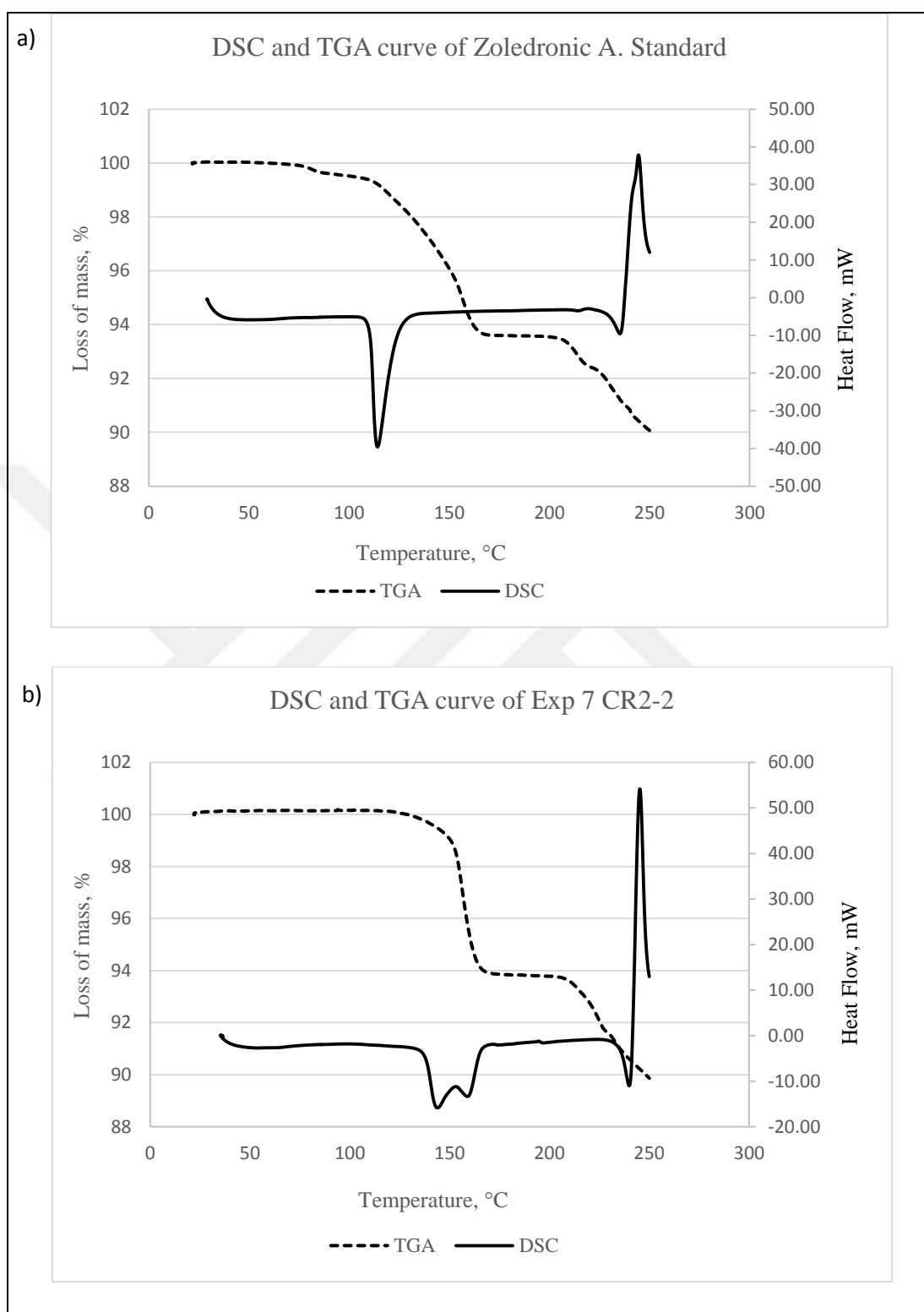


Figure 5.4. TGA and DSC curves of a) standard vs b) 7th experiment CR2-2

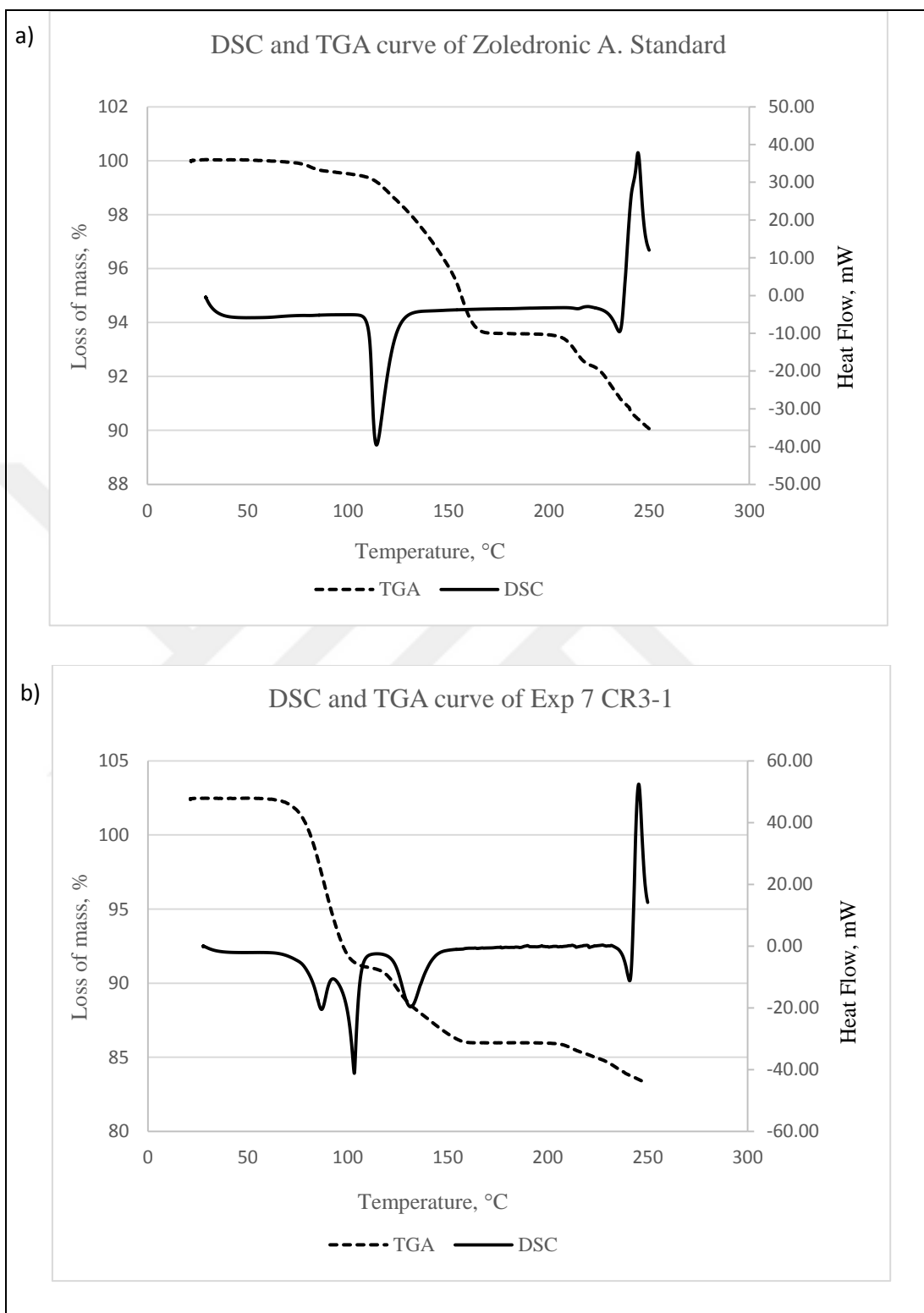


Figure 5.5. TGA and DSC curves of a) standard vs b) 7th experiment CR3-1

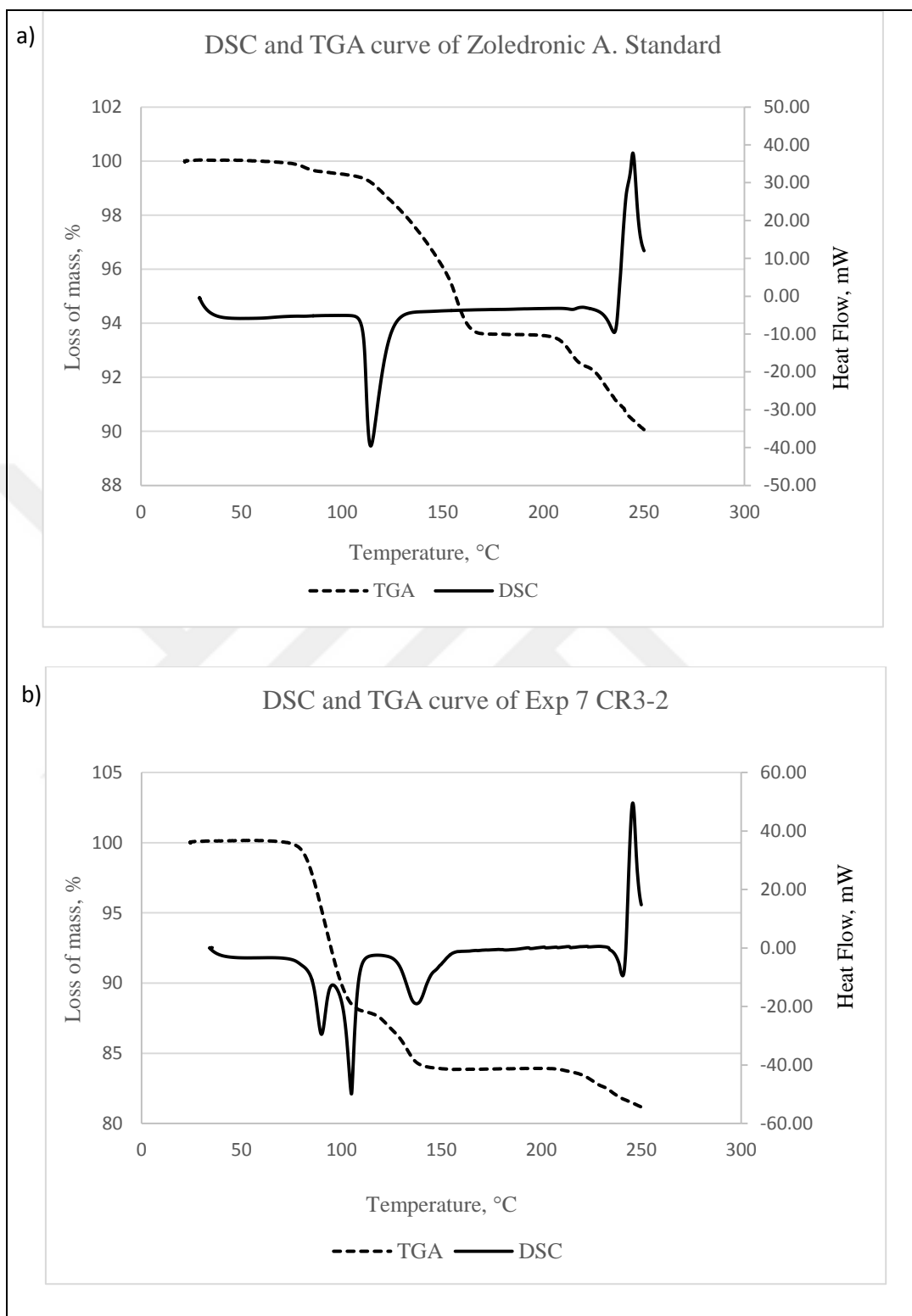


Figure 5.6. TGA and DSC curves of a) standard vs b) 7th experiment CR3-2

The first part as cooled down to 25 °C then 0 °C, gives a product with 12.21 per cent moisture, which bring the yield of crystallization to 72 per cent. DSC result shows

decomposition at 241 °C for the first part (Figure 5.5). The DSC curve shows, multiple endothermic peaks at 87 °C, 104 °C, 132 °C. These gradual peaks in this interval can be interpreted as a melting process and/or the gradual water loss. Another endothermic peak is visible at 241 °C interpreted for decomposition. The peak changed directly into an exothermic peak at 245 °C.

3:1 (water:ethanol) is added to the second half at 25 °C. The obtained amount is 14.91 g with 11.93 per cent moisture content, resulting in a better yield of 87.5 per cent. The DSC curve for second part (Figure 5.6) also shows, multiple endothermic peaks at 90 °C, 105 °C and 138 °C similarly. These gradual peaks can be interpreted with a melting process and/or the gradual water loss. The gradual mass loss could be also seen in DSC results in Figure A.32 and Figure A.35. A visible peak at 241 °C gives endothermic behavior and is interpreted for decomposition. The peak observed at 245 °C reveals exothermic feature resulted by further heating. From this trial it was seen that effect of addition of ethanol helps to precipitation of the substance after crystallized in water.

5.1.4.1.4. Fourth Crystallization Trial

Using water : ethanol in 1:1 ratio for crystallization let to incomplete dissolution of the synthesized product, 4:1 water : ethanol ratio is also tried. This time zoledronic acid is dissolved at 78-80 °C. The obtained amount is 17.4 g with 1 per cent moisture content, resulting in a yield of 69 per cent. The DSC and TGA curve (Figure 5.7) shows, an endothermic peak at 121 °C. Another endothermic peak is visible at 240 °C interpreted for decomposition. This peak changes into an exothermic peak at 245 °C.

Results obtained from crystallization trials are summarized in Table 5.8. Based on this results, the crystallization procedure which will be used in the production is the one described in trial 3-2, where zoledronic acid is dissolved in water at 90-95 °C and cooled down to 25 °C followed by addition of ethanol in 3:1 (water : ethanol) ratio and cooling down to 0-5 °C. The addition of ethanol and low temperature effects are shown to enhance the precipitation of zoledronic acid and increase the yield of pure product. In the drying period there is a deviation and a trihydrate molecule is obtained for trial 3rd and this is overcome with the corrected drying time.

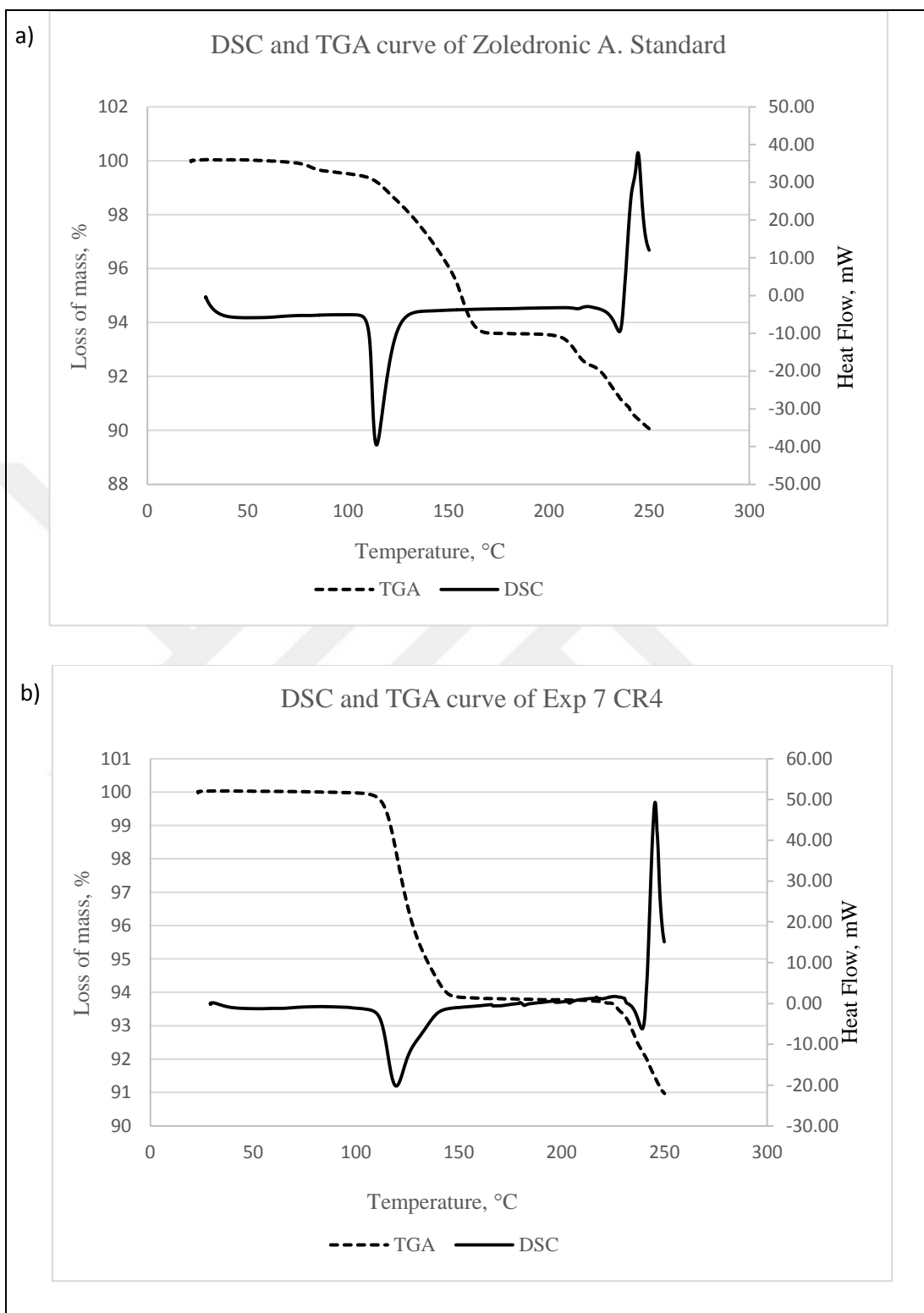


Figure 5.7. TGA and DSC curves of a) standard vs b) 7th experiment CR4

Even if there is a process deviation trial 3 has a high yield considering other trials, marking for trial 2nd, the material is not completely dissolved because of the low boiling point of ethanol. The results obtained from different crystallization processes are summarized in Table 5.8.

Table 5.8. Summary of results obtained in 7th experiment

Tests	Standard	Trial 1	Trial 2		Trial 3		Trial 4
			Trial 2-1	Trial 2-2	Trial 3-1	Trial 3-2	
Assay %	-	102.24	98.77	99.7	99.1	98.7	99.16
Decomposition °C	235	233	237	240	241	241	240
Water Loss %	6.33	7.13	5.95	6.13	15.83	15.94	6.11
Yield %	-	73	84	84	72	87.5	69

5.1.4.2. 8th Experiment

The experiment is repeated with the established crystallization method, where water is used to dissolve zoledronic acid at 90 °C and ethanol : water /1:3 is used for precipitation in cold media. The production yield for reaction is 51 per cent and for crystallization yield is calculated as 75 per cent.

IR results show 0.999 fit with the reference standard (Figure A.39) approving the substance is zoledronic acid. Karl-Fischer result shows 6.35 per cent water content, approving the monohydrate form (Figure A.42). Assay result is found 100.3 per cent considering the water content. Related chromatograms are attached (Figure A.40 and Figure A.41).

5.1.5. Effect of pH

5.1.5.1. 10th and 11th Experiments

The yield found was lower for lower pH value when the effect of change in pH is experimented with parallel experiments. The yield, decreased from 51 per cent to 43 per cent for pH values 0.7 and 0.4 respectively. Assay results however shows that the both products have good purity, as 99.75 per cent, 99.95 per cent respectively, (Figure A.44, Figure A.45 and Figure A.48 and Figure A.49) with the addition of KF results as 6.01 per cent, 6.35 per

cent respectively (Figure A.46, Figure A.50). IR results shows 0.99, 0.99 correlation with the reference standard, respectively (Figure A.43 and Figure A.47). The obtained results approving the obtained products are pure zoledronic acid monohydrate.

The same experiment carried out at pH 1 lead to the precipitation of a product that was not zoledronic acid. Lower pH values reduced the reaction yield therefore the pH of the medium was kept as pH 0.6-0.8 as described in US8952172 [230].

5.1.6. Excess of Halo Phosphorous Compound

5.1.6.1. 12th Experiment

In 12th experiment excess amount of halophosphorus compound, ie. PCl_3 is used where instead of 1: 3 carboxylic acid: halophosphorous ratio, excess PCl_3 is at 1:4.5 ratio is employed [214]. No yield difference is observed, so the ratio 1:3 kept as optimum amount for this reactant. Assay results shows considerably lower purity, as 96.63 per cent (Figure A.52 and Figure A.53). However, IR result shows 0.99 correlation with the reference standard (Figure A.51). KF result is as expected as 6.31 per cent for the monohydrate content (Figure A.54).

5.1.7. Excess of Phosphorous Acid

5.1.7.1. 9th Experiment

The experiment is repeated with excess amount of phosphorylation agent (25 per cent excess) where carboxylic acid: phosphorous acid ratio is increased 1:2 to 1:2.5. Total yield increased from 32 to 37 per cent. Assay results shows that the product has good purity, as 100.00 per cent with the same retention time of the standard (Figure A.56 and Figure A.57). KF result is found as 16.64 per cent that proving the synthesized material is a trihydrate form and drying will be applied to get the monohydrate form (Figure A.58). However, IR result shows 0.88 correlation with the reference standard (Figure A.55). This is found not an expected correlation and the difference is mainly causing by the 600-1000 cm^{-1} region. The unique peaks for zoledronic acid is 671, 712, 766, 975, 1301, 1323, 1406, 1460, 1550, 2826,

3154, and 3484, $\pm 5 \text{ cm}^{-1}$ and directly transition from trihydrate form to monohydrate form is possible with drying [232]. The region is related mainly C-C stretching. A volatile impurity could cause such difference since loss on drying test is applied and the same result is approved.

In this experiment drying was terminated in 5 hours and this could cause a trihydrate form according to the assay result with the moisture content.

5.1.7.2. 13th Experiment

Phosphorylation agent is used with increased excess amount (50 per cent excess) and having molar ratio of 1:3. The total yield is increased to 44 g (58 per cent). Assay results shows that the product has good purity, as 96.87 per cent (Figure A.60 and Figure A.61) considering KF result as 3.83 per cent (Figure A.62). The purity is found considerably low with the reference monohydrate due to the lower hydrate content. This could be caused by the drying time. IR result shows 0.99 correlation with the reference standard (Figure A.59).

5.1.8. Reproducibility

5.1.8.1. 14th, 15th, 16th Experiments

Three production trials are repeated as validation batches. Synthesis yield increased from 30 per cents to 50 per cent at the end of the trials. Analytical tests is performed according to the methods given in the Materials and Methods in Chapter 3. Purity results are found in the range of 98-102 per cent in HPLC. The finally accepted procedure will have the details as below, and related chromatograms are attached.

A reliable assay method for zoledronic acid ion-change chromatography is used since it is an ionic substance. Zoledronic acid assay methods were tried to establish a validated method. The method uses HPLC system with C18 column. The details of method for assay are represented in the Materials and Methods in Chapter 3.

Analytical method is referenced above is validated in the below according to the ICH guideline Validation of Analytical Procedures: Text and Methodology Q2 (R1), ICH

Harmonised Tripartite Guideline. The validation is taken in six parts are system suitability, selectivity, precision, linearity, solution stability, zoledronic acid LOD and LOQ values. The results obtained to check the reproducibility of the obtained procedure is summarized in Table 5.9.

H-NMR results (Figure A.67 for 14th experiment, Figure A.81 for 15th experiment, Figure A.96 for 16th experiment) shows parallel results for three of experiments and consistent results with the literature and previous experiments. This time some peak splitting is observed after a while the experiment is finalized. This splitting is caused by the electromagnetic effects of phosphorous. Following results are obtained from H-NMR analysis; as deuterium (D₂O) as solvent (Table 5.10).

Table 5.9. Results obtained for reproducibility

Results	14 th experiment	15 th experiment	16 th experiment	Reference
IR, correlation ratio	0.99	0.99	0.99	Figure A.63 Figure A.77 Figure A.92
KF, %	7.18	6.47	6.76	Figure A.66 Figure A.80 Figure A.95
Assay, %	99.93	99.47	99.0	Figure A.64 - Figure A.65 Figure A.78 - Figure A.79 Figure A.93 - Figure A.94

Table 5.10. ¹H-NMR results of reproducibility batches

Experiment No	Chemical shifts, ppm			
	Ethane 2-CH ₂	Imidazole H-4	Imidazole H-5	Imidazole H-2
14 th experiment	4.626-4.674 (m)	7.335-7.344 (t)	7.536-7.544 (t)	8.656-8.663 (t)
15 th experiment	4.629-4.677 (m)	7.339-7.347 (t)	7.538-7.546 (t)	8.663-8.670 (t)
16 th experiment	4.629-4.677 (m)	7.338-7.347 (t)	7.537-7.546 (t)	8.662-8.665 (t)

C-NMR results (Figure A.70 for 14th experiment, Figure A.84 for 15th experiment, Figure A.99 for 16th experiment) shows parallel results for three of experiments and consistent

results with the literature and previous experiments. The results are given in Table 5.11. A peak splitting on the carbons which are close to the phosphate groups are observed.

Table 5.11. ^{13}C -NMR results of reproducibility batches

Experiment No	Chemical Shifts, ppm				
	Ethane C-2	Ethane C-1	Imidazole C-4	Imidazole C-5	Imidazole C-2
14 th experiment	55.906-55.963	74.218-76.706	121.474	126.565	138.645
15 th experiment	55.899-55.857	74.218-76.712	121.416	126.571	138.619
16 th experiment	55.906-55.963	74.231-76.719	121.429	126.578	138.632

COSY spectrums are represented in Figure A.72 for the 14th experiment, Figure A.86 for 15th experiment, Figure A.101 for the 16th experiment. Zoledronic acid has two peaks giving relation with the imidazole 4-H and imidazole 5-H protons which are symmetric to the diagonal (Figure A.14 and Figure A.15). COSY is a homo nuclear correlation spectroscopy where plot is between two protons molecules which are attached directly or a little away [233]. A lower density peak is observed between the imidazole H-2 and imidazole C-4 and imidazole C-5 this time different to the previous experiment.

HSQC spectrums are represented in Figure A.73 for the 14th experiment, Figure A.87 for 15th experiment, Figure A.102 for the 16th experiment. HSQC shows parallel results for three of experiments and consistent results with the literature and previous experiments. C-NMR and one axis to H-NMR and peaks are seen as associating hydrogen peaks in H-NMR and related carbon peaks of C-NMR.

HMBC spectrums are represented in Figure A.74 for the 14th experiment, Figure A.89 for the 15th experiment, Figure A.104 for the 16th experiment. HMBC shows parallel results for three of experiments and consistent results with the literature and previous experiments. Imidazole C-2 has three bond correlation with H-4 and H-5 and H2 on ethane. Imidazole C-5 has two bond correlation with imidazole H-4, three bond correlation with imidazole H-2 and ethane H-2. Imidazole C-4 has two bond correlation with imidazole H-5 and three bond correlation with imidazole H-2. The difference between two bond and three bond correlations could be seen as the density of the peaks.

Mass spectrums are represented in Figure A.76 for the 14th experiment, Figure A.91 for the 15th experiment, Figure A.106 for the 16th experiment. Mass analyses show parallel results for three of experiments and consistent results with the literature and previous experiments. Highest peak on the spectrum is on 273 m/z. The common molecule is found at 271 m/z. This two or three weight difference could be caused by the common carbon isotope ¹²C and ¹³C, ¹⁴N and ¹⁵N [228].

5.2. EXERGY RESULTS AND DISCUSSIONS

The synthesis was carried out with the reaction of imidazole 1-yl-acetic acid HCl (C₅H₇ClN₂O₂, Wudi Reaction Pharma & Chemicals co., Ltd., Shandong Province, China), with phosphorous acid (H₃PO₃, Sigma Aldrich, USA), in the presence of phosphorous trichloride (PCl₃, Sigma Aldrich, USA) in methane sulphonic acid solvent (CH₃SO₃H, Sigma Aldrich, USA). Sodium hydroxide (NaOH, Merck, Germany) and ethanol (C₂H₅OH, J.T. Baker, Poland) were also used for pH adjustment and crystallization, respectively. All the chemicals used in production were pharma grade, NaOH had more than 97 per cent, C₂H₅OH had more than 96 per cent and all the other chemicals had more than 99 per cent purity. Amounts of the reactants and the crystallization conditions are optimized to achieve higher yields. Reactor capacity was chosen to satisfy approximately 1/6th of the market share, e.g., 50 g zoledronic acid corresponding to 10,000 bottles. The sale numbers suggest that the need for this drug was approximately 60 thousand bottles per year in Turkey [234]. For a 5 mg/bottle product, the batch size was sufficient to satisfy the market share. Production of the API and the injectable solution were carried out in the sterile rooms complying with the ISO standards.

The starting material, e.g., imidazol-1-ylacetic acid hydrochloride (C₅H₇ClN₂O₂), reacts with phosphorylation agent (PCl₃) at 60-65 °C. The pH of the reaction medium was adjusted with sodium hydroxide (NaOH). The product was precipitated by adding ethanol (C₂H₅OH) to the mixture and cooling. The system boundary encloses the zoledronic acid synthesis (Figure B.1) and the injectable zoledronic acid solution production (Figure B.2). Amounts of the raw materials required to produce 50 g of API were regarded as one batch. Components of each stream are considered as ideal homogenous mixtures. Pressure was

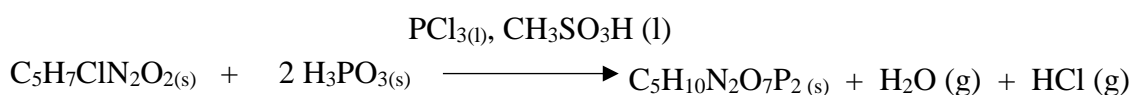
considered as 1 atm throughout the process. The temperature is also assumed to be spatially homogenous and equal to the boundary temperature.

Exergy analyses are performed for the synthesis of the API, zoledronic acid as well as for its unpackaged and packaged sterile solution. Energy and exergy utilization for production of the raw materials, excipients and packaging materials; and carrying out the unit operations are considered in the analysis.

5.2.1. Zoledronic Acid and Injectable Solution Synthesis

Flow diagrams for the synthesis of zoledronic acid ($C_5H_{10}N_2O_7P_2$) and production of the injectable preparation are presented in Figure B.1 and Figure B.2, respectively. The synthesis process was analyzed in five steps to carry out the calculations: (Step 1.1), reaction with heating under stirring, (Step 1.2) filtration, (Step 1.3) pH adjustment, (Step 1.4) precipitation, (Step 1.5) crystallization and drying as summarized in Figure B1. All the processes described in these figures are carried out by electric power utilization. Thermodynamic properties of the chemicals employed during synthesis of zoledronic acid are given in Table B.5. The cumulative exergy, $C_{ex}C$ of the electric power utilization was 4.17 kJ/kJ [235]. In the reaction stage, the solvent i.e., methane sulphonic acid (CH_3SO_3H) and the reaction agents, i.e., phosphorous trichloride (PCl_3) and phosphorous acid (H_3PO_3) are mixed. The amounts of the input materials are arranged to obtain 50 g of product. The reaction mixture is heated to 65 °C under mechanical stirring for 20 hours (Figure 5.8) at an optimum rate of 300 rpm with the motor power of 0.250 kJ/s. In this period, phosphorylation agent was added dropwise.

Phosphorylation of 1-h-imidazole acetic acid HCl, ($C_5H_7ClN_2O_2$), with phosphorous acid (H_3PO_3) to yield zoledronic acid may be described with the chemical reaction:



(5.1)

Heating of the reactants under continuous mixing is an irreversible process, where a fraction of the work potential is wasted. Exergy utilization for stirring is calculated from the maximum mixing power of the equipment. A 2 L glass reactor was used for the synthesis of zoledronic acid and its phosphorilization with 4 kJ/s of heating (Figure 5.8). After the completion of the reaction, the mixture was cooled down and the product was filtered with Nutsche apparatus, where cooling apparatus utilized 1.61 kJ/s energy (motor power= 0.25 kJ/s).

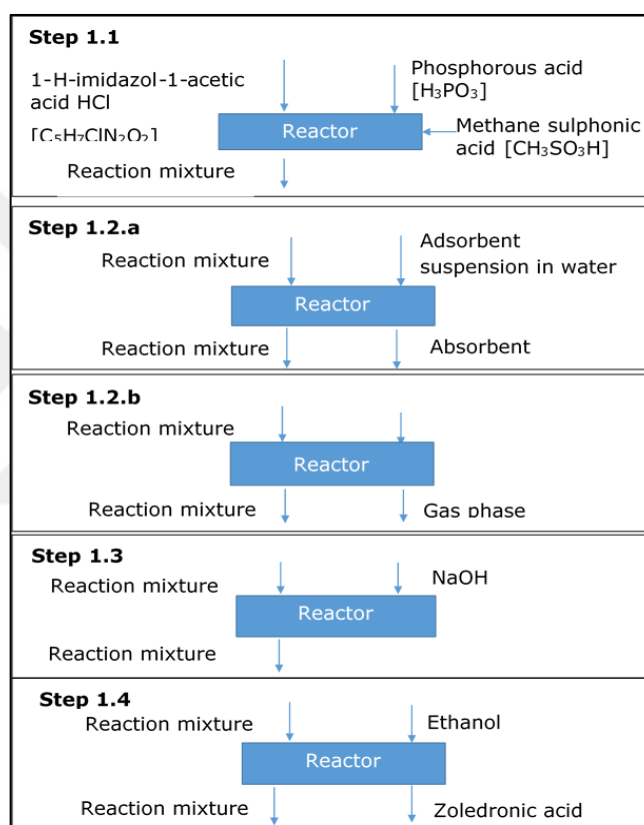


Figure 5.8. Schematic description of the steps of the zoledronic acid synthesis, separation and purification steps

It was calculated from the energy balance that; 20 kJ is used to heat up the ingredients and the exergy destruction $X_{\text{destroyed}}$ is calculated from Equation (3.3) as 2.8 kJ/batch (Table B.1). Enthalpy change of the synthesis reaction at the reaction temperature was -856 kJ/mol and $X_{\text{destroyed}}$ was calculated as 223.7 MJ/batch (Table B.1). Exergy destroyed in Step 1.1 was due to 20 h of continuous stirring and heating. During this long period, dissipation of heat from the reactor and irreversibility of stirring resulted in high exergy loss. In Step 1.2 reaction mixture was cooled from 338 K to 323 K (Figure 5.8); heat given to the

surroundings in this stage of the process was 10 kJ, whereas $X_{\text{destroyed}}$ was calculated as 939 kJ/batch (Table B.1). The total energy requirement of the synthesis reaction was 227.5 MJ/batch including cooling (Table B.1). Product was separated from the reaction mixture after the completion of the reaction with filtration, followed by precipitation, recrystallization and drying. Absorbent is added to the reaction mixture in the filtration step (Figure 3), and the mixture is heated up to 75 °C using a water bath. The solution is then filtered hot through Nutsche 150 μ size filter by the help of a suction pump (Senco, China, Model 2XZ-1; 0.25 kW) and absorbent is separated from the mixture after adsorbing most of the impurities from the mixture (Step 1.2). Work entering into the system via the suction pump and stirring equipment, and mass input was in the form of absorbent and water are calculated as 40.9 kJ; $X_{\text{destroyed}}$ in this stage for the separation as 6,369 kJ (Table B.1). The reaction mixture was cooled down to 5 °C to after filtration, improve the reaction yield. 5.8). Amount of the pH adjustment agent is optimized to adjust the pH to obtain a higher product yield. Addition of sodium hydroxide (NaOH) is performed slowly under controlled temperature. In this stage $X_{\text{destroyed}}$ is calculated for the cooling and the buffer addition steps as 1,222 kJ (Table B.1). When the reaction mixture was then cooled to less than 70 °C, and the pH was adjusted to 0.6-0.7, ethanol ($\text{C}_2\text{H}_5\text{OH}$) is added to the mixture with stirring (Step 1.4 in Figure 5.8) to precipitate the zoledronic acid. Total exergy for precipitation and collection of the precipitate was 17 MJ. The crude zoledronic acid was then crystallized to obtain a higher-purity product. Crystallization of zoledronic acid is performed under GMP conditions in Step 1.5 (Table B.1), where class C, HVAC equipment was employed (0.5 kW/m² considering a 4 m² room size adapted from Clean Room Technology (2014) [236]. In this stage, the precipitate is dissolved in water again by heating and mixing around 90 °C. Zoledronic acid starts to dissolve at 70-80 °C. Solution is then filtered again hot and allowed to cool down to 20 °C, to precipitate the solids once more. Drying takes place in a vacuum oven. Exergy utilization in the drying stage was 360 MJ (Table B.1). The total exergy destruction in the synthesis process, (step 1), was 202 MJ (Table B.1), including the chemical exergies of the inputs, e.g., starting materials, pH adjustment reagents, etc. The total chemical plus the physical exergies of the input species was approximately 0.4 MJ (Table B.2). Heat transfer and work were the main causes of the exergy loss. Molecular chemical exergy for the product zoledronic acid was 3,594 kJ/mole and physical exergy is -1,921 kJ/mole at the reaction step. Product exergy itself is 1,004 kJ for 0.6 mole of zoledronic acid.

The main inputs of the synthesis process were the starting materials and the solvent. In the last step of the production of zoledronic acid, i.e. crystallization, exergy destruction was approximately 553 MJ (Table B.1, Figure 5.9). The CDP was calculated to be 1.47×10^{-4} .

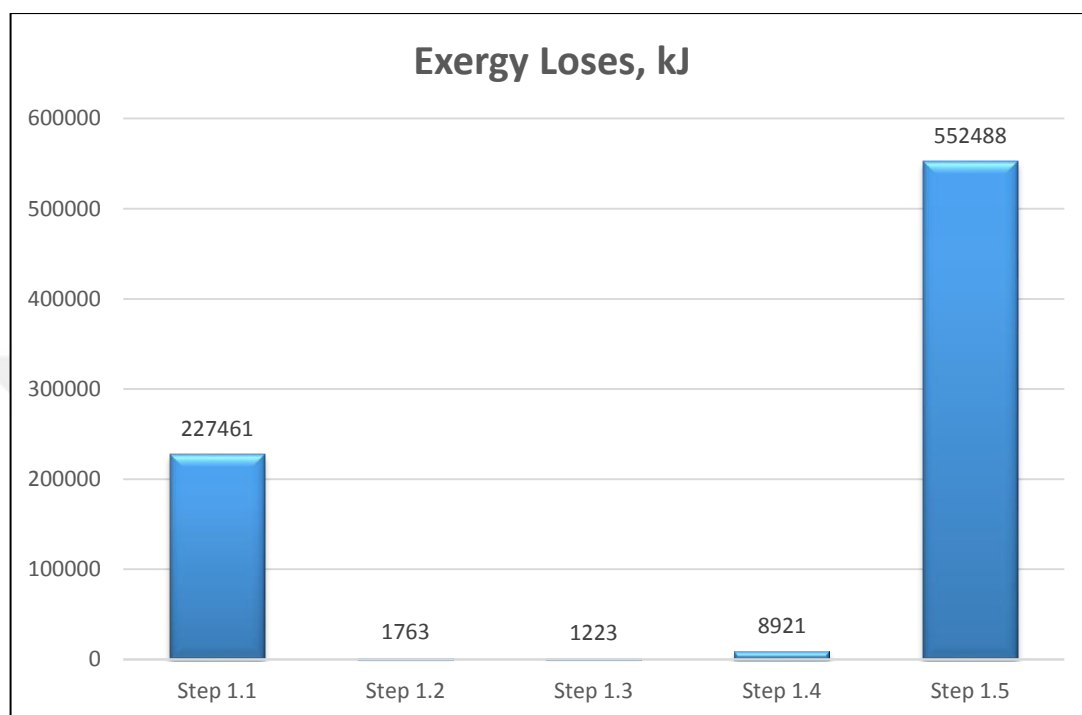


Figure 5.9. Exergy loss in each step of the zoledronic acid production process Step 1.

5.2.2. Production of The Injectable and Parenteral Zoledronic Acid Solution

Production of the injectable parenteral zoledronic acid solution (Step 2) is described in Figure 5.10. Intravenous zoledronic acid solution production requires the use of conventional incipient; an isotonic agent, a pH adjustment agent, e.g., sodium citrate ($C_6H_5Na_3O_7$) and injectable grade water. In the present study as isotonic agent mannitol ($C_6H_{14}O_6$) is employed which the most preferred agent in the industry.

Sterile mixing is carried out in a class C room, whereas sterile filling took place in B class room. For packaging of filled bottles, D class HVAC system is operated. Energy utilized by the HVAC system depends on the class and area of the room. Sterile room classifications are adapted from Clean Room Technology (2014) as 1.52 kW/m^2 , 0.50 kW/m^2 and 0.41 kW/m^2 for class B, C and D, respectively.

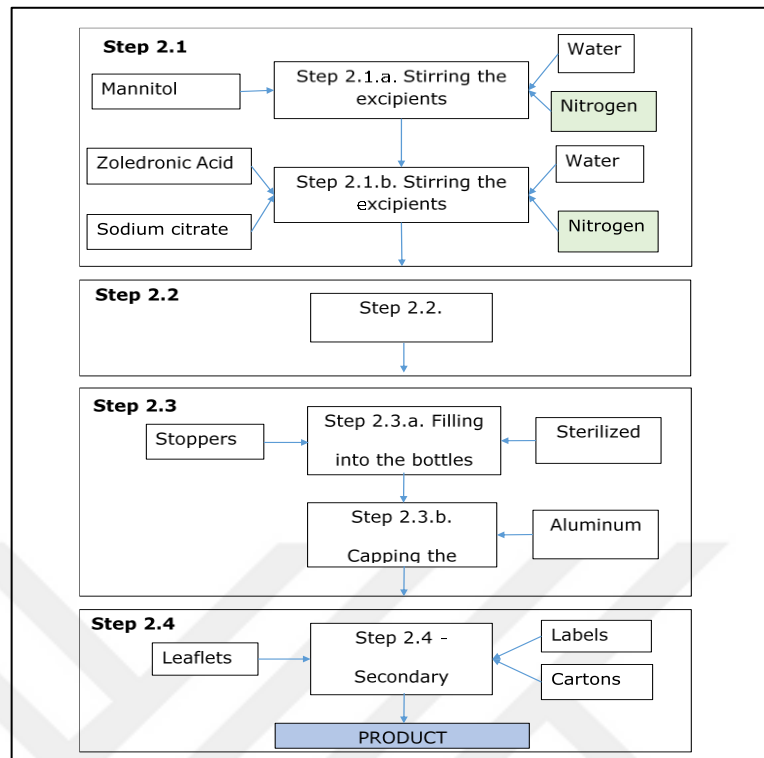


Figure 5.10. Schematic description of the injectable zoledronic acid solution production and its packaging.

Water purified in the reverse osmosis plant is used to prepare the injectable solution, where 5.4 MJ of energy is utilized. All the excipients were dissolved together by stirring until a homogenous solution is obtained in a 1,000 L stainless steel vessel equipped with 0.75 kW mixer (Step 2.1a). Mannitol ($C_6H_{14}O_6$) is dissolved in water under nitrogen atmosphere with 0.5 kW/m^2 of energy utilization in a 1.0 m x 2.5 m x 4.0 m class C room (Figure B.4). There was no heating or cooling in this stage, but there was an entropy change that is caused by the mixing of streams. Work contribution arises from the mechanical mixing during the aeration of water with nitrogen for 30 minutes and followed by mixing for 15 minutes to dissolve mannitol ($C_6H_{14}O_6$) in and the HVAC system electricity, to keep the pressure level of the room in the limits to create class C room, which is the requested class to prepare the bulk solution for sterile production. At this stage since mixing is an irreversible process, work required for mixing and the work to provide class C room is calculated as $X_{\text{destroyed}}$ (Table B.4).

In the second stage of solution preparation step, zoledronic acid and sodium citrate ($C_6H_5Na_3O_7$) is added to the solution (Step 2.1b in Figure B.4). Along with some more water,

solution is mixed for 40 minutes. HVAC system was operating during this mixing stage. At the inlet of the filling line, the bulk solution was filtered through a 0.2 μm pore size filter (Figure B.4). A typically used peristaltic pump has a power utilization rate of 3.3 MJ (RISEN RH series industrial peristaltic pump). According to the pumping capacity with considered peristaltic pump and 0.2 μm filtration capacity as 12,000 L / h and 200 L / minute, respectively, for 1,000 L solution 5 min of operation time is considered. The filtration operation is carried out when the class C HVAC system is on. Exergy of the energy consumption from work is 8 MJ (Step 2.2 in Table B.4).

The filter cartridge production machine produces 2,000 pieces/day of 10-inch filters with running power of 20 kJ/s, therefore the energy utilization during production of each cartridge was 864 kJ. The cartridge was made of nylon. Energy utilization for production of nylon is 0.156 MJ/m and for 10 inch nylon filter the energy requirement for the production the material is calculated as 39 kJ. Therefore, the total exergy utilization for the production of the filter was found to be 3.7 MJ (Table B.3).

Aseptic filling operation is done under B class room conditions (Step 2.3). Primary packaging materials (i.e. bottles and stoppers) are sterilized prior to use. The filling operation took place in a closed machine in a laminar flow cabinet operating as Class A room. Primary packaging material is supplied to the machine, where the bottles are filled with the prepared bulk solution and are capped in aseptic conditions. (Figure B.4). Bottles, stoppers and caps are the used materials during filling as primary packaging materials. Each of which are produced at an energy cost. In the next section, these are calculated.

The glass bottles that are used in pharmaceutical products have at least their internal surfaces coated with a transparent, heat sterilized plastic material [237]. Exergy of the coated glass is calculated as a two-stage operation where the first stage consists of the production of the glass and the second coating with silicone. In the filling stage, silicon coated glass bottles are used. Coating is necessary to prevent any leaching from glass to the product. Mainly glass containers are coated with a material that is first heated to a molten state followed by cooling without crystallization. Metallic oxides which may be used for this purpose include SiO_2 , B_2O_3 , P_2O_5 and GeO_2 . Among these oxides, SiO_2 is the one which is used most commonly for medical glass making processes including containers for sterile dosage forms [238]. Production exergy for glass bottle making is taken from the literature as 8.4 MJ / t glass (adapted from UNIDO, 1993) [239]. A 100 ml-bottle weighs 120 g, therefore energy

consumption per bottle is 1.008 kJ. For a batch of 10,000 bottles the exergy consumed is 10.080 MJ. Coating is achieved by dissolving a silicone in an organic solvent where this solution is introduced to the bottle to be coated and remains as a film on the inner walls of the container. Evaporation of the organic solvent at high temperatures also provide the baking of silicone coating which stabilizes and fixes the coating on the surface. However, the temperature should be higher than the vaporization temperature of silicon. It is believed that the silicone layer is molecularly fused to the walls of the container, particularly when the container is glass [240]. The most energy consuming stage of the process is heating the residual film of silicone to bake. Glass is heated for about 1.5 hours in an oven at 300 °C. Promake (China) model QHJ tray drier with capacity of holding 48 trays is used with this purpose. Each tray is capable of drying 256 bottles (considering 5 cm bottle diameter and 1 m² trays area) and one batch (10,000 bottles) can be dried using 40 trays, so 48-tray capacity is matching the requirement of one batch. Power consumption of the typical tray dryer machine comes from heating power (24 kJ/s) and fan power (0.45 kJ/s) which for 1.5 h operation time gives 132 MJ electrical consumption. Methyl silicone (R-OSi)_n and chloroform (CHCl₃) are the used material for such a coating. Silicone production energy consumption is considered as 5 kWh/ kg Si [241]. One bottle coating is assumed to consume 1 g Si. According to this assumption 180 MJ energy is used for silicon coating of one batch of bottles. Organic solvent chloroform is assumed to be recovered so not considered in the calculations. Sterilization of bottles is performed within the filling machine. Bottles are washed with WFI water at 85 °C, followed by drying using sterilized air. The washing machine has the capacity of 10,000 bottles/h, and one-hour operation is considered. The sterilization tunnel operates as high temperature sterilization at 300 °C. Total electrical energy consumed by the washing machine is 3.2 kW (4 KVA considering conversion factor 0.8) whereas 1-hour operation of sterilization tunnel for 10,000 bottles is 11.52 MJ, that sums up to C_{ex}C to be 48 MJ. During the washing process, water is recycled for 1 hour in a recycling unit, having 6 kW power capacity. Additional 1-hour air sterilization in the sterilization tunnel feeding 750 m³ air consumes 30 kW which sums up to 36 kW energy consumption in addition to the electrical energy consumption of 129.6 MJ. A total of 589 MJ exergy consumption is calculated for sterilization (Table B.4).

A stopper typically consists of a rubber part and a coating barrier. Similar to the bottles the coating serves as a barrier for leaching materials into the medicament. Barrier films based

on expanded PTFE (C_2F_4)_n can provide for thin and strong barrier layers to leachable and extractable materials from the stopper. The densified PTFE (C_2F_4)_n film is thermoformed to make a preform. Thermoforming is done at process temperatures sufficiently above the melting to ensure melt forming while preserving the barrier properties. The thermoformed, densified PTFE (C_2F_4)_n preform can be combined with the elastomer body by injection molding, compression molding, priming and post laminating [242].

The production of the rubber part of the stopper consists of molding of rubber. Teflon (C_2F_4)_n coated stoppers used are produced in the same manner. The amount of Teflon (C_2F_4)_n coating is very low compared to the rubber part, so the exergy of Teflon (C_2F_4)_n production itself is neglected. Considering the main process steps such as thermoforming at elevated temperatures and compression molding, electrical consumption of the machines are taken into consideration neglecting other terms such as materials used in the production. In thermoforming process, close to 400 °C operation temperature and a thermoforming machine that uses 100 kJ/s is considered. Such machine has the capacity of 40 pieces / min, giving 250-minute operation time for 10,000 bottles. Total energy consumed is calculated as 1,500 MJ and $C_{ex}C$ as 6,255 MJ). (Table B.6).

Typically, energy consumption for rubber molding range from 1080 kJ/kg to 7200 kJ/kg and 3,600 kJ/kg is taken as average. The rubber part of one stopper neglecting the coating weighs 1 g, and for one batch 10,000 stoppers are used needing 10 kg rubber, resulting in a total of 36 MJ electrical consumption for its production. Total exergy consumed is for the stoppers used in the process is 1,536 MJ and $C_{ex}C$ is 6,405 MJ (Table B.4 and Table B.6).

Aluminum caps are used over the rubber stoppers for the closure of the bottles. Exergy consumption is calculated considering the production of caps (Figure B.4). Exergy utilization for the production of aluminum is adapted from [243, 244] as 30 MJ/kg. One cap weighs 2 g and 10,000 caps for one batch requires 20 kg of aluminum, resulting in 600 MJ exergy consumption for its production (Table B.6). Onto the aluminum caps a plastic cover is injection molded. The caps are first made and inserted into a machine where plastic is injected on top [245]. Throughout this process, injection molding is the highest energy consuming step, therefore other contributions are neglected, and 33 kJ/s (heating + motor power) for injection molding is taken from literature reference as typical electrical consumption for an injection molding machine. A single cap weight consists about 1 g plastic and for one batch 10,000 caps are used, giving a total of 10 kg with injection rate 200 g/s.

Injection is completed in 50 s which consumes 1.6 MJ in total resulting in C_{exC} of 6.67 MJ. (Table B.6)

Compression molding machine is used for shaping of the elastomer part. Here materials are pressed around 4-ton pressure at around 100 – 150 °C, and the process takes about 1.15 h. A compression molding machine using around 45,000 J/s energy is considered, giving 776.87 MJ exergy consumption (Table B.6).

Aseptic filling operation is done under B class room conditions. Primary packaging materials (i.e. bottles and stoppers) are sterilized prior to use. The filling operation took place in a closed machine in a Laminar flow cabinet which operates as Class A room, according to EU cGMP classifications (Gröninger vial filling and closing line, DFVK 6000, Germany). Primary packaging material is supplied to the machine, where the bottles are filled with the prepared bulk solution and are capped in aseptic conditions (Figure B4). After the sterilization of primary packaging material, 100 mL of the prepared bulk solution is filled to the bottles. Sterilized stoppers are inserted onto the bottles.

Nitrogen gas (0.9 mole N_2) is supplied throughout the process where 10 L nitrogen capacity is used. ($Ex_{chem} = 0.72$ kJ/ mole), Ex_{chem} is 0.64 kJ which is negligible considering the electrical power consumed. The filling machine has a capacity of 2,500 bottles/h therefore 4 h of operation is required. The filling operation takes place in an A class LAF cabinet (730 J/s) that is operated for 4 h where this cabinet is placed in a B class room. During aseptic filling operation, machine work for filling and stoppering have an energy consumption of 144 MJ (C_{exC} , 601 MJ), where the overall energy consumption adds up to 733 MJ including sterilization (C_{exC} , 3,058 MJ) (Table B.4). Capping machine operates at 1,760 J/s (2.2 KVA for considering 0.8 conversion factor) for 1 hour during which 6.3 MJ is consumed as electrical energy (Step 2.3 in Table B.4).

Once bottles are filled with the medicament, a secondary packaging step is required (Step 2.4). Packaging materials used in final packaging includes all the labels, boxes, leaflets, and cartoons for labelling and cartooning. Second phase weight controls are also performed and added to exergy analyses. All the materials and transport of these materials are contributions to exergy.

Labels used on the bottles are polypropylene. C_{exC} of polypropylene is 85.2 MJ/kg [246]. One piece of label used for one bottle is 0.45 g. For one batch 4.5 kg polypropylene is used,

giving $C_{ex}C$ of 383 MJ (91.84 MJ energy). Labelling machine, has a capacity of 150 bottles / min and consumes 1.5 kJ/s. (Shanghai Peiyu Machinery Ltd., China, model SPC – 150 B). Considering one batch, 1 h of operation time is required, which adds up to 5.4 MJ ($C_{ex}C$, 22.5 MJ) energy consumption. (Table B.6)

In every box with 12 bottles one information leaflet is placed. For 10,000 bottles, 834 boxes (i.e. 834 leaflets) are needed. The dimensions of one leaflet is 160 x 245 mm (area 0.04 m²) and a paper quality 60 g/m² is used, making one leaflet 2.4 g. Therefore, for a batch, 2 kg paper is consumed. Energy for paper production is 16.59 MJ/kg [235] hence 33.18 MJ ($C_{ex}C$, 138 MJ) is consumed in one batch. (Table B.6)

Leaflets are printed with a leaflet printing machine having capacity of average 5000 sheets/h, consuming 2.55 kJ/s electrical power. 834 leaflets are printed in 0.167 h (600 s), making the energy consumption of printing leaflets for one batch, i.e. 834 leaflets, is 1.54 MJ ($C_{ex}C$, 6.42 MJ). (Table B.6)

The cardboard boxes where the bottles are placed have dimensions of 44x34x27 cm (area 0.72 m²); 10,000 bottles require 834 boxes (834 x 0.72 = 600.5 m²) where the energy needed for cardboard production is 1 MJ/ m² on average [247] making the total energy consumed 600.5 MJ. Once the cardboard is produced, the material should be turned into a box with some information printed on the box. Box making and printing machine is considered to produce 250 boxes/min consuming 135 kJ/s energy (Shanghai Liu (China)). To produce 834 boxes with 250 boxes / min, 3.4 minutes (204 s) is sufficient which brings the consumption to 27.5 MJ ($C_{ex}C$, 114.68 MJ) for one batch (Table B.6).

The exergies of the excipients, e.g., mannitol (C₆H₁₄O₆), zoledronic acid, sodium citrate (C₆H₅Na₃O₇) and water and electrical energy used during manufacturing were those of the raw materials under sterile conditions before filling, i.e. 23.005 MJ. Exergy of the product was sum of the chemical exergies of all excipients composing the sterile solution, i.e. 22.968 kJ. The exergy efficiency of the solution before filling is 17 per cent.

Exergy efficiency for finished product form is calculated to consider packaging of the product. Details of the calculations presented in Table B.8. Packaging could differ for different applications, in this study 100 ml glass bottle, Teflon coated stoppers and aluminum caps are evaluated. Chemical and physical exergies of the excipients in the sterile solution, production exergy of the sterile water and the exergies of the packaging materials were added

up to calculate the exergy of the product (14,224 MJ). Total exergy obtained of the finished product, ready for shipment, was 18,805 MJ and its exergy efficiency was 75 per cent.

5.2.3. Analytical Testing

Analytical testing was done at two stages of the production, first after the synthesis of zoledronic acid, for the identification and purity of the compound. Other analytical tests are performed for quality control purposes where the finished product form is tested to comply with the regulations. Both testing mainly comprises of assay and impurity testing with HPLC (Shimadzu, model LC-2030 C, Japan). The standards for the HPLC analyses were purchased from U.S. Pharmacopeial Convention, (US). HPLC grade methanol and other materials i.e., tetra butyl ammonium hydrogen sulphate, potassium dihydrogen phosphate, triethylamine were obtained from Merck Millipore (Germany). Chemical analyses which are carried out to assure the product quality are presented in Table B.7. Thermodynamic properties of the chemicals, which are used in analytical testing are presented in Table B.7a. Analysis carried out in short time with consumption of trivial amounts of chemicals, such as determination of the melting point or water content with Karl Fisher method not included in the calculations and the overall exergy cost of the analysis carried out for quality control are presented in Table B.7b. Total exergy cost for analytical testing is calculated to be 22.2 MJ.

Stability studies are performed in different stability conditions to show there is no sign of degradation of the product until the expiry date. Stability studies are performed both under accelerated conditions where the temperature is 40 °C with 75 per cent relative humidity for 6 months and under long term conditions where the temperature is 25 °C with 65 per cent relative humidity for two years, testing for changes in the chemical structure with the aforementioned analytical methods. Testing frequency is every 3 months for the first year and every six months for the following year, as described in ICH Q1A. Release tests are performed two and six times during the storage in accelerated and long-term conditions, respectively. During stability studies, energy utilization for analytical testing was 177.16 MJ and that of release testing as 22.15 MJ, adding up to 199 MJ (or the total exergy of 827 MJ) (Table B.6).

Quality control is an important task accompanying the production of the pharmaceuticals. The finished product is analyzed by using an HPLC to assess the presence of the impurities.

According to the procedure, 20 injections (6 sample injection, 12 standard injections for assay and impurity, and placebo, diluted injections) are required per sample and each injection takes 40 minutes. Approximate exergy consumption of analyses for 800 minutes of HPLC operation was found as 22 MJ (Table B.7).

5.2.4. Transportation of The Materials

Transportation of the raw materials for the production of the active ingredient is neglected, because of the small, e.g., 50 g, batch size of the Zoledronic acid production process. The main excipient used in injectable finished product formulation is water and the volumes of the other excipients are negligible. The bottles are received in 100-bottle packages (dimensions: 25 cm x 25 cm x 42 cm with four layers of 25 bottles). The total volume of 10,000 bottles, e.g., 26.25 m³ occupy 65 per cent of the 40 m³ truck load. The product, which is placed in 834 boxes occupy 34 m³ of volume corresponding to 90 per cent of a truck load. Assuming an average travel velocity of 90 km/h, utilizing 0.287 L/km of diesel (density 0.832 kg/L, energy equivalency of 57.5 MJ/kg of diesel) [248]. The energy consumption for distribution to one-hour distance of a full truck is 1,373 MJ. With the location the production unit, most distribution is considered to take place within one hour. Therefore, the transport of raw materials costs 892 MJ (1,373 MJ/truck x 0.65 truck) energy whereas the distribution energy cost is 1,236 MJ (1,373 MJ/truck x 0.9 truck), making the total transport energy consumption 2,128 MJ (Table B.6).

5.2.5. Renewability of The Process

Renewability indicator was defined as:

$$I_r = \frac{(W_p - W_r)}{W_p} \quad (5.2)$$

where, W_p is the useful work obtained by the product, W_r is the restoration work. If the maximum work potential of the product is extracted via reversible process, then W_p equals to X_p [249, 250, 224].

Table 5.12. Summary of the results

Step and sub-steps of the process	$X_{\text{destroyed}}$ (MJ)	CDP (%)	Renewability index
Zoledronic acid synthesis			
Step 1.1 Reaction	227.46	2.29×10^{-2}	-319.24
Step 1.2 Filtration	6.37		
Step 1.3 pH adjustment	6.35		
Step 1.4 Precipitation	16.67		
Step 1.5 Crystallization and drying	552.49		
Unpackaged injectable zoledronic acid solution production			
Step 2.1 (dissolving of excipients)	102.30	17	-123.83
Step 2.2 (filtering)	11.76		
Packaged injectable zoledronic acid solution production			
Injectable zoledronic acid solution total (total of steps 2.1 and step 2.2)	114.06	75	0.68
Step 2.3a (sterilization and filling)	10,806.43		
Step 2.3b (capping)	4,224.69		
Step 2.4 (secondary packaging)	3,659.84		

The restoration work, is the cost of producing an energy source, without causing an environmental damage or pollution. Restoration work is defined as the sum of net cumulative exergy consumptions (CNE_x) of the production and the waste treatment.

$$W_r = CNE_{x_{\text{production}}} + CNE_{x_{\text{waste treatment}}} \quad (5.3)$$

Renewability indicator calculated for Step 1, e.g., for synthesis of the zoledronic acid, and for the injectable drug production before packaging, at Step 2.2 and after the whole

production process, including packaging at Step 2.4 and found as -319, -123 and 0.68, respectively (Table 5.12). The negative RI values indicate non-renewability of the process. A renewable energy source does not destroy exergy [224]. The total work to produce the energy source and to restore the environment should be smaller than the work produced by the energy source. An exergy source, is not renewable, considering the work consumed to restore environment is much larger than the produced work [251]. In a small-scale drug synthesis, the impact on the environment needs much more work than the work done to produce the product itself. For the injectable, large scale drug production, since all the package materials are renewable, like glasses, card board, and no waste is produced, therefore the renewability factor was positive.

6. CONCLUSION AND FUTURE WORK

The aim of this work was to increase the production yield of zoledronic acid monohydrate, an active pharmaceutical used for bone diseases. For this purpose, a conventional synthesis method is employed multiple times under different reaction conditions. The parameters which are varied to increase the product yield are temperature, reaction medium, i.e. the solvent, and stoichiometry of the reactants. For a chemical process, apart from the yield, the energy efficiency is of crucial importance. Therefore, in the second half of the study exergy analysis of the synthesis was carried out for the production of injectable product, e.g. the finished dosage form of the zoledronic acid.

The production yield was determined with different analytical methods. HPLC is used to check the purity, IR, DSC and the decomposition temperature were used for identification; NMR methods and mass spectrum were used for structural testing. Karl Fisher method and TGA were used to determine the water content of the molecule. Structural and analytical testing for the reproducibility of the established process proved that the synthesized material was pure zoledronic acid monohydrate and was the same as the standard of the USP and the literature references.

Batch production was carried out with the expired patents, and the product was precipitated in water, the recovery ratio was approximately 32 per cent. In the case of crystallization with water followed by ethanol precipitation 38 per cent recovery ratio was obtained. After using 20 per cent excess H_3PO_3 the recovery ratio became 43 per cent. With the use of 50 per cent excess H_3PO_3 recovery ratio became 50 per cent. Exergy efficiency of the entire process was the highest in this case. When, 75 per cent of the ethanol, employed in the crystallization step was recovered with distillation, the efficiency decreased due to the exergy expenditure for distillation. With the use of 50 per cent excess H_3PO_3 , the highest recovery ratio, 50 per cent, and the highest exergy efficiency, 3.52×10^{-2} per cent, were obtained (Table 6.1). The highest energy utilizing steps were the crystallization carried out under class C conditions and the HVAC work. Exergy efficiency was very low in all of the aforementioned cases. Although recovery of 50 per cent of the waste heat was found to improve the exergy efficiency by about 1.8 folds, recovering 75 per cent of the ethanol employed for crystallization did not cause any enhancement in exergy efficiency, but helped to improve the product to waste ratio.

Table 6.1. Variation of the yield and the exergetic efficiency under different reaction conditions

Reaction conditions	Recovery ratio	Exergy efficiency	Exergy efficiency after recovering 50 % of the waste heat	Product to waste ratio
Case 1: crystallization with water	32 %	1.47×10^{-4}	2.26×10^{-4}	0.035
Case 2: crystallization with water followed by ethanol precipitation	38 %	1.74×10^{-4}	2.68×10^{-4}	0.027
Case 3: % 20 excess H_3PO_3 crystallization with water followed by ethanol precipitation	43 %	1.97×10^{-4}	3.02×10^{-4}	0.031
Case 4: % 50 excess H_3PO_3 crystallization with water followed by ethanol precipitation	50 %	2.29×10^{-4}	3.52×10^{-4}	0.036
Case 5: % 50 excess H_3PO_3 crystallization with water followed by ethanol precipitation; 75 % of ethanol recovered with distillation	50 %	2.28×10^{-4}	3.49×10^{-4}	0.048

Exergy analysis was carried out for each step of manufacturing of the sterile finished product, including the mixing of the excipients, filtering to ensure the sterility, filling and packaging, quality control and transportation of the product. Manufacturing was carried out in the sterile rooms to ensure GMP quality standards. For each class of room, energy consumption is evaluated. Since filling is performed in Class A room to ensure sterile production, more electric power was employed in comparison with the other production steps due to the ventilation of the system to create a clean environment. Primary packaging materials contribute to the energy consumption during filling. Besides production of high quality packaging materials for sterile production, satisfying all the requirements of the solution stability, sterilization of the primary packaging materials was also consuming energy, therefore filling was found to be the most energy consuming step. However, since the package material is considered as a part of the finished product, the sum of wasted energy by the HVAC systems, sterilization, irreversible mixing, and materials used during the

manufacturing resulted in a relatively high CDP, 75 per cent. Renewability index of the chemical synthesis step was -319. The renewability index, RI, values were -123 for the unpackaged injectable solution production. Upon packaging RI became 0.68 since all of the packaging materials used were renewable. The CDP of the zoledronic acid synthesis and the unpackaged and the packaged injectable solution steps were 2.29×10^{-2} , 17, and 75 per cent, respectively. Running the system at the maximum conversion and exergy efficiency caused maximum product to waste ratio and minimum waste generation.

The finished dosage forms for zoledronic acid were mainly injectable forms. Considering the active pharmaceutical product amounts are very low in this product, the starting materials used in the process were also very low and it is not economically worthy to change the experimental set-up. According to the exergy analysis the most energy consuming step for the overall process was drying after the chemical synthesis. Additional work could be applied to optimize the drying time and vacuum pressure. Additionally, there are different synthesis methods in the recent patents with different reaction conditions which could be studied for higher yields in the future.

REFERENCES

1. Menschutkin M. Ueber die Einwirkung des Chloracetyls auf phosphorige Säure. *Ann Chem Pharm.* 1865;133:317-320.
2. Russell RG, Rogers MJ. Bisphosphonates: from the laboratory to the clinic and back again. *Bone.* 1999;25:97–106.
3. Fleisch H, Russell RGG, Bisaz S, Casey P, Mühlbauer R. The influence of pyrophosphate analogues (diphosphonates) on the precipitation and dissolution of calcium phosphate in vitro and in vivo. *Calcif Tissue Res.* 1968;2:10-10a.
4. Fleisch H, Development of bisphosphonates. *Breast Cancer Res.* 2002;4:30-34
5. Fleisch H, Russell RGG, Straumann F. Effect of pyrophosphate on hydroxyapatite and its implications in calcium homeostasis. *Nature.* 1966;212:901-903.
6. Nancollas GH, Tang R, Phipps RJ. Novel insights into actions of bisphosphonates on bone: differences in interactions with hydroxyapatite. *Bone.* 2006;38:617–627.
7. Russell RG, Watts NB, Ebtino FH. Mechanisms of action of bisphosphonates: similarities and differences and their potential influence on clinical efficacy. *Osteoporosis International.* 2008;19:733–759.
8. Giger EV, Castagner B, Leroux J-C. Biomedical applications of bisphosphonates. *Journal of Controlled Release.* 2013;167:175–188.
9. Papapoulos SE. Bisphosphonates: how do they work?. *Best Practice & Research Clinical Endocrinology & Metabolism.* 2008;22(5):831–847.
10. Bauer DC, Black DM, Garnero P. Change in bone turnover and hip, non-spine, and vertebral fracture in alendronate-treated women: the fracture intervention trial. *Journal of Bone and Mineral Research.* 2004;19:1250–1258.

11. Rogers MJ. New insights into the molecular mechanisms of action of bisphosphonates. *Curr Pharm Des.* 2003;9:2643-58.
12. Brooker RJ, Widmaier E, Graham L, Stiling P. *Biology*, New York: McGraw-Hill; 2007.
13. Sato M, Grasser W, Endo N, Akins R, Simmons H, Thompson DD. Bisphosphonate action. Alendronate localization in rat bone and effects on osteoclast ultrastructure. *J Clin Invest.* 1991;88:2095-2105.
14. Felix R, Guenther HL, Fleisch H. The subcellular distribution of ¹⁴C dichloromethylene bisphosphonate and ¹⁴C-1-hydroxyethylidene-1,1-bisphosphonate in cultured calvaria cells. *Calcif Tissue Int.* 1984;36:108-13.
15. Boonekamp PM, Van der Wee-Pals LJ, Van Wijk-Van Lennep MM, Thesing CW, Bijvoet OL. Two modes of action of bisphosphonates on osteoclastic resorption of mineralized matrix. *Bone Miner.* 1986;1:27-39.
16. Russel RGG. Bisphosphonates: The first 40 years. *Bone.* 2011;49:2-19.
17. Fleisch H. Development of bisphosphonates. *Breast Cancer Res.* 2002;4:30-34
18. Benedict JJ. The physical chemistry of the diphosphonates-Its relationship to their structural activity. *Symposium CEMO IV. Nyon Switzerland, Medecine est Hygiene.* 1982;1-19.
19. Thompson K, Rogers MJ, Coxon FP, Crockett JC. Cytosolic entry of bisphosphonate drugs requires acidification of vesicles after fluidphase endocytosis, *Mol Pharmacol*, 2006, 69, 1624-32.
20. Baron R, Neff L, Louvard D, Courtoy PJ. Cell-mediated extracellular acidification and bone resorption: evidence for a low pH in resorbing lacunae and localization of a 100-

- kD lysosomal membrane protein at the osteoclast ruffled border. *J. Cell Biol.* 1985;101:2210–2222.
21. Blair H, Teitelbaum S, Ghiselli R, Gluck S. Osteoclastic bone resorption by a polarized vacuolar proton pump. *Science.* 1989;245:855–857.
 22. Frith JC, Mönkkönen J, Blackburn GM, Russell RGG, Rogers MJ. Clodronate and liposome-encapsulated clodronate are metabolized to a toxic ATP analog, adenosine 5'-(β , γ -dichloromethylene) triphosphate, by mammalian cells in vitro. *J. Bone Miner. Res.* 1997;12:1358–1367.
 23. Lehenkari PP, Kellinsalmi M, Nöpänkangas JP, Ylitalo KV, Mönkkönen J, Rogers MJ, Azhayev A, Väänänen HK, Hassinen IE. Further insight into mechanism of action of clodronate: inhibition of mitochondrial ADP/ATP translocase by a nonhydrolyzable, adenine-containing metabolite. *Mol. Pharmacol.* 2002;61:1255–1262.
 24. Van Beek E, Pieterman E, Cohen L, Löwik C, Papapoulos S. Farnesyl pyrophosphate synthase is the molecular target of nitrogen-containing bisphosphonates. *Biochem. Biophys. Res. Commun.* 1999;264:108–111.
 25. Luckman SP, Hughes DE, Coxon FP, Russell RGG, Rogers MJ. Nitrogen-containing bisphosphonates inhibit the mevalonate pathway and prevent post-translational prenylation of GTP-binding proteins, including Ras. *J Bone Miner Res.* 1998;13:581–9.
 26. Benford HL, Frith JC, Auriola S, Mönkkönen J, Rogers MJ. Farnesol and geranylgeraniol prevent activation of caspases by aminobisphosphonates: biochemical evidence for two distinct pharmacological classes of bisphosphonate drugs. *Mol Pharmacol.* 1999;56:131–40.
 27. Amin D, Cornell SA, Gustafson SK, Needle SJ, Ullrich JW, Bilder GE. Bisphosphonates used for the treatment of bone disorders inhibit squalene synthase and cholesterol biosynthesis. *J Lipid Res.* 1992;33:1657–63.

28. Goldstein JL, Brown MS. Regulation of the mevalonate pathway. *Nature*. 1990;343:425–30.
29. Rogers MJ, Crockett JC, Coxon FP, Mönkkönen J. Biochemical and molecular mechanisms of action of bisphosphonates. *Bone*. 2011;49(1):34-41.
30. Zhang FL and Casey PJ. Protein isoprenylation: Molecular mechanisms and functional consequences. *Annu Rev. Biochem*. 1996;65:241-269.
31. Ory S, Brazier H, Pawlak G, Blangy A. Rho GTPases in osteoclasts: orchestrators of podosome arrangement. *Eur J Cell Biol*. 2008;87:469–77.
32. Dunford JE, Rogers MJ, Ebetino FH, Phipps RJ, Coxon FP. Inhibition of protein prenylation by bisphosphonates causes sustained activation of Rac, Cdc42 and Rho GTPases. *J Bone Miner Res*. 2006;21:684–94.
33. Coxon FP, Helfrich MH, van't Hof RJ, Sehti SM, Ralston SH, Hamilton AD. Protein geranylgeranylation is required for osteoclast formation, function, and survival: inhibition by bisphosphonates and GGTI-298. *J Bone Miner Res*. 2000;15:1467–76.
34. Bergstrom JD, Bostedor RG, Masarachia PJ, Reszka AA, Rodan G. Alendronate is a specific, nanomolar inhibitor of farnesyl diphosphate synthase. *Arch Biochem Biophys*. 2000;373:231–41.
35. Staal A, Frith JC, French MH, Swartz J, Gungor T, Harrity TW. The ability of statins to inhibit bone resorption is directly related to their inhibitory effect on HMG-CoA reductase activity. *J Bone Miner Res*. 2003;18:88–96.
36. Fisher JE, Rodan GA, Reszka AA. In vivo effects of bisphosphonates on the osteoclast mevalonate pathway. *Endocrinology*. 2000;141:4793–6.
37. Sato M, Grasser W. Effects of bisphosphonates on isolated rat osteoclasts as examined by reflected light microscopy. *J Bone Miner Res*. 1990;5(1):31–40.

38. Coxon FP, Rogers MJ. The role of prenylated small GTP-binding proteins in the regulation of osteoclast function. *Calcif Tissue Int.* 2003;72:80–4.
39. Zhao H, Laitala-Leinonen T, Parikka V, Vaananen HK. Downregulation of small gtpase rab7 impairs osteoclast polarization and bone resorption. *J Biol Chem.* 2001;276: 39295–302.
40. Pavlos NJ, Xu J, Riedel D, Yeoh JS, Teitelbaum SL, Papadimitriou JM. Rab3D regulates a novel vesicular trafficking pathway that is required for osteoclastic bone resorption. *Mol Cell Biol.* 2005;25:5253–69.
41. Coxon FP, Helfrich MH, Larijani B, Muzylak M, Dunford JE, Marshall D. Identification of a novel phosphonocarboxylate inhibitor of Rab geranylgeranyl transferase that specifically prevents Rab prenylation in osteoclasts and macrophages. *J Biol Chem.* 2001;276:48213–22.
42. Glantschnig H, Fisher JE, Wesolowski G, Rodan GA, Reszka AA. M-CSF, TNFalpha and RANK ligand promote osteoclast survival by signaling through mTOR/S6 kinase. *Cell Death Differ.* 2003;10:1165–77.
43. Rodan GA, Martin TJ. Therapeutic approaches to bone diseases. *Science.* 2000;289: 1508–1514.
44. Bansal G, Wright JEI, Kucharski C, Uludag H. A dendritic tetra(bisphosphonic acid) for improved targeting of proteins to bone. *Angew. Chem. Int.* 2005;44:3710–3714.
45. Ogawa K, Mukai T, Arano Y, Ono M, Hanaoka H, Ishino S, Hashimoto K, Nishimura H, Saji H. Development of a rhenium-186-labeled MAG3-conjugated bisphosphonate for the palliation of metastatic bone pain based on the concept of bifunctional radiopharmaceuticals. *Bioconjug. Chem.* 2005;16:751–757.
46. Morioka M, Kamizono A, Takikawa H, Mori A, Ueno H, Kadowaki S-I, Nakao Y, Kato K, Umezawa K. Design, synthesis, and biological evaluation of novel estradiol–

- bisphosphonate conjugates as bone-specific estrogens. *Bioorg. Med. Chem.* 2010;18:1143–1148.
47. Danenberg HD, Fishbein I, Epstein H, Waltenberger J, Moerman E, Mönkkönen J, Gao J, Gathi I, Reichi R, Golomb G. Systemic depletion of macrophages by liposomal bisphosphonates reduces neointimal formation following balloon-injury in the rat carotid artery. *J. Cardiovasc. Pharmacol.* 2003;42:671–679.
 48. Danenberg HD, Fishbein I, Gao J, Mönkkönen J, Reich R, Gati I, Moerman E, Golomb G. Macrophage depletion by clodronate-containing liposomes reduces neointimal formation after balloon injury in rats and rabbits. *Circ. Res.* 2002;106:599–605.
 49. Portet D, Denizot B, Rump E, Lejeune J-J, Jallet P. Nonpolymeric coatings of iron oxide colloids for biological use as magnetic resonance imaging contrast agents. *J. Colloid Interface Sci.* 2001;238:37–42.
 50. Rosales RTM, Tavaré R, Glaria A, Varma G, Protti A, Blower PJ. ^{99m}Tc-bisphosphonate-iron oxide nanoparticle conjugates for dual-modality biomedical imaging. *Bioconjug. Chem.* 2011;22:455–465.
 51. Chapon C, Franconi F, Lacoëuille F, Hindré F, Saulnier P, Benoit J-P, Le Jeune J-J, Lemaire L. Imaging E-selectin expression following traumatic brain injury in the rat using a targeted USPIO contrast agent. *Magn. Reson. Mater. Phys. Biol. Med.* 2009;22:167–174.
 52. Greiner SH, Wildemann B, Back DA, Alidoust M, Schwabe P, Haas NP, Schmidmaier G. Local application of zoledronic acid incorporated in a poly(D, L-lactide)-coated implant accelerates fracture healing in rats. *Acta Orthop.* 2008;79:717–725.
 53. Stadelmann VA, Terrier A, Gauthier O, Bouler JM, Pioletti DP. Prediction of bone density around orthopedic implants delivering bisphosphonate. *J. Biomech.* 2009;42:1206–1211.

54. Gartrell BA, Coleman RE, Fizazi K, Miller K, Sternberg CN, Galsky MD, Saad F. Toxicities Following Treatment with Bisphosphonates and Receptor Activator of Nuclear Factor- κ B Ligand Inhibitors in Patients with Advanced Prostate Cancer. *European Urology*. 2014;65(2):278–286.
55. Camm JA. Review of the Cardiovascular Safety of Zoledronic Acid and Other Bisphosphonates for the Treatment of Osteoporosis. *Clinical Therapeutics*. 2010;32(3):426-36.
56. Zuradelli M, Masci G, Biancofiore G, Gullo G, Scorsetti M, Navarria P. High incidence of hypocalcemia and serum creatinine increase in patients with bone metastases treated with zoledronic acid. *Oncologist*. 2009;14:548-56.
57. Arboleya L, Alperi M, Alonsa S. Adverse effects of bisphosphonates. *Reumatol Clin*. 2011;7(3):189-197.
58. Black DM, Delmas PD, Eastell R, Reid IR, Boonen S, Cauley JA. Once-yearly zoledronic acid for treatment of postmenopausal osteoporosis. *N Engl J Med*. 2007;356: 1809-22.
59. Silverman S. Osteonecrosis of the Jaw (ONJ). *American College of Rheumatology*. 2012;1-4.
60. Marx RE. Pamidronate (Aredia) and Zoledronate (Zometa) induced avascular necrosis of the jaws: a growing epidemic. *Journal of Oral and Maxillofacial Surgery*. 2003;61: 1238-9.
61. Ruggiero SL, Mehrotra B, Rosenberg TJ, Engroff SL. Osteonecrosis of the jaws associated with the use of bisphosphonates: a review of 63 cases. *Journal of Oral and Maxillofacial Surgery*. 2004;62:527-34.

62. Bamias A, Kastritis E, Bamia C, Moulopoulos LA, Melakopoulos I, Bozas G. Osteonecrosis of the jaw in cancer after treatment with bisphosphonates: incidence and risk factors. *J Clin Oncol*. 2005;23:8580-7.
63. Woo SB, Hellstein JW, Kalmar JR. Narrative review: bisphosphonates and osteonecrosis of the jaws. *Ann Intern Med*. 2006;144:753-61.
64. Burr DB, Allen M.R. Mandibular necrosis in beagle dogs treated with bisphosphonates. *Orthod Craniofac Res*. 2009;12:221-8.
65. Pazianas M, Miller P, Blumentals WA, Bernal M, Kothawala P. A Review of the literature on osteonecrosis of the jaw in patients with osteoporosis treated with oral bisphosphonates: Prevalence, risk factors, and clinical characteristics. *Clin Ther*. 2007;29(8):1548-58.
66. Saeki T, Sasaki Y, Itoh K, Igarashi T, Minami H. Zoledronate: phase I and pharmacokinetics/pharmacodynamics study in cancer patients. *Bone*. 2000;26:41S.
67. Chen T, Berenson J, Vescio R. Pharmacokinetics and pharmacodynamics of zoledronic acid in cancer patients with bone metastases. *J Clin Pharmacol*. 2002;42:1228–36.
68. Brown JE, Ellis SP, Lester JE. Prolonged efficacy of a single dose of the bisphosphonate zoledronic acid. *Clin Cancer Res*. 2007;13:5406–10.
69. Bone HG, Hosking D, Devogelaer JO, Tucci JR, Emkey RD, Tonino RP, Rodriguez-Portales JA, Downs RW, Gupta J, Santora AC, Liberman U. Alendronate phase III osteoporosis treatment study group. Ten years' experience with alendronate for osteoporosis in postmenopausal women. *N Engl J Med*. 2004;350:1189–99.
70. Walsh JP, Ward LC, Stewart GO, Will RK, Criddle RA, Prince RL, Stuckey BG, Dhaliwal SS, Bhagat CI, Retallack RW, Kent GN, Drury PJ, Vasikaran S, Gutteridge

- DH. A randomized clinical trial comparing oral alendronate and intravenous pamidronate for the treatment of Paget's disease of bone. *Bone*. 2004;34:747–54.
71. Wellington K, Goa KL. Zoledronic acid: a review of its use in the management of bone metastases and hypercalcaemia of malignancy. *Drugs*. 2003;63:417–37.
72. Lane JM, Khan SN, O'Connor WJ, Nydick M, Hommen JP, Schneider R, Tomin E, Brand J, Curtin J. Bisphosphonate therapy in fibrous dysplasia. *Clin Orthop*. 2001;382:6–12.
73. Lehmann H.J., Mouritzen U., Christgau S., Cloos P.A., Christiansen C., Effect of bisphosphonates on cartilage turnover assessed with a newly developed assay for collagen type II degradation products. *Ann Rheum Dis*. 2002;61:530–3.
74. Maksymowych WP. Bisphosphonates for arthritis—a confusing rationale. *J Rheumatol*. 2003;30:430–4.
75. Aspray TJ, Francis RM. Treatment of osteoporosis in women intolerant of oral bisphosphonates. *Maturitas*. 2012;71(1):76-8.
76. Wilkes MM, Navickis RJ, Chan WW, Lewiecki EM. Bisphosphonates and osteoporotic fractures: across-design synthesis of results among compliant/persistent postmenopausal women in clinical practice versus randomized controlled trials. *Osteoporosis International*. 2010;21(4):679–88.
77. von Knoch F, Jaquier C, Kowalsky M, Schaeren S, Alabre C, Martin I, Rubash HE, Shanbhag AS. Effects of bisphosphonates on proliferation and osteoblast differentiation of human bone marrow stromal cells. *Biomaterials*. 2005;26(34):6941-9.
78. Jansen JP, Bergman GJ, Huels J, Olson M. The efficacy of bisphosphonates in the prevention of vertebral, hip, and nonvertebral-nonhip fractures in osteoporosis: a network meta-analysis. *Semin Arthritis Rheum*. 2011;40(4):275-84.

79. Naidu A, Dechow PC, Spears R, Wright JM, Kessler HP, Opperman LA. The effects of bisphosphonates on osteoblasts in vitro. *Oral Surg Oral Med Oral Pathol Oral Radiol Endod.* 2008;106(1):5-13.
80. Rääkkönen J, Mönkkönen H, Auriola S, Mönkkönen J. Mevalonate pathway intermediates downregulate zoledronic acid-induced isopentenyl pyrophosphate and ATP analog formation in human breast cancer cells. *Biochem Pharmacol.* 2010;79(5):777-83.
81. Skerjanec A, Berenson J, Hsu C, Major P, Miller Jr WH, Ravera C. The pharmacokinetics and pharmacodynamics of zoledronic acid in cancer patients with varying degrees of renal function. *J Clin Pharmacol.* 2003;43:154-62.
82. Coxon F.P., Thompson K., Roelofs A.J., Ebetino F.H., Rogers M.J., Visualizing mineral binding and uptake of bisphosphonate by osteoclasts and non-resorbing cells. *Bone*, 2008; 42: 848-60.
83. Roelofs AJ, Coxon FP, Ebetino FH, Lundy MW, Henneman Z.J., Nancollas G.H., Fluorescent risedronate analogues reveal bisphosphonate uptake by bone marrow monocytes and localization around osteocytes in vivo. *J Bone Miner Res.* 2010;25:606-16.
84. Mönkkönen H, Kuokkanen J, Holen I, Evans A, Lefley DV, Jauhiainen M. Bisphosphonate-induced ATP analog formation and its effect on inhibition of cancer cell growth. *Anticancer Drugs.* 2008;19:391-9.
85. Aparicio A, Gardner A, Tu Y, Savage A, Berenson J, Lichtenstein A. In vitro cytoreductive effects on multiple myeloma cells induced by bisphosphonates. *Leukemia.* 1998;12:220-9.
86. Corso A, Ferretti E, Lunghi M, Zappasodi P, Mangiacavalli S, De Amici M. Zoledronic acid down-regulates adhesion molecules of bone marrow stromal cells in

- multiple myeloma: a possible mechanism for its antitumor effect. *Cancer*. 2005;104:118-25.
87. Gordon S, Helfrich MH, Sati HI, Greaves M, Ralston SH, Culligan DJ. Pamidronate causes apoptosis of plasma cells in vivo in patients with multiple myeloma. *Br J Haematol*. 2002;119:475-83.
 88. Guenther A, Gordon S, Tiemann M, Burger R, Bakker F, Green JR. The bisphosphonate zoledronic acid has antimyeloma activity in vivo by inhibition of protein prenylation. *Int J Cancer*. 2010;126:239-46.
 89. Tassone P, Forciniti S, Galea E, Morrone G, Turco MC, Martinelli V. Growth inhibition and synergistic induction of apoptosis by zoledronate and dexamethasone in human myeloma cell lines. *Leukemia*. 2000;14:841-4.
 90. Ural AU, Yilmaz MI, Avcu F, Pekel A, Zerman M, Nevruz O. The bisphosphonate zoledronic acid induces cytotoxicity in human myeloma cell lines with enhancing effects of dexamethasone and thalidomide. *Int J Hematol*. 2003;78:443-9.
 91. Tassone P, Galea E, Forciniti S, Tagliaferri P, Venuta S. The IL-6 receptor super-antagonist Sant7 enhances antiproliferative and apoptotic effects induced by dexamethasone and zoledronic acid on multiple myeloma cells. *Int J Oncol*. 2002;21:867-73.
 92. Saag K, Lindsay R, Kriegman A, Beamer E, Zhou W. A single zoledronic acid infusion reduces bone resorption markers more rapidly than weekly oral alendronate in postmenopausal women with low bone mineral density. *Bone*. 2007;40(5):1238-43.
 93. Galasko CSB. *Skeletal Metastases*. London: Butterworth; 1986.
 94. Parker SL, Tong T, Bolden S. Cancer statistics. *CA Cancer J Clin*. 1997;47:5-27.

95. Coleman RE. Clinical features of metastatic bone disease and risk of skeletal morbidity. *Clin Cancer Res.* 2006;12:6243s–9s.
96. Brown JE, Cook RJ, Major P, Lipton A, Saad F, Smith M. Bone turnover markers as predictors of skeletal complications in prostate cancer, lung cancer, and other solid tumors. *J Natl Cancer Inst.* 2005;97(1):59–69.
97. Jacobs SC, Lawson RK. Mitogenic factor in human prostate extracts. *Urology.* 1980;16: 488.
98. Goltzman D. Mechanisms of the development of osteoblastic metastases. *Cancer.* 1997; 80:1581–1587.
99. Fournier P, Boissier S, Filleur S. Bisphosphonates inhibit angiogenesis in vitro and testosterone-stimulated vascular regrowth in the ventral prostate in castrated rats. *Cancer Res.* 2002;62:6538–44.
100. Boissier S, Ferreras M, Peyruchaud O. Bisphosphonates inhibit breast and prostate carcinoma cell invasion, an early event in the formation of bone metastases. *Cancer Res.* 2000;60:2949–54.
101. Fromigue O, Lagneaux L, Body JJ. Bisphosphonates induce breast cancer cell death in vitro. *J Bone Miner Res.* 2000;15:2211–21.
102. Senaratne SG, Pirianov G, Mansi JL, Arnett TR, Colston KW. Bisphosphonates induce apoptosis in human breast cancer cell lines. *Br J Cancer.* 2000;82(8):1459–1468.
103. Verdijk R, Franke HR, Wolbers F, Vermes I. Differential effects of bisphosphonates on breast cancer cell lines. *Cancer Lett.* 2007;246:308–12.
104. Wood J, Bonjean K, Ruetz S. Novel antiangiogenic effects of the bisphosphonate compound zoledronic acid. *J Pharmacol Exp Ther.* 2002;302:1055–61.

105. Senaratne SG, Mansi JL, Colston KW. The bisphosphonate zoledronic acid impairs Ras membrane [correction of impairs membrane] localisation and induces cytochrome c release in breast cancer cells. *Br J Cancer*. 2002;86:1479–86.
106. Hiraga T, Williams PJ, Ueda A, Tamura D, Yoneda T. Zoledronic acid inhibits visceral metastases in the 4T1/luc mouse breast cancer model. *Clin Cancer Res*. 2004;10:4559–67.
107. Jagdev SP, Coleman RE, Shipman CM, Rostami HA, Croucher PI. The bisphosphonate, zoledronic acid, induces apoptosis of breast cancer cells: evidence for synergy with paclitaxel. *Br J Cancer*. 2001;84:1126–34.
108. Green JR. Bisphosphonates: preclinical review. *Oncologist*. 2004;9(4):3–13.
109. Kanis JA, Powles T, Patterson AHG, McCloskey EV, Ashley S. Clodronate decreases the frequency of skeletal metastases in women with breast cancer. *Bone*. 1996;19(6):663–667.
110. Powles TJ, Patterson S, Kanis JA. Randomized, placebocontrolled trial of clodronate in patients with primary operable breast cancer. *J Clin Oncol*. 2002;20:3219–3224.
111. Diel IJ, Solomayer EF, Costa S. Reduction in new metastases in breast cancer with adjuvant clodronate treatment. *N Engl J Med*. 1998;339:357–363.
112. Saarto T, Blomqvist C, Virkkunen P, Elomaa I. Adjuvant clodronate treatment does not reduce the frequency of skeletal metastases in node-positive breast cancer patients: 5-year results of a randomised controlled trial. *J Clin Oncol*. 2001;19(1):10–17.
113. Mardiak J, Bohunicky L, Chovanec J, Salek T, Koza I. Adjuvant clodronate therapy in patients with locally advanced breast cancer-long term results of a double blind randomised trial. Slovak Clodronate Collaborative Group. *Neoplasma*. 2000;47(3):177–180.

114. Shipman CM, Croucher PI, Russell RG, Helfrich MH, Rogers MJ. The bisphosphonate incadronate (YM175) causes apoptosis of human myeloma cells in vitro by inhibiting the mevalonate pathway. *Cancer Res.* 1998;58:5294-7.
115. Boise LH, Gonzalez-Garcia M, Postema C.E., Bcl-x, a bcl2-related gene that functions as a dominant regulator of apoptotic cell death. *Cell.* 1993;74:597-608.
116. Boisser SS, Vaananen HK, Harkonene PL, Lakkakorpi PT. Alendronate inhibits invasion of PC-3 prostate cancer cells by affecting the mevalonate pathway. *Cancer Res.* 2002;62:2708-2714.
117. Teronen O, Heikkila P, Konttinen YT. MMP inhibition and downregulation by bisphosphonates. *Ann N Y Acad Sci.* 1999;878:453-465.
118. Neville-Webbe HL, Holen I, Coleman RE. The anti-tumour activity of bisphosphonates. *Cancer Treat Rev.* 2002;28(6):305-19.
119. van der Pluijm G, Vloedgraven H, van Beek E, van der WeePals L, Lowik C, Papapoulos S. Bisphosphonates inhibit the adhesion of breast cancer cells to bone matrices in vitro. *J Clin Invest.* 1996;98(3):698-705.
120. Hortobagyi GN. Novel approaches to the management of bone metastases in patients with breast cancer. *Semin Oncol.* 2002;29(11):134-44.
121. Coleman RE. Metastatic bone disease: clinical features, pathophysiology and treatment strategies. *Cancer Treat Rev.* 2001;27:165-76.
122. Mundy GR. Metastasis to bone: causes, consequences and therapeutic opportunities. *Nat Rev Cancer.* 2002;2:584-93.
123. Janjan N. Bone metastases: approaches to management. *Semin Oncol.* 2001;28:28-34.

124. Boissier S, Magnetto S, Frappart L. Bisphosphonates inhibit prostate and breast carcinoma cell adhesion to unmineralised and mineralised bone extracellular matrices. *Cancer Res.* 1997;57(18):3890–3894.
125. Rosen LS, Gordon D, Kaminski M. Long-term efficacy and safety of zoledronic acid compared with pamidronate disodium in the treatment of skeletal complications in patients with advanced multiple myeloma or breast carcinoma: a randomized, double-blind, multicenter, comparative trial. *Cancer.* 2003;98:1735–44.
126. Fitzpatrick JM, Colombel M, Saad F, Sternberg CN, Tubaro A. Treatment strategies in advanced prostate cancer/genitourinary malignancies: The use of bisphosphonates across the continuum. *European Urology Supplements.* 2009;8 (9):733-737.
127. Smith MR. Zoledronic acid to prevent skeletal complications in cancer: corroborating the evidence. *Cancer Treat Rev.* 2005;31(3):19-25.
128. Saad F. New research findings on zoledronic acid: Survival, pain, and anti-tumour effects. *Cancer Treatment Reviews.* 2008;34(2):183-192.
129. Clézardin P. Anti-tumour activity of zoledronic acid. *Cancer Treat Rev.* 2005;31(3):1-8.
130. Dinçer I, Rosen MA. *Exergy*, London: Elsevier; 2007.
131. Dinçer I. Exergy as a potential tool for sustainable drying systems. *Sustainable Cities and Society.* 2011;1: 91-96.
132. Jokandan MJ, Aghbashlo M, Mohtasebi SS. Comprehensive exergy analysis of an industrial-scale yogurt production plant. *Energy.* 2015;93:1832-1851.
133. Moran MJ. *Availability Analysis: A Guide to Efficient Energy Use.* New York:ASME; 1989.

134. Moran MJ, Sciubba E. Exergy analysis: Principles and practice. *J. Engineering for Gas Turbines and Power*. 1994;116:285–290.
135. Rosen MA, Dincer I. Thermal storage and exergy analysis: The impact of stratification. *Trans. CSME*. 1999;23(1B):173–186.
136. Dincer I, Dost S, Li X. Performance analyses of sensible heat storage systems for thermal applications. *Int. J. Energy Research*. 1997;21(10):1157–1171.
137. Degerli B, Nazir S, Sorgüven E, Hitzmann B, Özilgen M. Assessment of energy and exergy efficiencies of farm to fork grain cultivation and bread making processes in Turkey and Germany. *Energy*. 2015;93:421-434.
138. Genç S, Hepbasli A. Performance assessment of a potato crisp frying process. *Dry Technol*. 2015;33(7):865-875.
139. Pelvan E, Özilgen M. Assessment of energy efficiency and renewability of black tea, instant tea and ice tea production and waste valorization processes. *Sustainable Production and Consumption*. 2017;12:59-77.
140. Nasiri F, Aghbashlo N, Rafiee S. Exergy analysis of an industrial-scale ultrafiltrated (UF) cheese production plant: a detailed survey. *Heat and mass transfer*. 2017;53: 407-424.
141. Genç M, Genç S, Goksungur Y. Exergy analysis of wine production: Red wine production process as a case study. *Applied Thermal Engineering*. 2017;117:511-521.
142. Nimkar SC, Mewada RK. An overview of exergy analysis for chemical process industries. *International Journal of Exergy*. 2014;15(4):468-507.
143. Madloul NA, Saidur R, Rahim NA, Islam MR, Hossian MS. An exergy analysis for cement industries: An overview. *Renewable and Sustainable Energy Reviews*. 2012; 16:921–932.

144. Luis P. Exergy as a tool for measuring process intensification in chemical engineering. *Journal of Chemical Technology and Biotechnology*. 2013; 88(11):1951–1958.
145. Thompson T. Sustainable medicine: good for the environment, good for people. *British Journal of General Practice*. 2011;61(582):3–4.
146. Redshaw CH, Stahl-Timmins WM, Fleming LE, Davidson I, Depledge MH. Potential changes in disease patterns and pharmaceutical use in response to climate change. *Journal of Toxicol. Environ. Health B Crit Rev*. 2013;16(5):285-320.
147. Thomas F, Depledge M. Medicine ‘misuse’: Implications for health and environmental sustainability. *Social Science and Medicine*. 2015;143:81-87.
148. Hawker DW, Cropp R, Boonsaner M. Uptake of zwitterionic antibiotics by rice (*Oryza sativa* L.) in contaminated soil. *Journal of Hazardous Materials*. 2013;263:458-466.
149. Herrmann M, Olsson O, Fiehn R, Herrel M, Kümmerer K. (2015). The significance of different health institutions and their respective contributions of active pharmaceutical ingredients to wastewater. *Environment International*. 2015;85: 61-76.
150. California UO. An Introduction to NMR Spectroscopy. LibreTexts, Chemistry; [cited 2014, 21 Aug]. Available from: [https://chem.libretexts.org/Textbook_Maps/Organic_Chemistry_Textbook_Maps/Map%3A_Organic_Chemistry_\(Bruice\)/14%3A_A_NMR_Spectroscopy/14.01_The_Nature_of_Acids_and_Bases](https://chem.libretexts.org/Textbook_Maps/Organic_Chemistry_Textbook_Maps/Map%3A_Organic_Chemistry_(Bruice)/14%3A_A_NMR_Spectroscopy/14.01_The_Nature_of_Acids_and_Bases).
151. Paula Yurkanis B. *Organic Chemistry*. USA: Prentice Hall, 2004.
152. Reich HJ. 5-HMR-2 Chemical Shift. University of Wisconsin; [cited 2017, 12 June]. Available from: <https://www.chem.wisc.edu/areas/reich/nmr/05-hmr-02-delta.htm>
153. Reich HJ. Proton Chemical Shifts. Department of Chemistry at University of Wisconsin; [cited 2017, 03 March]. Available from: <https://www.chem.wisc.edu/areas/reich/nmr/h-data/hdata.htm>

154. Agilent Technologies brings ease of use to NMR with ProPulse system; [cited 2017, 03 March]. Available from: https://www.manufacturingchemist.com/news/article_page/Agilent_Technologies_brings_ease_of_use_to_NMR_with_ProPulse_system/93169
155. Columbia University. HMBC; [cited 2017, 05 July]. Available from: <http://www.columbia.edu/cu/chemistry/groups/nmr/HMBC.html>
156. Reusch W. Mass spectrometry. Michigan State University; [cited 2017, 05 July]. Available from: <https://www2.chemistry.msu.edu/faculty/reusch/virttxtjml/spectrpy/massspec/masspec1.htm>
157. Shimadzu Cooperation, Total Ion Chromatogram (TIC); [cited 2017, 05 July]. Available from: http://www.shimadzu.com/an/total_ion.html
158. Chrom Academy, Mass Spectrometry Fundamental LC-MS Mass Analysers; [cited 2017, 05 July]. Available from: http://www.chromacademy.com/lms/sco36/Fundamental_LC-MS_Mass_Analysers.pdf
159. Ion Source, Mass Spectrometry Educational Resource, Introduction to MS Quantitation and Modes of LC/MS Monitoring; [cited 2017, 05 July]. Available from: <http://www.ionsource.com/tutorial/msquan/intro.htm>
160. KRSS Ltd. Used Micromass Quattro Micro Mass Spectrometer; [cited 2018, 03 March]. Available from: <http://www.krssltd.com/used-refurbished-mass-spectrometer/triple-quad/micromass-quattro-micro>
161. FTIR / Fourier Transform Infra-Red Spectrophotometer. LDP Lab Services; [cited 2017, 10 July]. Available from: http://www.lpdlabservices.co.uk/analytical_techniques/chemical_analysis/ftir.php
162. Stuart, B. Introduction. *Infrared Spectroscopy: Fundamentals and Applications*. 2004:1-15.

163. Prasanthi MM, Rao BA, Rao BVN, Krishna YP, Ramana DV. Formulation and evaluation of zoledronic acid for injection by lyophilization technique. *International Research Journal of Pharmacy*. 2017;8(2):50-56.
164. IRAffinity-1S Fourier Transform Infrared Spectrophotometer. Shimadzu Corporation, Analytical and Measuring Instruments; [cited 2018, 3 March]. Available from: https://www.shimadzu.com/an/molecular_spectro/ftir/affinity/iraf.html
165. Schöffski K. Der lange weg zur gif treien karl-fischer titration. *Sonderdruckj aus GIT*, 1998;7:98.
166. Caro CA. Efficient, precise and fast water determination by the Karl Fischer titration. *Food Control*. 2001;12:431-436.
167. Toledo M. Good Titration Practice™ in KF Titration; [cited 2017, 1 May]. Available from: <http://www.ecslabonline.com/pdf/mettler-toledo-dogru-titrasyon-uygulamalari-ipuclari.pdf>
168. Mitsubishi Chemical Corp. What is the Karl Fischer method?; [cited 2017, 1 May]. Available from: <http://mckkf.com/english/kf-basic/what.html>
169. 841 Titrand. Metrohm; [cited 2018, 5 March]. Available from: <https://www.metrohm.com/en/products/28410010>
170. Toledo M. Karl Fischer Applications; [cited 2017, 1 May]. Available from: https://www.mt.com/dam/MT-NA/KarlFischerHelpPage/KF_Chemicals.pdf
171. Anderson Materials Evaluation, Differential Scanning Calorimetry (DSC) Thermal Analysis; [cited 2017, 29 June]. Available from: Inc.: <http://www.andersonmaterials.com/dsc.html>

172. Malvern Instruments Ltd. Differential Scanning Calorimetry; [cited 2017, 29 August]. Available from: <https://www.malvern.com/en/products/technology/differential-scanning-calorimetry>.
173. Biocompare, Lab Equipments, HPLC Systems; [cited 2017, 17 April]. Available from: <http://www.biocompare.com/Lab-Equipment/13035-HPLC-Systems/>
174. Vallano PS. Determination of risedronate in human urine by column-switching ion-pair high performance liquid chromatography with ultraviolet detection. *J. Chromatogr. B*, 2003;794:23–33.
175. Pettersson KN. Determination of phosphonoformate (foscarnet) in biological fluids by ion-pair reversed-phase liquid chromatography. *J. Chromatogr.* 1989;488:447–455.
176. Kwong EA. HPLC analysis of an amino bisphosphonate in pharmaceutical formulations using post-column derivatization and fluorescence detection. *J. Chromatogr. Sci.* 1990;445:233–238.
177. Daley-Yates PG. Assay of 1-hydroxy-3-aminopropylidene-1,1-bisphosphonate and related bisphosphonates in human urine and plasma by high performance ion chromatography. *J. Chromatogr.* 1989;490:329–338.
178. Aluoch AR. Stability indicating ion-pair HPLC method for the determination of risedronate in a commercial formulation. *J of Liquid Chromotography and Related Technologies.* 2004; 27(17):2799–2813.
179. Matuszewski L, Matuszewska A., Mazurkiewicz T, Rogalski J, Cho N-S, Ohga S. Determination of bisphosphonates by ion-pair HPLC. *J. Fac. Agr.* 2011;56(2):213–216.
180. Liquid Chromatography. Shimadzu Corporation, Analytical and measuring instruments; [cited 2018, 3 March]. Available from: <https://www.shimadzu.com/an/hplc/>

181. Ettre LS. Nomenclature for chromatography. *Pure and Appl. Chem.* 1993;65:819-872.
182. Supryniewicz ZB. Determination of veratric acid and its metabolites in biological material by ion-pair high-performance liquid chromatography. *J. Chromatogr.* 1984;286:253-260.
183. Prasad V, Pranothi M, Diwan VP, Kishore C. Development of HPLC Method for the Identification Related substances and Assay of Zoledronic acid in a tablet form. *British Biomedical Bulletin.* 2013;44-055.
184. Shanmugasundaram P, Sumithra MS. Development and Validation of Zoledronic Acid by using RP - HPLC method. *International Journal of Frontiers in Science and Technology.* 2013; 62-75.
185. Reddy LM, Reddy KJ, Reddy PR. A simple RP-HPLC Method for related substances of zoledronic acid in pharmaceutical products. *Arabian Journal of Chemistry.* 2017;10:196-204.
186. Mastanamma SK, Suresh G, Sindu Priya D, Seshagiri Rao JVLN. A Validated RP-HPLC Method for The Estimation of Zoledronic acid. *IJPSR.* 2011;3(3):826-829.
187. Nandan SR. A new Analytical Method for Estimation of zoledronic acid in commercial pharmaceutical injections by Ion-Exchange (IEC) High Performance Liquid. *Journal of Liquid Chromatography & Related Technologies.* 2011;34:476-489.
188. Nandan SR, Reddy R, Rao S, Ravindranath LK. Regulatory requirement – validated, specific, and stability indicating analytical method for zoledronic acid and its related impurities by Ion Pair Reversed Phase Liquid Chromatography (IP-RPLC). *Journal of Liquid Chromatography & Related Technologies.* 2009;32: 2307-2321.
189. PerkinElmer; Thermogravimetric Analysis (TGA), Beginners Guide; 2010, [cited 2017, 10 November]. Available from: file:///C:/Users/acer/Desktop/ZZAA/zoledronic%20acid/Literatural%20search/44-74556GDE_TGABeginnersGuide.pdf

190. TGA7 thermogravimetric Analyzer Perkin Elmer. UCL Engineering [cited 2018, 10 March]. Available from: <https://www.natureinspiredengineering.org.uk/facility/equipment/thermal-analyses/tga7-perkin-elmer>
191. Automatic Melting Point Apparatus, SMP 40. Jepson Bolton's International Catalogue; [cited 2018, 10 March]. Available from: <http://www.jepbol.com/sect3/SMP40.html>
192. European Pharmacopoeia (Ph. Eur.) 9th Edition, General Chapters 2.2.14.
193. Blum H, Worms K-H. Hydroxy-aminopropane-di:phosphonic acids prepn-from beta-alanine or poly-beta-alanine and phosphorous acid-phosphorus oxychloride. 1977. European Patent No. DE2702631.
194. Bosies E, Gall R. Diphosphonic acid derivatives. 1987. US Patent No. US4666895.
195. Sturtz G, Guervenou J. Synthesis of novel functionalized gem-bisphosphonates. *Synthesis, Journal of synthetic Organic Chemistry*. 1991;8:661-662.
196. Nugent WA, RajanBabu TV, Burk MJ. Beyond Nature's Chiral Pool: Enantioselective catalysts in industry. *Science*. 1993;259:479-483.
197. Kieczkowski GR, Jobson BR, Melillo DG, Reinhold DF, Grenda VJ, Shinkai I. Preparation of (4-Amino-1-Hydroxybutylidene)bisphosphonic acid sodium salt, MK-217 (alendronate sodium). An improved procedure for the preparation of 1-Hydroxy-1,1-bisphosphonic Acids. *J. Org. Chem*. 1995;60(25):8310–8312.
198. Kleemann A, Engel J, Kutscher B, Reichert D. *Pharmaceutical Substances, Syntheses, Patents and Applications of the most relevant APIs*. Stuttgart-New York: Theme; 2009.

199. Niju S., Begum M., Anantharaman N. Preparation of biodiesel from waste frying oil using a green and renewable solid catalyst derived from egg shell, *Environmental Progress & Sustainable Energy*. 2014; doi: 0.1002/ep.11939
200. Rosini S, Staibano G. Pharmacologically active biphosphonates, process for the preparation thereof and pharmaceutical compositions therefrom. 1986. US Patent No. US4621077.
201. Jaeggi KA, Widler L. Substituted alkanediphosphonic acids and pharmaceutical use. 1990. US Patent No. US 4939130.
202. Blum H, Worms K-H. Process for the production of 3-amino-1-hydroxypropane-1,1-diphosphonic acid. 1982. US Patent No. US 4327039.
203. Jary J, Rihakova V, Zobacova A. 6-Amino-1-hydroxyhexylidene diphosphonic acid, salts and a process for production thereof. 1981. US Patent No. US 4304734.
204. Blum H, Hempel H-U, Worms K-H. Hydroxyalkane diphosphonic acids. 1981. US Patent No. US4267108.
205. Blum H, Worms K-H. 1-Hydroxy-3-amino-alkane-1,1-diphosphonic acids and salts. US Patent No. US4054598.
206. Kieczkowski GR, Melillo DG, Jobson RB. Process for preparing 4-amino-1-hydroxybutylidene-1,1-bisphosphonic acid or salts thereof. 1990. US Patent No. US 4922007.
207. Kieczkowski GR. Process for preparing 4-amino-1-hydroxybutylidene-1,1-bisphosphonic acid (ABP) or salts thereof. 1991. US Patent No. US 5019651.
208. Dauer RR, DiMichele L, Futran M, Kieczkowski GR. Process for producing N-amino-1-hydroxy-alkylidene-1,1-bisphosphonic acids. 1996. US Patent No. US 5510517.

209. De FL, Turchetta S, Massardo P, Casellato P. Preparation of biphosphonic acids and salts thereof. 2003. Patent No. WO 2003093282.
210. Lifshitz-Liron R, Lidor-Hadas R. Process for purification of zoledronic acid. 2005. Patent No. WO 2004075860.
211. Kim J-D, Shin J-Y. Process for preparing sodium risedronate hemipentahydrate. 2012. US Patent No. US 8193355.
212. Mohakhud P, Murki V, Kishore Nandanmudi K, Babu M, Banerjee S. Crystalline form of zoledronic acid. 2006. US Patent No. US20060178439.
213. Danda SR, Garimella NKASS, Divvela SRVN, Dandala R, Meenakshisunderam S. Process for the preparation of biphosphonic acids. 2009. US Patent No. US 7528280.
214. Lerstrup K, Preikschat HF, Fischer E. Reagent and use thereof for the production of bisphosphonates. 2008. Patent No. WO2008058722.
215. Siverstein RM, Webster FX, Kiemle DJ. *Spectrometric Identification of Organic Compounds*. New York: John Wiley & Sons. 2005.
216. Srinivasa Rao DVN, Dandala R, Narayanan GKASS, Lenin R, Sivakumaran M, Naidu A. Novel Procedure for the synthesis of 1-hydroxy-1,1-bisphosphonic acids using phenols as medium. *Synthetic Communications: An International Journal for Rapid Communication of Synthetic Organic Chemistry*. 2007; 37(24):4359-4365.
217. Ratrouf SS, Al Sarabi AM, Sweidan KA. A One-pot and efficient synthesis of zoledronic acid starting from tert-butyl imidazol-1-yl acetate. *Pharmaceutical Chemistry Journal*. 2015;48(12):837-841.
218. NMR Predict, Institute of Chemical Sciences and Technoogy. [cited 2017 11 November]. Available from: http://www.nmrdb.org/new_predictor/index.shtml?v=v2.82.3

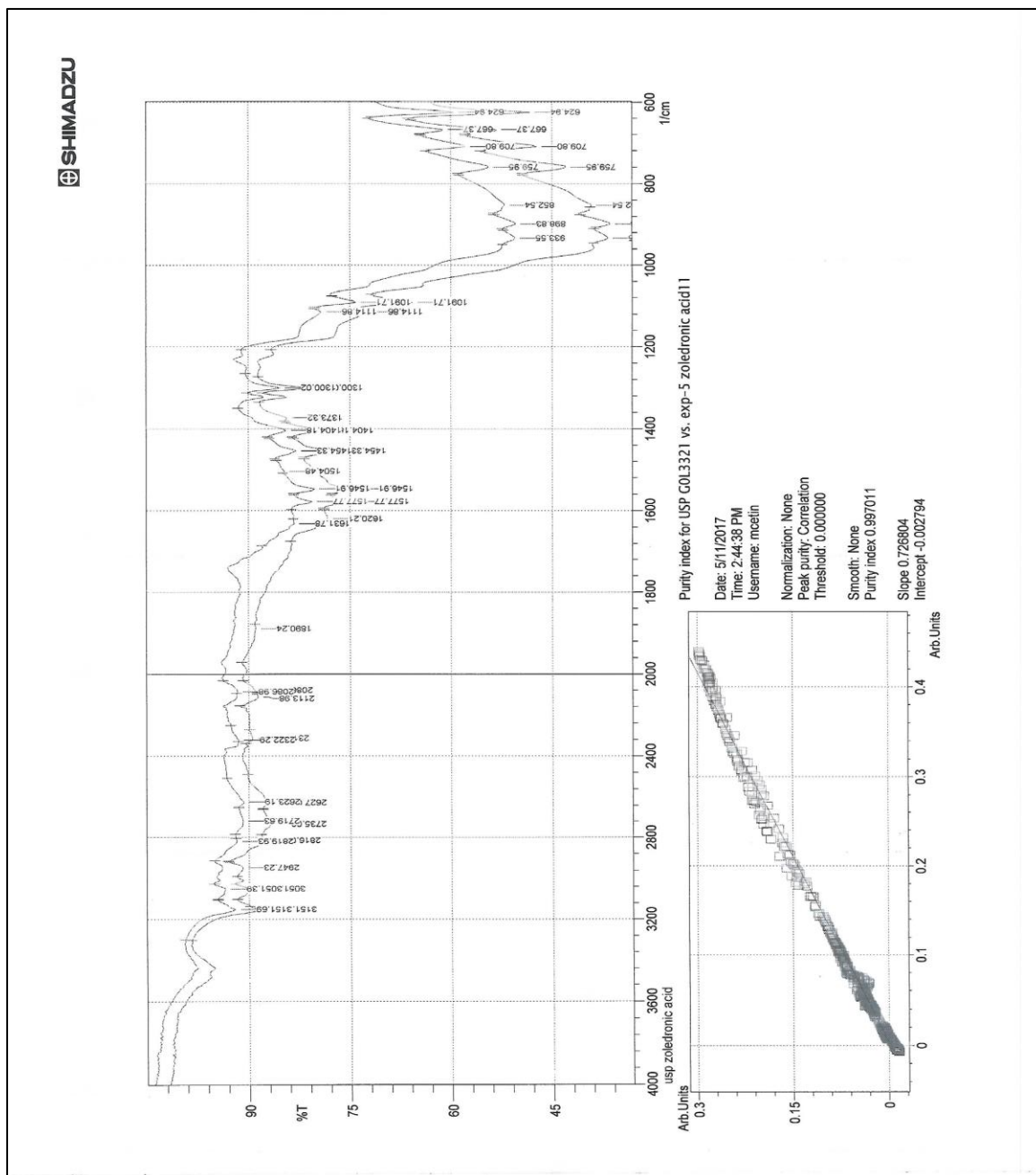
219. Samsel EG, Wu T-C. Process for manufacturing bisphosphonic acids. 2008. European Patent no. EP1996599.
220. Nuclear Magnetic Resonance Spectroscopy. [cited 2017 11 November]. Available from: <https://www2.chemistry.msu.edu/faculty/reusch/virttxtjml/spectrpy/nmr/nmr1.htm>
221. Pinto DCGA, Santos CMM, Silva AMS. Advanced NMR techniques for structural characterization of heterocyclic structures. *Recent Research Developments in Heterocyclic Chemistry*. 2007:397-475.
222. Chemistry, Libretexts, 5.8: NMR of phosphorylated molecules. [cited 2017 11 November]. Available from: [https://chem.libretexts.org/Textbook_Maps/Organic_Chemistry_Textbook_Maps/Map%3A_Organic_Chemistry_with_a_Biological_Emp_hasis_\(Soderberg\)/Chapter_05%3A_Structure_Determination_II/5.8%3A_NMR_of_phosphorylated_molecules](https://chem.libretexts.org/Textbook_Maps/Organic_Chemistry_Textbook_Maps/Map%3A_Organic_Chemistry_with_a_Biological_Emp_hasis_(Soderberg)/Chapter_05%3A_Structure_Determination_II/5.8%3A_NMR_of_phosphorylated_molecules)
223. U NMR Lab; COSY; [cited 2017 11 November]. Available from: <http://chem.ch.huji.ac.il/nmr/techniques/2d/cosy/cosy.html>
224. Parella T. Bruker Biospin; NMR Guide 3.5: 2D Experiments. [cited 2017 11 November]. Available from: http://triton.iqfr.csic.es/guide/eNMR/eNMR2_Dinv/hsqc2d.html
225. Columbia University: Chemistry: NMR: HMBC. [cited 2017 11 November]. Available from: <http://www.columbia.edu/cu/chemistry/groups/nmr/HMBC.html>
226. Reusch W. Mass Spectrometry. [cited 2017 14 November]. Available from: <https://www2.chemistry.msu.edu/faculty/reusch/virttxtjml/spectrpy/massspec/masspec1.htm>

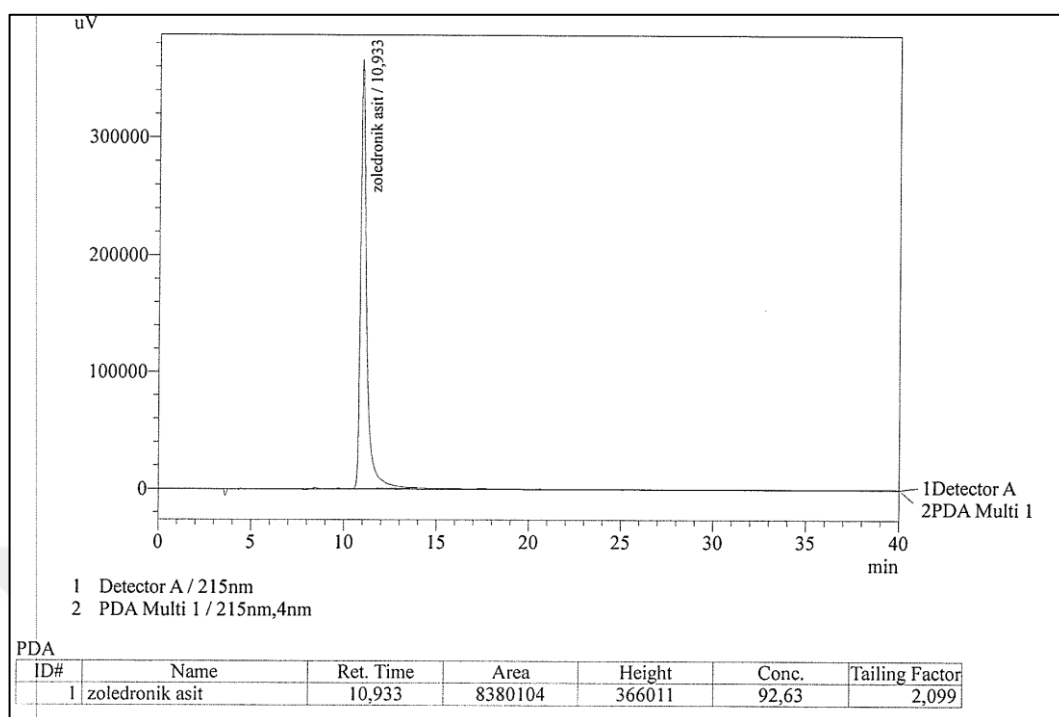
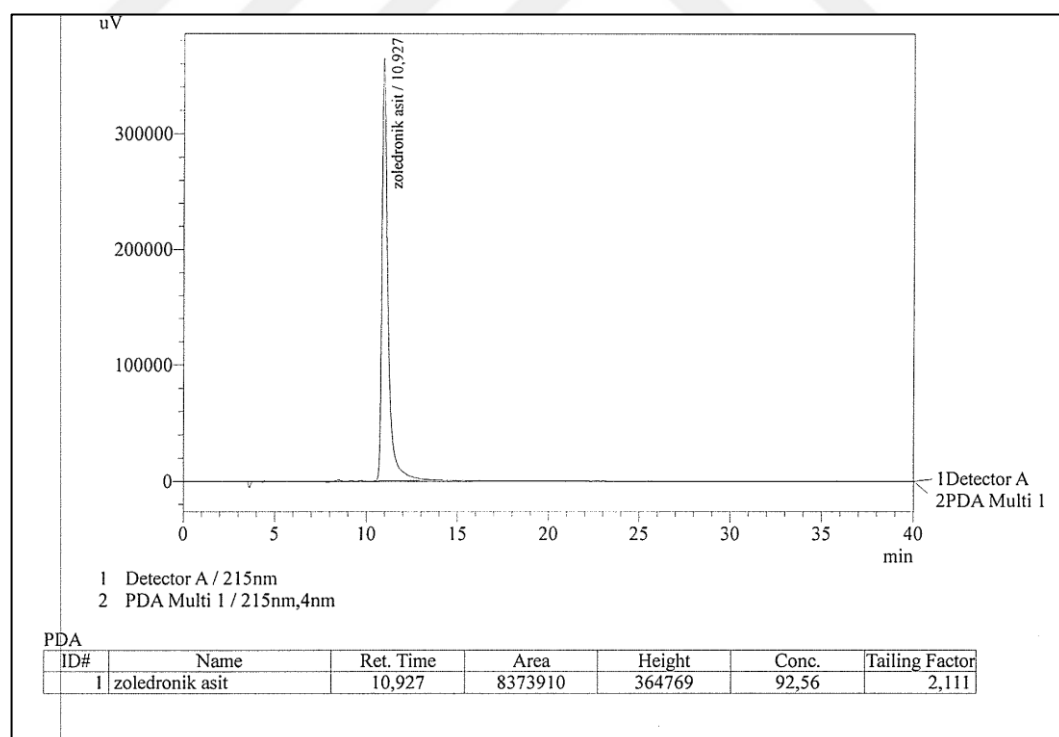
227. Premier Biosoft, Accelerating Research in Life Sciences. Mass Spectrometry. [cited 2017 14 November]. Available from: http://www.premierbiosoft.com/tech_notes/mass-spectrometry.html
228. Raccor BS, Sun J, Lawrencea RF, Li L, Zhang H, Somermanc MJ, Totah RA. Quantitation of zoledronic acid in murine bone by liquid chromatography coupled with tandem mass spectrometry. *Journal of Chromatography B*. 2013;935:54–60.
229. Aronhime J, Lifshitz-Liron R. Zoledronic acid crystal forms, zoledronate sodium salt crystal forms, amorphous zoledronate sodium salt, and processes for their preparation. 2003. US Patent No. US20050054616.
230. Mettler Toledo: Thermal Analysis of Zoledronic Acid Hydrate. [cited 2017 14 November]. Available from: https://www.mt.com/be/en/home/supportive_content/matchar_apps/MatChar_UC333.html
231. Labriola RA, Tombari DG, Vechhioli A. Crystalline form of the zoledronic acid, a process to obtain it and the pharmaceutical composition comprising it. 2005. US Patent No. US8952172.
232. Mohakhud P, Murki V, Kishore Nandanmudi K, Babu M, Banerjee S. Crystalline trihydrate of zoledronic acid. 2008. European Patent No. EP 1931326 A1.
233. Vasavi1 Y, Parthiban N, Kumar DS, Banji D, Srisutherson N, Ghosh S, Kumar Chakravarthy MV. Heteronuclear multiple bond correlation spectroscopy-An overview. *International Journal of Pharm Tech Research*. 2011;3(3):1410-1422.
234. RxMediaPharma 2016, Interactive pharmaceuticals information resource (in Turkish). [cited 2017 14 November]. Available from: <http://www.eczanet.com/>, accessed on August 10, 2017.
235. Szargut J. Energy and exergy analysis of the preheating of combustion reactants. *International Journal of Energy Research*. 1988;12:45–58.

236. Bioclean: Clean Room Technology. [cited 2017 14 November]. Available from: https://www.cleanroomtechnology.com/technical/article_page/Saving_energy_in_cleanrooms/100623
237. Glausch A, Löffler R, Sigg J. Pharmaceutical products comprising bisphosphonates. 2006. European Patent No. EP 1663314.
238. Nema S, Ludwig JD. (2010). *Pharmaceutical dosage forms- Parenteral medications*, 3rd ed. Vol. 1, CRC Press. New York.
239. UNIDO. 1993. Output of a seminar on energy conservation in glass industry; [cited 2017 14 November]. Available from: https://www.unido.org/fileadmin/import/user_files/puffk/glass.pdf, accessed June 19, 2014
240. Goldman R, Drain-clear container for aqueous-vehicle liquid pharmaceutical preparations. 1950. US Patent No. US 2504482.
241. Marstein ES. Sustainable silicon production. Centre for Environment-friendly Energy Research. 2016. [cited 2017 14 November]. Available from: <https://www.naturviterne.no/getfile.php/1318742/Nettside%202017/Bilder/Bilder%20-%20gamle%20format/002%20Artikkelbilder/2016/Naturviterforum%202016/presentasjoner/Marstein%20%40%20Naturviterne%20101116.pdf>
242. Ashmead EG, Gunzel EC, Moritz MP. Syringe stopper. 2010. USA Patent No. US8722178.
243. Choate WT, Green JAS. U.S. Energy requirements for aluminum production: historical perspective, theoretical limits and new opportunities. *TMS Annual Meeting*. 2003:99-113.
244. Best Available Techniques Reference Document in the non ferrous metals. (2001). European Commission, Integrated Pollution Prevention and Control (IPPC). [cited

- 2017 14 November]. Available from: http://eippcb.jrc.ec.europa.eu/reference/BREF/NFM/JRC107041_NFM_Bref_2017.pdf
245. Nielsen OSM, Jarsskov ET. Container closure and a method of making the same. 1978. USA Patent No. US4205754.
246. Langenhove JD. Thermodynamic optimization of the life cycle of plastics by exergy analysis. *International Journal of Energy Search*. 2004; 28(11):969-976.
247. Chow S, Hackett B, Ganji AR. Opportunities for energy efficiency and demand response in corrugated cardboard manufacturing facilities. Energy systems laboratory. *Industrial Energy Technology Conference on*; 2005.
248. Roy P, Nei D, Okadome H, Nakamura N, Orikasa T, Shiina T. Life cycle inventory analysis of fresh tomato distribution systems in Japan considering the quality aspects. *J Food Eng*. 2008;86:225-33.
249. Sorguven E, Özilgen M. Thermodynamic assessment of algal biodiesel utilization. *Renewable Energy*. 2010;35:1956-1966.
250. Ptansinski KJ. *Efficiency of biomass energy; an exergy approach to biofuels, power, and biorefineries*. New Jersey: John Wiley and Sons. Hoboken; 2016.
251. Özilgen M & Sorguven E. *Biothermodynamics, principles and applications*. USA; CRC Press;2017.

APPENDIX A: RESULTS OF THE INSTRUMENTAL ANALYSIS

Figure A.1. IR result of 4th experiment

Figure A.2. HPLC (run 1) data obtained for 4th experimentFigure A.3. HPLC (run 2) data obtained for 4th experiment

PC Control PC Control	Serial number 1111270515 Printed	Program version 4.0 2017-06-19 11:33:17		
Result report				
Determination	Method KF Numune Analizi Last saved on 2016-12-08 14:32:18 ver. 9 Method status saved Determination Zoledronik Asit-20170619-112619 Determ. time 2017-06-19 11:26:19 Status of deter. original Sample number 11 User mkepur Full name Mahmut Kepur			
Sample data	Numune adi Zoledronik Asit Batch seri no. deneme-05 Sample size 0.30 g			
03 KFT Ipol	Karl Fischer titration Ipol			
Sensor	Metal electrode			
Titrant	Hydranal Composite 5			
	Concentration	1.000 mol/L		
	Titer	5.1636 mg/mL		
	Date titer det.	2017-06-19 09:49:27		
Titration	EP1	4.1250 mL		
	Regular stop			
Results	Nem	7.10 %		
Statistics	n	Mean	s +/-	s rel
	Nem 2	7.15 %	0.071 %	0.99 %
Curve				
03 KFT Ipol	Karl Fischer titration Ipol			
Date	Signature			
Reason				

Figure A.4. KF data of 4th experiment

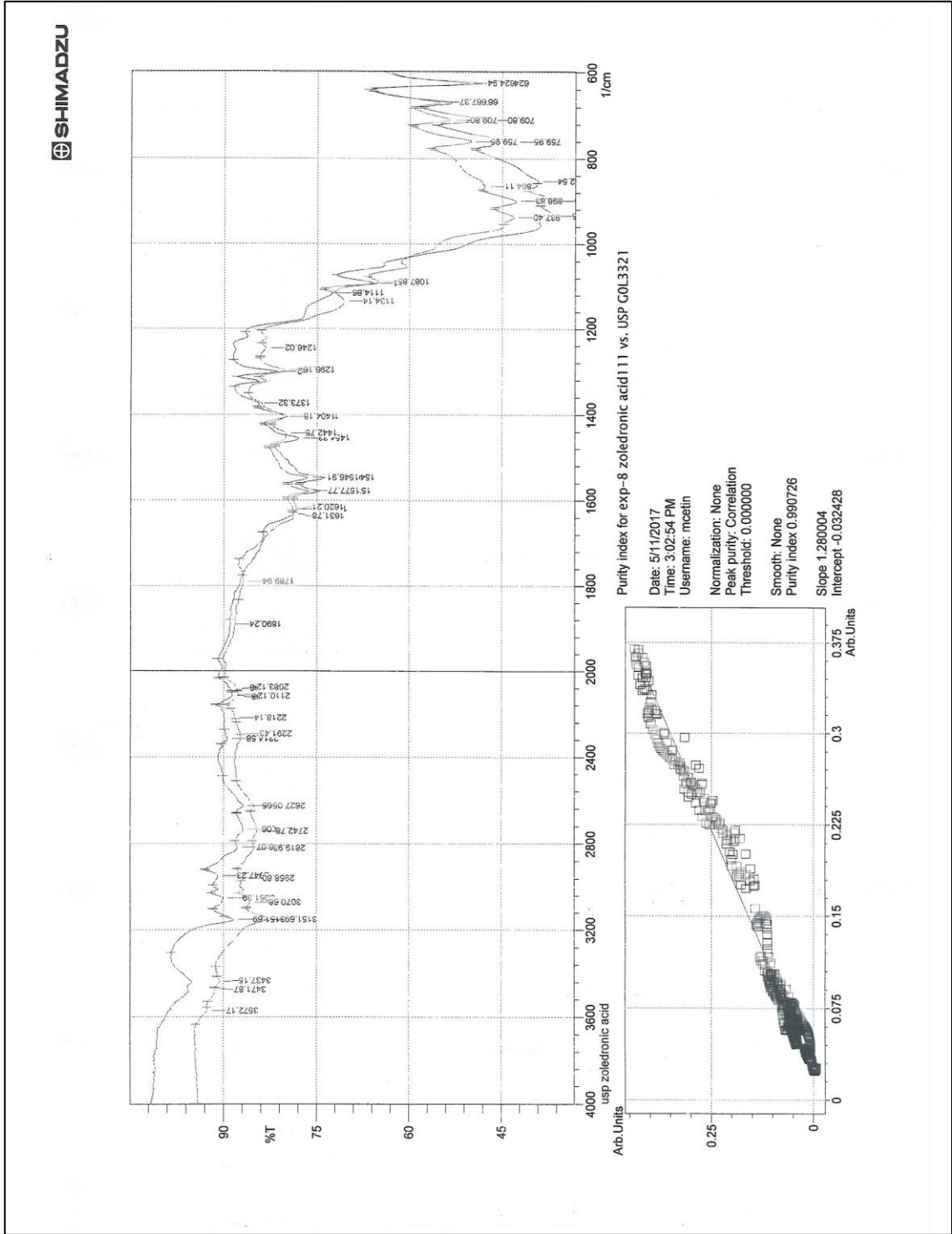
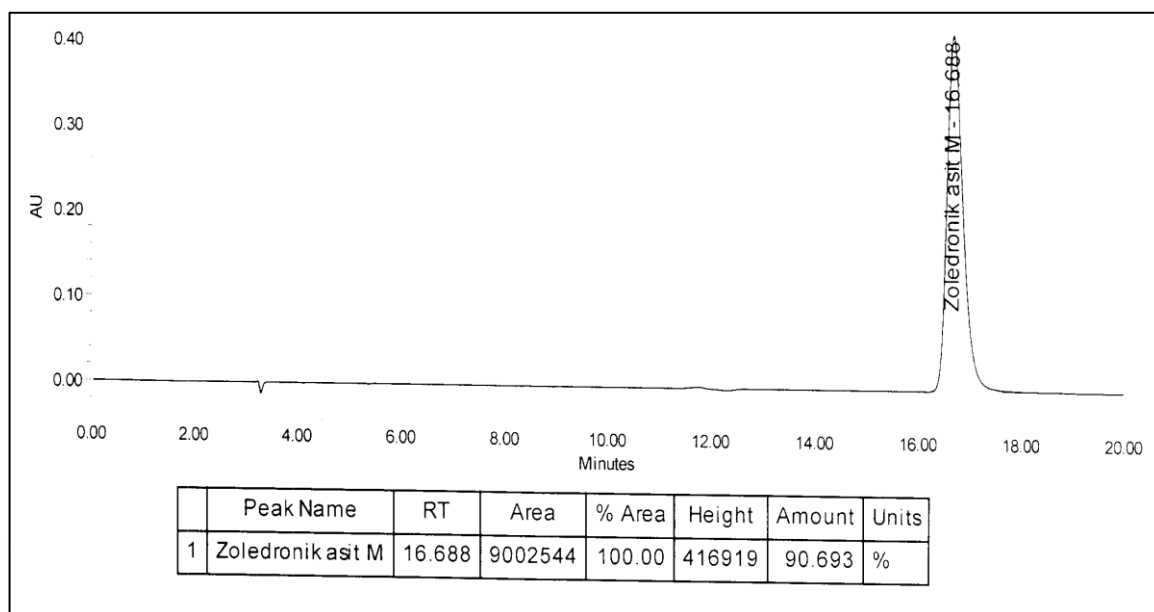
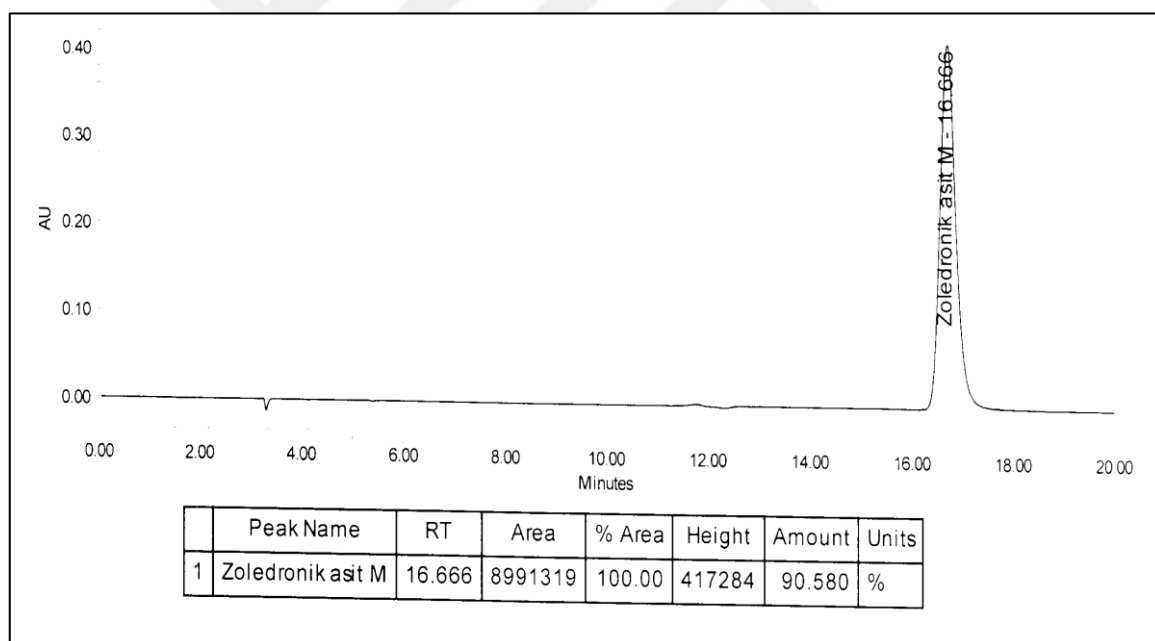


Figure A.5. IR result of 6th experiment

Figure A.6. HPLC (run 1) result of 6th experimentFigure A.7. HPLC (run 2) result of 6th experiment

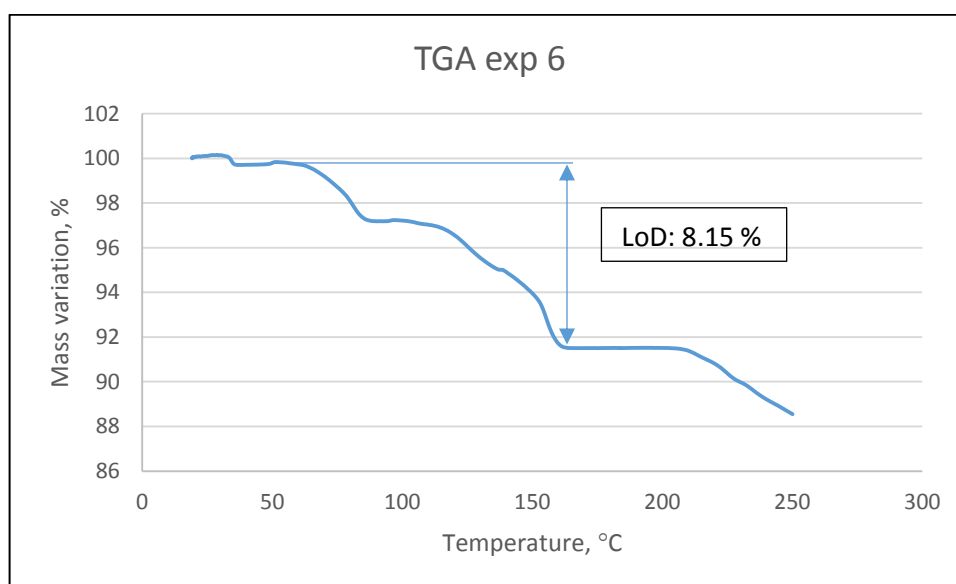
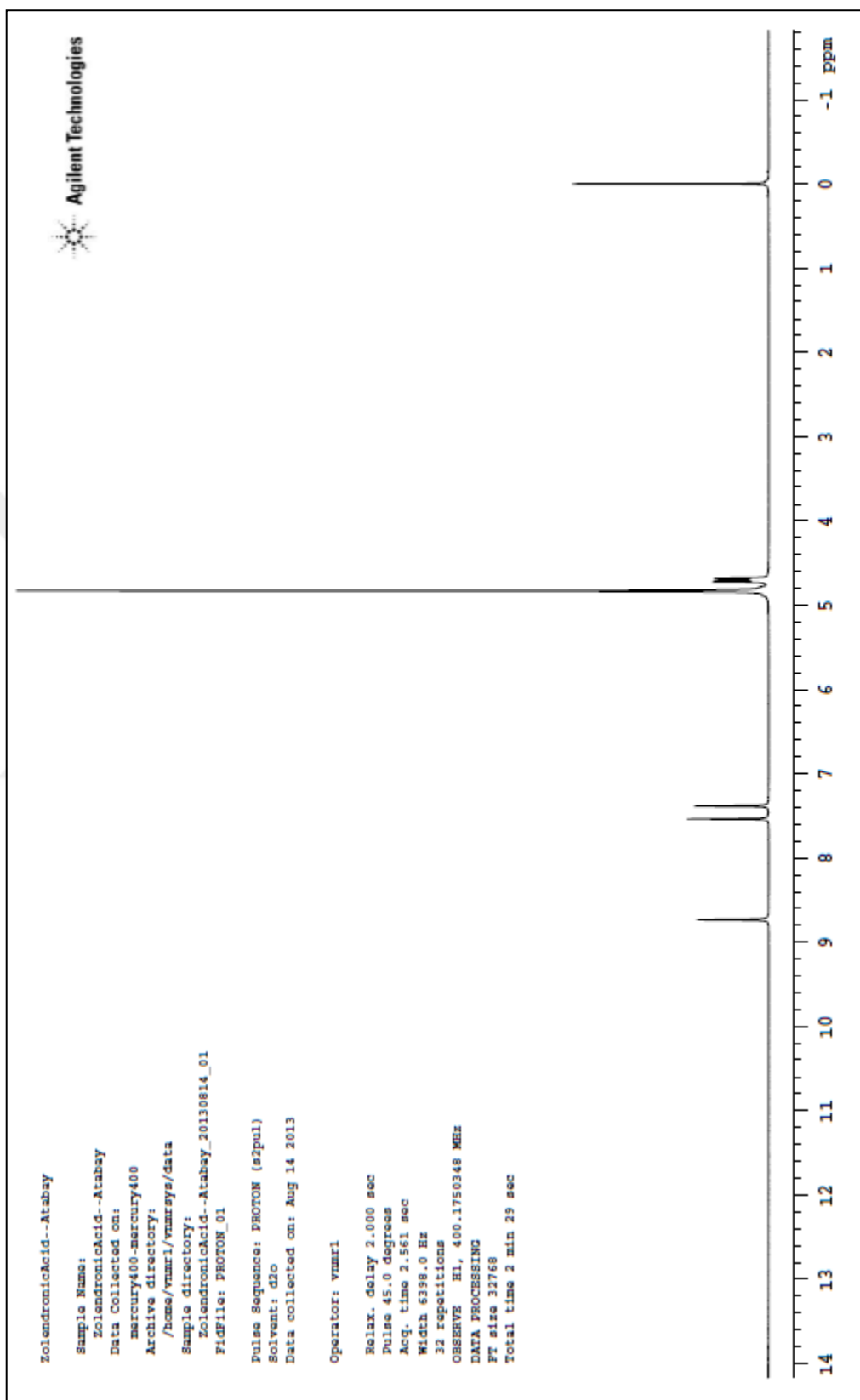


Figure A.8. TGA results of 6th experiment

Figure A.9. ^1H -NMR spectrum of 6th experiment

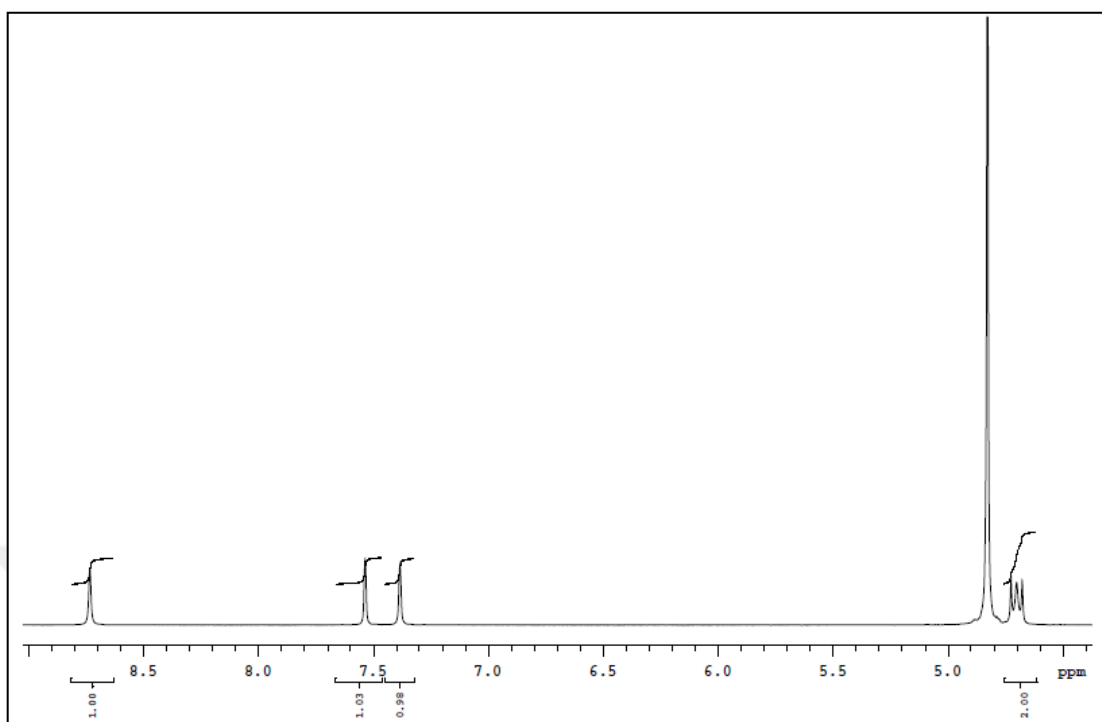


Figure A.10. $^1\text{H-NMR}$ spectrum of 6th experiment with magnitudes

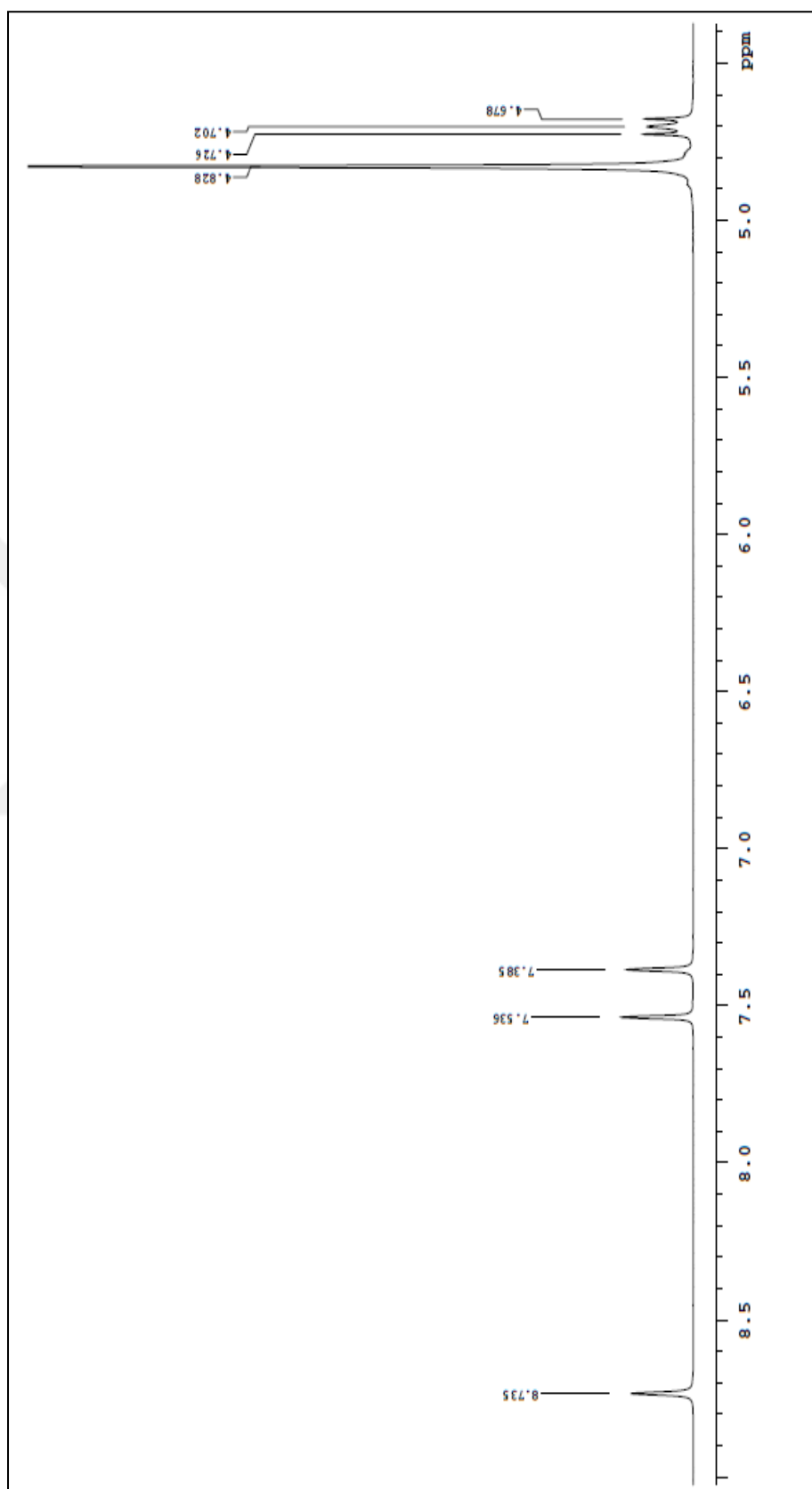
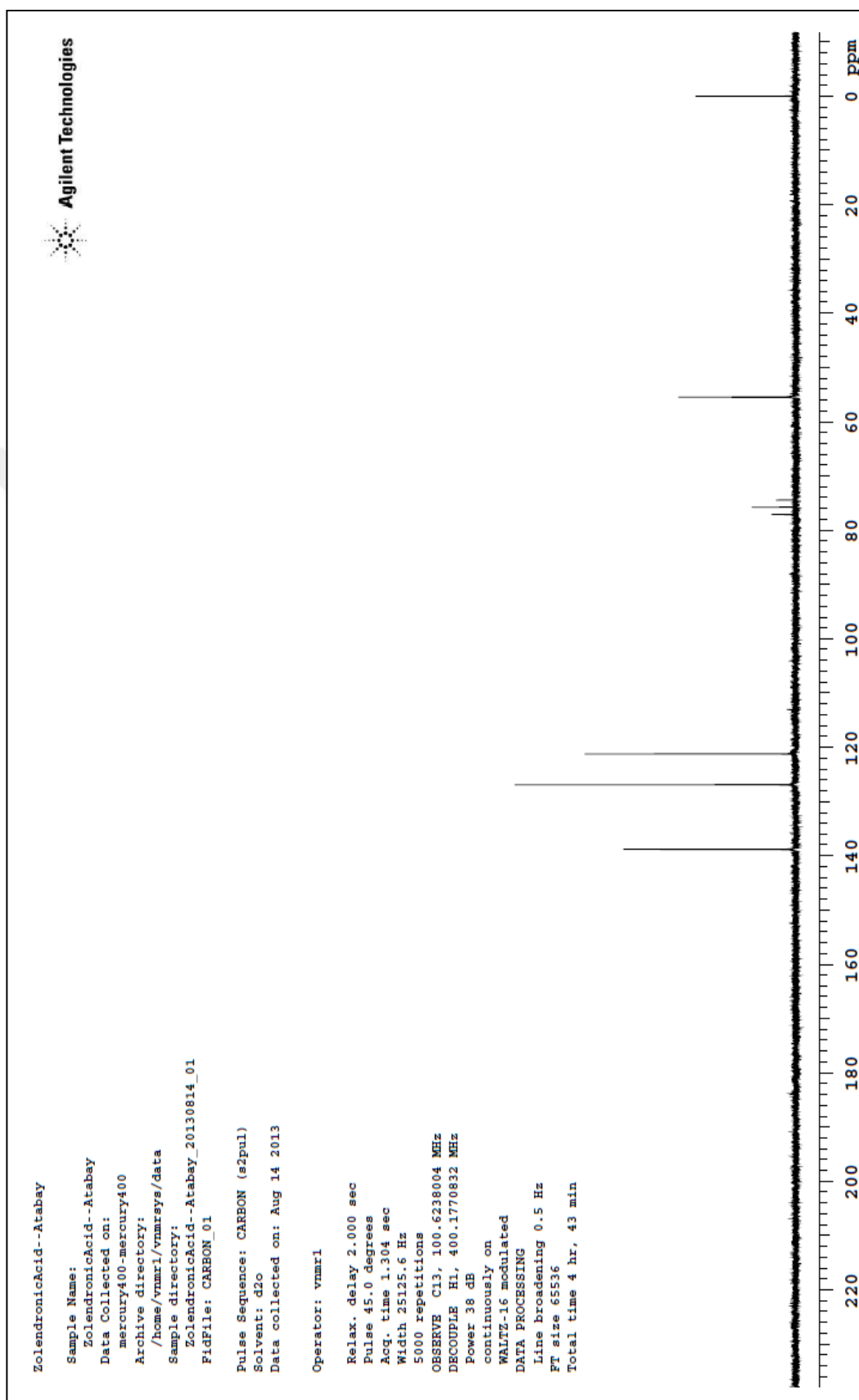


Figure A.11. $^1\text{H-NMR}$ spectrum details of 6th experiment

Figure A.12. ^{13}C -NMR spectrum of 6th experiment

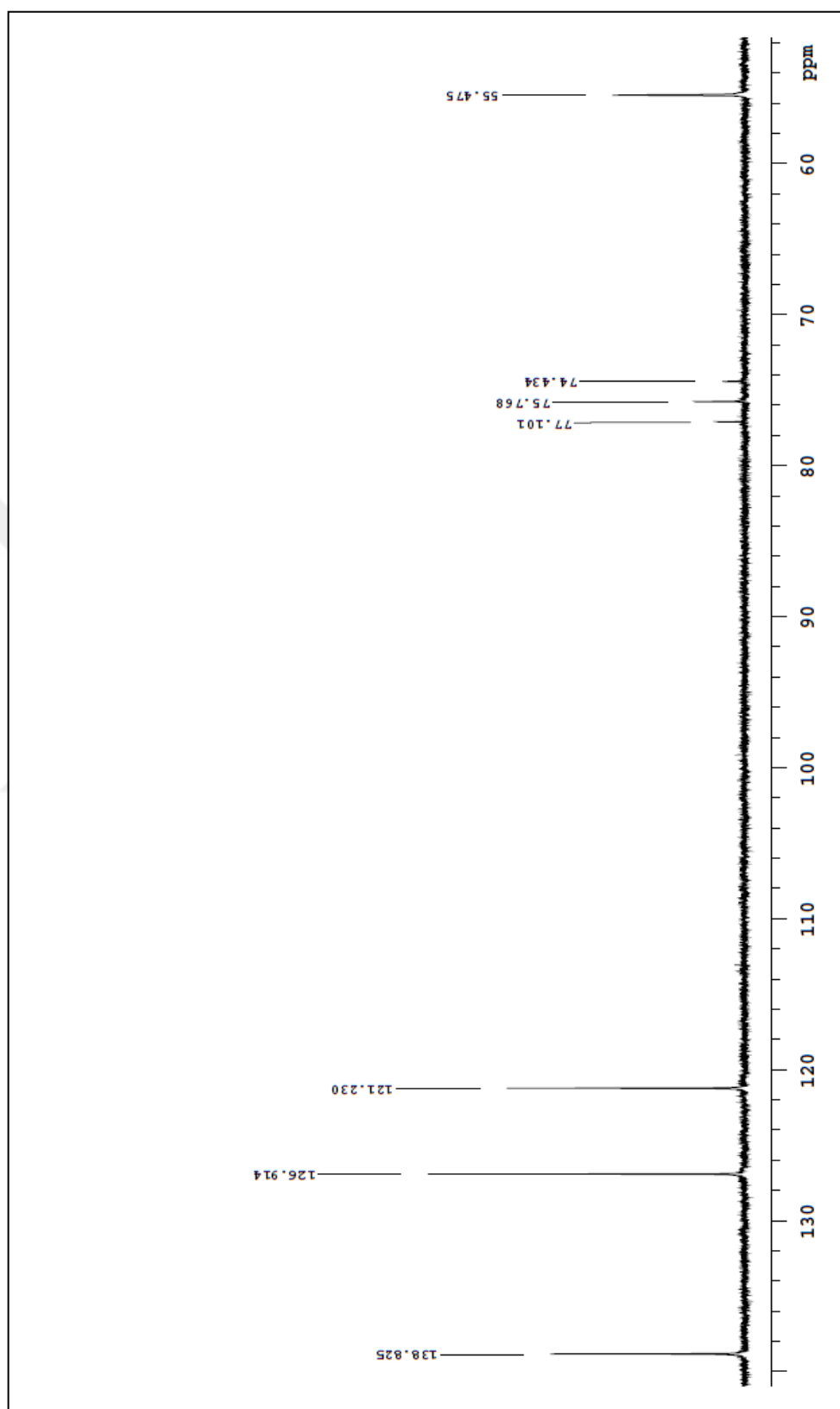
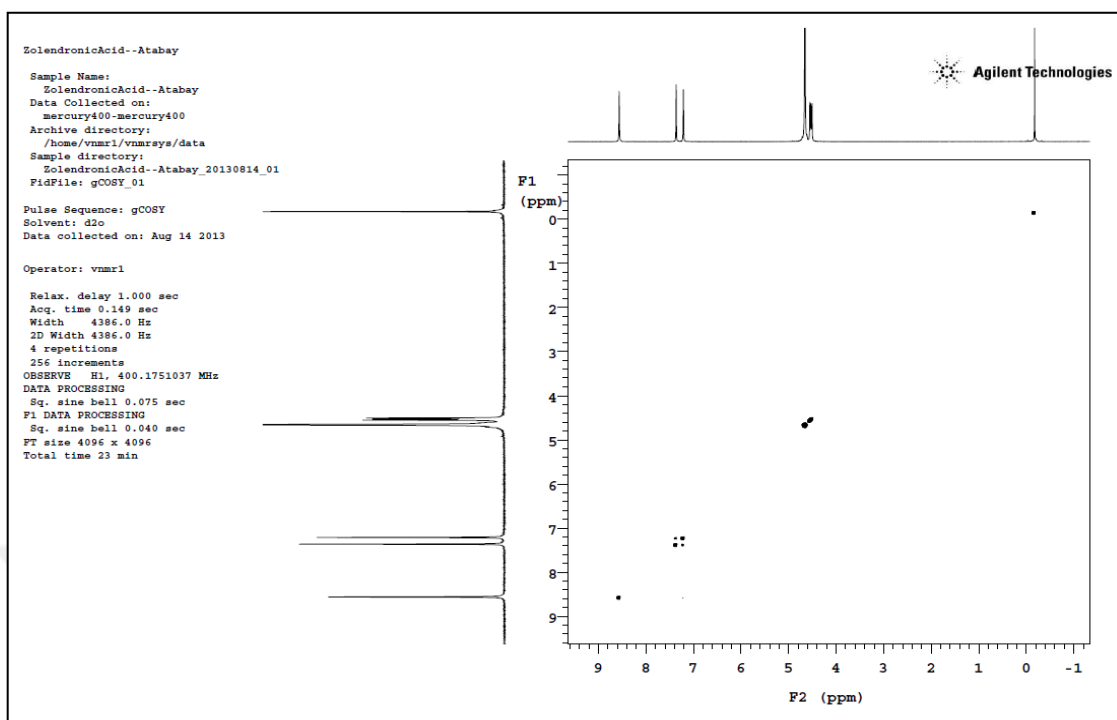
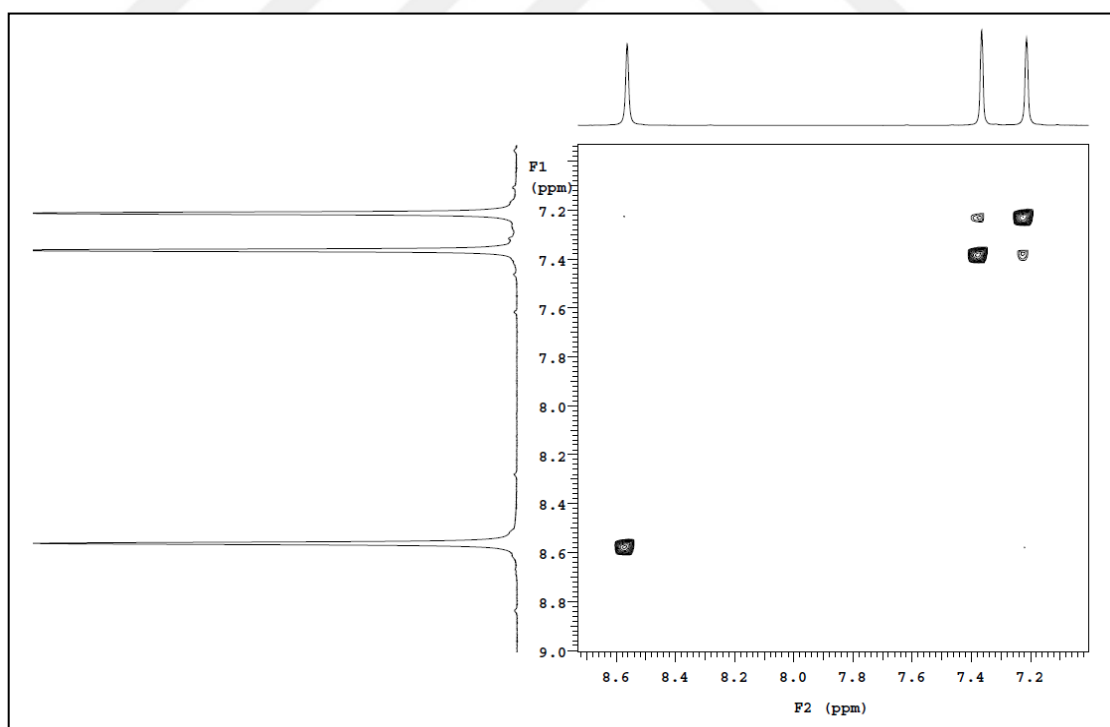
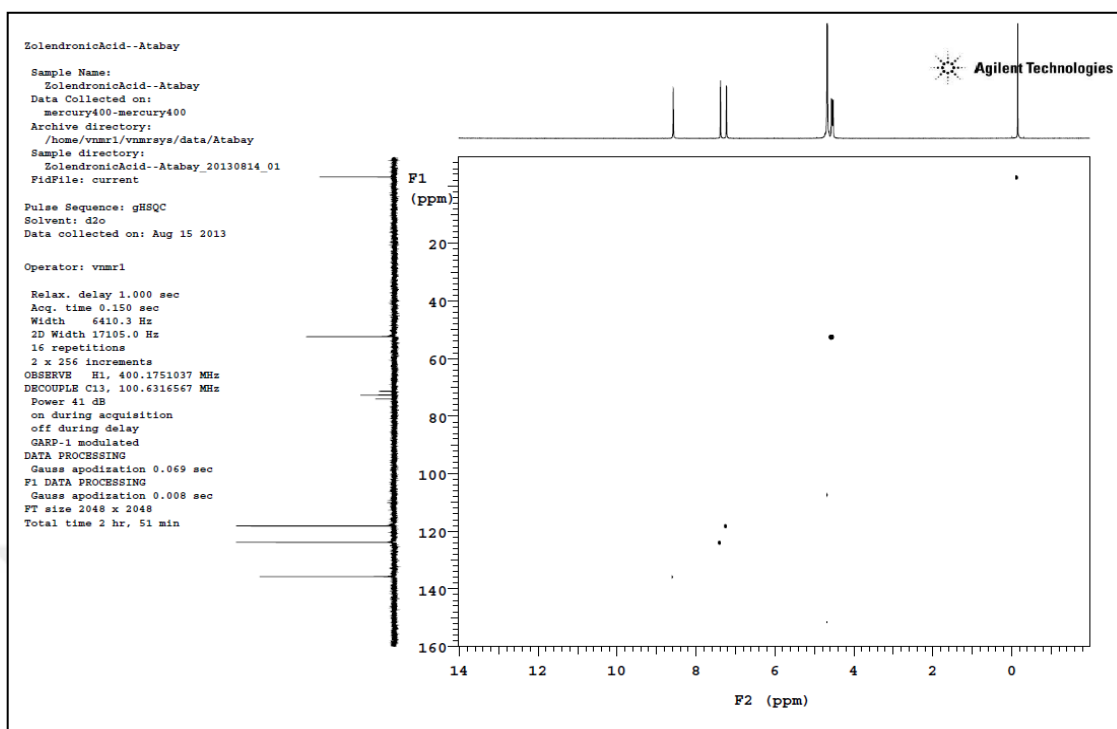
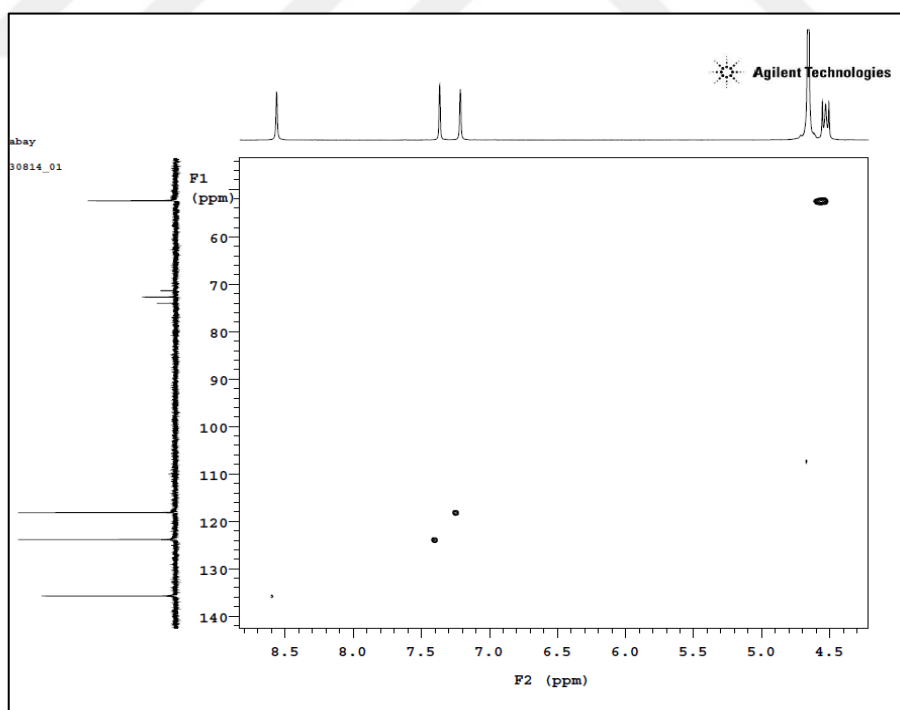
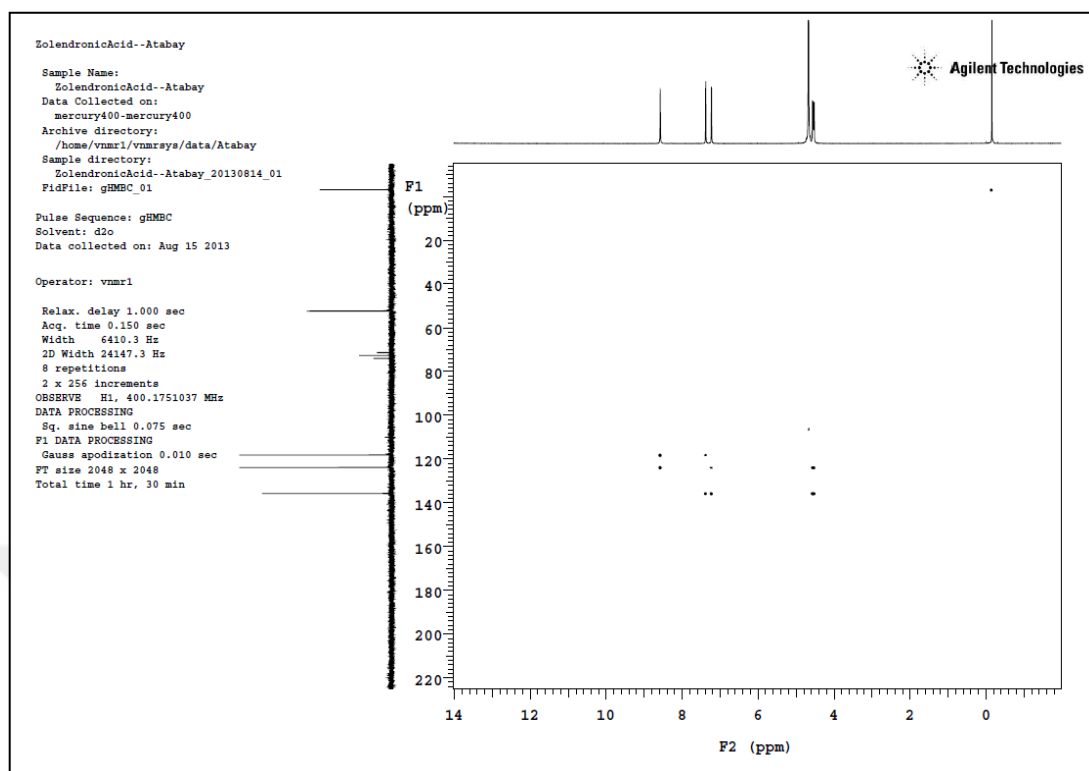
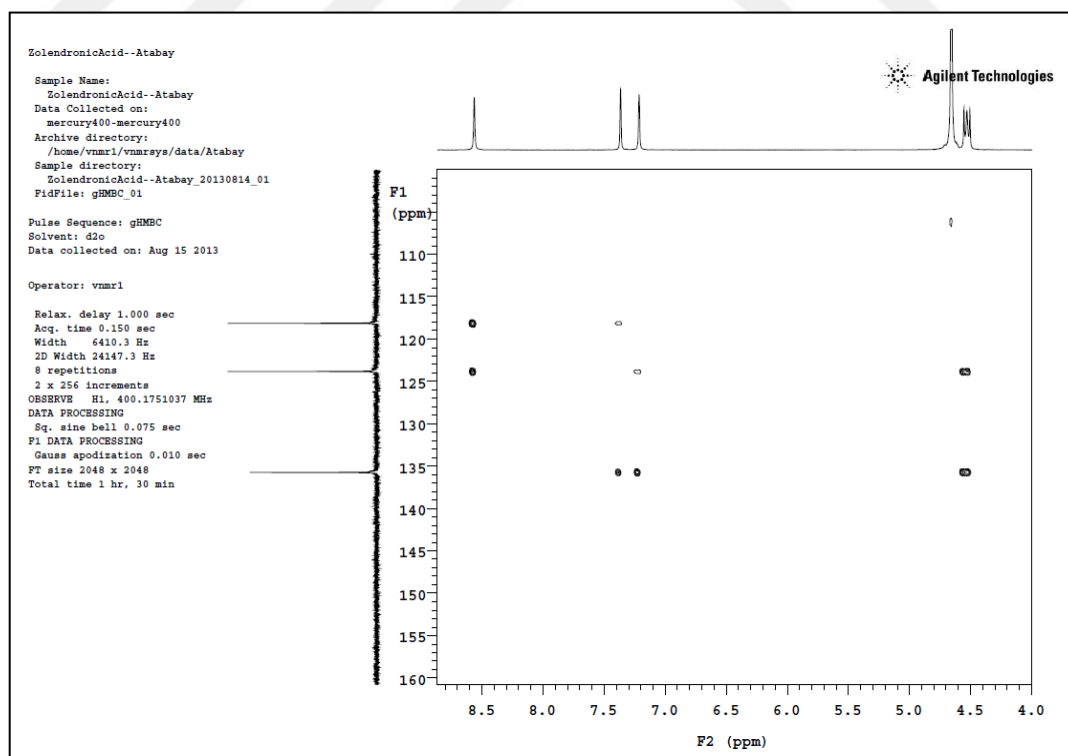
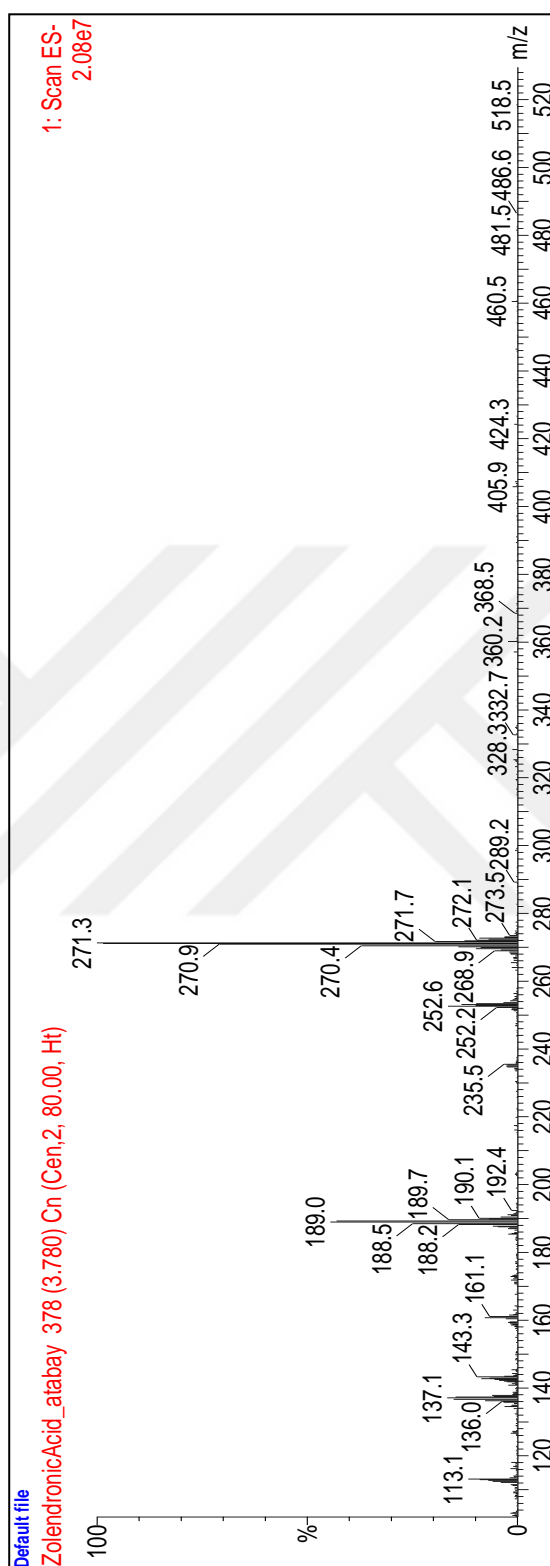


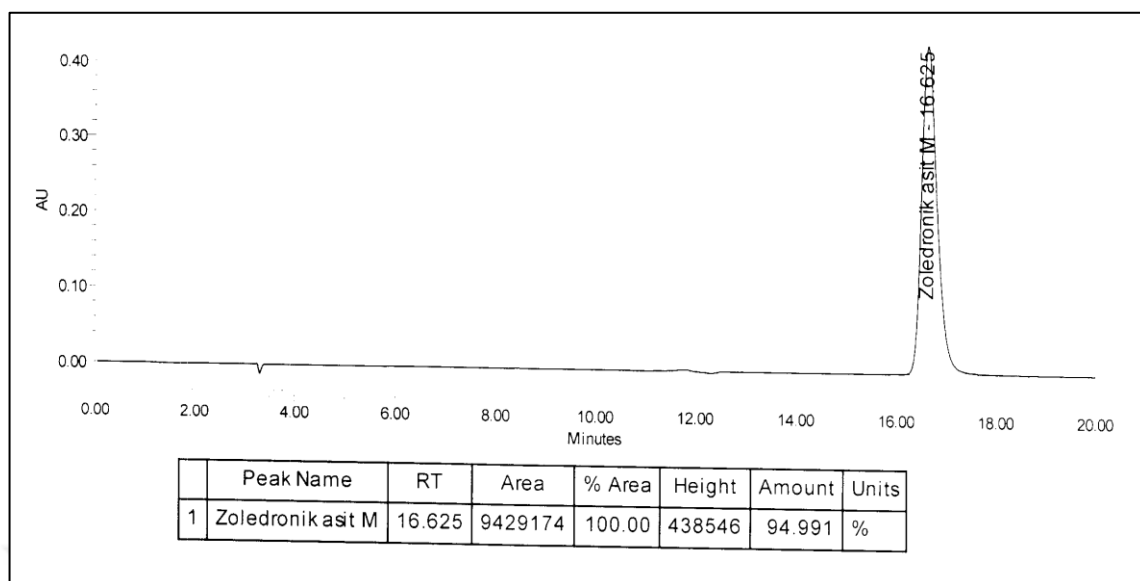
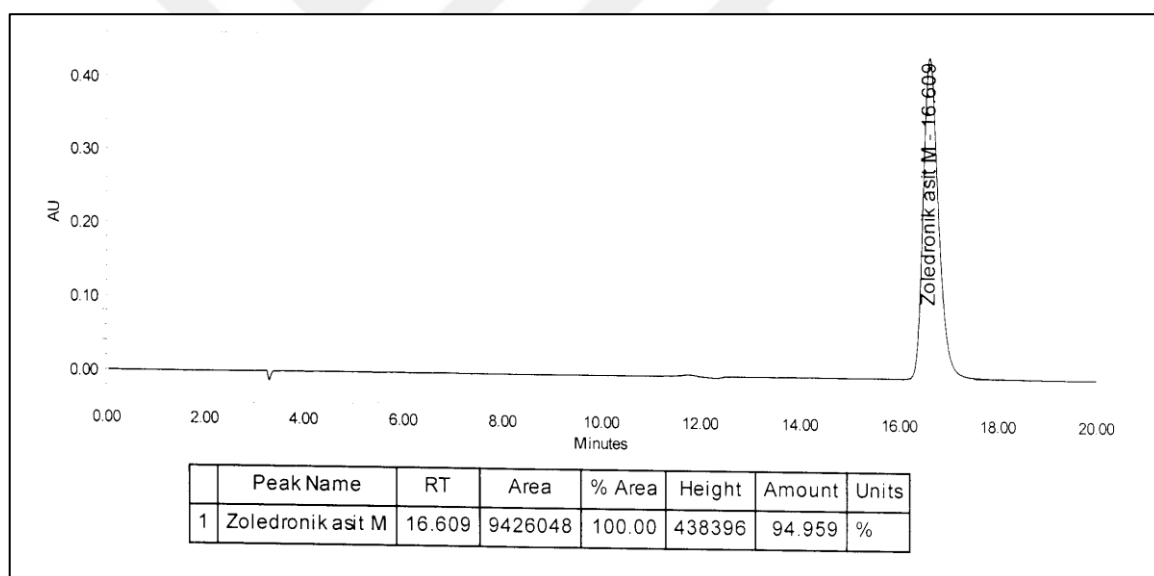
Figure A.13. ^{13}C -NMR spectrum details of 6th experiment

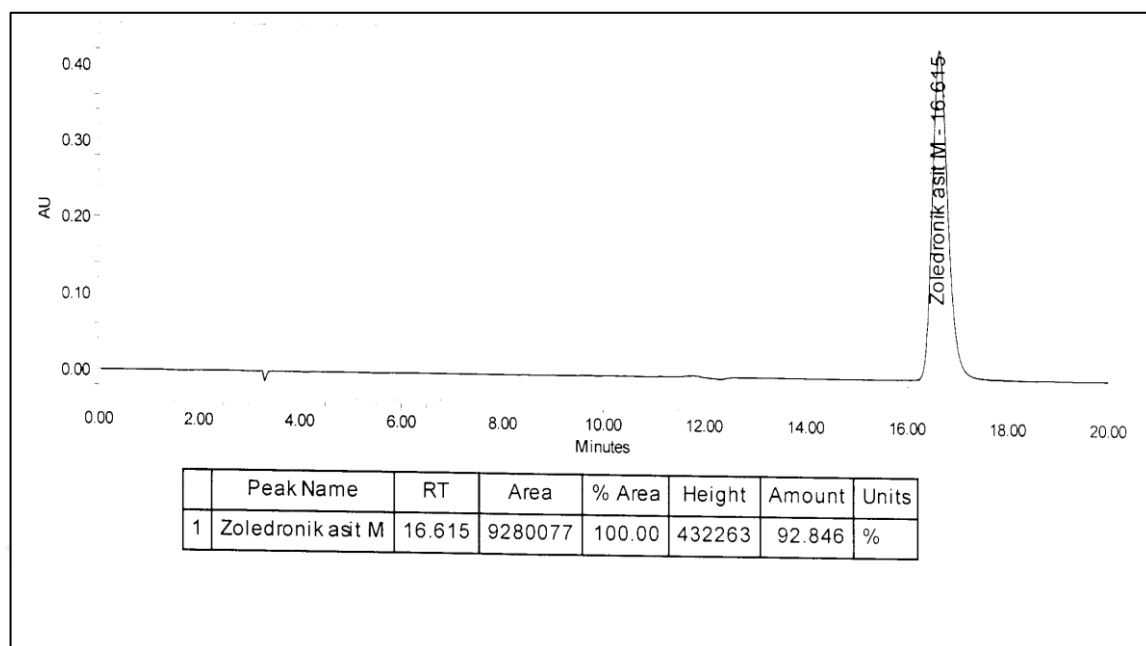
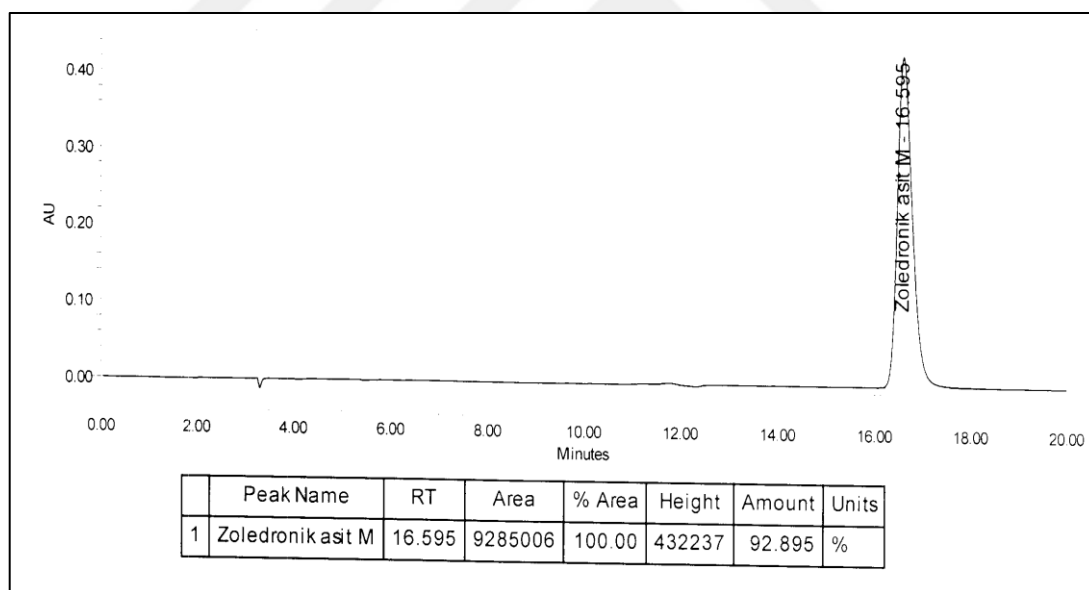
Figure A.14. COSY spectrum of 6th experimentFigure A.15. COSY spectrum details of 6th experiment

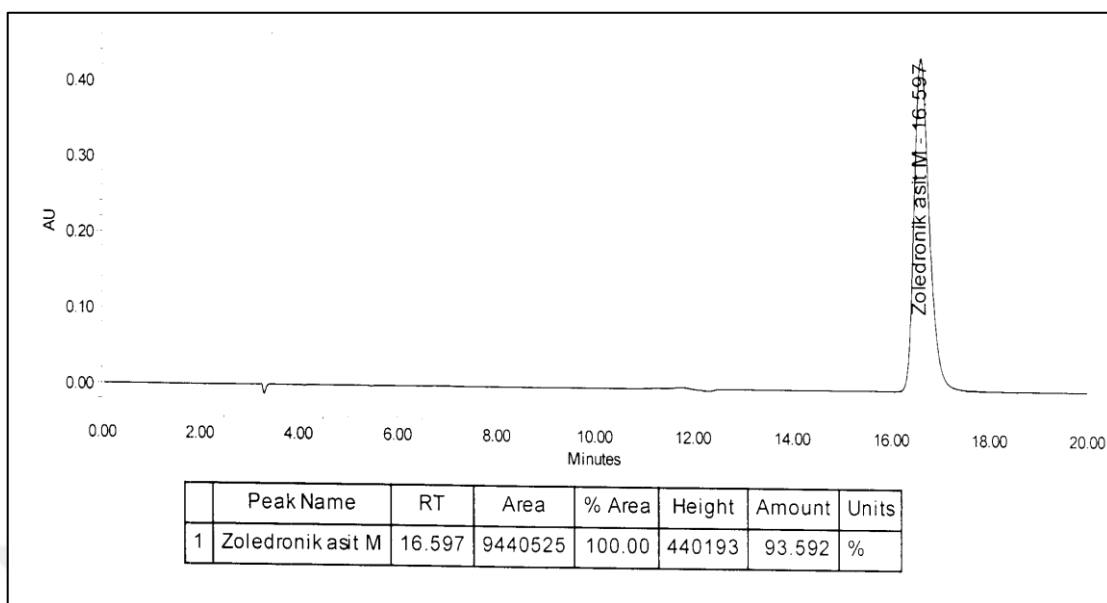
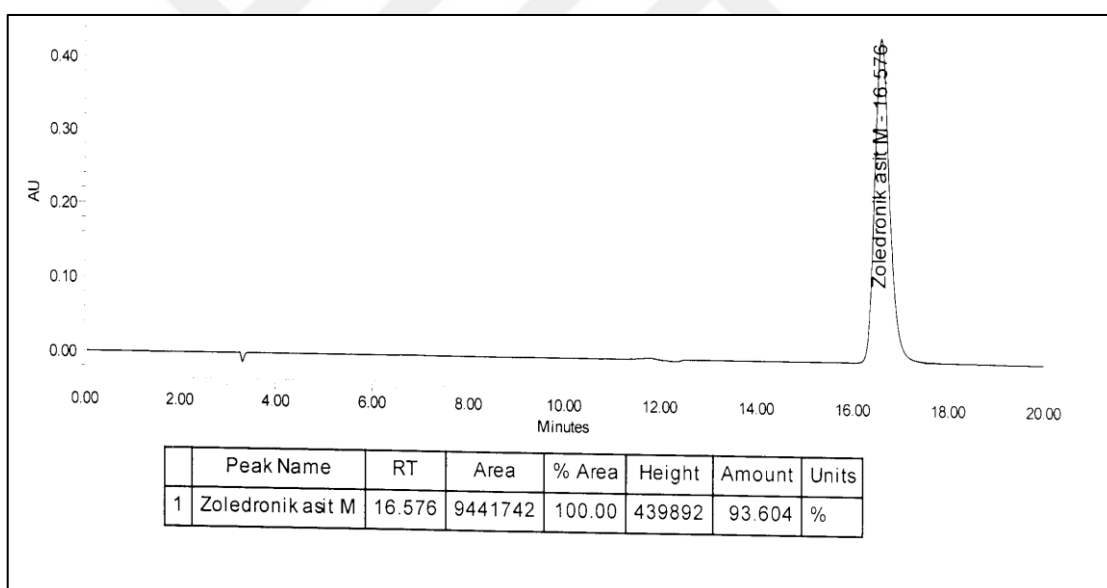
Figure A.16. HSQC spectrum of 6th experimentFigure A.17. HSQC spectrum details of 6th experiment

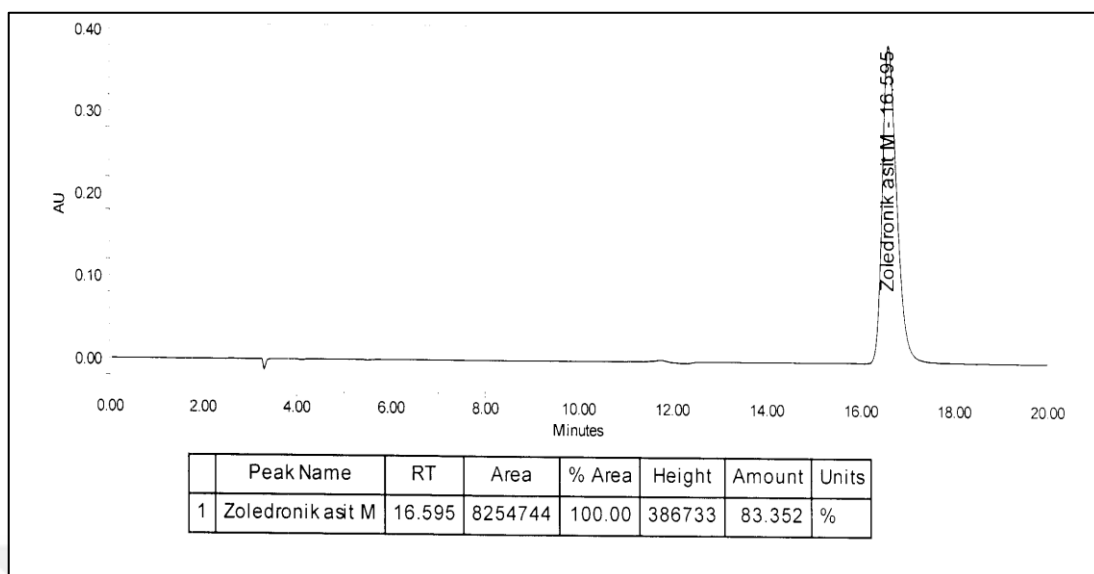
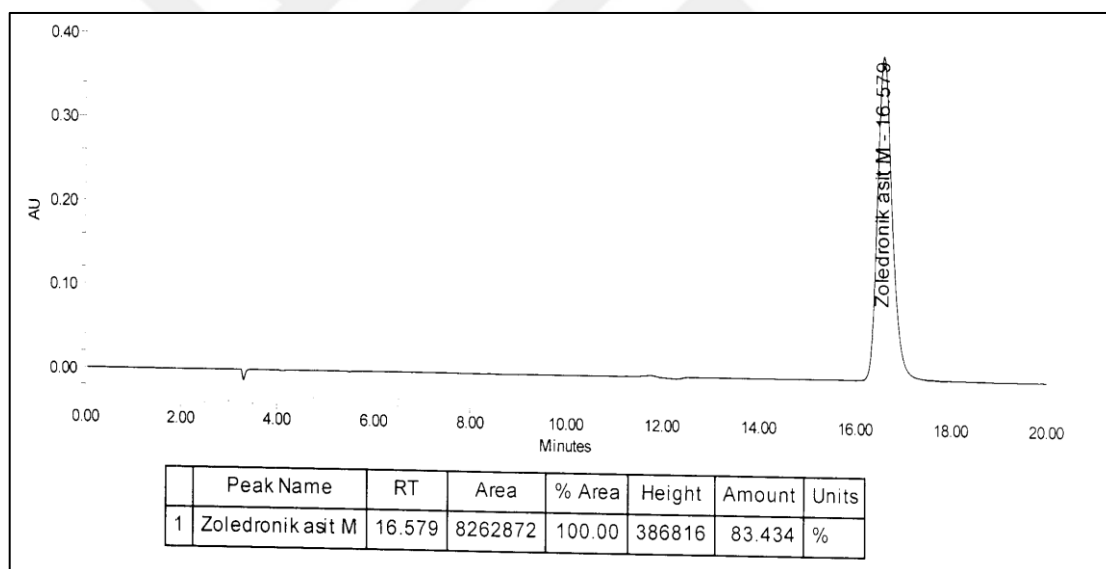
Figure A.18. HMBC spectrum details of 6th experimentFigure A.19. HMBC spectrum details of 6th experiment

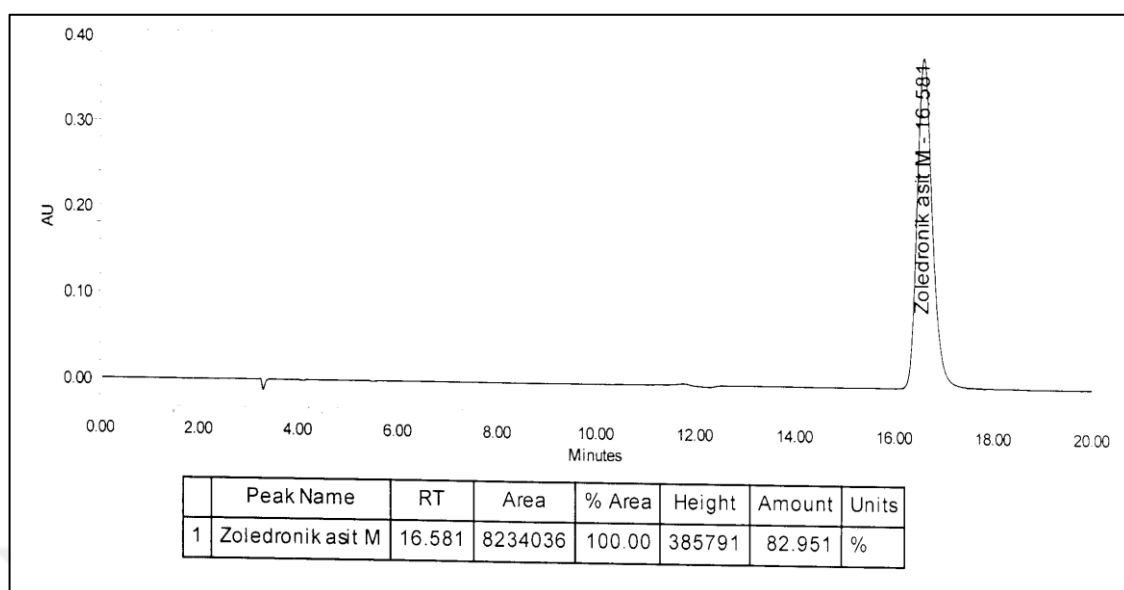
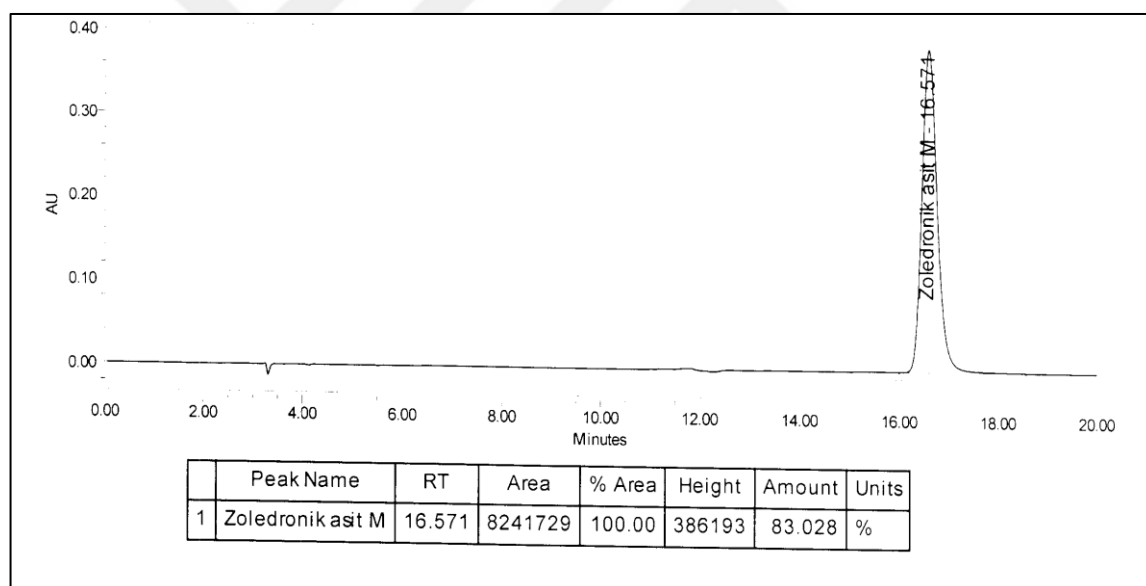
Figure A.20. Mass spectrum details of 6th experiment

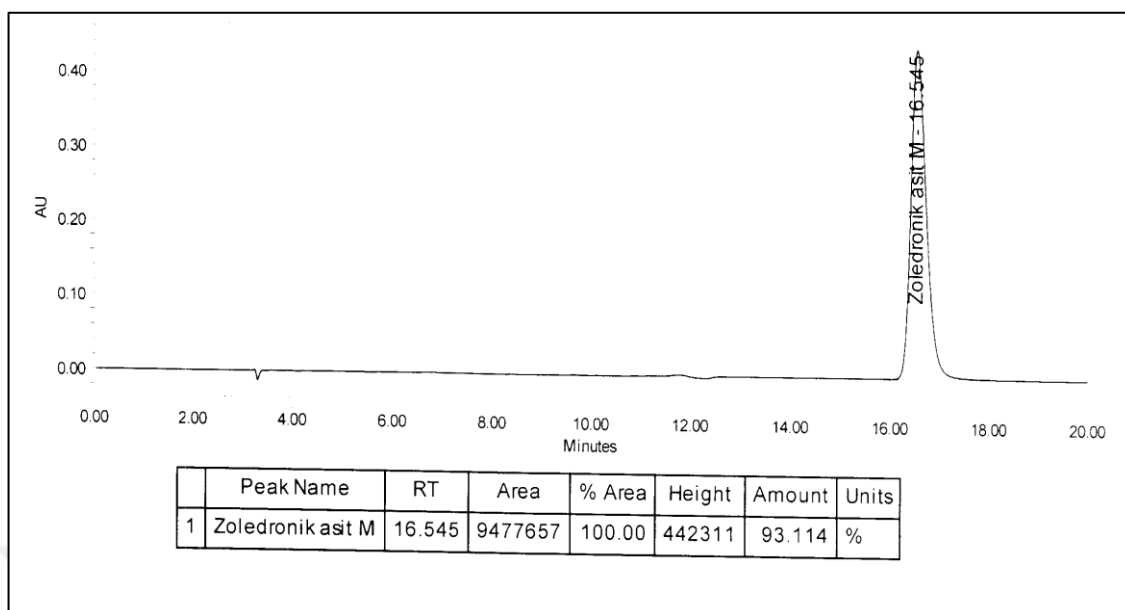
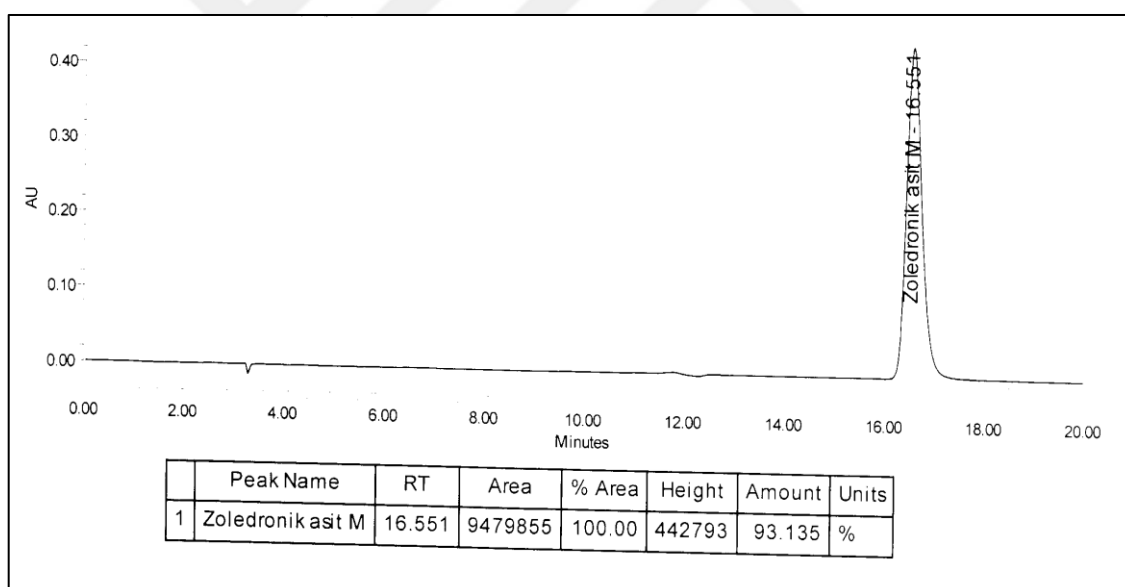
Figure A.21. HPLC results (run 1) of 7th experiment CR1Figure A.22. HPLC results (run 2) of 7th experiment CR1

Figure A.23. HPLC results (run 1) of 7th experiment CR2-1Figure A.24. HPLC results (run 2) of 7th experiment CR2-1

Figure A.25. HPLC results (run 1) of 7th experiment CR2-2Figure A.26. HPLC results (run 2) of 7th experiment CR2-2

Figure A.27. HPLC results (run1) of 7th experiment CR3-1Figure A.28. HPLC results (run1) of 7th experiment CR3-1

Figure A.29. HPLC results (run1) of 7th experiment CR3-2Figure A.30. HPLC results (run2) of 7th experiment CR3-2

Figure A.31. HPLC results (run 1) of 7th experiment CR4Figure A.32. HPLC results (run 2) of 7th experiment CR4

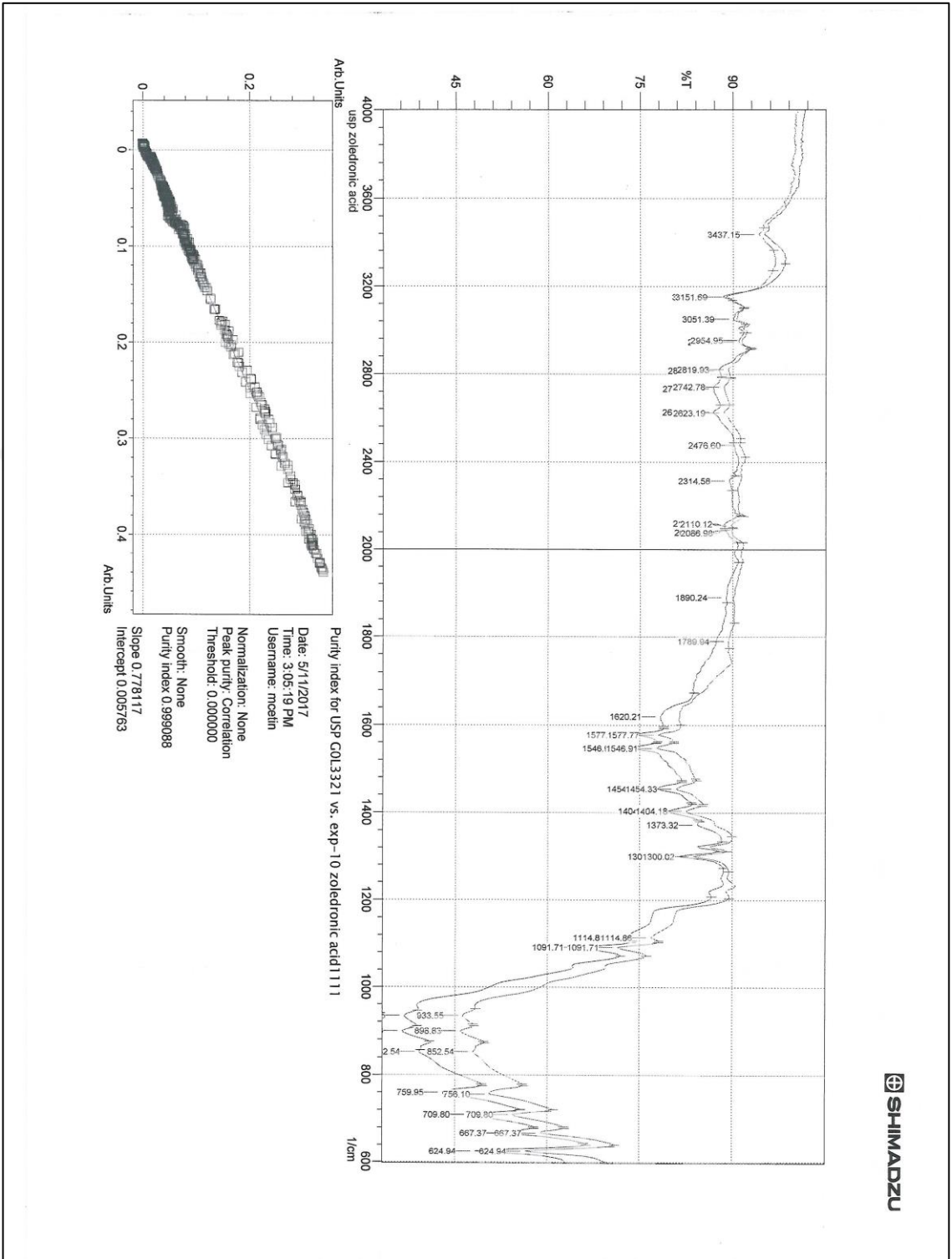
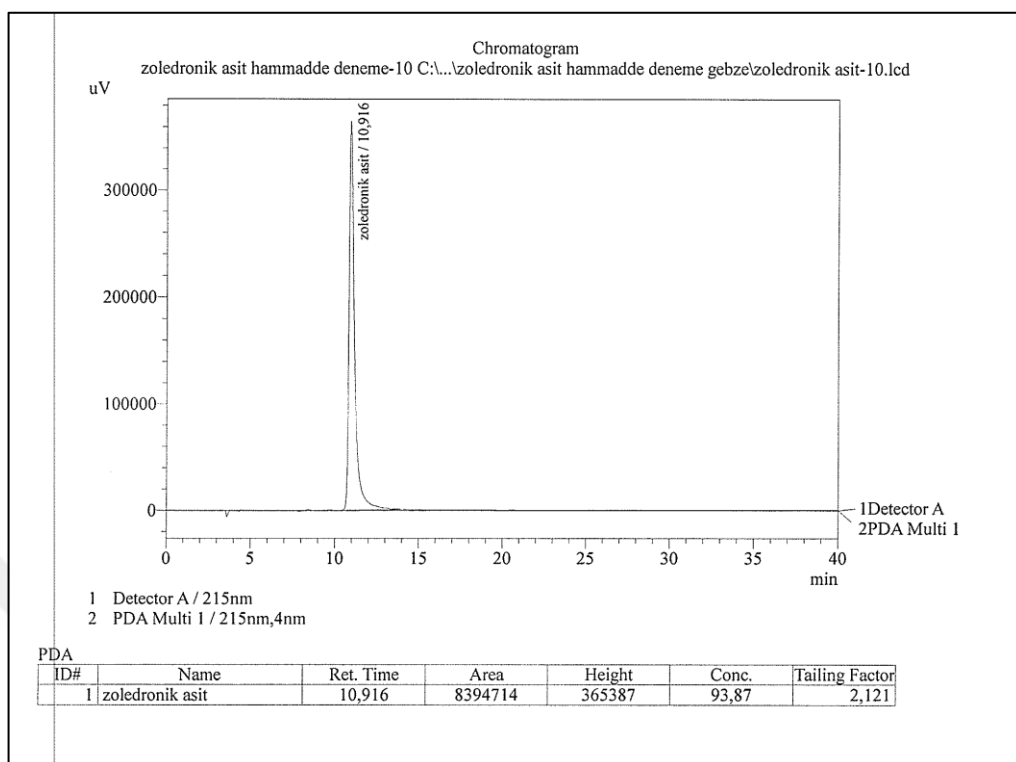
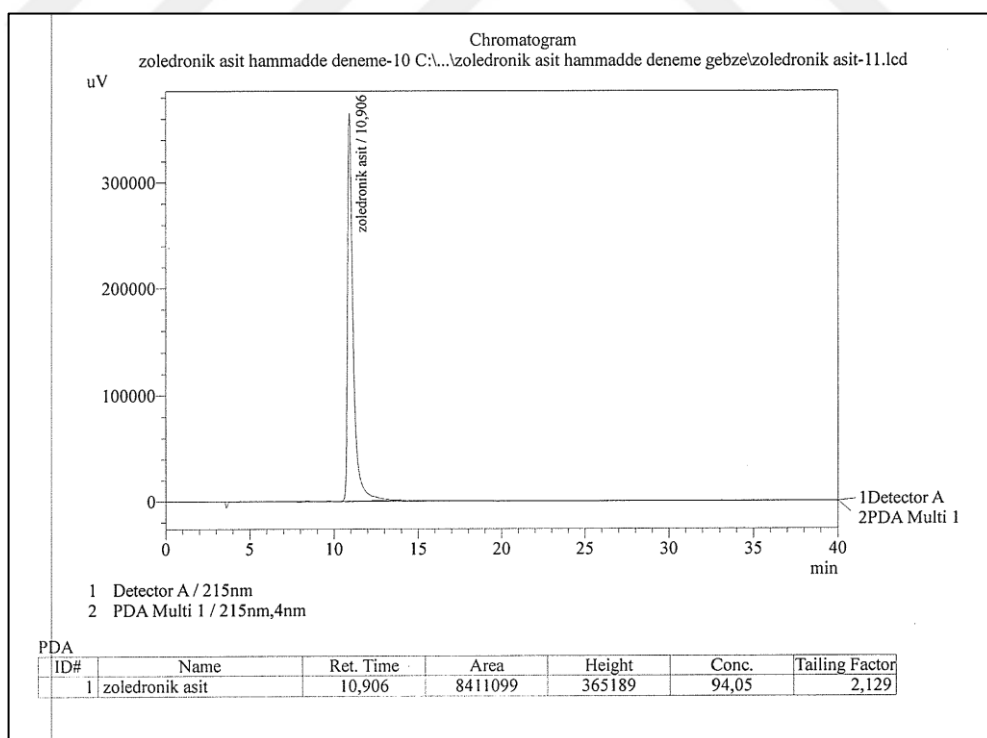


Figure A.33. IR result of 8th experiment

Figure A.34. HPLC result (run 1) of 8th experimentFigure A.35. HPLC result (run 2) of 8th experiment

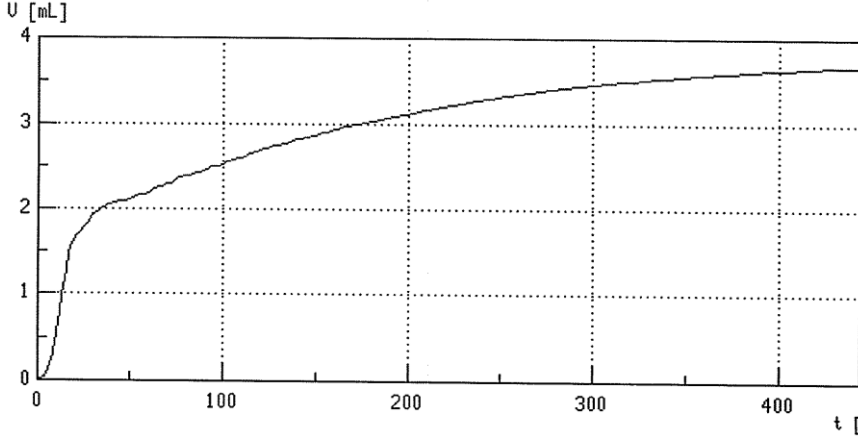
PC Control PC Control	Serial number 1111270515 Printed	Program version 4.0 2017-06-19 14:17:51
Result report		
Determination	Method KF Numune Analizi Last saved on 2016-12-08 14:32:18 ver. 9 Method status saved Determination Zoledronik Asit-20170619-140601 Determ. time 2017-06-19 14:06:01 Status of deter. original Sample number 16 User mkepur Full name Mahmut Kepur	
Sample data	Numune adi Zoledronik Asit Batch seri no. deneme-10 Sample size 0.2995 g	
03 KFT Ipol	Karl Fischer titration Ipol Sensor Metal electrode Titrant Hydranal Composite 5 Concentration 1.000 mol/L Titer 5.1636 mg/mL Date titer det. 2017-06-19 09:49:27 Titration EP1 3.6840 mL Regular stop	
Results	Nem 6.35 %	
Statistics	n	Mean
	s +/-	s rel
	Nem 1	6.35 %
Curve		
03 KFT Ipol	Karl Fischer titration Ipol 	
Date Reason	Signature	

Figure A.36. KF data of 8th experiment

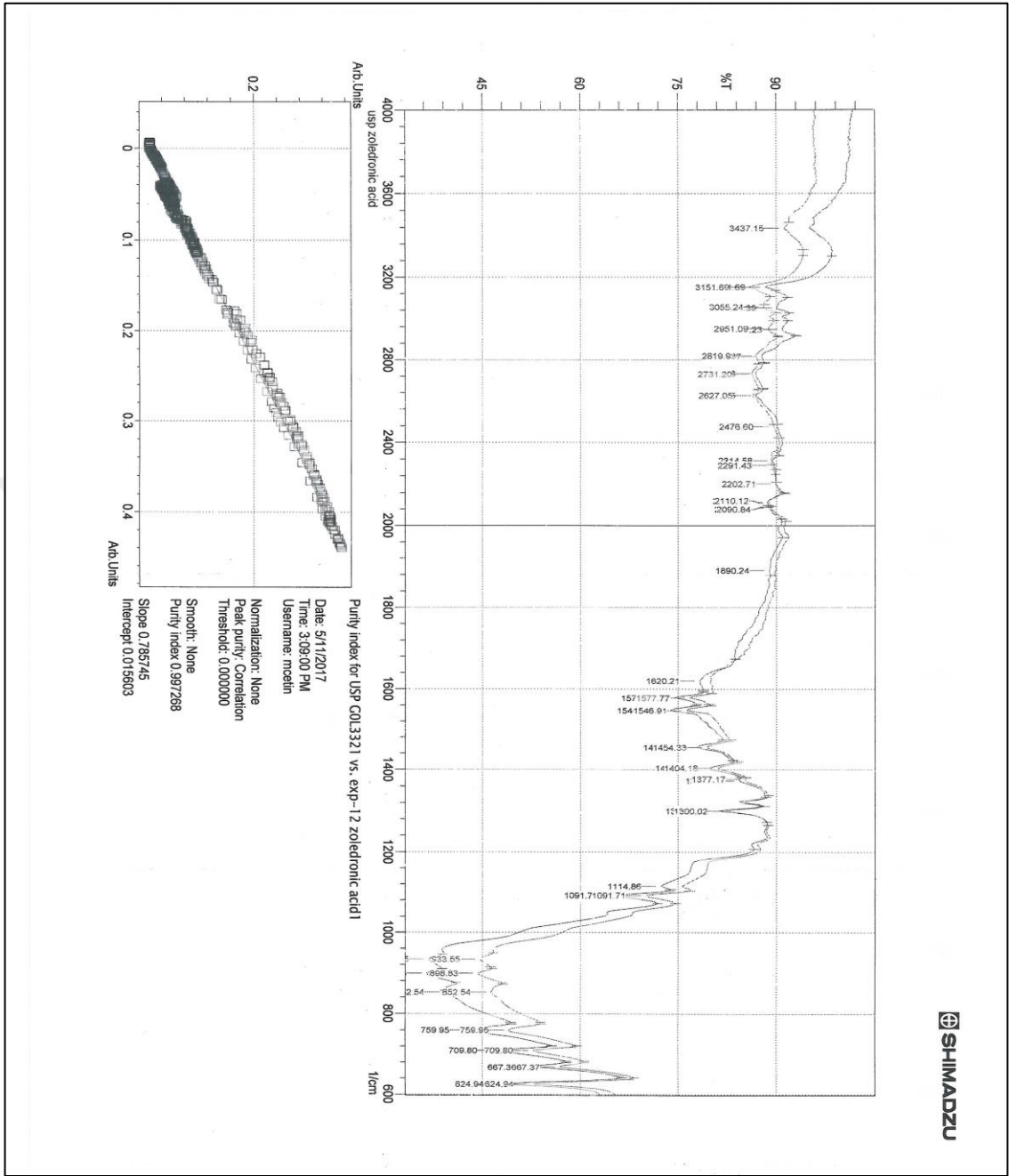
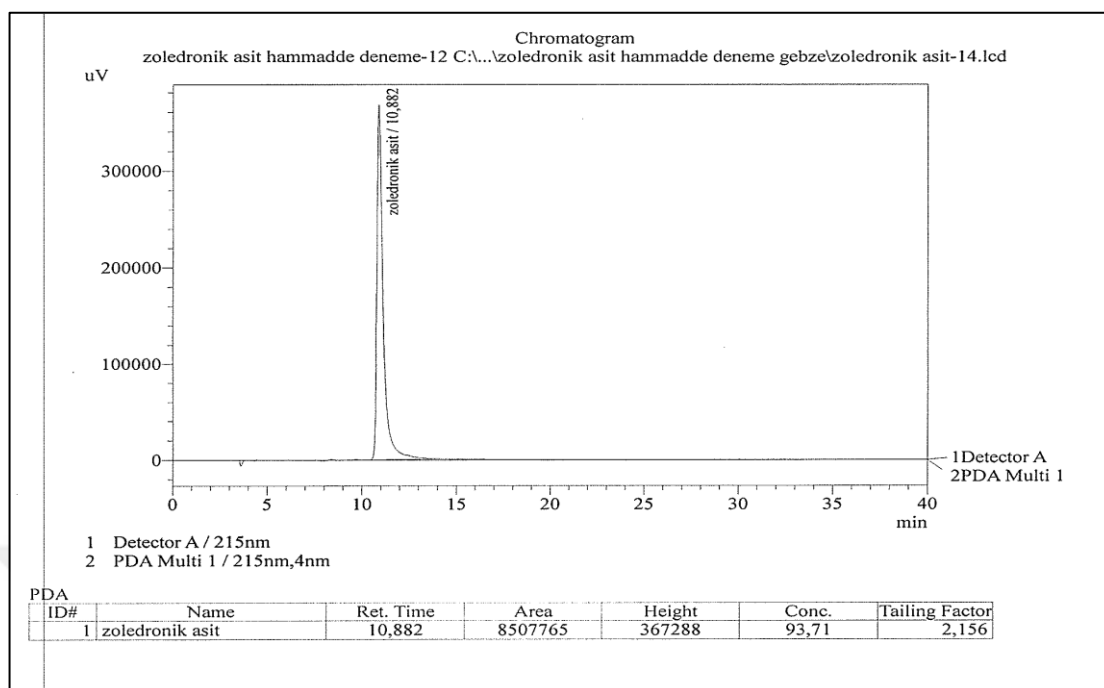
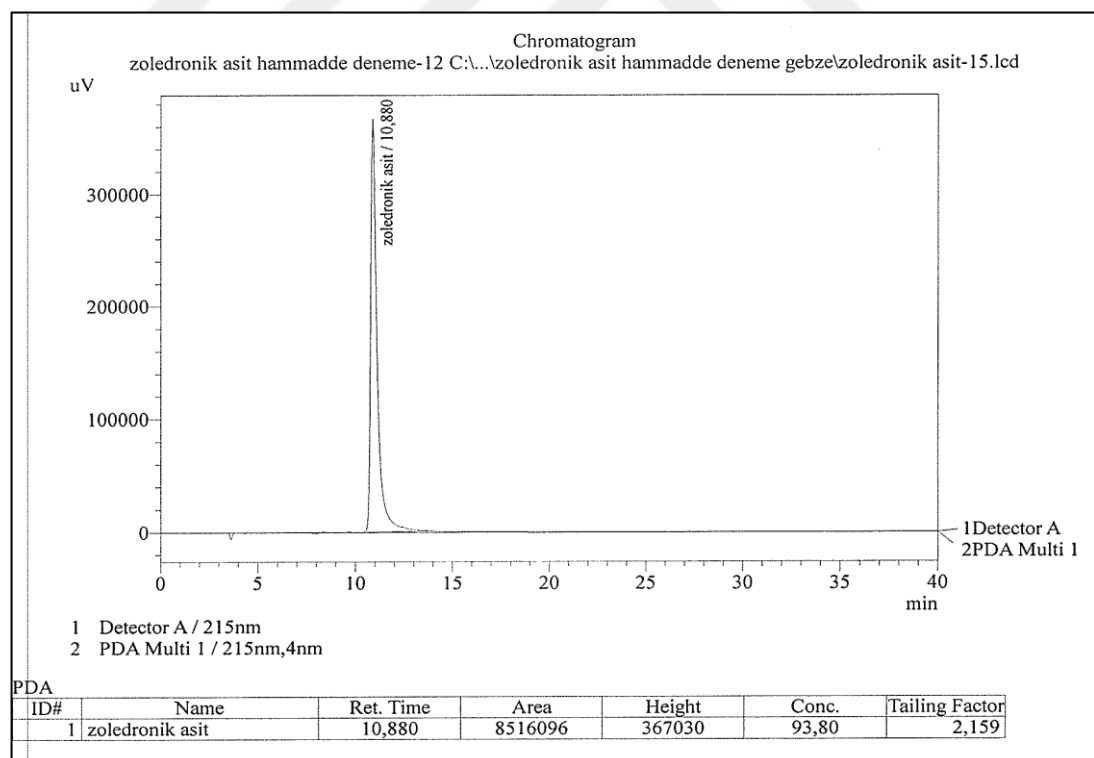


Figure A.37. IR result of 10th experiment

Figure A.38. HPLC result (run 1) of 10th experimentFigure A.39. HPLC result (run 2) of 10th experiment

PC Control PC Control	Serial number 1111270515 Printed	Program version 4.0 2017-06-24 18:12:49		
Result report				
Determination	Method KF Numune Analizi Last saved on 2016-12-08 14:32:18 ver. 9 Method status saved Determination Zoledronic acid-20170624-180940 Determ. time 2017-06-24 18:09:40 Status of deter. original Sample number 30 User ekamo Full name Erdogan Kamo			
Sample data	Numune adi Zoledronic acid Batch seri no. deneme 12 Sample size 0.1265 g			
03 KFT Ipol	Karl Fischer titration Ipol Sensor Metal electrode Titrant Hydranal Composite 5 Concentration 1.000 mol/L Titer 4.9974 mg/mL Date titer det. 2017-06-24 13:25:26 Titration EP1 1.5210 mL Regular stop			
Results	Nem 6.01 %			
Statistics	n	Mean	s +/-	s rel
	Nem	1	6.01 %	
Curve				
03 KFT Ipol	Karl Fischer titration Ipol			
Date Reason	Signature			

Figure A.40. KF data of 10th experiment

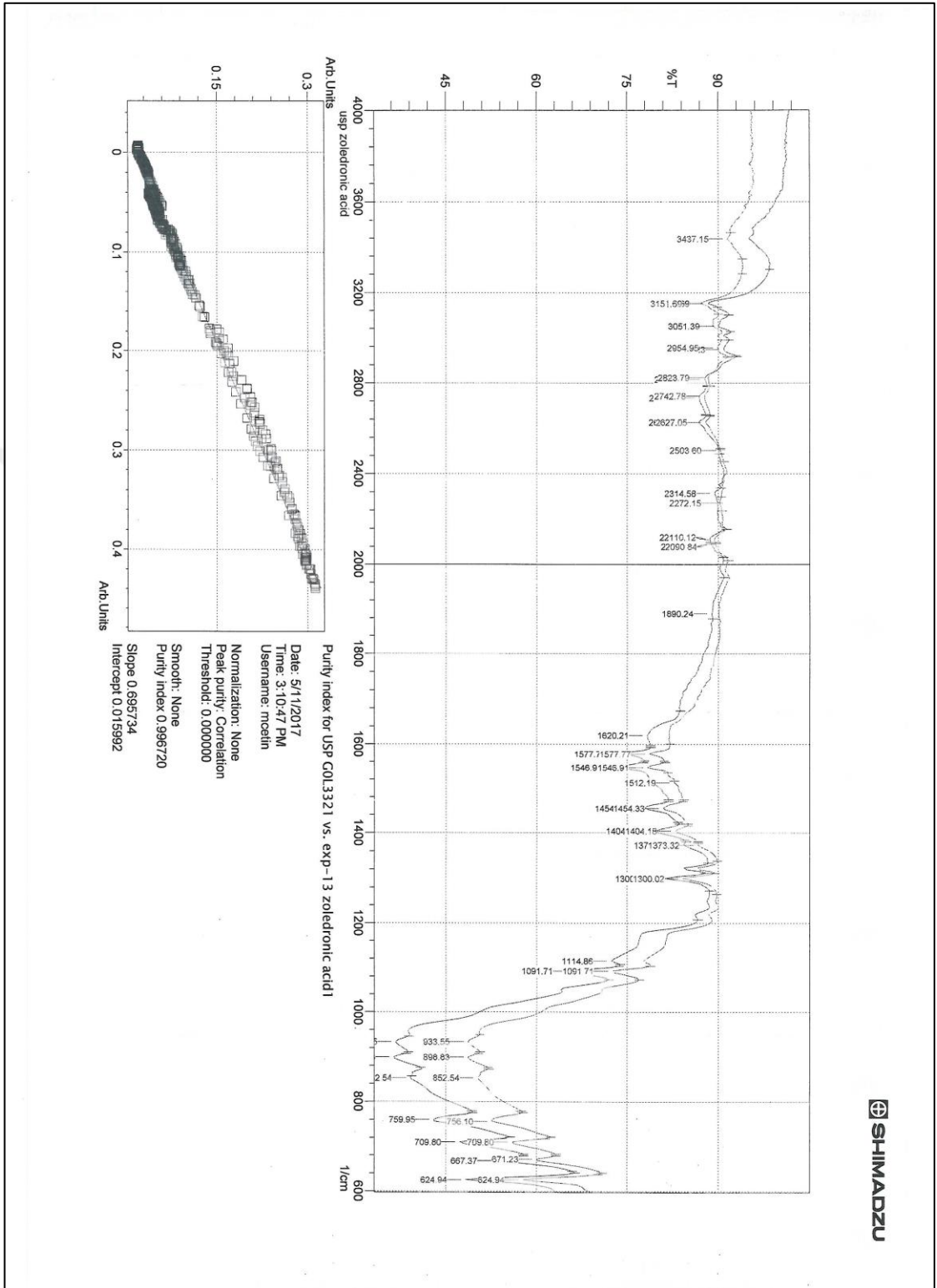
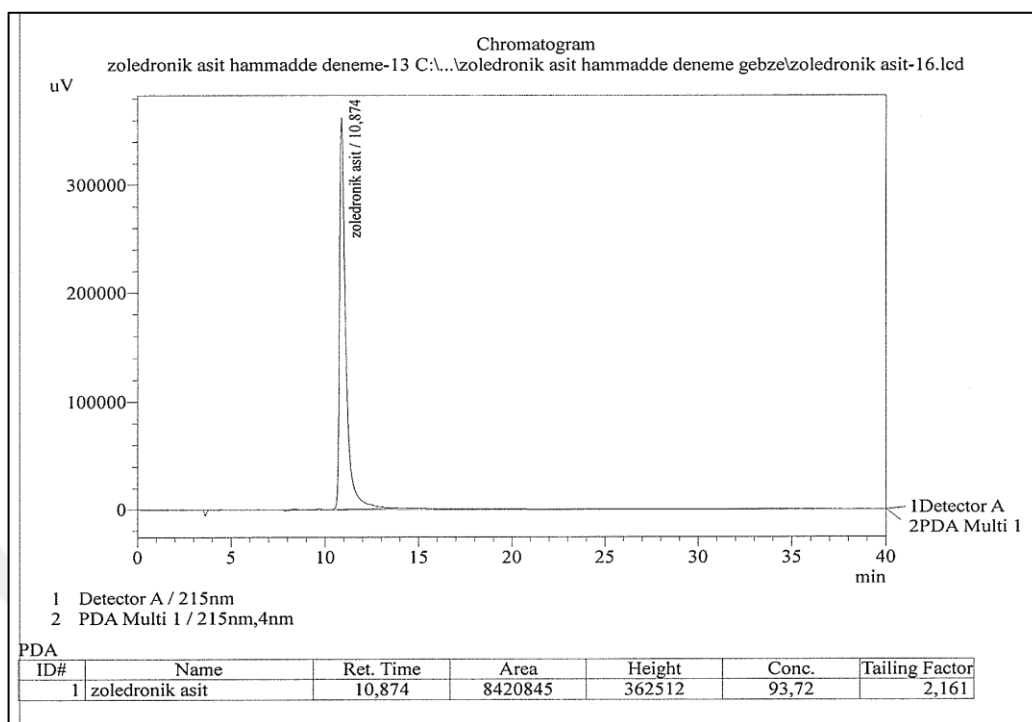
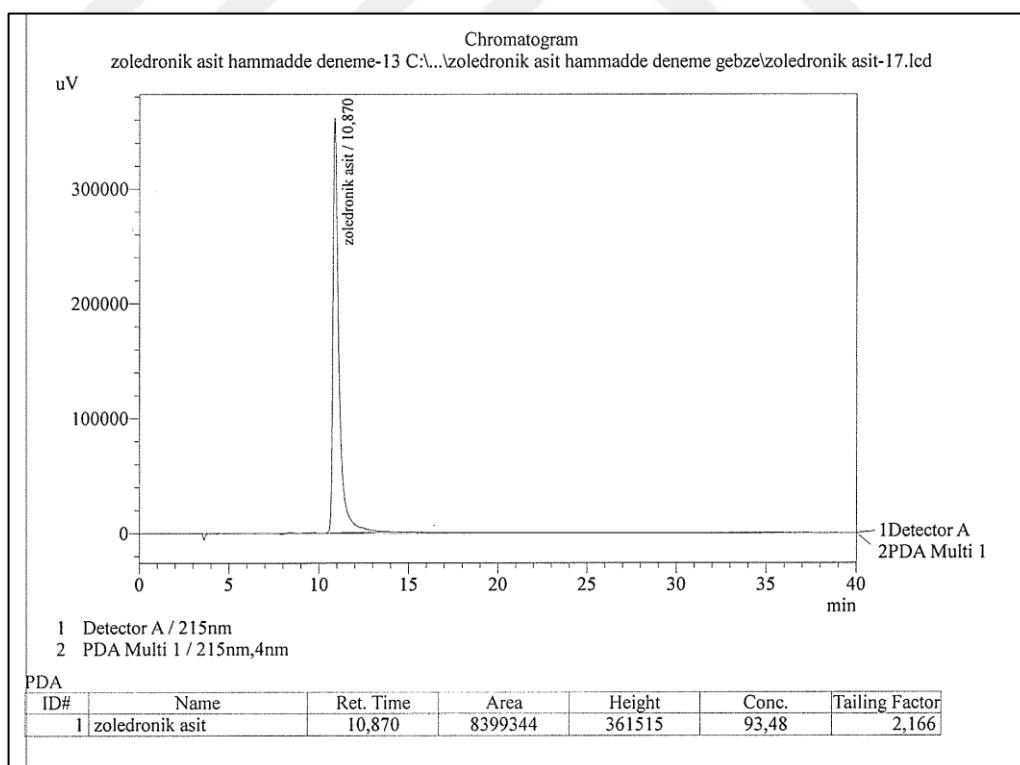


Figure A.41. IR result of 11^h experiment

Figure A.42. HPLC result (run 1) of 11th experimentFigure A.43. HPLC result (run 2) of 11th experiment

PC Control PC Control	Serial number 1111270515 Printed	Program version 4.0 2017-06-19 18:21:15
Result report		
Determination	Method KF Numune Analizi Last saved on 2016-12-08 14:32:18 ver. 9 Method status saved Determination Zoledronic Acid-20170619-180702 Determ. time 2017-06-19 18:07:02 Status of deter. original Sample number 29 User mkepur Full name Mahmut Kepur	
Sample data	Numune adi Zoledronic Acid Batch seri no. Exp 13 Sample size 0.2950 g	
03 KFT Ipol	Karl Fischer titration Ipol Sensor Metal electrode Titrant Hydranal Composite 5 Concentration 1.000 mol/L Titer 5.1636 mg/mL Date titer det. 2017-06-19 09:49:27 EP1 3.6300 mL Regular stop	
Results	Nem 6.35 %	
Statistics	n	Mean
	s +/-	s rel
	Nem 2	4.56 %
	2.524 %	55.35 %
Curve		
03 KFT Ipol	Karl Fischer titration Ipol	
Date	Signature	
Reason		

Figure A.44. KF data of 11th experiment

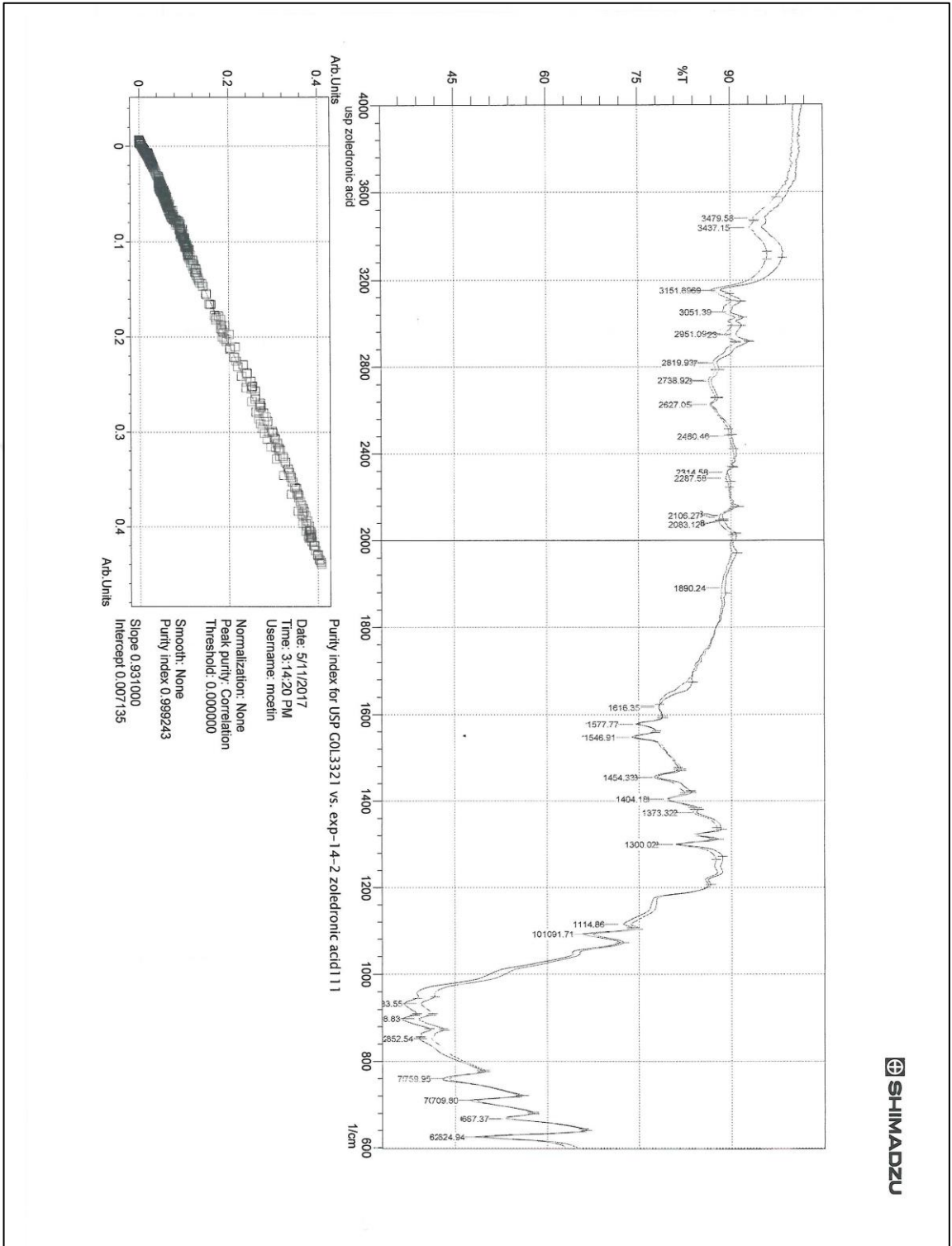
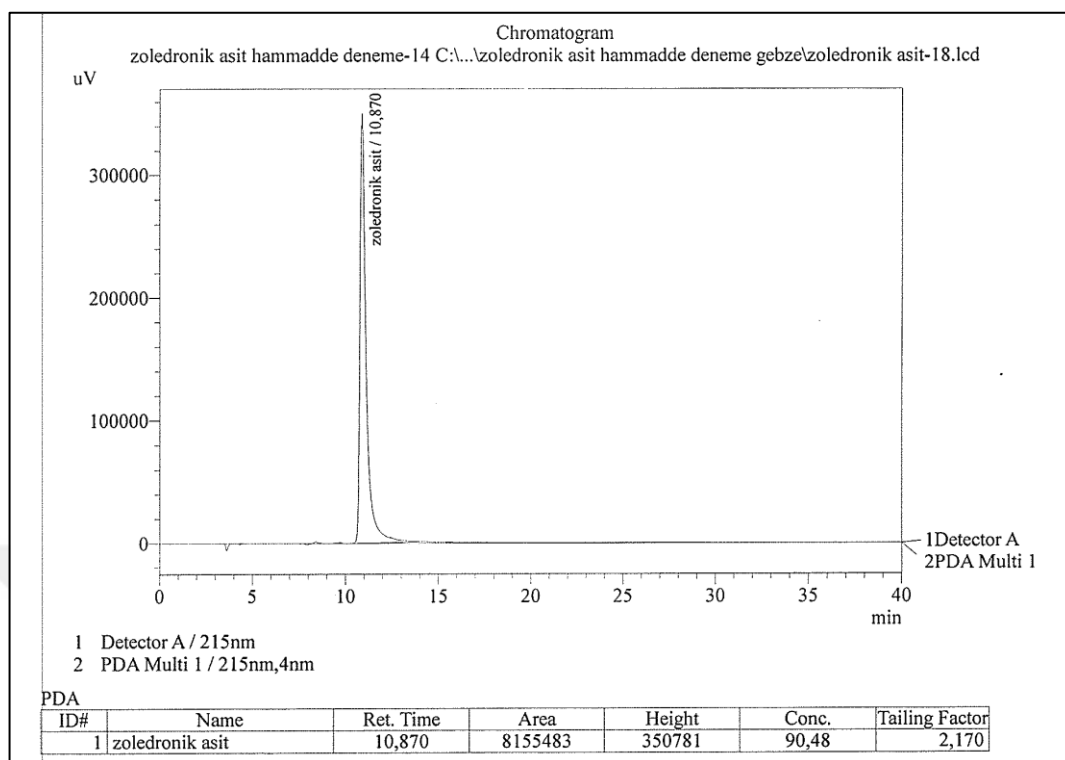
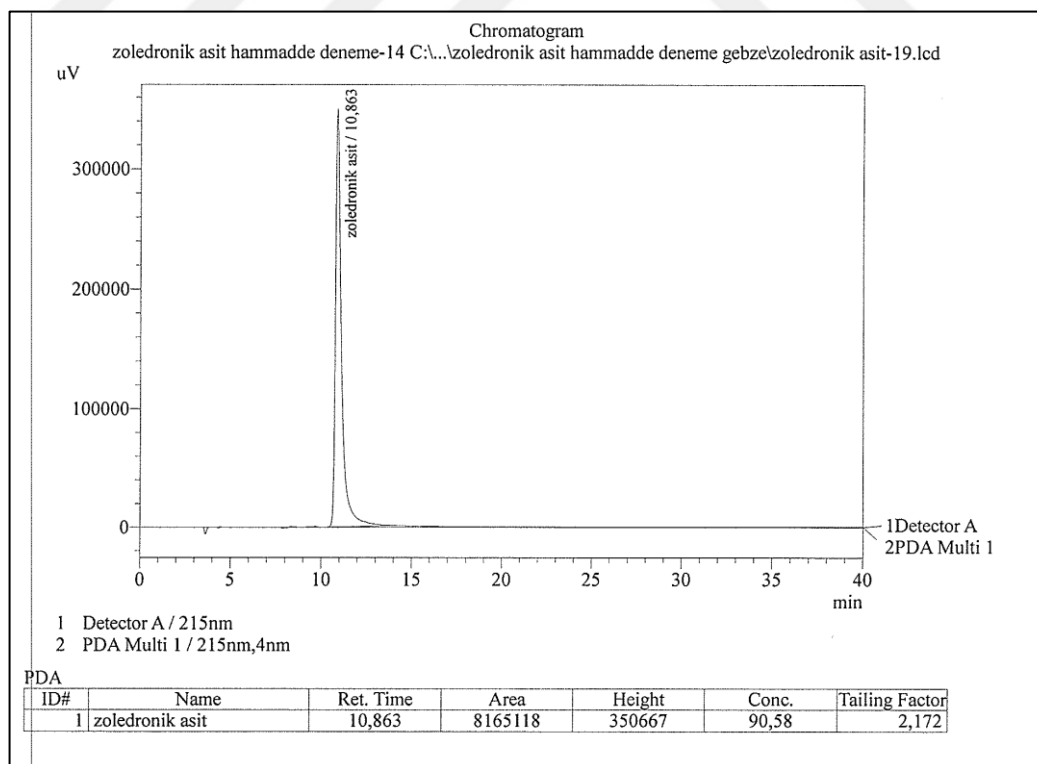


Figure A.45. IR result of 12th experiment

Figure A.46 HPLC result (run 1) of 12th experimentFigure A.47. HPLC result (run 2) of 12th experiment

PC Control PC Control	Serial number 1111270515 Printed	Program version 4.0 2017-06-19 18:33:25		
Result report				
Determination	Method KF Numune Analizi Last saved on 2016-12-08 14:32:18 ver. 9 Method status saved Determination Zoledronic Acid-20170619-182527 Determ. time 2017-06-19 18:25:27 Status of deter. original Sample number 30 User mkepur Full name Mahmut Kepur			
Sample data	Numune adi Zoledronic Acid Batch seri no. Exp 14 Sample size 0.3038 g			
03 KFT Ipol	Karl Fischer titration Ipol Sensor Metal electrode Titrant Hydranal Composite 5 Concentration 1.000 mol/L Titer 5.1636 mg/mL Date titer det. 2017-06-19 09:49:27 EP1 3.7150 mL Regular stop			
Results	Nem 6.31 %			
Statistics	n	Mean	s +/-	s rel
	Nem 1	6.31 %		
Curve				
03 KFT Ipol	Karl Fischer titration Ipol			
Date Reason	Signature			

Figure A.48. KF data of 12th experiment

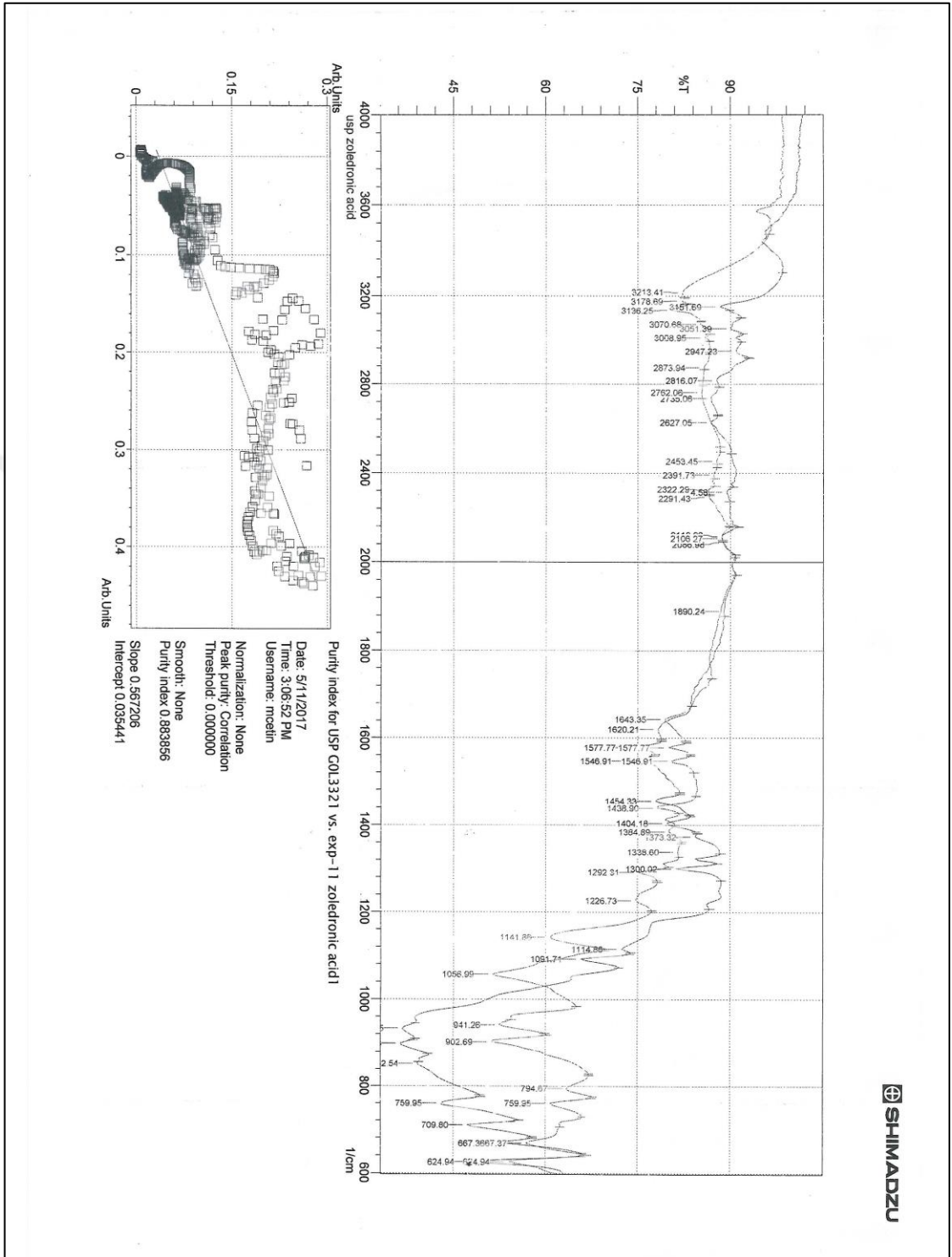
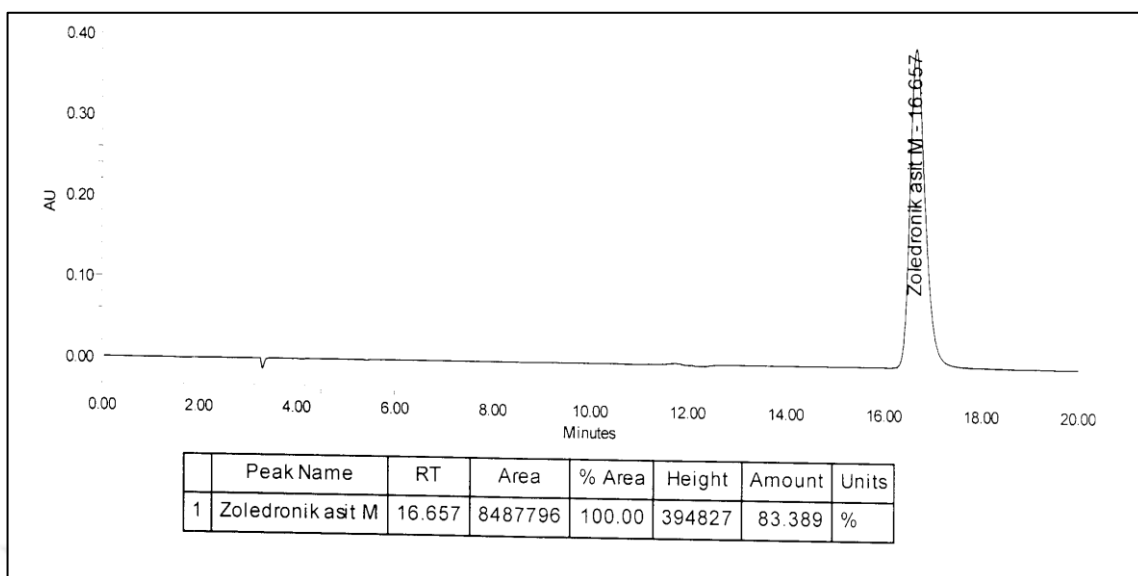
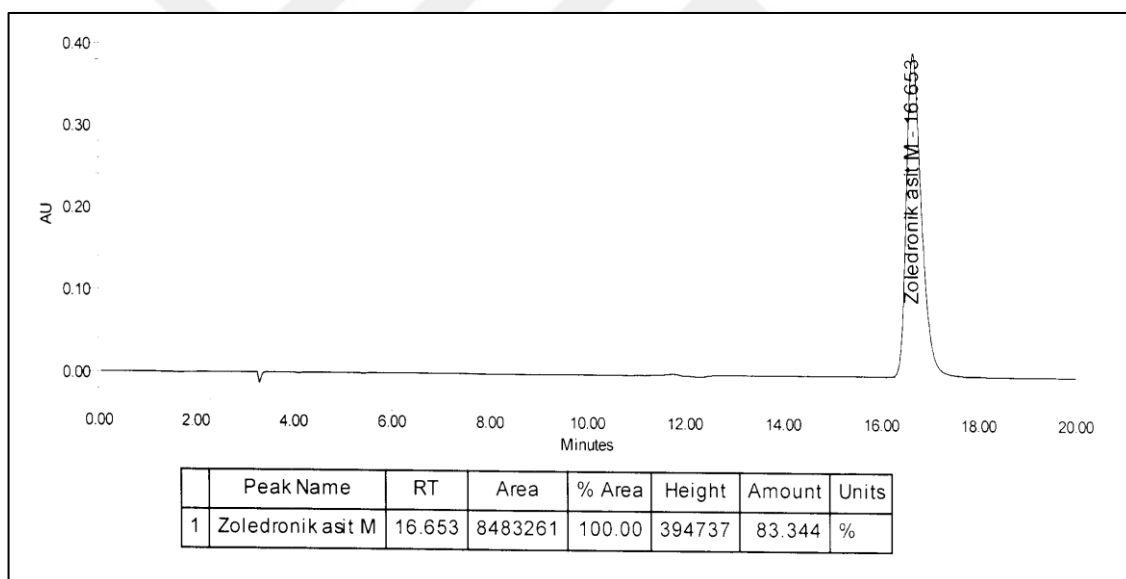


Figure A.49. IR result of 9th experiment

Figure A.50. HPLC result (run 1) of 9th experimentFigure A.51. HPLC result (run 2) of 9th experiment

PC Control PC Control	Serial number 1111270515 Printed	Program version 4.0 2017-06-19 14:30:51										
Result report												
Determination	Method KF Numune Analizi Last saved on 2016-12-08 14:32:18 ver. 9 Method status saved Determination Zoledronik Asit-20170619-142052 Determ. time 2017-06-19 14:20:52 Status of deter. original Sample number 17 User mkepur Full name Mahmut Kepur											
Sample data	Numune adi Zoledronik Asit Batch seri no. deneme-11 Sample size 0.3018 g											
03 KFT Ipol	Karl Fischer titration Ipol Sensor Metal electrode Titrant Hydranal Composite 5 Concentration 1.000 mol/L Titer 5.1636 mg/mL Date titer det. 2017-06-19 09:49:27 Titration EP1 9.7270 mL Regular stop											
Results	Nem 16.64 %											
Statistics	<table border="1"> <thead> <tr> <th></th> <th>n</th> <th>Mean</th> <th>s +/-</th> <th>s rel</th> </tr> </thead> <tbody> <tr> <td>Nem</td> <td>2</td> <td>11.50 %</td> <td>7.276 %</td> <td>63.27 %</td> </tr> </tbody> </table>			n	Mean	s +/-	s rel	Nem	2	11.50 %	7.276 %	63.27 %
	n	Mean	s +/-	s rel								
Nem	2	11.50 %	7.276 %	63.27 %								
Curve												
03 KFT Ipol Karl Fischer titration Ipol												
Date Reason	Signature											

Figure A.52. KF data of 9th experiment

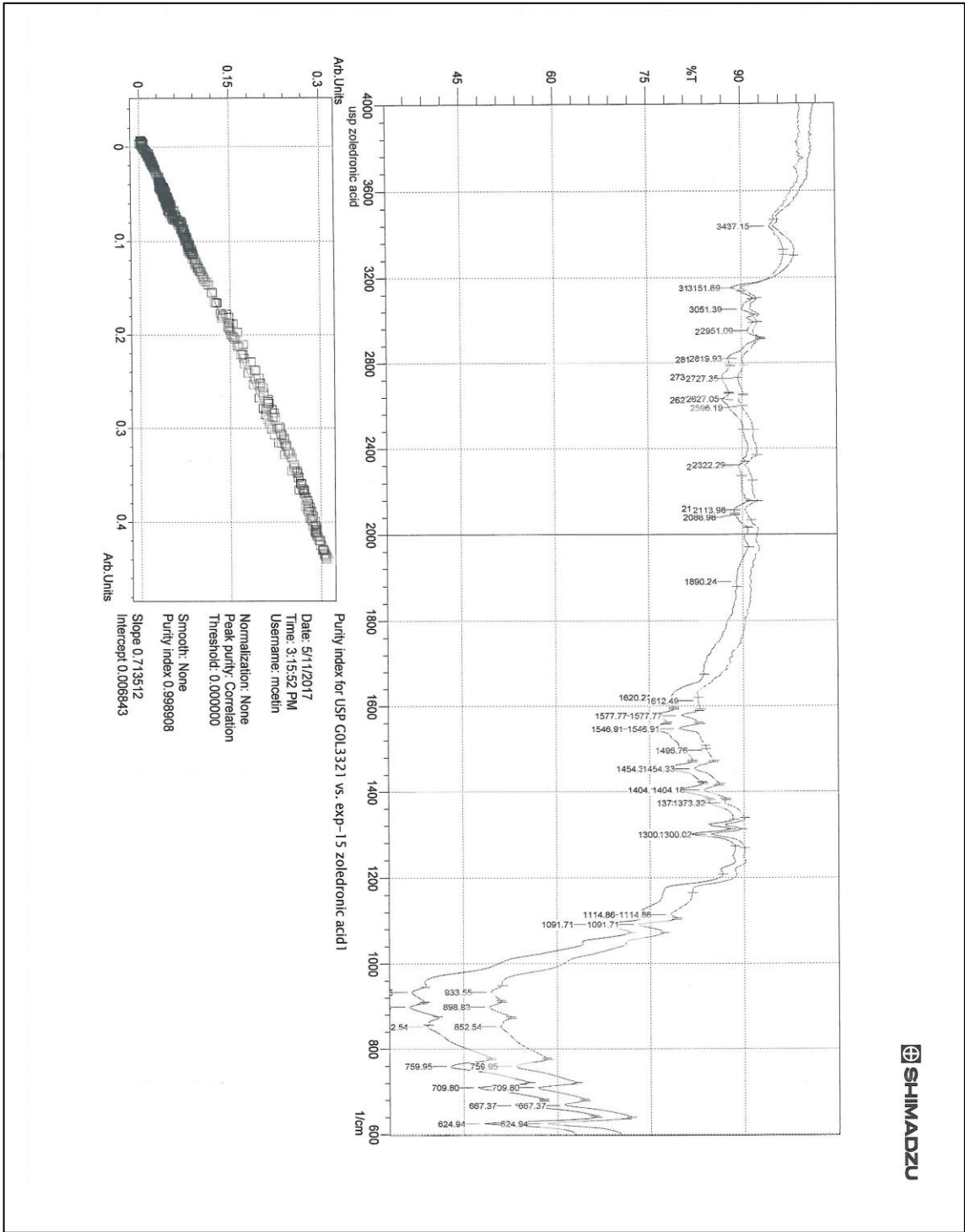
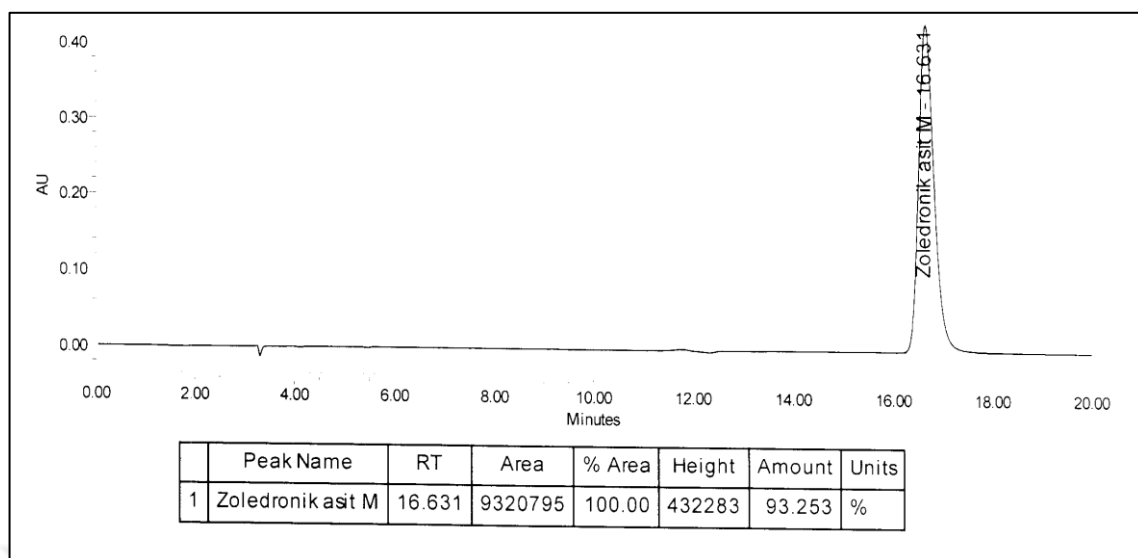
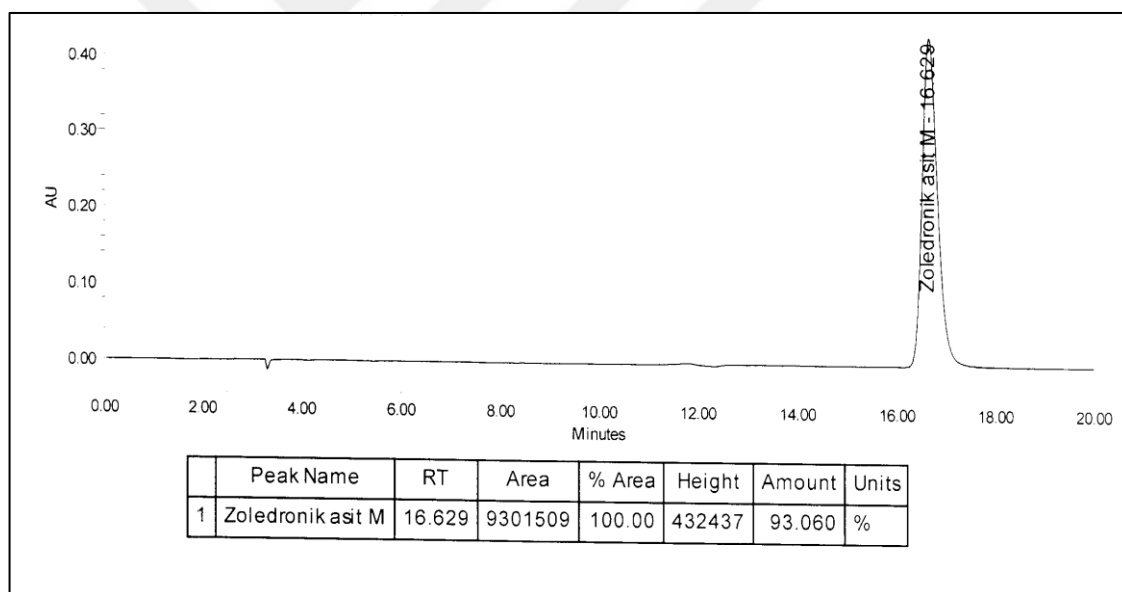


Figure A.53. IR result of 13th experiment

Figure A.54. HPLC result (run 1) of 13th experimentFigure A.55. HPLC result (run 2) of 13th experiment

PC Control PC Control	Serial number 1111270515 Printed	Program version 4.0 2017-06-24 18:33:01		
Result report				
Determination	Method KF Numune Analizi Last saved on 2016-12-08 14:32:18 ver. 9 Method status saved Determination Zoledronic acid-20170624-183129 Determ. time 2017-06-24 18:31:29 Status of deter. original Sample number 33 User ekamo Full name Erdogan Kamo			
Sample data	Numune adi Zoledronic acid Batch seri no. deneme 15 Sample size 0.0550 g			
03 KFT Ipol	Karl Fischer titration Ipol Sensor Metal electrode Titrant Hydranal Composite 5 Concentration 1.000 mol/L Titer 4.9974 mg/mL Date titer det. 2017-06-24 13:25:26 Titration EP1 0.4210 mL Regular stop			
Results	Nem 3.83 %			
Statistics	n	Mean	s +/-	s rel
	Nem 2	3.62 %	0.297 %	8.20 %
Curve				
03 KFT Ipol	Karl Fischer titration Ipol			
Date	Signature			
Reason				

Figure A.56. KF data of 13th experiment

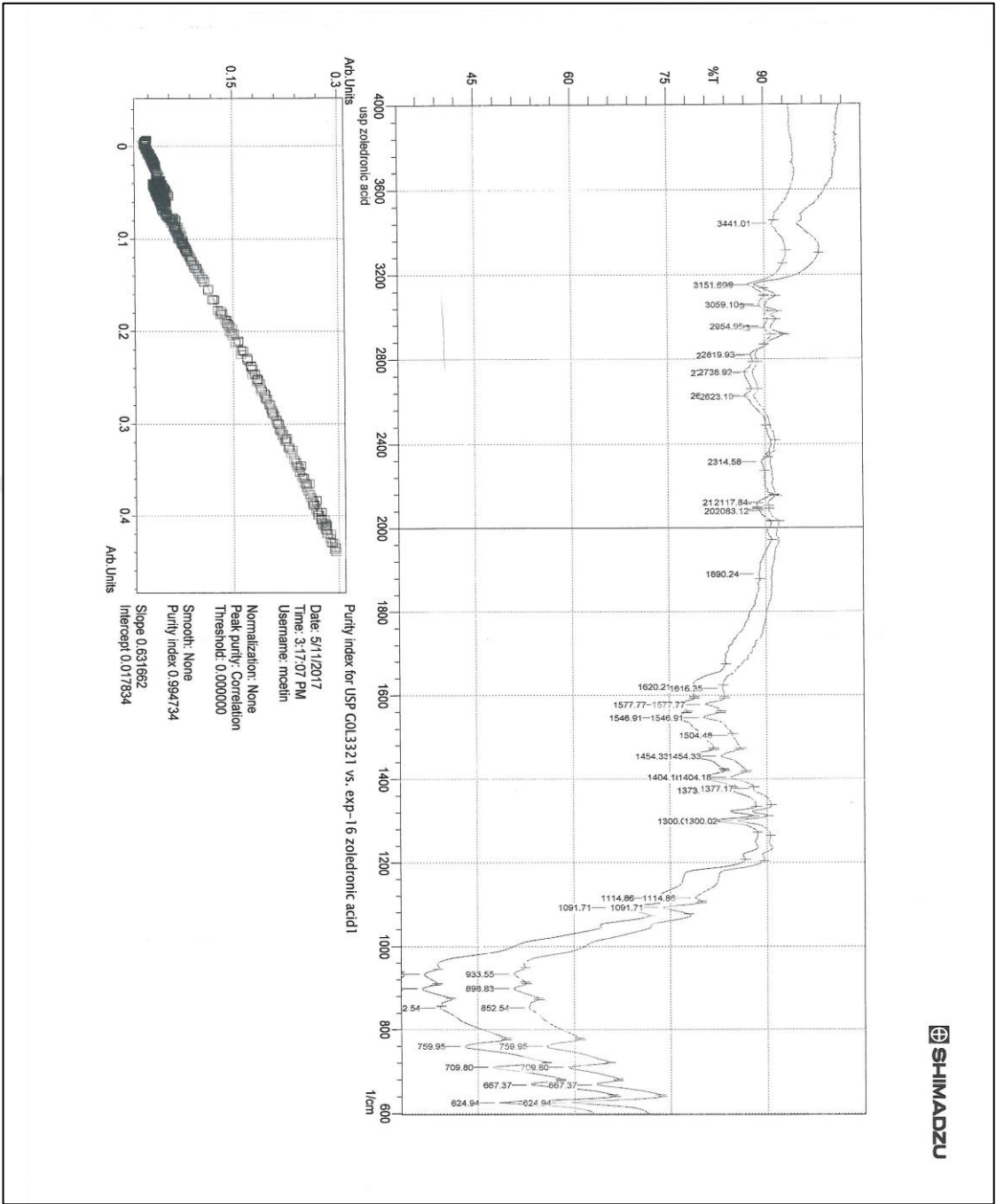
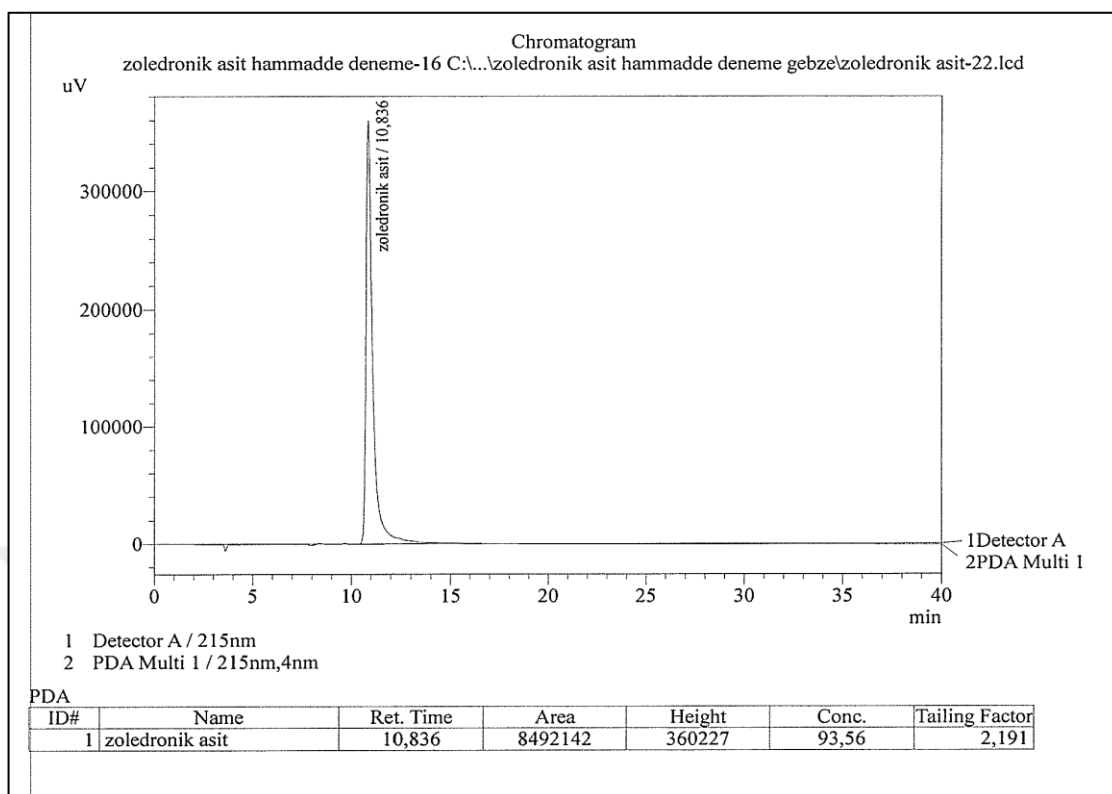
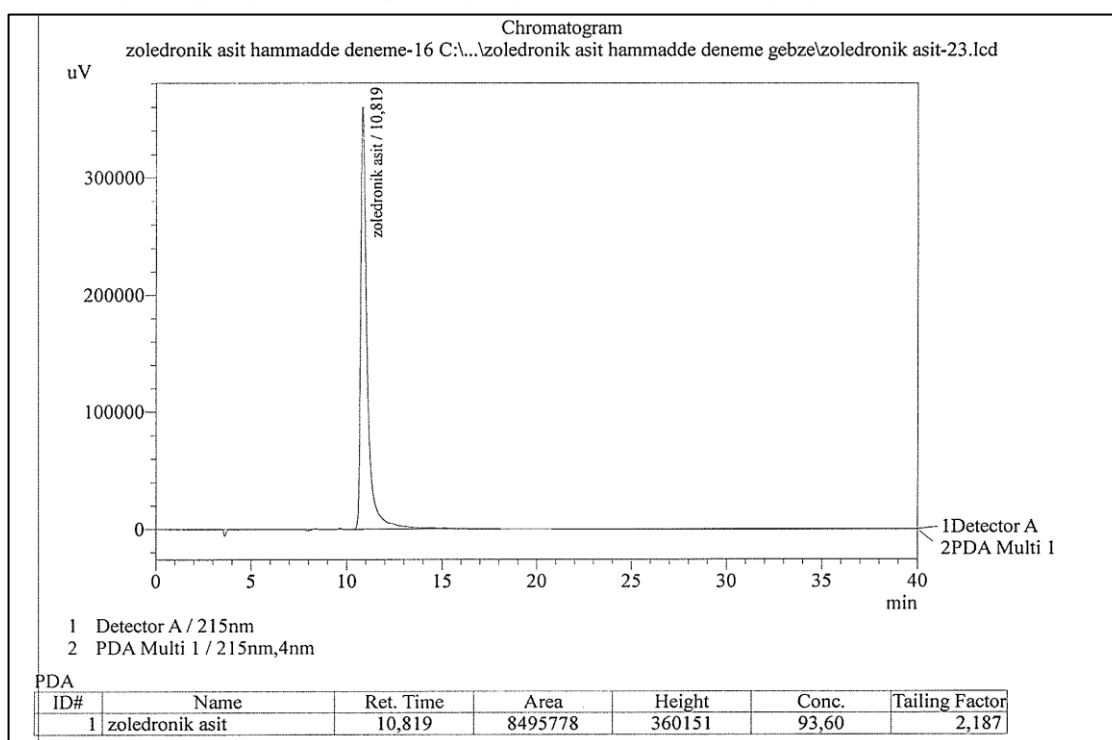
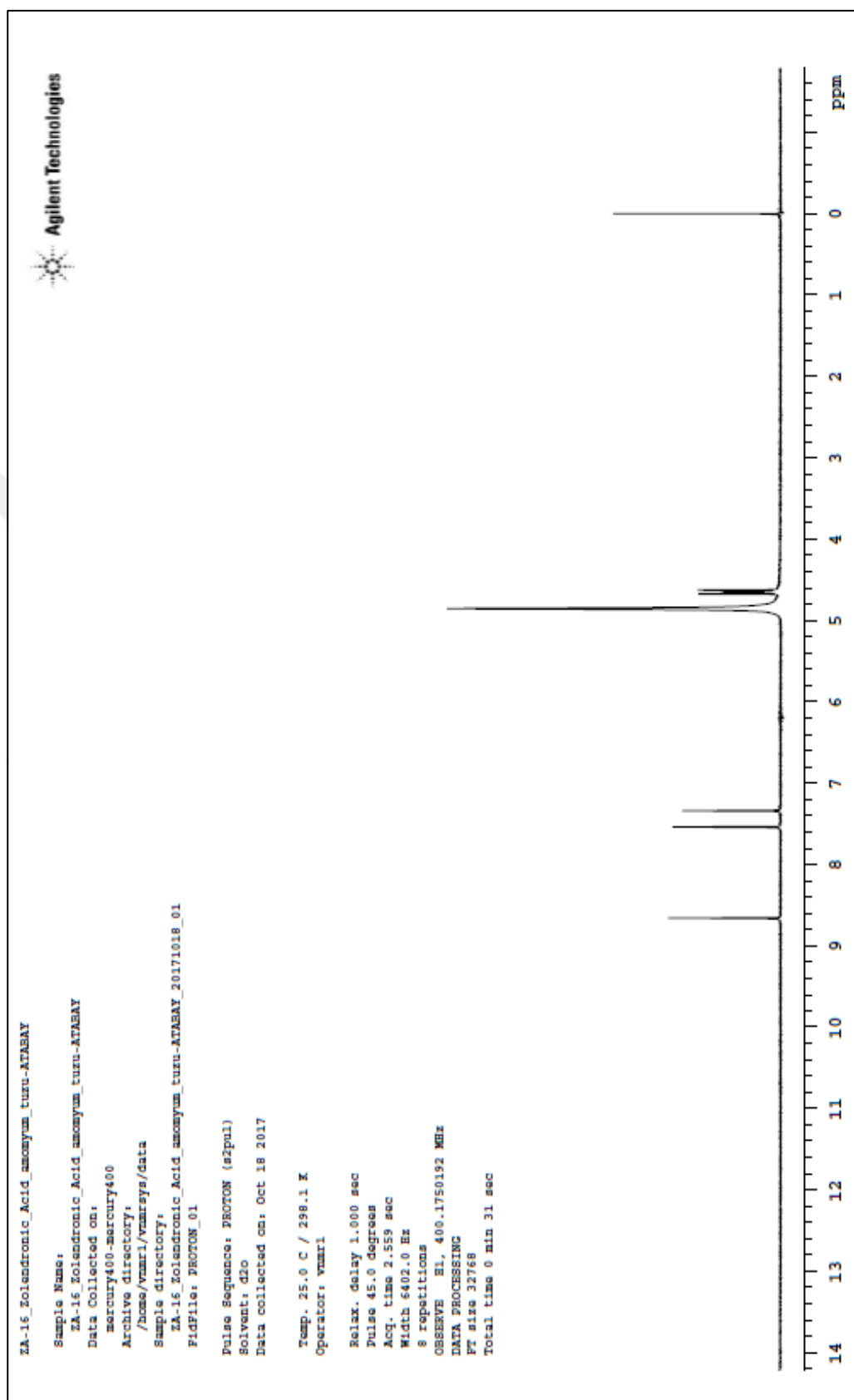


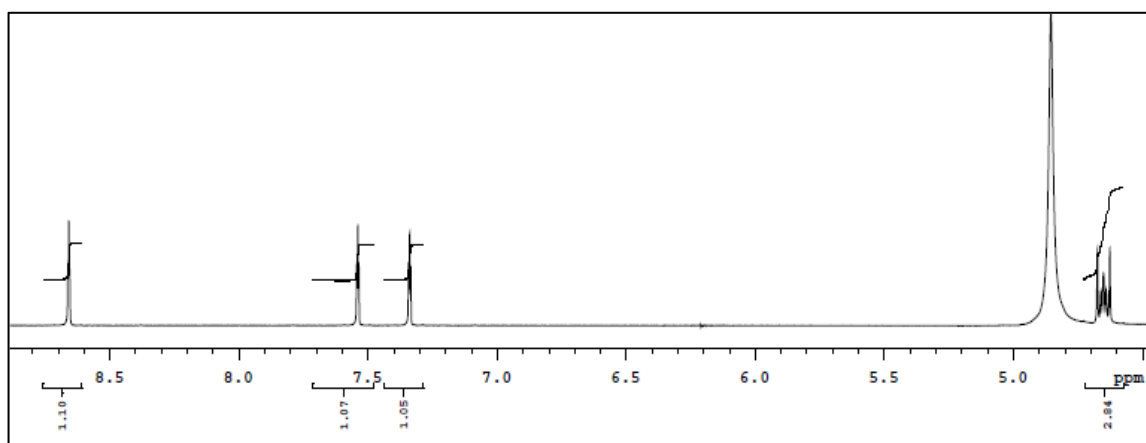
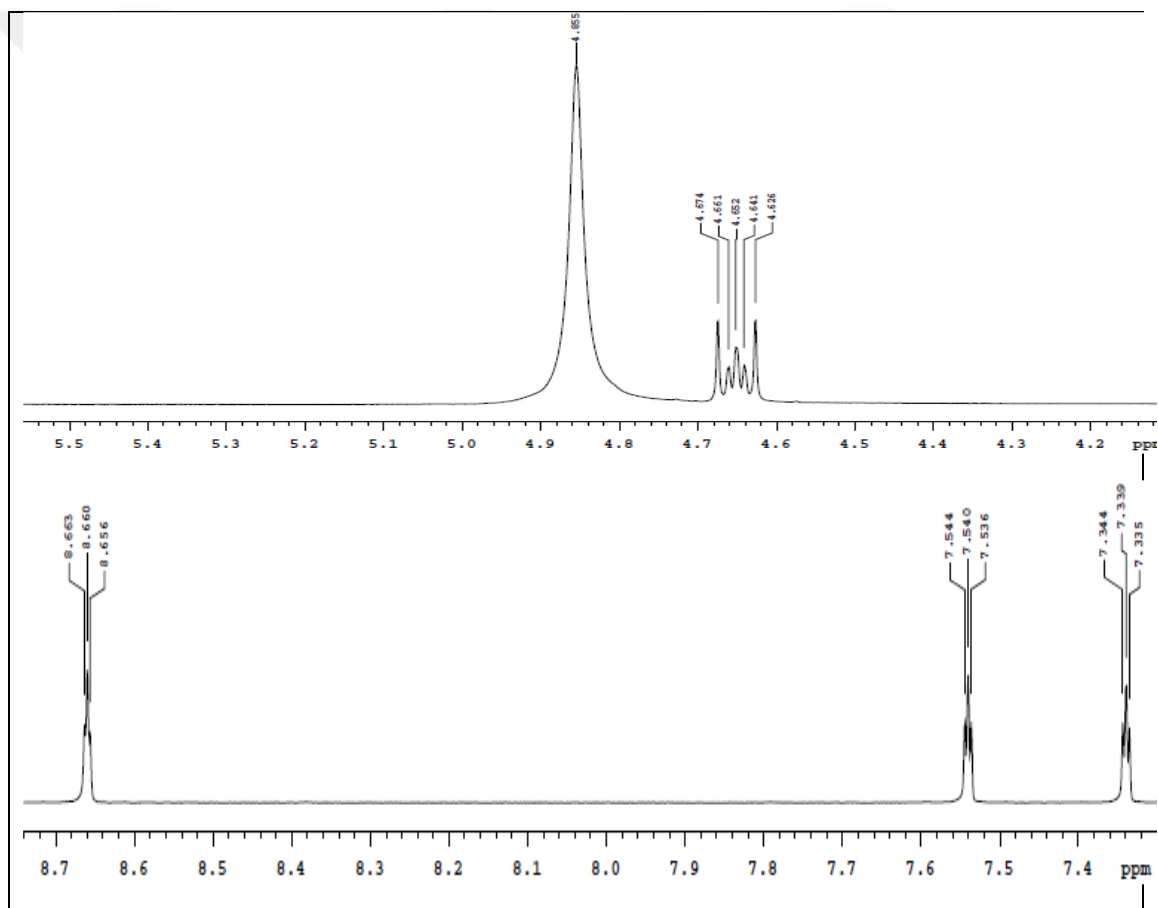
Figure A.57. IR result of 14th experiment

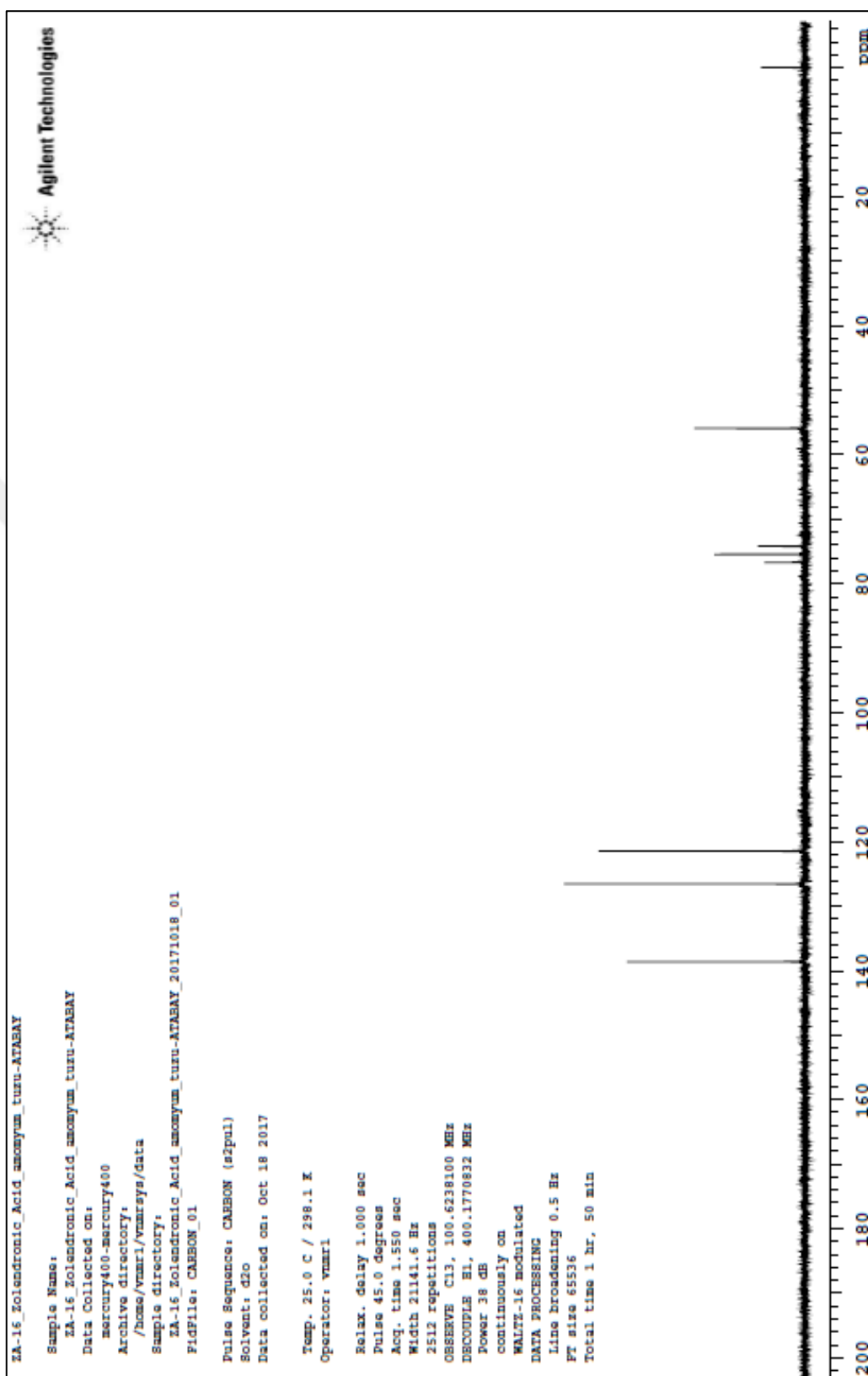
Figure A.58. HPLC result (run 1) of 14th experimentFigure A.59. HPLC result (run 2) of 14th experiment

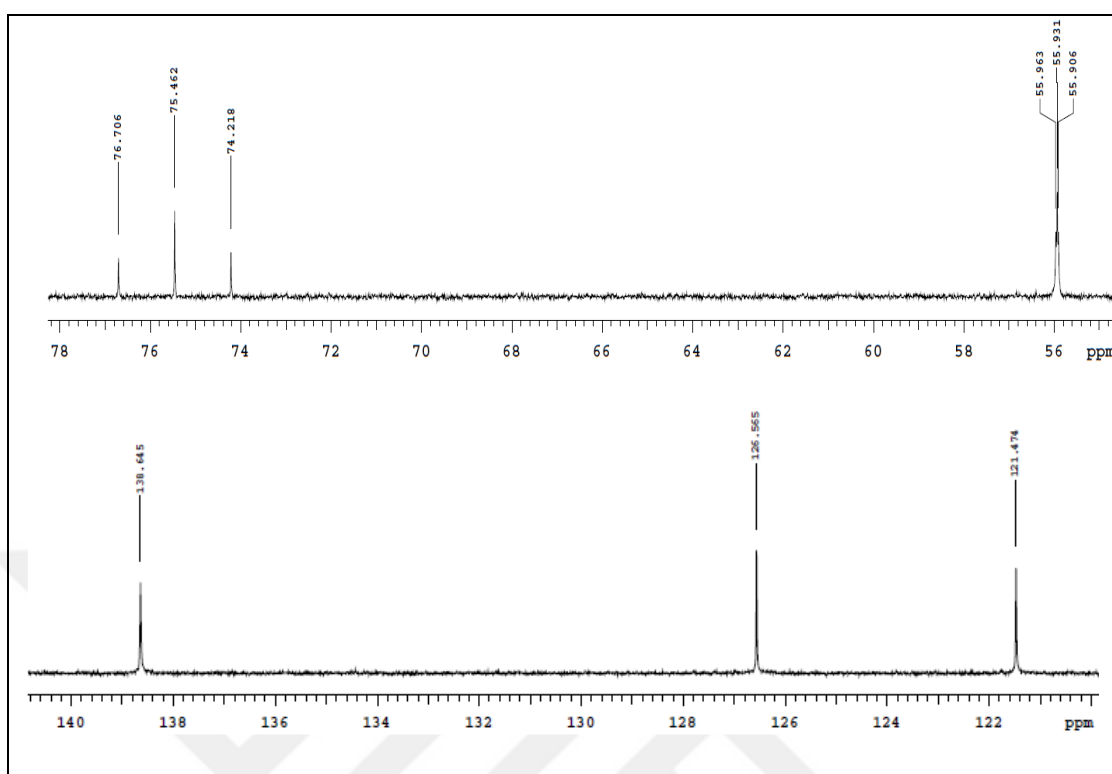
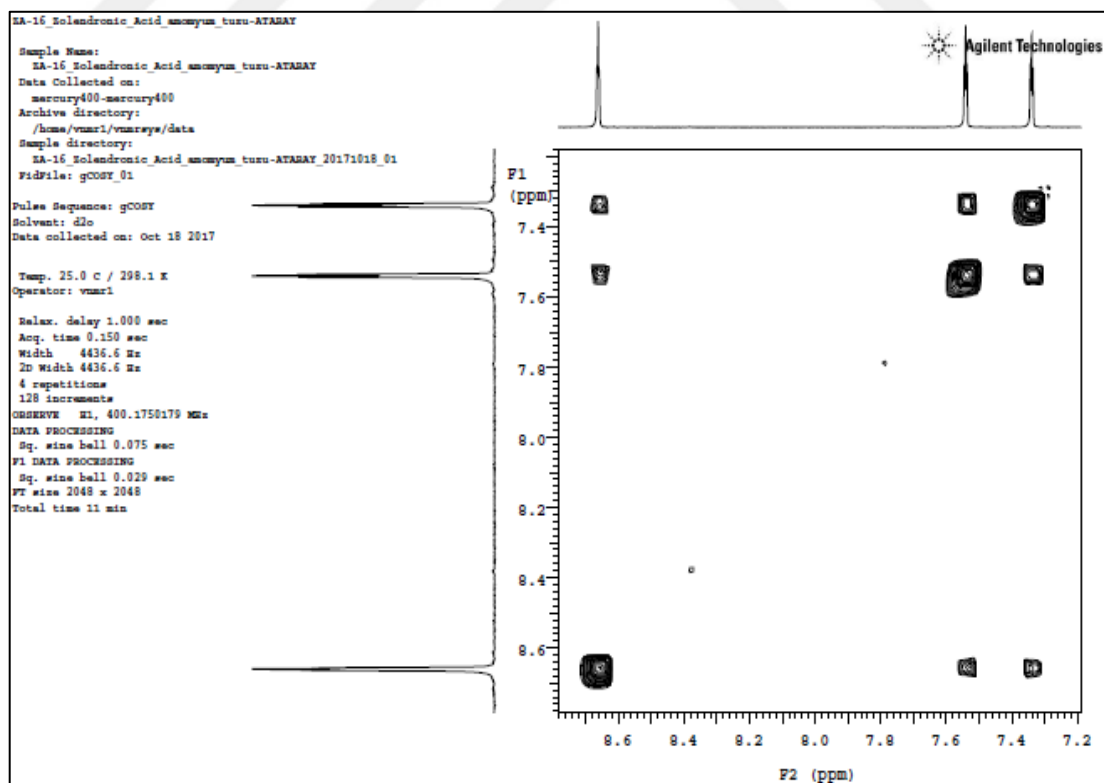
PC Control PC Control	Serial number 1111270515 Printed	Program version 4.0 2017-06-20 11:51:27
Result report		
Determination	Method KF Numune Analizi Last saved on 2016-12-08 14:32:18 ver. 9 Method status saved Determination Zoledronic acid-20170620-114313 Determ. time 2017-06-20 11:43:13 Status of deter. original Sample number 12 User mkepur Full name Mahmut Kepur	
Sample data	Numune adi Zoledronic acid Batch seri no. deneme 16 Sample size 0.1011 g	
03 KFT Ipol	Karl Fischer titration Ipol Sensor Metal electrode Titrant Hydranal Composite 5 Concentration 1.000 mol/L Titer 5.1434 mg/mL Date titer det. 2017-06-20 10:41:15 Titration EP1 1.4110 mL Regular stop	
Results	Nem 7.18 %	
Statistics	n	Mean
		s +/-
		s rel
	Nem 1	7.18 %
Curve		
03 KFT Ipol	Karl Fischer titration Ipol	
Date	Signature	
Reason		

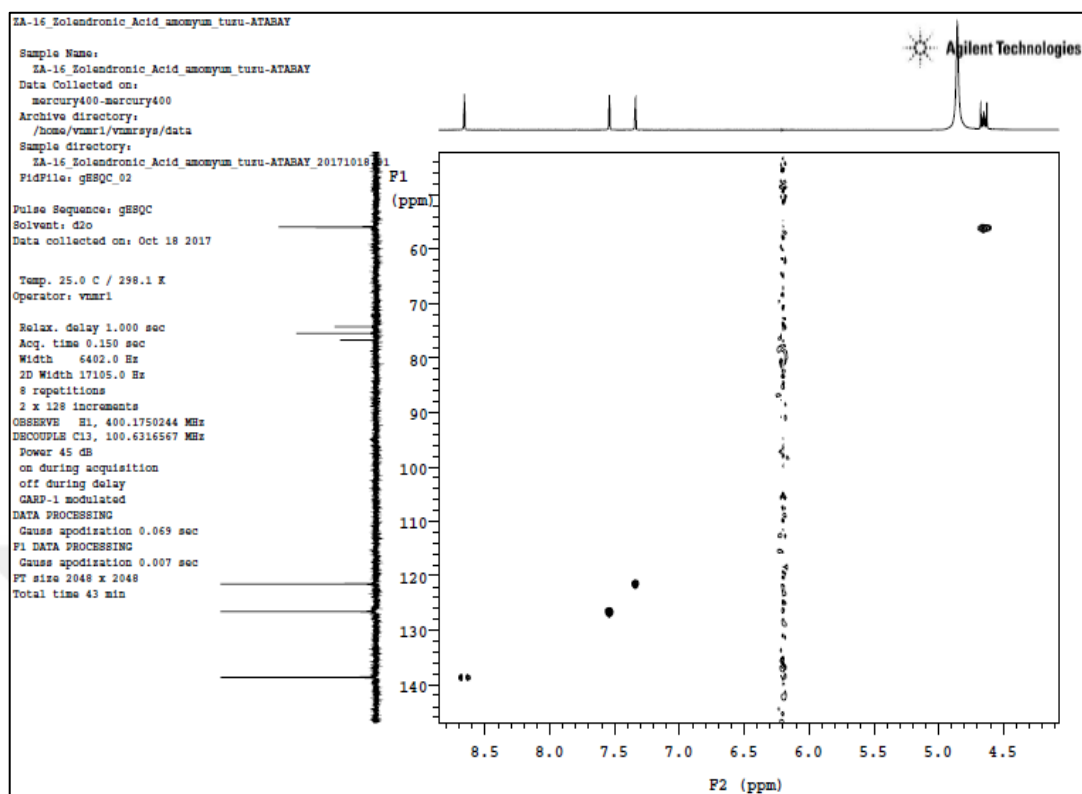
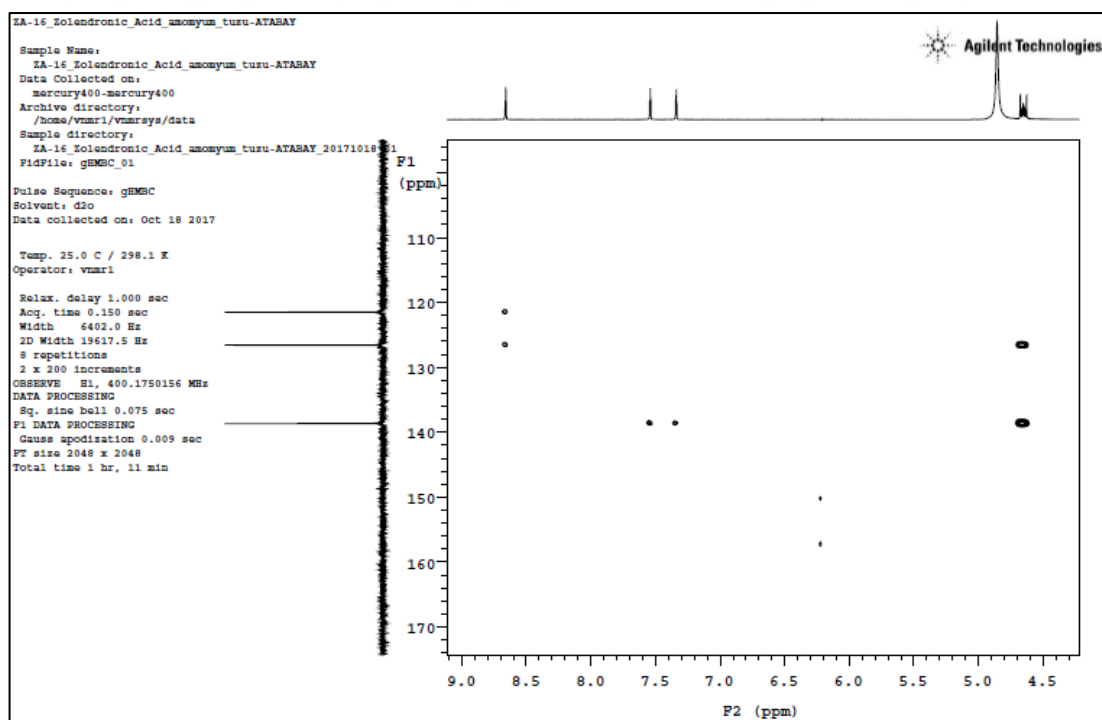
Figure A.60. KF data of 14th experiment

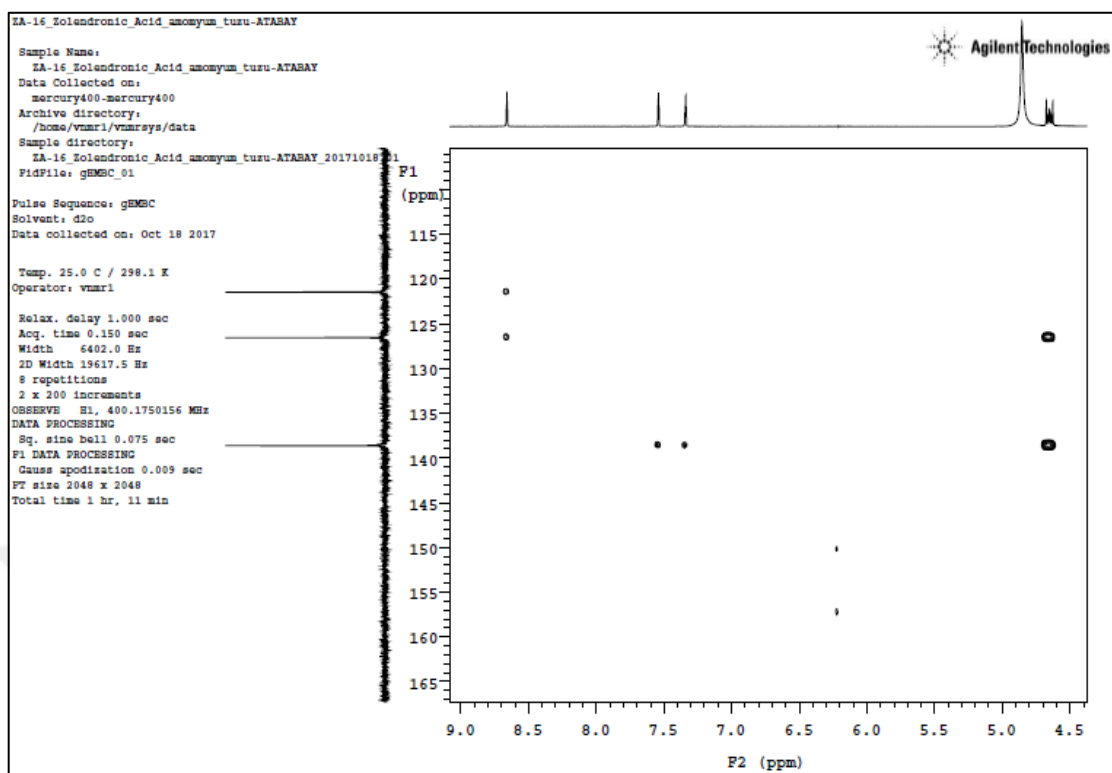
Figure A.61. H-NMR spectrum of 14th experiment

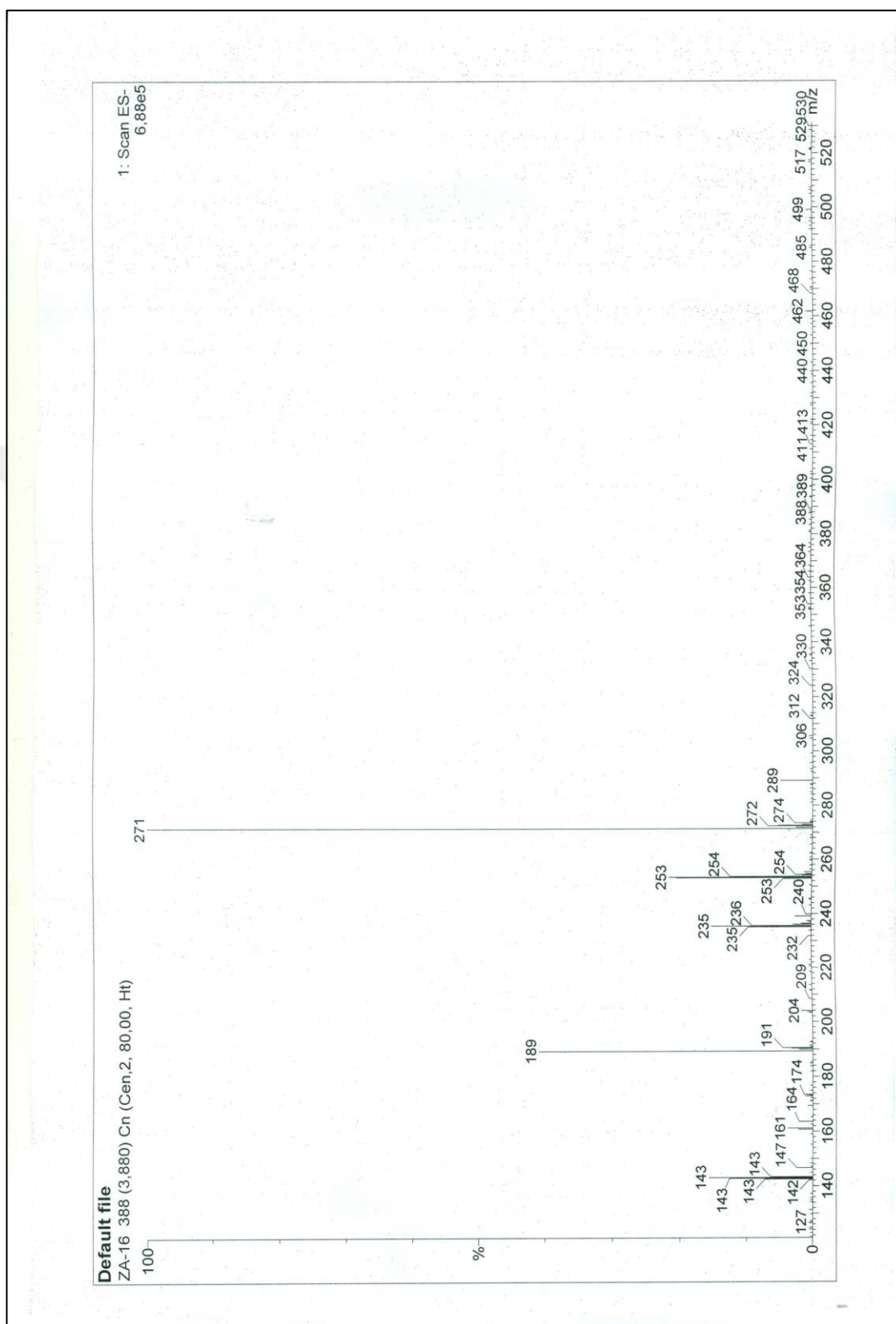
Figure A.62. H-NMR spectrum of 14th experiment with magnitudesFigure A.63. H-NMR spectrum details of 14th experiment

Figure A.64. C-NMR spectrum of 14th experiment

Figure A.65. C-NMR spectrum details of 14th experimentFigure A.66. COSY spectrum of 14th experiment

Figure A.67. HSQC spectrum of 14th experimentFigure A.68. HMBC spectrum details of 14th experiment

Figure A.69. HMBC spectrum details of 14th experiment

Figure A.70. Mass spectrum details of 14th experiment

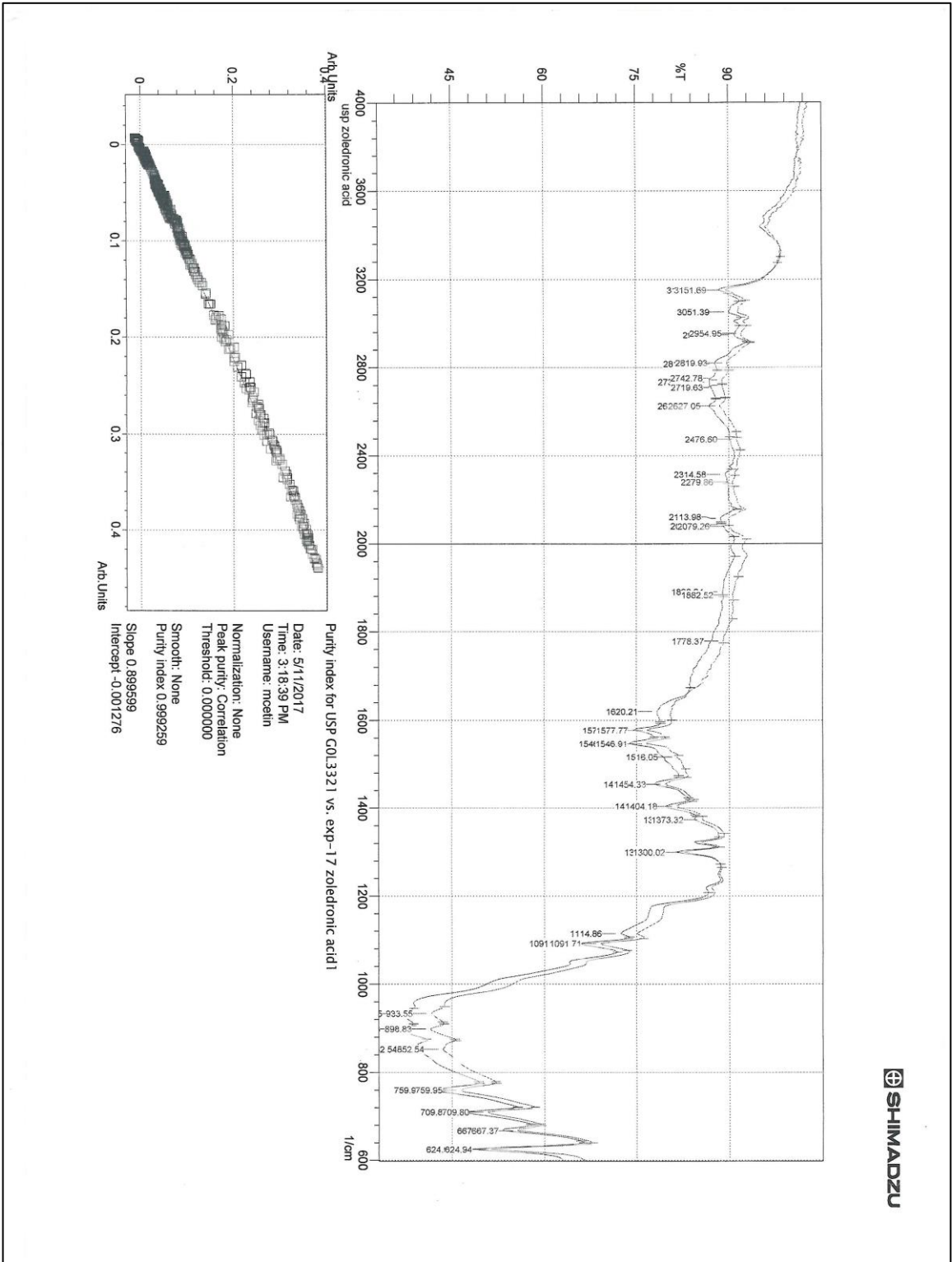
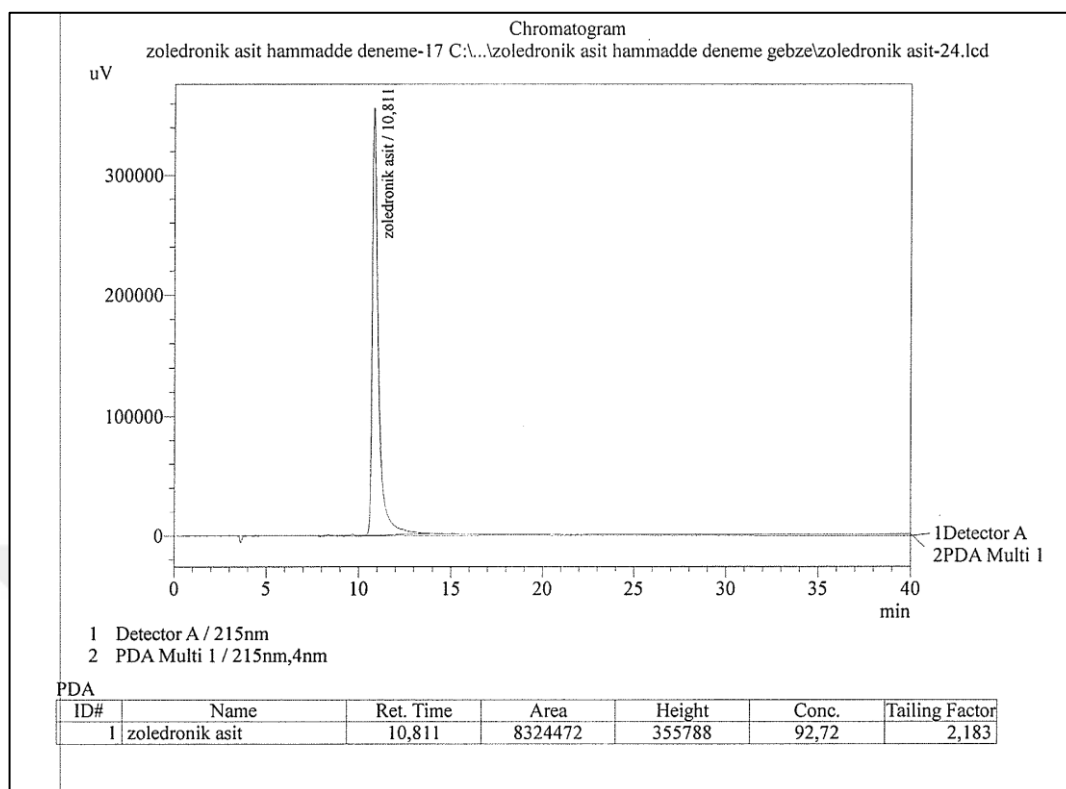
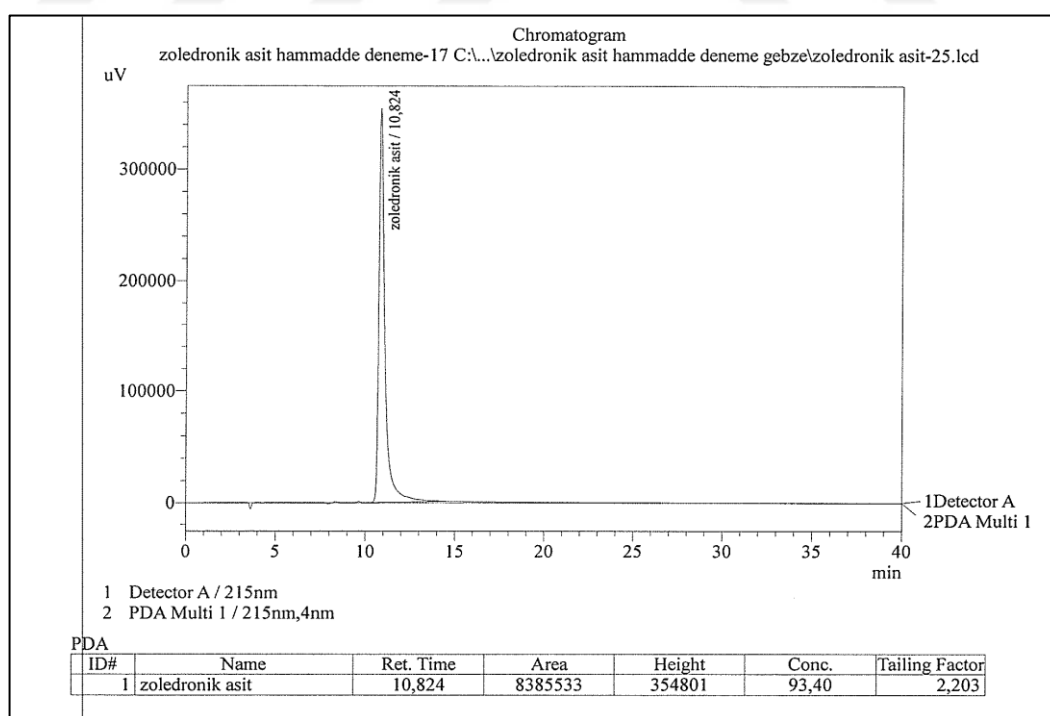
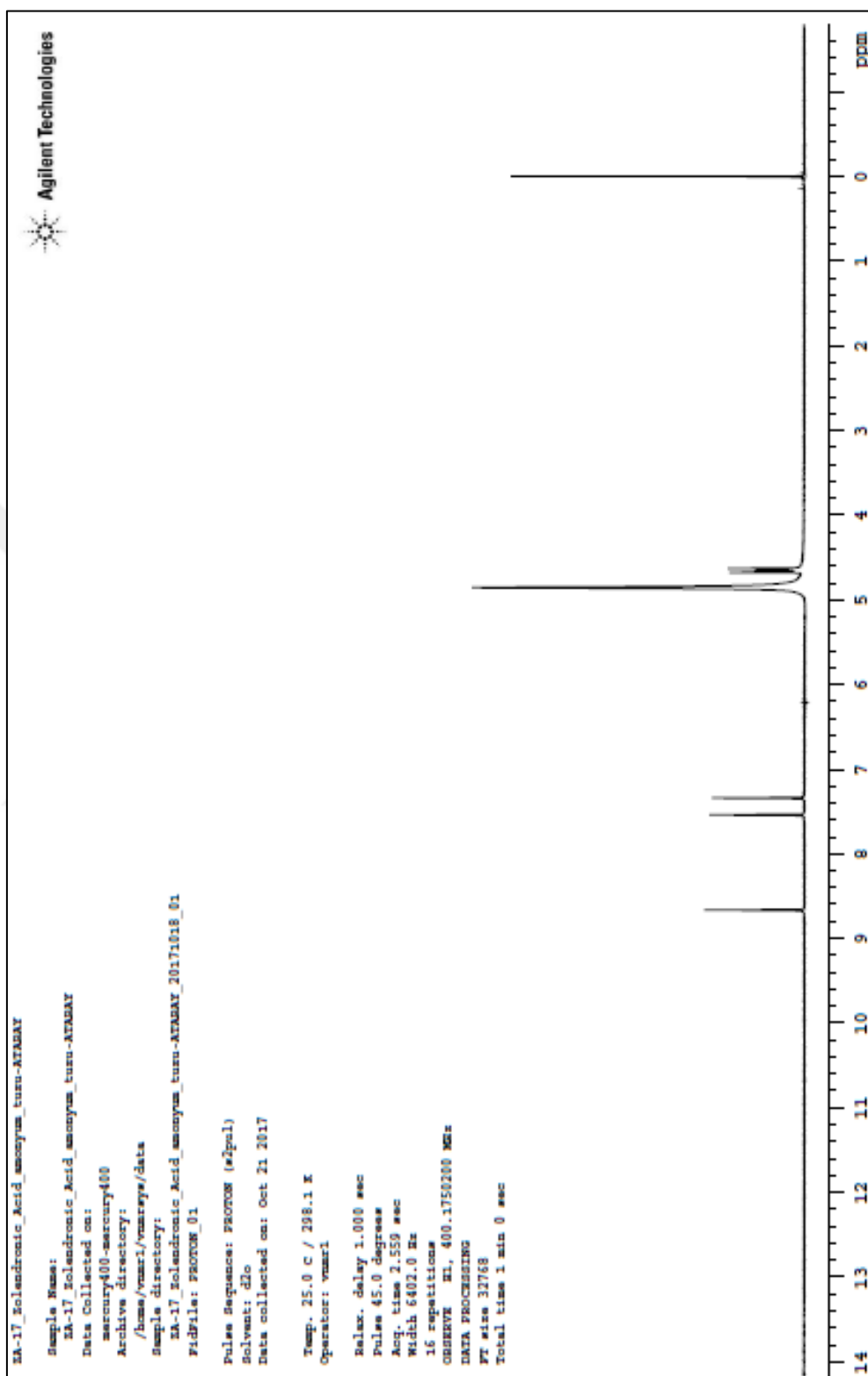


Figure A.71. IR result of 15th experiment

Figure A.72. HPLC result (run 1) of 15th experimentFigure A.73. HPLC result (run 2) of 15th experiment

PC Control PC Control	Serial number 1111270515 Printed	Program version 4.0 2017-06-20 12:20:16		
Result report				
Determination	Method KF Numune Analizi Last saved on 2016-12-08 14:32:18 ver. 9 Method status saved Determination Zoledronic acid-20170620-121319 Determ. time 2017-06-20 12:13:19 Status of deter. original Sample number 15 User mkepur Full name Mahmut Kepur			
Sample data	Numune adi Zoledronic acid Batch seri no. deneme 17 Sample size 0.1030 g			
03 KFT Ipol	Karl Fischer titration Ipol Sensor Metal electrode Titrant Hydranal Composite 5 Concentration 1.000 mol/L Titer 5.1434 mg/mL Date titer det. 2017-06-20 10:41:15 EP1 1.2950 mL Regular stop			
Results	Nem 6.47 %			
Statistics	n	Mean	s +/-	s rel
	Nem 2	6.00 %	0.658 %	10.97 %
Messages	Sample out of range			
Curve				
03 KFT Ipol	Karl Fischer titration Ipol			
Date	Signature			
Reason				

Figure A.74. KF data of 15th experiment

Figure A.75. H-NMR spectrum of 15th experiment

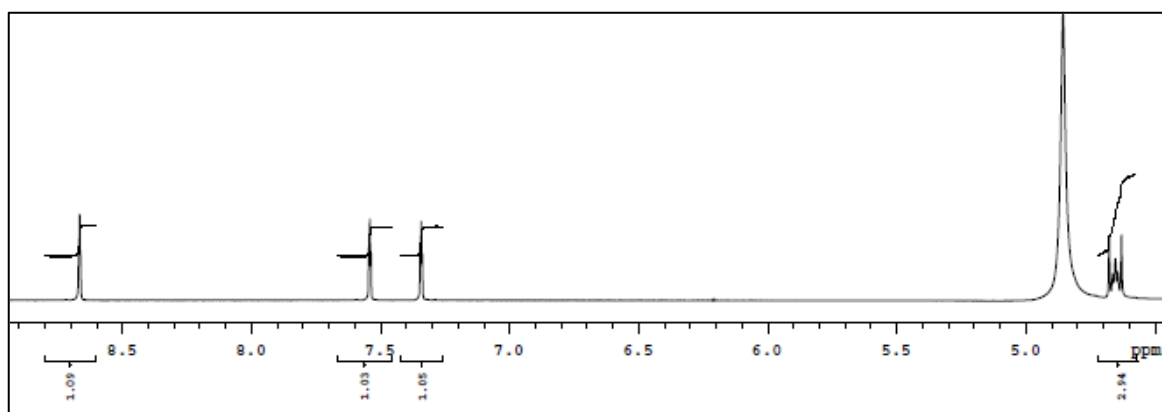


Figure A.76. H-NMR spectrum of 15th experiment with magnitudes

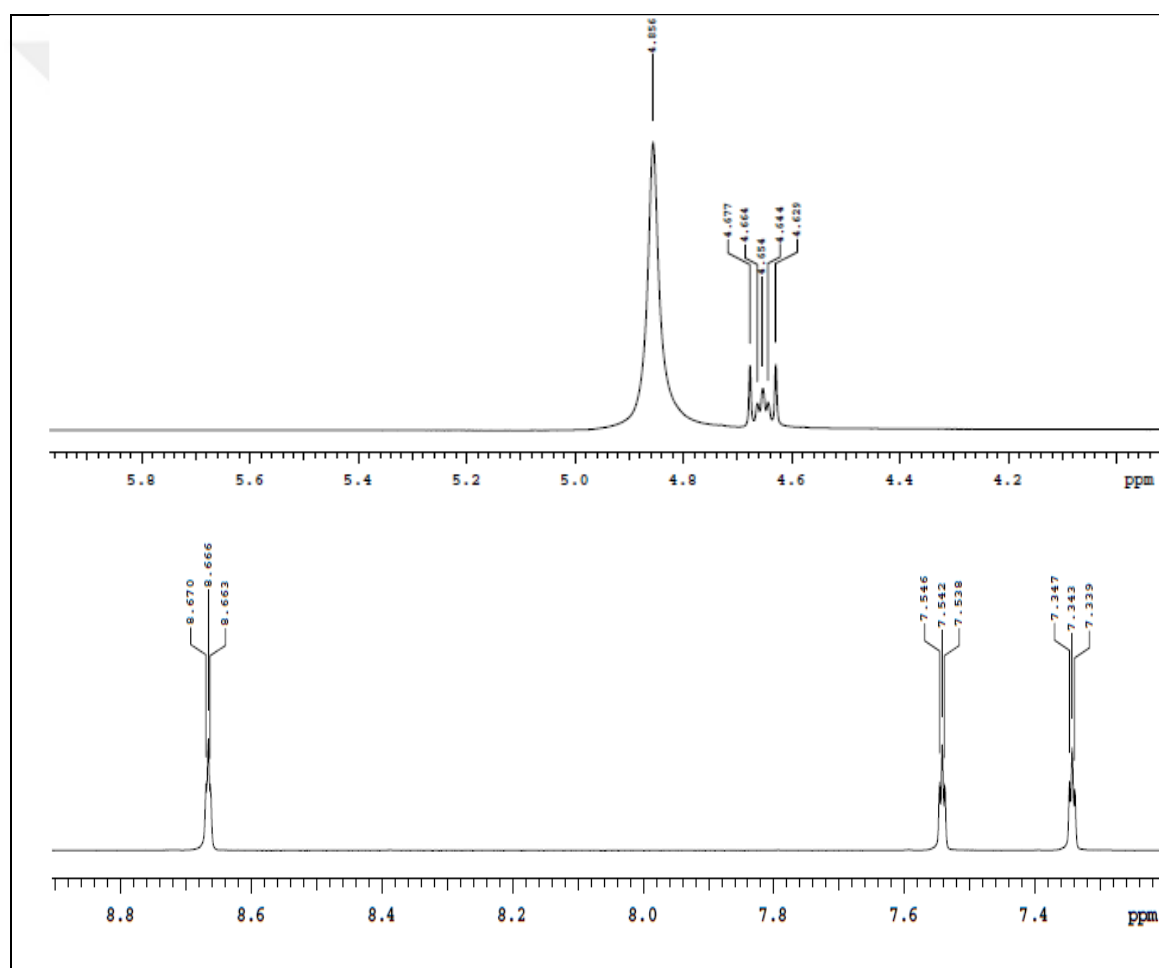
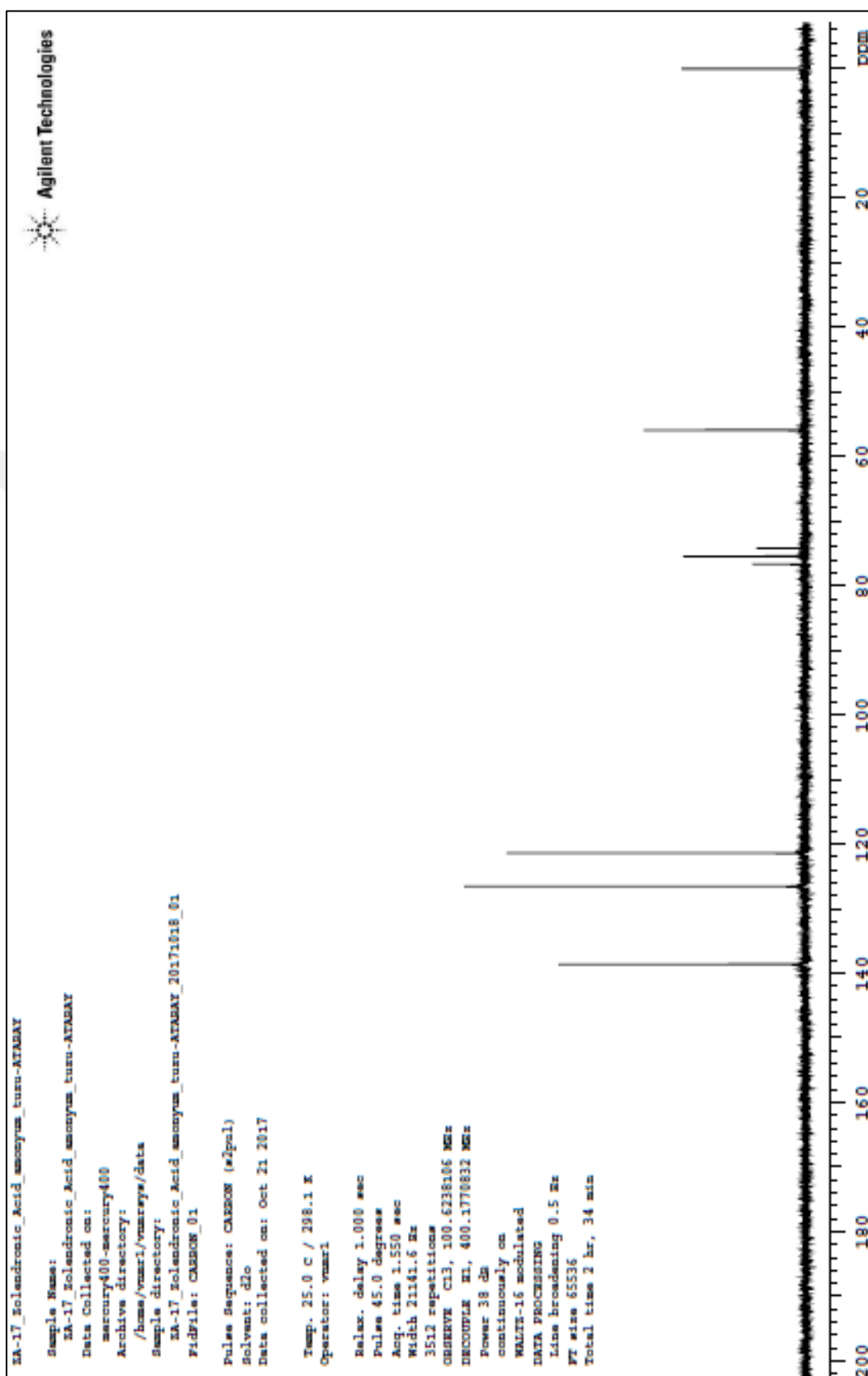


Figure A.77. H-NMR spectrum details of 15th experiment

Figure A.78. ^{13}C -NMR spectrum of 15th experiment

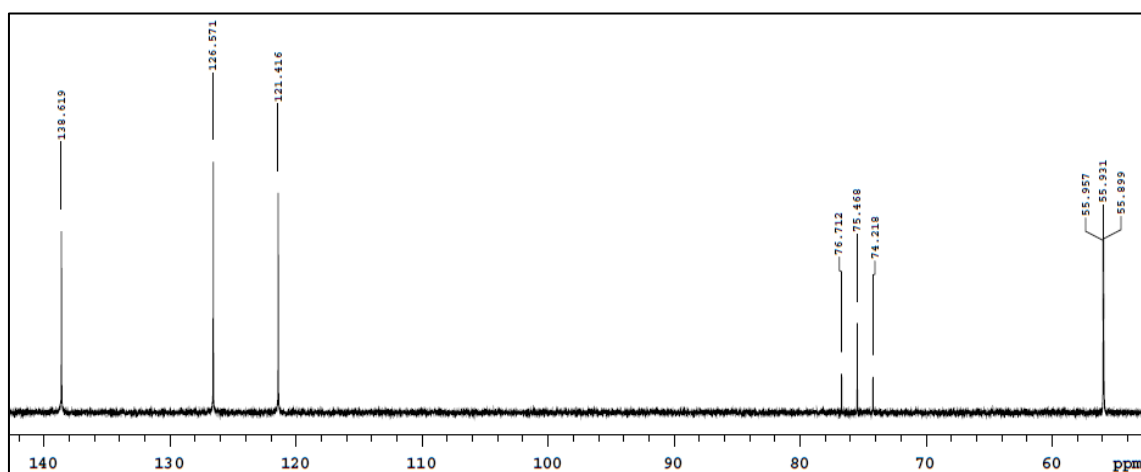


Figure A.79. ^{13}C -NMR spectrum details of 15th experiment

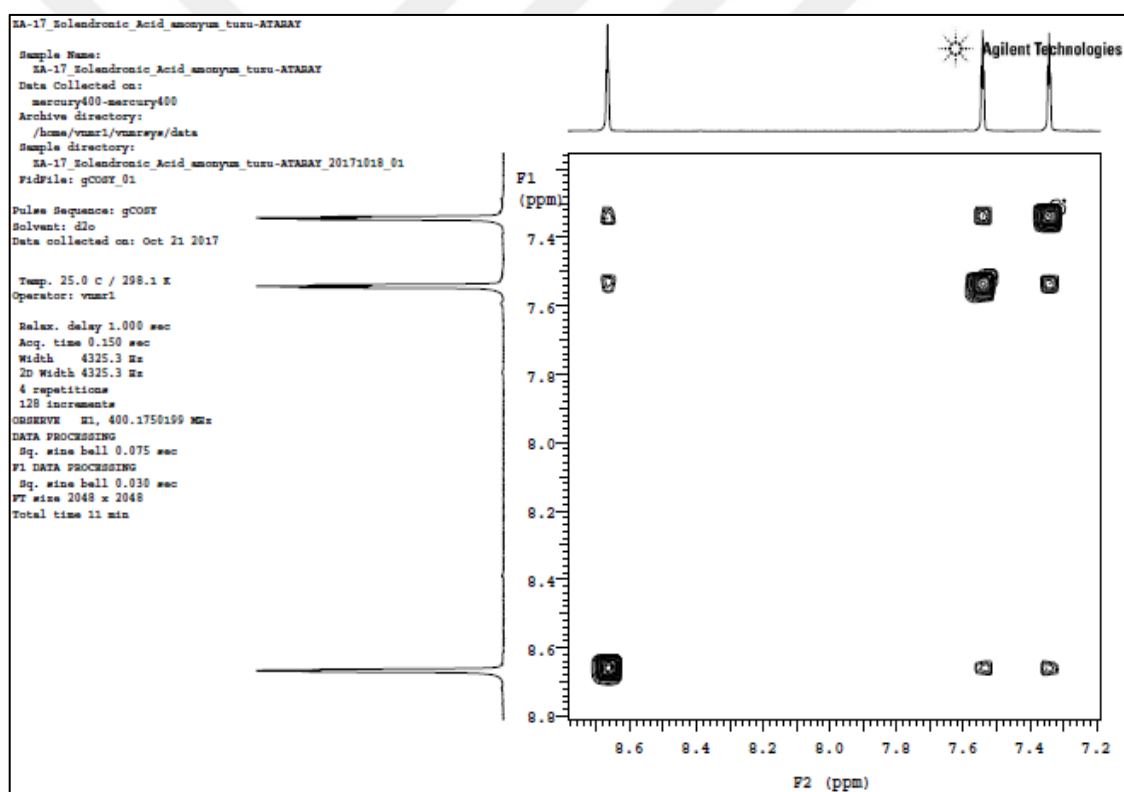
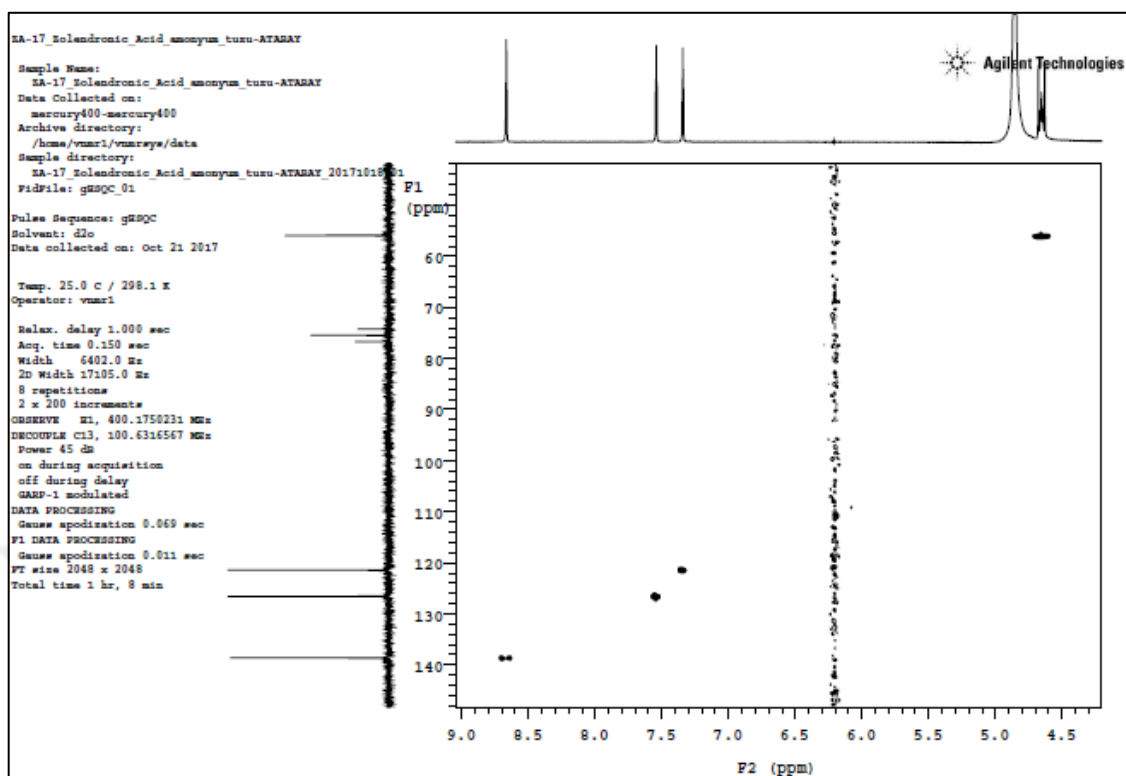
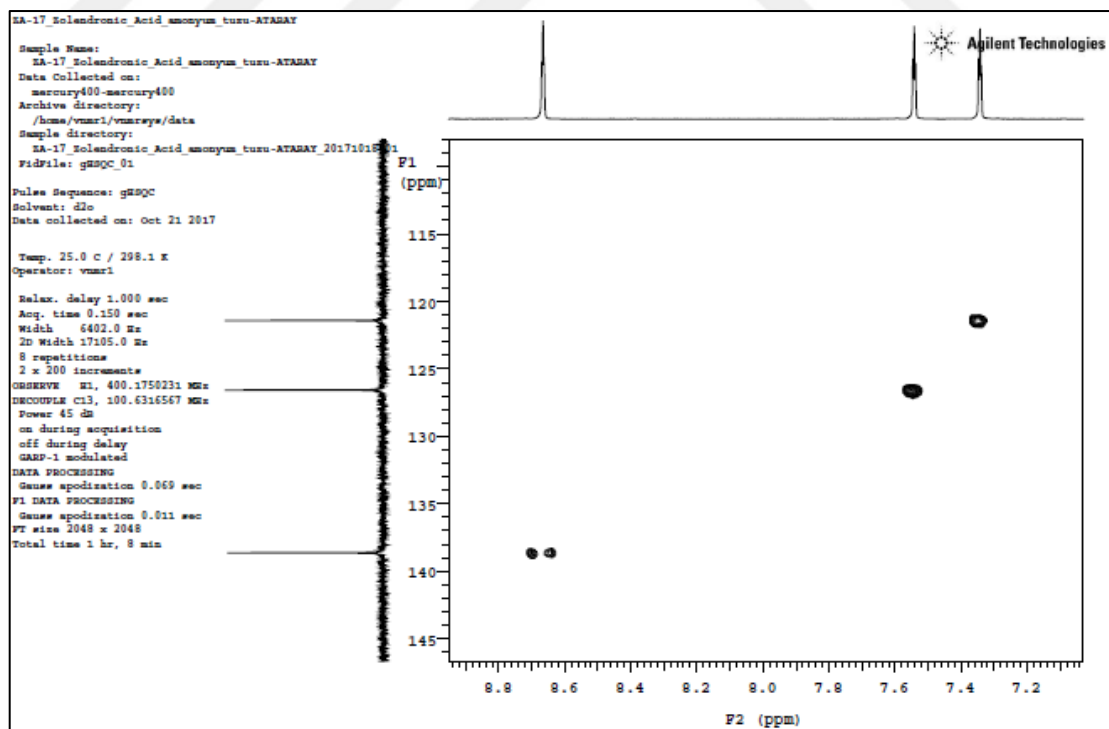
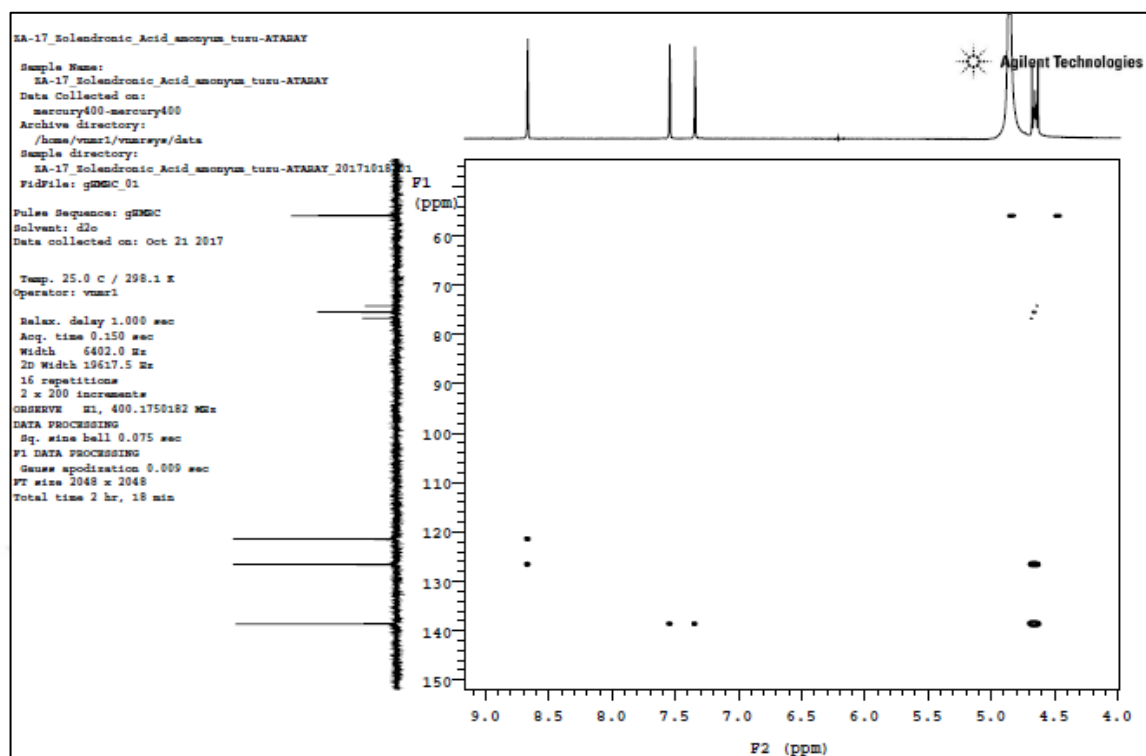
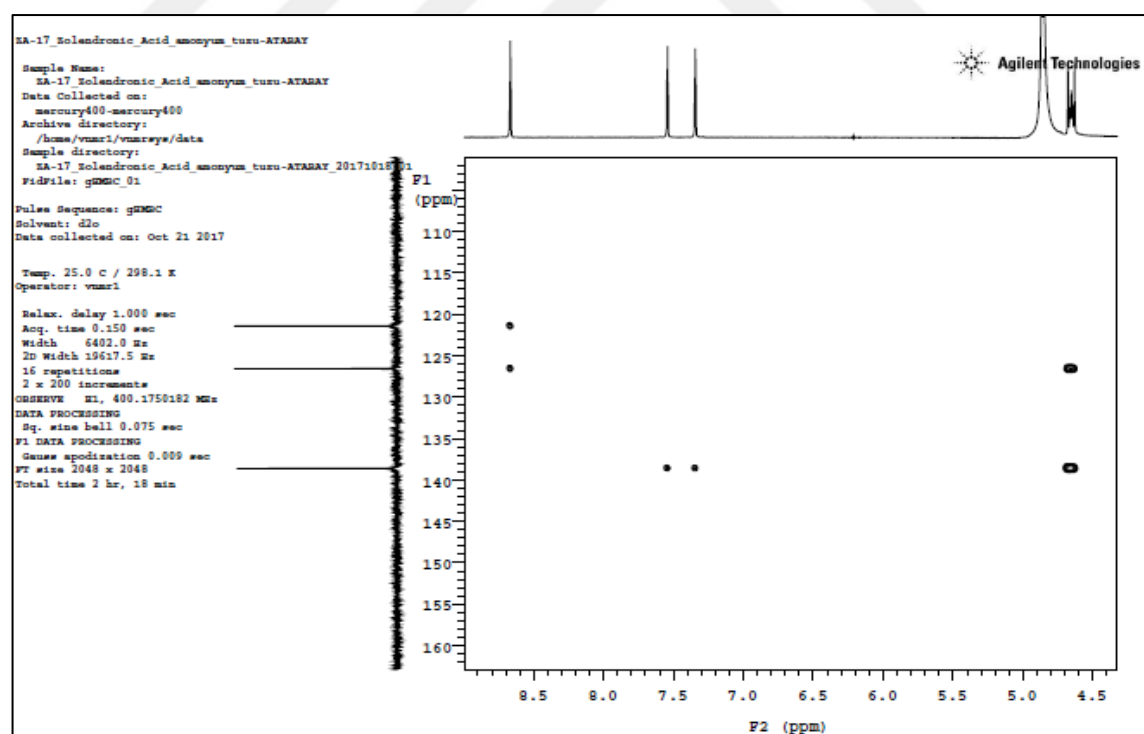
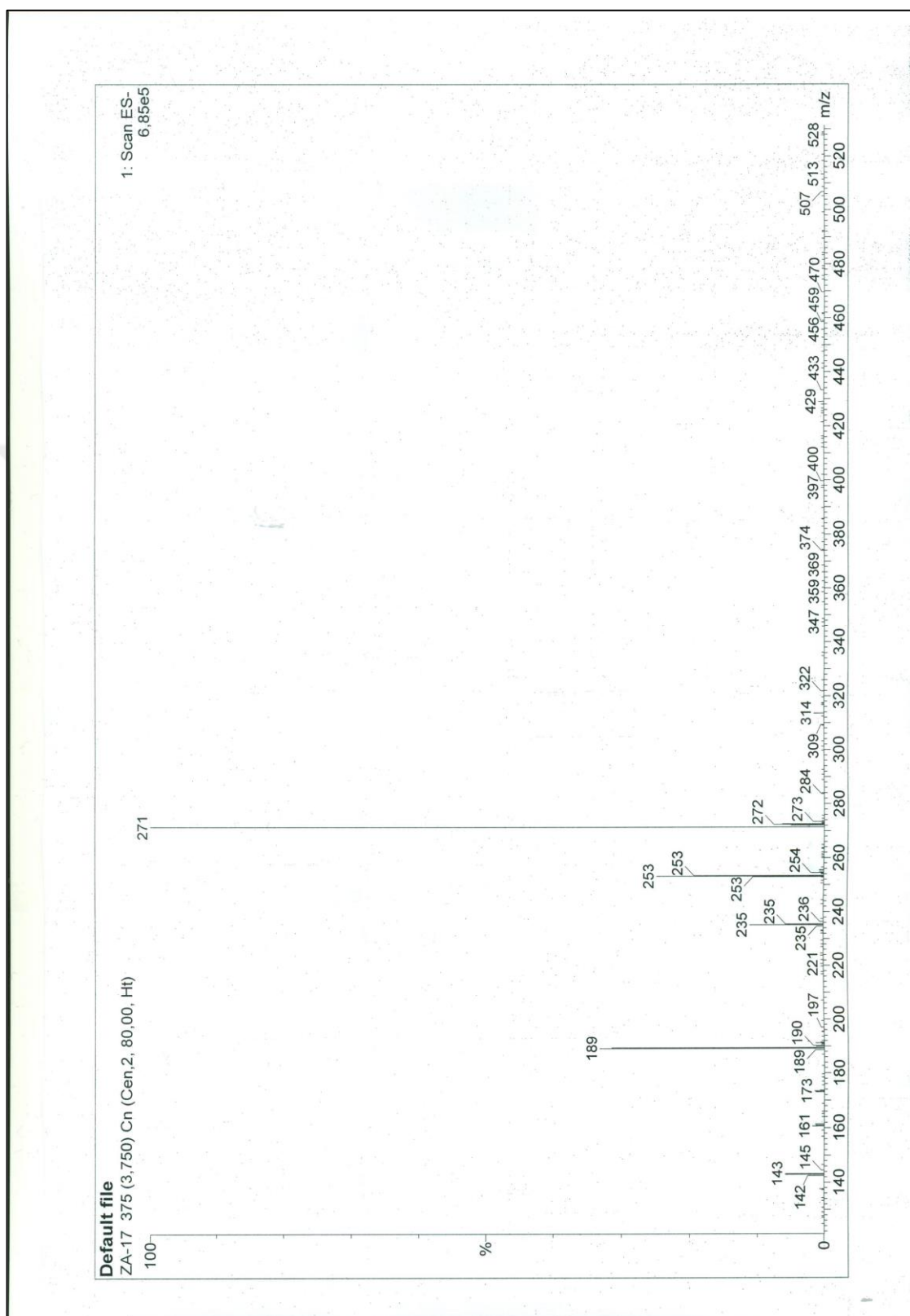


Figure A.80. COSY spectrum of 15th experiment

Figure A.81. HSQC spectrum of 15th experimentFigure A.82. HSQC spectrum details of 15th experiment

Figure A.83. HMBC spectrum details of 15th experimentFigure A.84. HMBC spectrum details of 15th experiment

Figure A.85. Mass spectrum details of 15th experiment

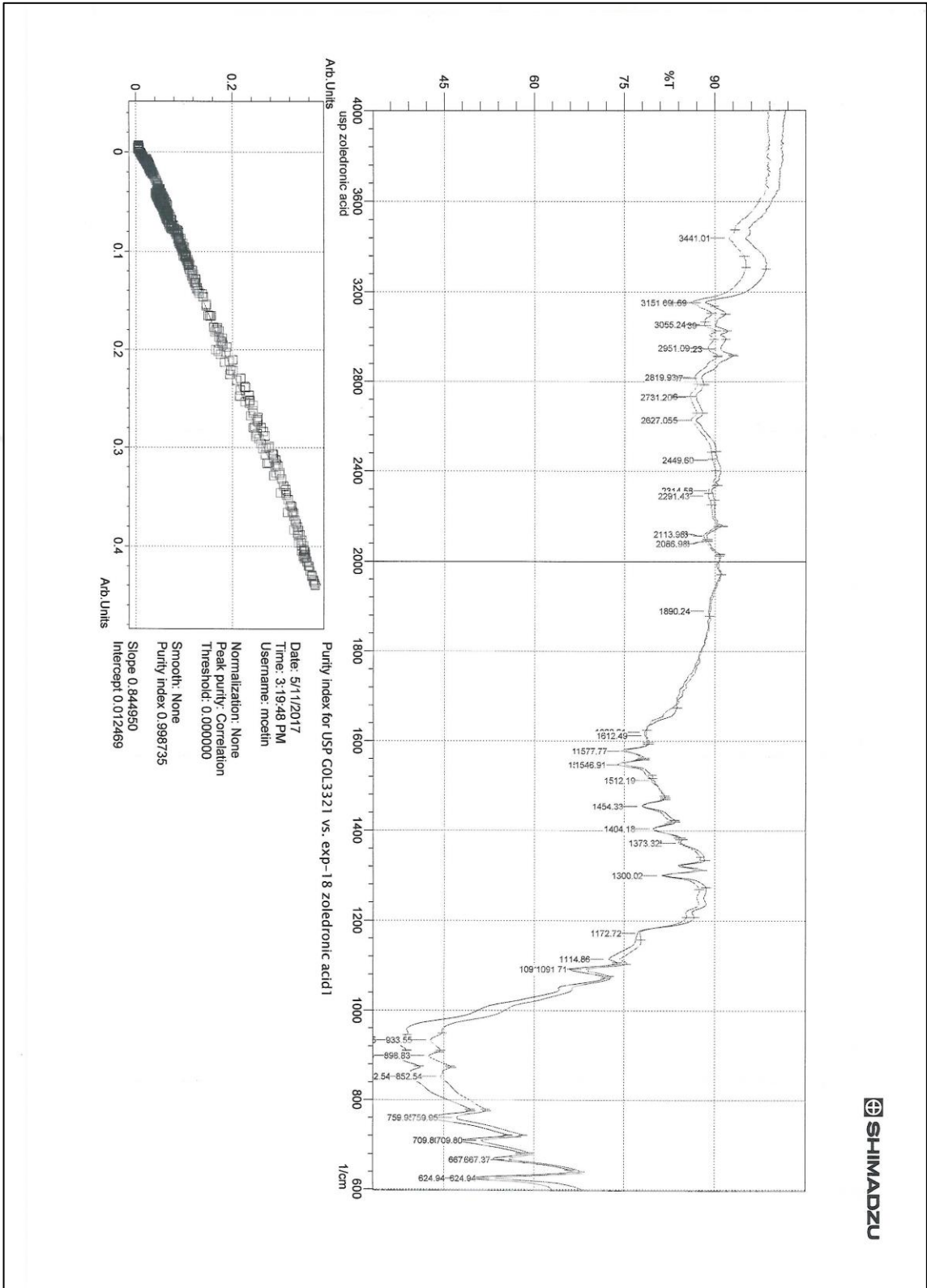
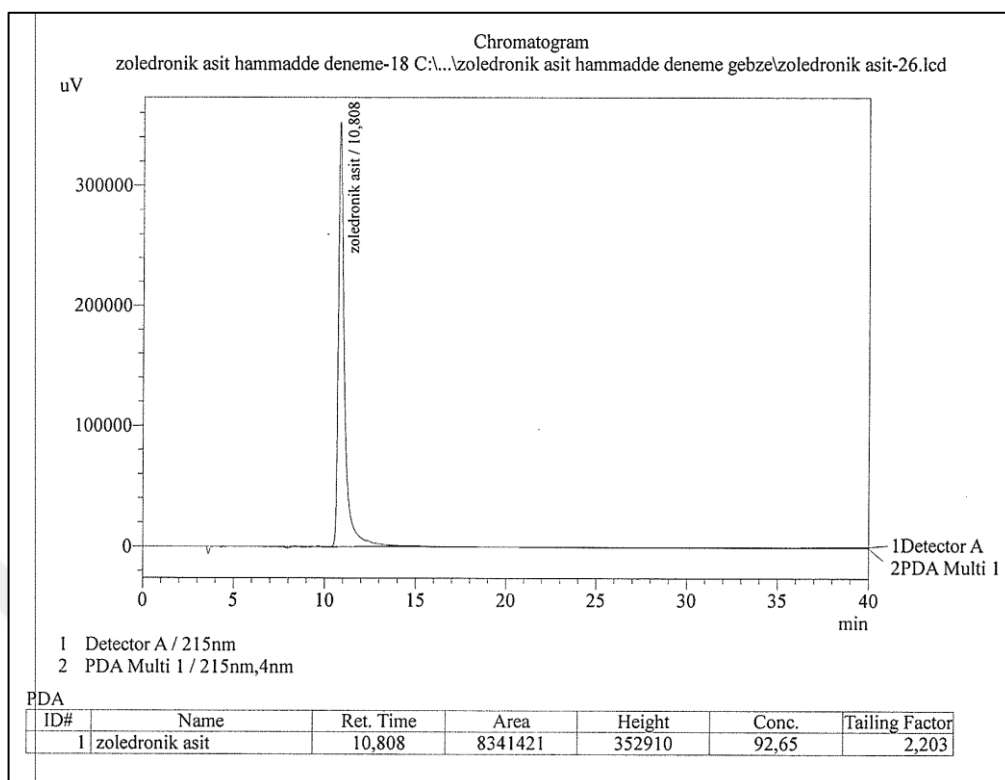
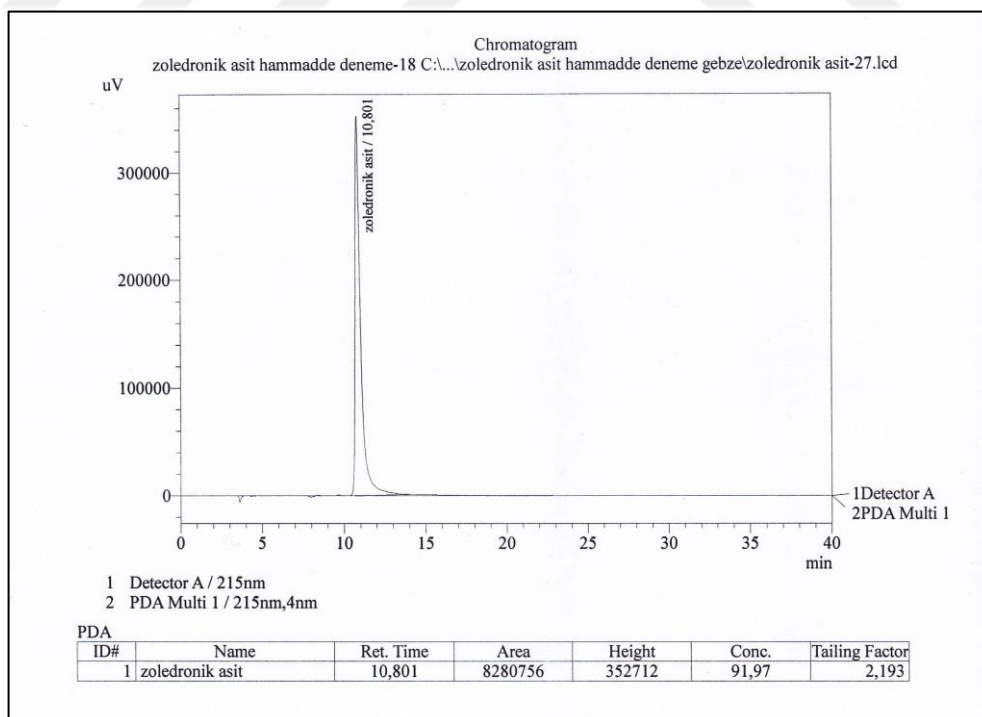
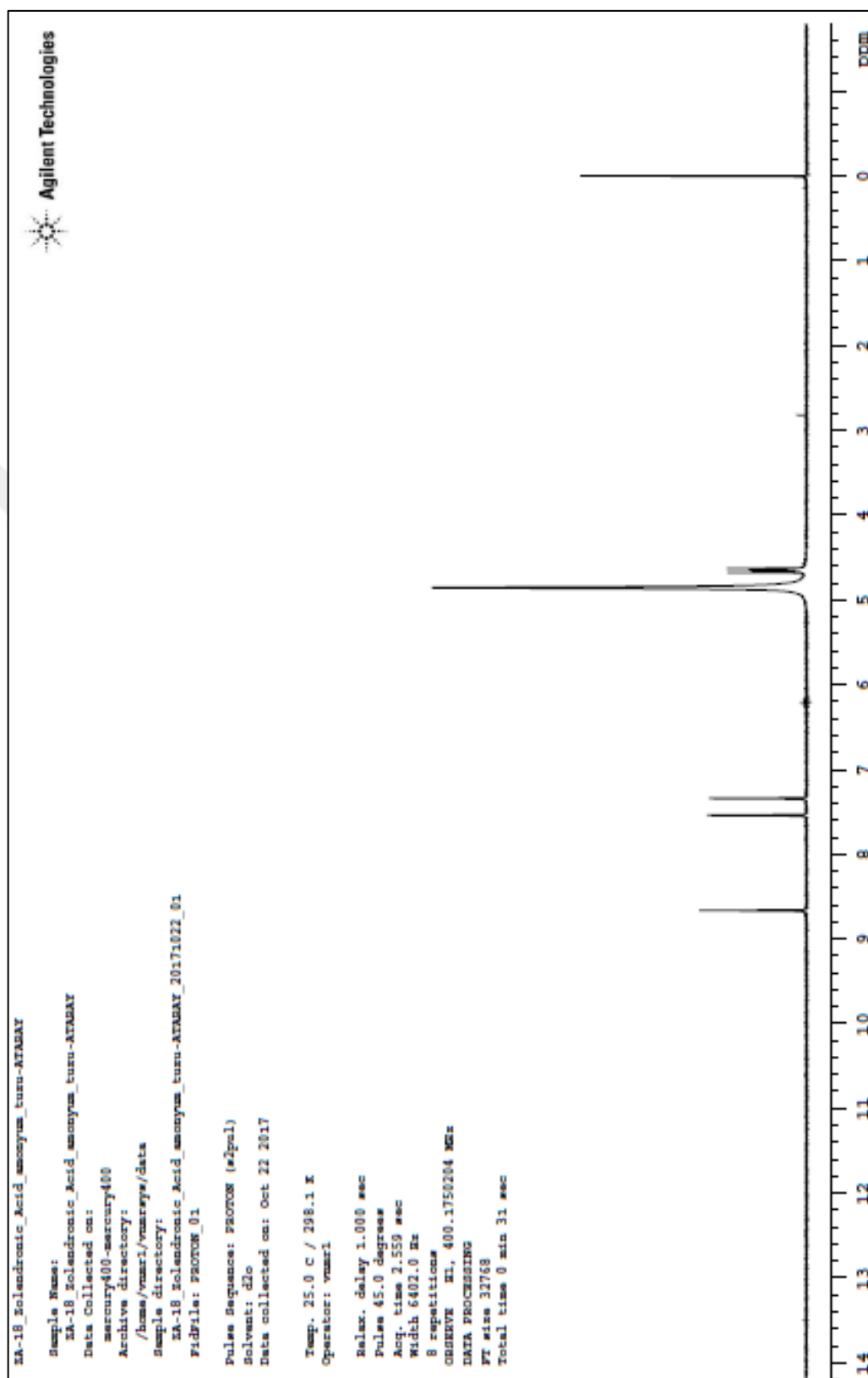


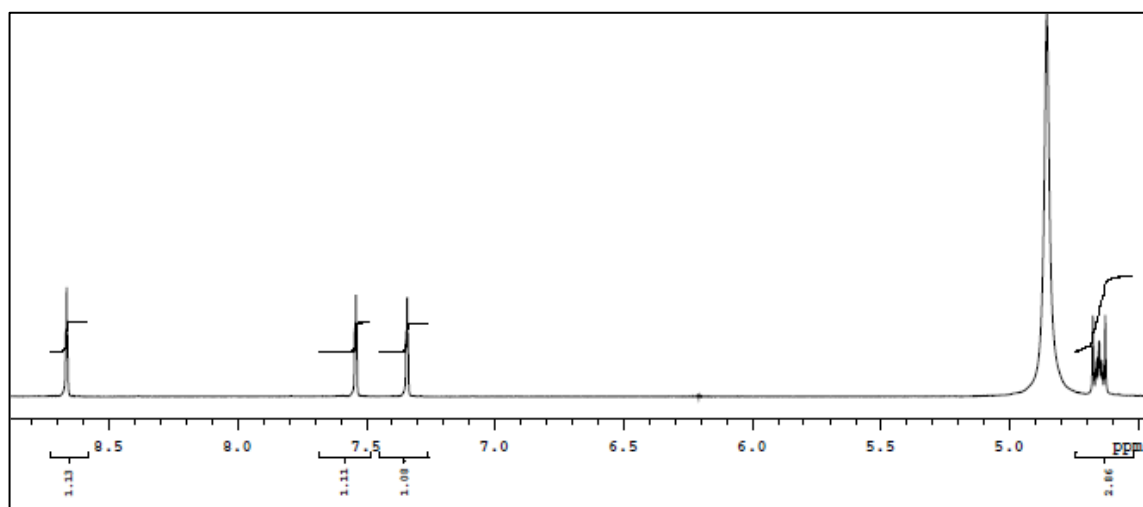
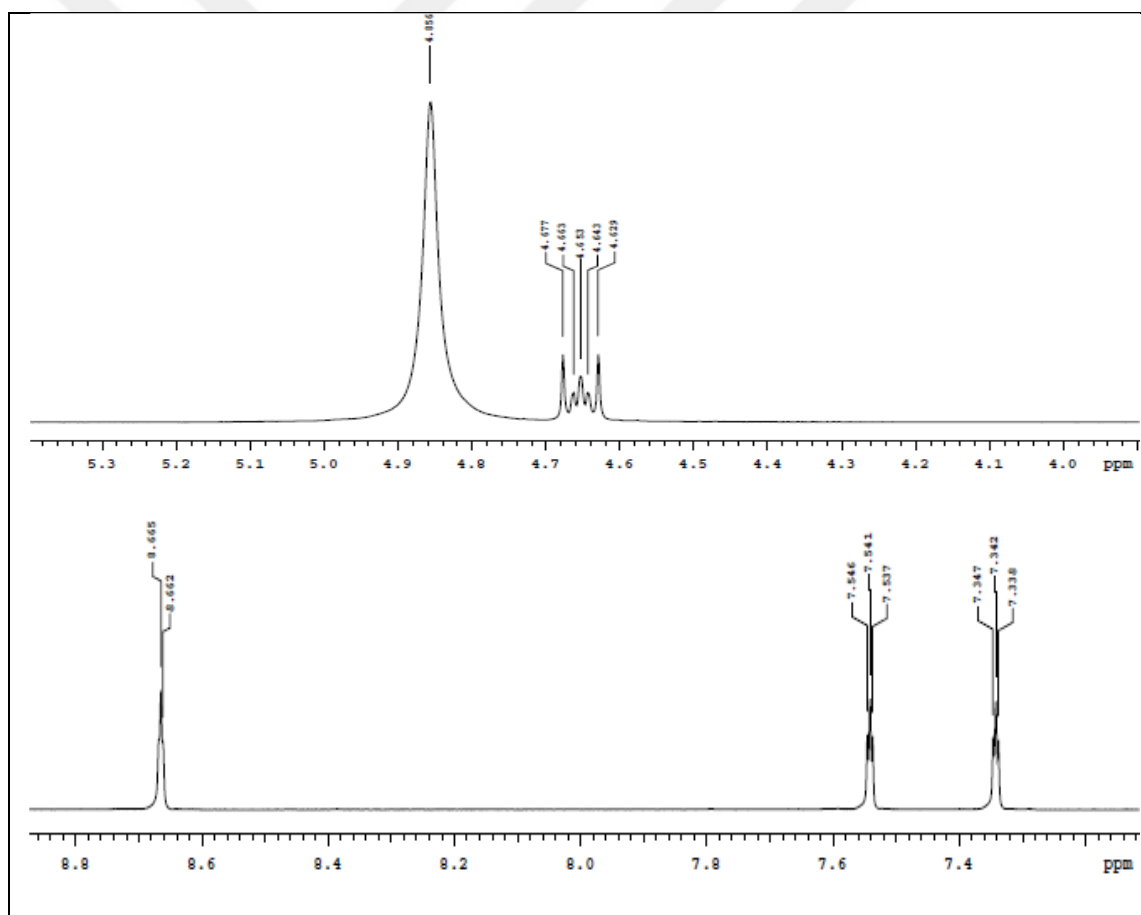
Figure A.86. IR result of 16th experiment

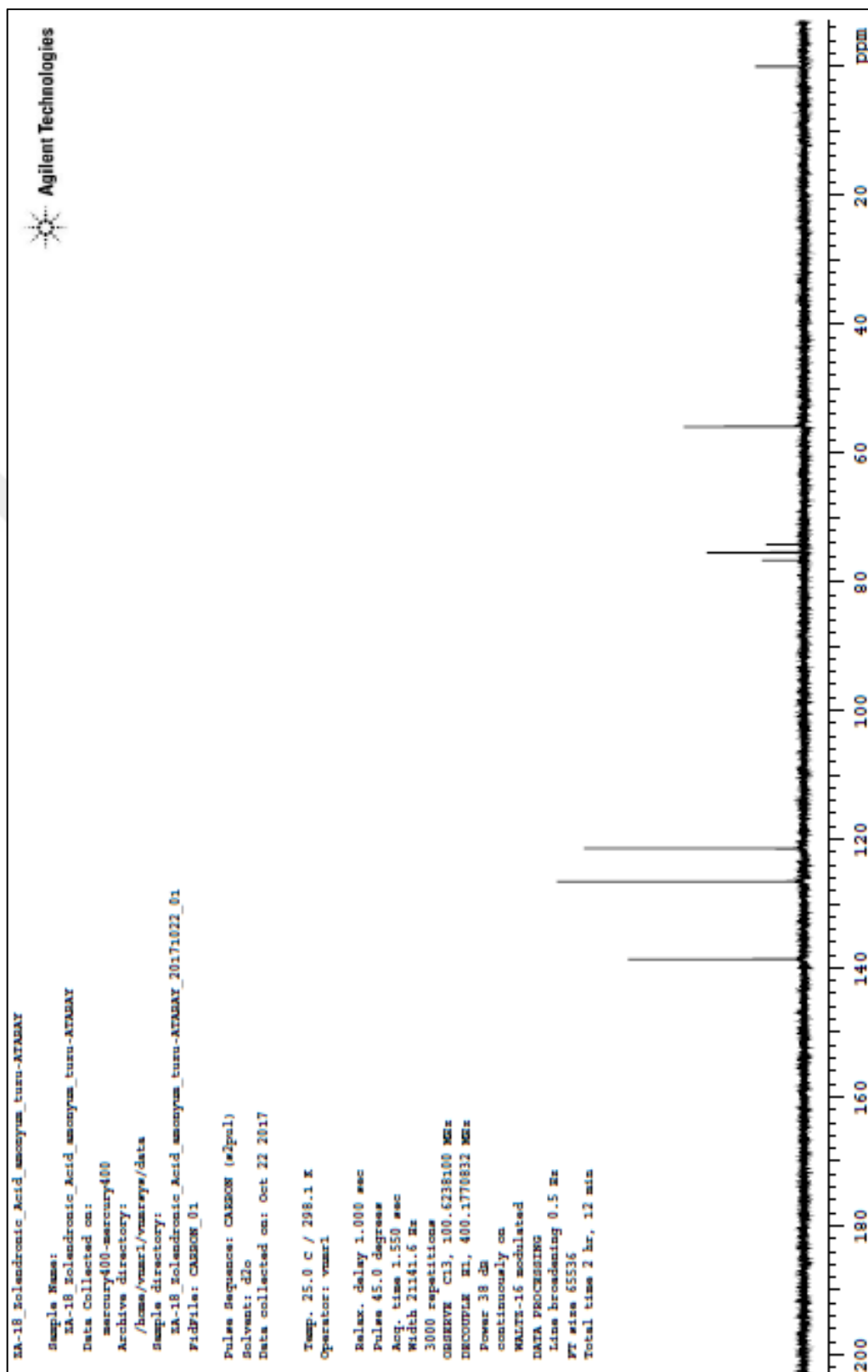
Figure A.87. HPLC result (run 1) of 16th experimentFigure A.88. HPLC result (run 2) of 16th experiment

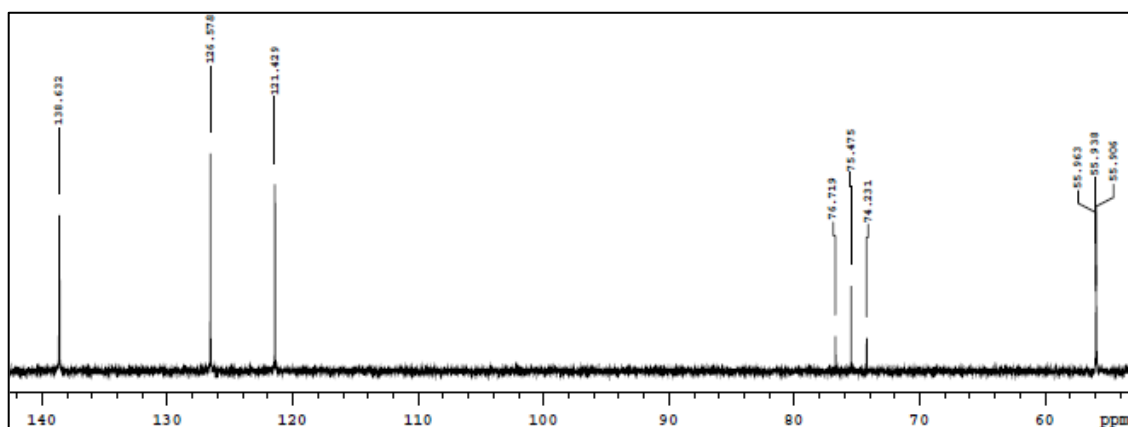
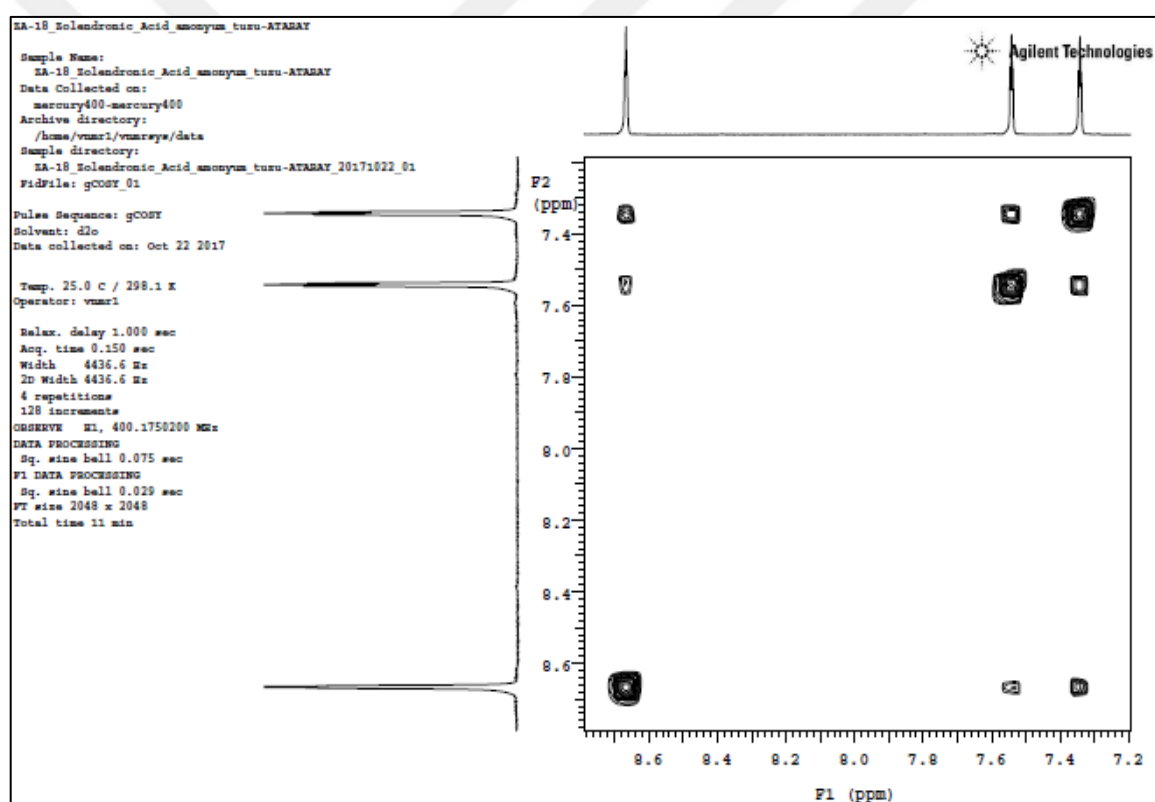
PC Control PC Control	Serial number 1111270515 Printed	Program version 4.0 2017-06-20 12:40:36		
Result report				
Determination	Method KF Numune Analizi Last saved on 2016-12-08 14:32:18 ver. 9 Method status saved Determination Zoledronic acid-20170620-123302 Determ. time 2017-06-20 12:33:02 Status of deter. original Sample number 16 User mkepur Full name Mahmut Kepur			
Sample data	Numune adi Zoledronic acid Batch seri no. deneme 18 Sample size 0.1021 g			
03 KFT Ipol	Karl Fischer titration Ipol			
Sensor	Metal electrode			
Titrant	Hydranal Composite 5			
	Concentration	1.000 mol/L		
	Titer	5.1434 mg/mL		
	Date titer det.	2017-06-20 10:41:15		
Titration	EP1	1.5450 mL		
	Regular stop			
Results	Nem 7.78 %			
Statistics	n	Mean	s +/-	s rel
	Nem	1	7.78 %	
Curve				
03 KFT Ipol	Karl Fischer titration Ipol			
Date	Signature			
Reason				

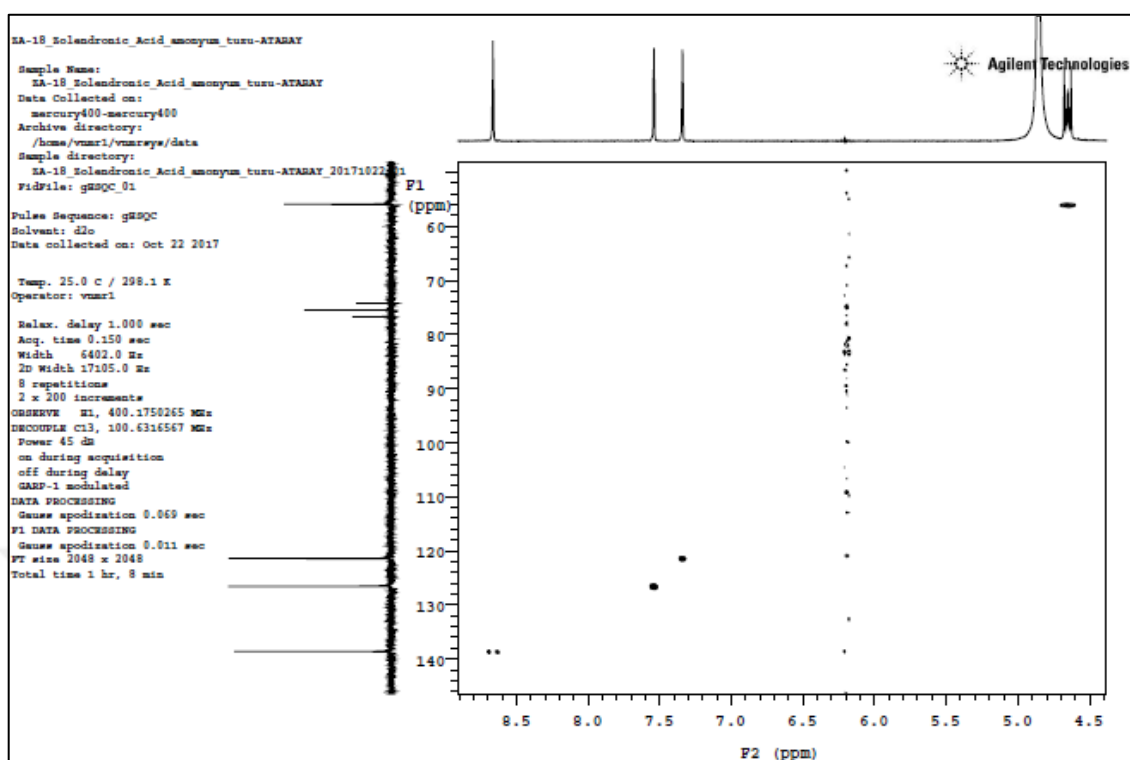
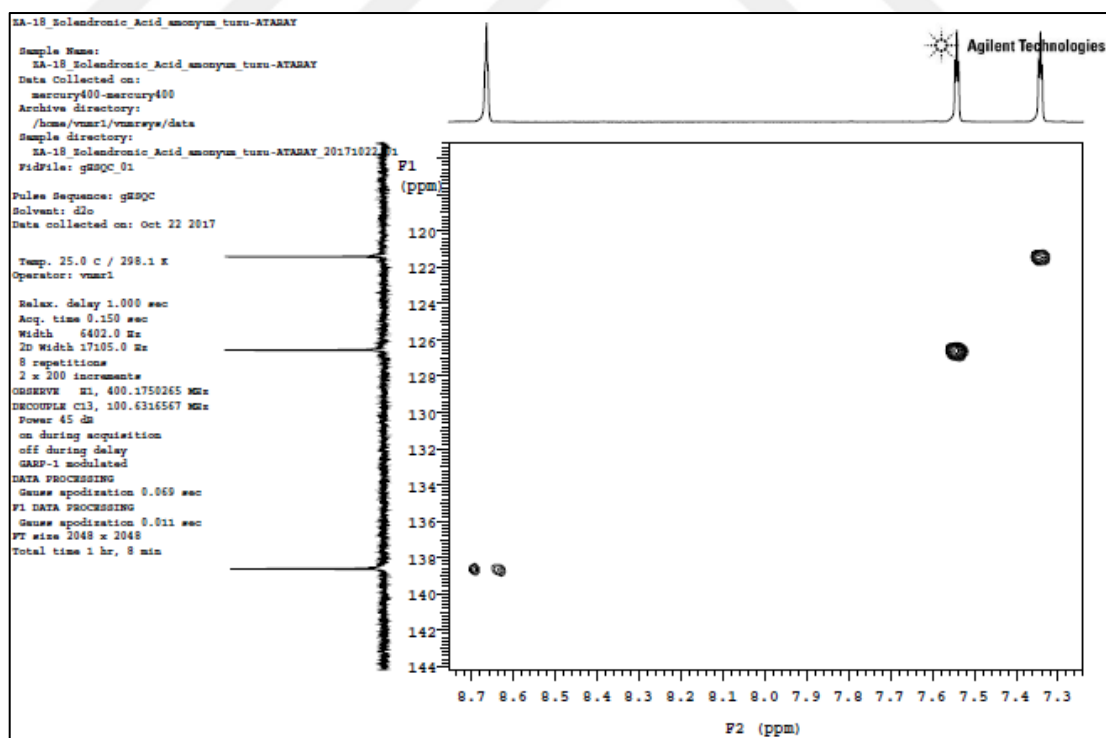
Figure A.89. KF data of 16th experiment

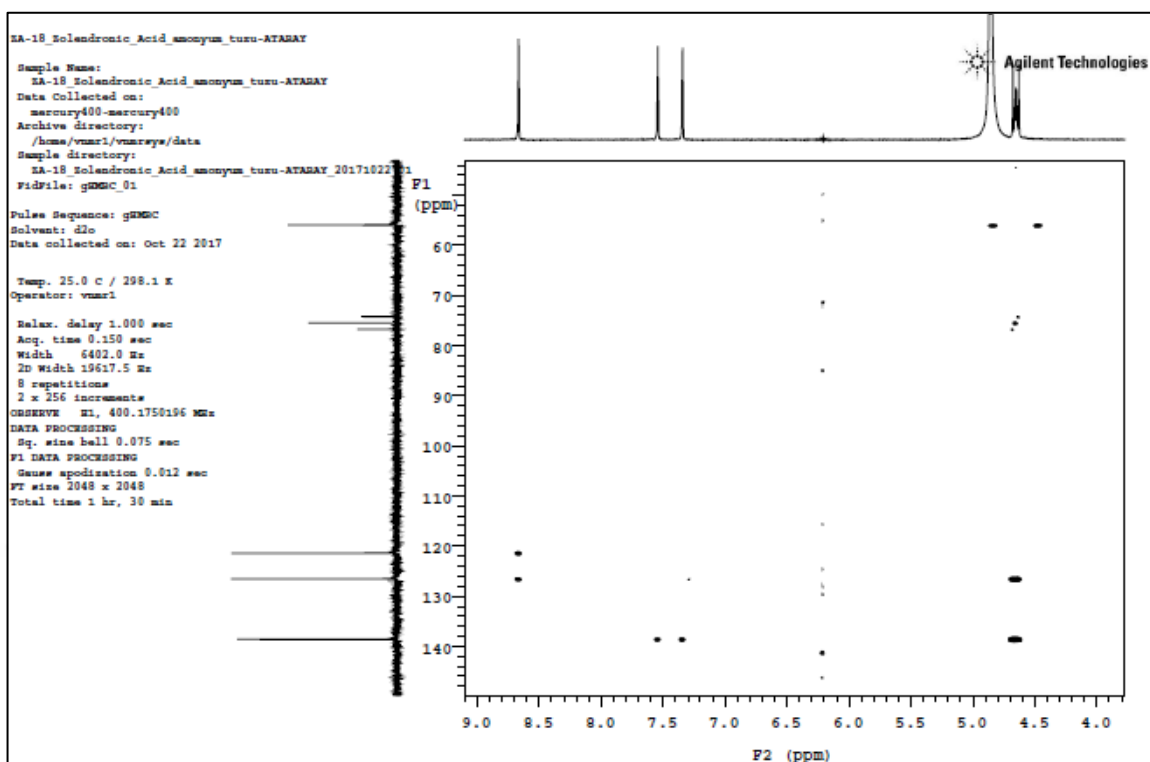
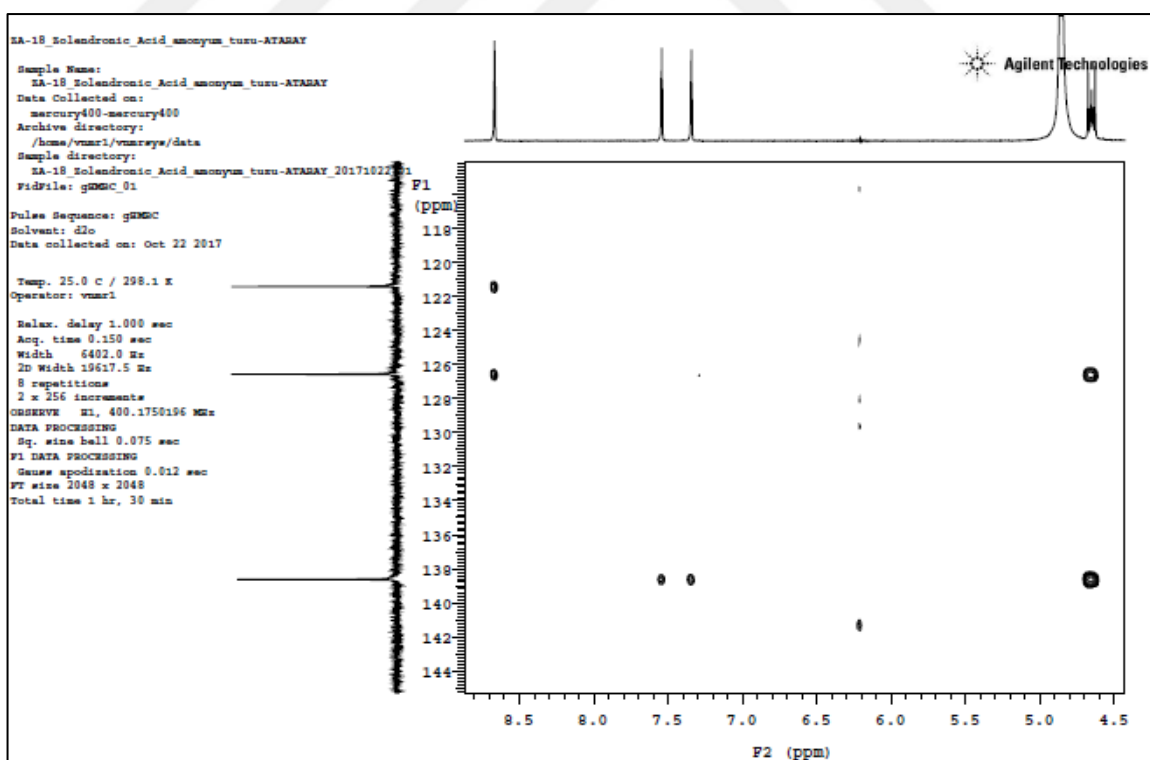
Figure A.90. ^1H -NMR spectrum of 16th experiment

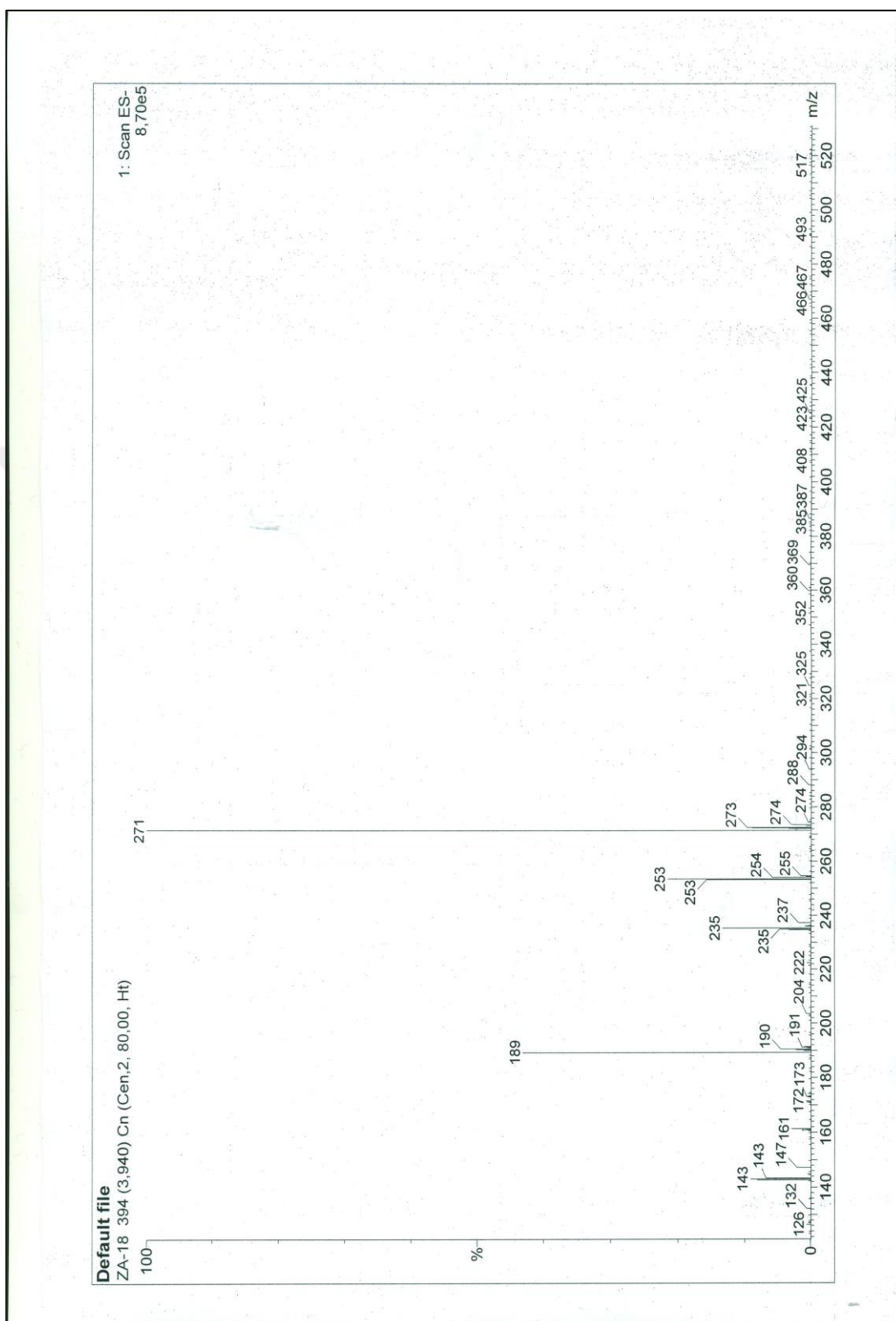
Figure A.91. ^1H -NMR spectrum of 16th experiment with magnitudesFigure A.92. ^1H -NMR spectrum details of 16th experiment

Figure A.93. ^{13}C -NMR spectrum of 16th experiment

Figure A.94. ^{13}C -NMR spectrum details of 16th experimentFigure A.95. COSY spectrum of 16th experiment

Figure A.96. HSQC spectrum of 16th experimentFigure A.97 HSQC spectrum details of 16th experiment

Figure A.98. HMBC spectrum details of 16th experimentFigure A.99. HMBC spectrum details of 16th experiment

Figure A.100. Mass spectrum details of 16th experiment

APPENDIX B: SUMMARY TABLES AND FIGURES FOR CALCULATIONS OF EXERGY

Table B.1. Exergy destruction in each sub-step of the zoledronic acid production process

Step and sub-steps of the process		X _{destroyed} (kJ)
Step 1.1 Reaction		
dissolving of the reactants		2,853
reaction after addition of PCl ₃		223,668
cooling of the reaction products		939
Total		227,461
Step 1.2 Filtration		
Heating and addition absorbent and water		3,871
Filtration of absorbent		2,497
Total		6,369
Step 1.3 pH adjustment a temperature lower than 0 °C		
Cooling		2,633
NaOH addition		3,718
Total		6,351
Step 1.4 Precipitation	Heating to room temperature	941
	Addition of ethanol	1,197
	Stirring	11,246
Total		13,383
Step 1.4 Precipitation	Cooling to a temperature lower than 0 °C	203
	Stirring	2,536
	Total	2,740
Filtration and collecting of the product		549
Step 1.5 Product recovery		
Crystallization at a temperature lower than 0 °C		0,321
Stirring the raw material and heating up		90,924
Cooling		31,452
Stirring		31,369
Filtration		8,137
Drying		360,285
Total		552,488
Total		809,340

Table B.2. Chemical and physical exergies calculated under the prevailing conditions of each stream when no excess chemicals are used

Materials consumed during the production	ex_{ch}^0 (kJ/mole)	Physical exergy input (kJ/mole)	Total input exergy of the species (kJ)
Methane sulphonic acid (l)	968.2	-346.6	2,486.4
Imidazole-1-yl-Acetic Acid HCl (s)	2,741.2	89.8	1,698.6
Phosphorous acid (s)	364.1	-916.7	-663.2
PCl ₃ (l)	775.2	-473.6	603.2
Water (l)	0.77	-310.84	-6,666.6
NaOH (l)	77.4	-490.1	-1,650.6
Ethanol (l)	1,356.0	-325.6	8,861.7
Total			366.7

Table B.3. Exergy of the materials used in filling

	Material	CExC (MJ)	Reference
Cartridge Filter	Nylon	3.7	(Ecotextiles, 2009) <i>Filter Cartridge Making Machine</i> , Wuxi ANGE, 30 kW power, Jiangsu, China
Bottles	100 ml glass, silicon coated	1,343	(Output of a Seminar on Energy Conservation in Glass Industry, 1993) (Marstein, 2016)
Stoppers	32 mm Teflon coated	6,405	<i>Thermoforming machine Auto Machine</i> , Guangdong, China, 100 kW power (Energy efficiency in rubber processing - Practical worksheets for industry, Accessed on 03.2017)
Caps	32 mm aluminum	3,286	<i>Composite material compression molding machine</i> , Dongguan Qiaolian Machinery Co., Ltd, Guangdong, China, 45 kW power
Cartoon Boxes	Cardboard	2,619	(Chow, 2005)
Leaflet	Paper	144	(Szargut, 1988)
Labels	Polypropylene	406	(Langenhove , 2004)

Table B.4. Exergy utilization during production of the finished dosage

	W (MJ) CexC of HVAC system	Δe (kJ)	Material contribution (CexC) (MJ)	X_{dest} (MJ)
Step 2.1a (dissolving of mannitol)	65	41.65	-	65
Step 2.2b (dissolving of all other excipients)	38	1.19	-	38
Step 2.2 (filtering)	8	0.00	4 (0.2 μ m nylon filter)	12
Step 2.3a (sterilization and filling)	3,058 (HVAC 1,826 MJ, 44 MJ from LAF, 601 MJ filling + stoppering and 589 MJ from sterilization tunnel)	0.00	1,343 (bottles) 6,405 (stoppers)	10,806
Step 2.3b (capping)	939 (HVAC + 26 MJ from capping)	0.00	3,286 (caps)	4,225
Step 2.4 (secondary packaging)	492	0.00	cartoon boxes 2,619 leaflet 144 labels 406	3,660
Total	-	-	-	18,805

Table B.5. Thermodynamic properties of the chemicals employed during synthesis of the zoledronic acid

Material	Enthalpy of formation (ΔH_f, kJ/mol)	Gibbs Energy (ΔG, kJ/mol)	Exergy of species (ΔE, KJ/mol)	Heat Capacity (C_p, kJ/mol K)	Standard molar Entropy (ΔS°, kJ/mol K)
Methane sulphonic acid(l)	-566.200	-527.30	968.16	0.190	-0.737
Imidazole 1yl Ac. Ac. HCl(s)	-536.300	-203.10	2741.20	0.217	-2.101
Phosphorous acid (s)	-965.525	-857.46	364.07	0.103	-0.164
Zoledronic Acid	-2032.960	-1375.30	3593.91	0.351	-0.571
Phosphorous trichloride (l)	-319.700	-272.30	775.15	0.120	0.516
Phosphorous trichloride (g)	-287.000	-267.80	779.65	0.072	0.422
Hydrochloric acid (g)	-92.300	-95.33	84.73	0.036	0.187
Water (g)	-241.820	-228.57	9.34	0.036	0.189
Water (l)	-285.830	-237.13	0.77	0.075	0.070
Absorbent (s)	0.000	0.00	410.25	0.012	0.006
Sodium hydroxide (l)	-425.610	-379.49	77.43	0.060	0.065
Ethanol (l)	-277.690	-174.78	1356.01	0.112	0.161

Table B.6. Exergy allocation for the production of the packaging materials and leaflets, transportation and quality assurance

Filling Operation			
Materials used	Operation	Energy (MJ)	CexC (MJ)
Bottles	Glass production	10.08	42.03
	Coating operation	132.00	550.44
	Silicone production	180.00	750.60
	Total	322.08	1,343.07
Stoppers	Teflon coating	1,500.00	6,255.00
	Rubber moulding	36.00	150.12
	Total	1,536.00	6,405.12
Aluminium caps	Aluminium production	600.00	2,502.00
	Injection moulding	1.60	6.67
	Compression moulding	186.30	776.87
	Total	787.90	3,285.54
Secondary Packaging			
Labels	Label production	91.85	383.00
	Labelling operation	5.40	22.50
	Total	97.24	405.50
Leaflets	Leaflet production	33.18	138.00
	printing machine	1.54	6.42
	Total	34.63	144.42
Cardboard boxes	Cardboard production	600.50	2,504.09
	Boxing and printing	27.50	114.68
	Total	628.00	2,618.76
Analytical Testing			
Testing by HPLC	Analytical methods applied for release and during shelf life (CexC for HPLC (22 MJ) and chemical exergy for used chemicals (0,145 MJ) including release tests and eight sampling points for stability)	199.31	826.97
Transportation of the materials			
Transportation by truck	Transport of raw material and package materials. and for distribution of the product	510.42	2,128.45

Table B.7. Thermodynamic properties of the chemicals used in analytical testing Exergy of the chemicals employed in the assay

Chemicals used in the assay	ΔG (kJ/mole)	ΔE (kJ)	Reference
Water	-237.30	0.0747	(Woods and Garrels, 1987)
Tetra-n-butyl ammonium hydrogen sulfate	-479.36	110.5056	(Jankowski et al., 2008)
Sodium hydroxide	-379.78	30.7880	(Weast, 1986)
Disodium hydrogen phosphate dihydrate	-2092.90	1.5365	(Woods and Garrels, 1987)
EDTA disodium	-1643.32	0.0047	-
Methanol	-166.40	1.7748	(Woods and Garrels, 1987)
USP Zoledronic acid monohydrate	-700.30	0.0024	-
2-(1-H- imidazole-1-yl) acetic acid, C ₅ H ₆ N ₂ O ₂	-145.50	0.0002	-
Imidazole	446.2	0.0004	-
Total		144.7	

Exergy requirement of making the analysis with HPLC (AB Sciex Pte. Ltd, HPLC System)

Power requirement 110 W, operation time 400 min, electric power utilization 11 MJ, CexC 45.9 MJ	22.2 MJ/t medication
---	----------------------

Table B.8. Exergy calculation for the production of finished product form

Systems used during each step of production, added as energy consumption as work															
Step No	Mixer Work, (J/s)	Pump Work, (J/s)	HVAC system work, (J/s)			Linear air flow cabinet, (J/s)	Filling line, (J/s)	Water purification system, (J/s)	Packaging line, (J/s)	Heat Supplied, Q (kJ)	Outlet Temp T, (K)	Inlet Temp, T ₀ , (K)	Mechanical Exergy W, (kJ)	Thermal Exergy, (kJ) Q*(1-T ₀ /T)	Total Exergy, (kJ) W+Q*(1-T ₀ /T)
			Class B	Class C	Class D										
2.1a	750	-	-	3,000	-	-	-	5,400	-	0.00	298	298	15,525	0.00	15,525
2.1b	750	-	-	3,000	-	-	-	-	-	0.00	298	298	9,000	0.00	9,000
2.2	-	3,300	-	3,000	-	-	-	-	-	0.00	298	298	1,890	0.00	1,890
2.3a	-	-	30,400	-	-	730	10,000	-	39,200	0.00	298	298	1156,752	0.00	1156,752
2.3b	-	-	60,800	-	-	-	-	-	1,760	0.00	298	298	225,216	0.00	225,216
2.4	-	-	-	-	16,400	-	-	-	-	0.00	298	298	118,080	0.00	118,080

Mixer is operated:

Step 2.1a : Mixing of the firstly added excipients

Step 2.1b : Mixing of the secondly added excipients

- Pump is operated to transfer the solution through 0.2 µm filter in filtration step 2

- HVAC system operated during whole production. Consumptions are calculated considering room area and HVAC energy consumption during the operation time

- LAF cabinet was operated during the filling as part of the machine

- Filling line operation includes;

Step 2.2: Filling of the solution to the bottles and stoppering

- Water purification system is considered in step 1, for 1000 kg of water

- Packaging line operation includes

Step 2.3a: Bottle washing and drying unit

Step 2.3b: Capping operation

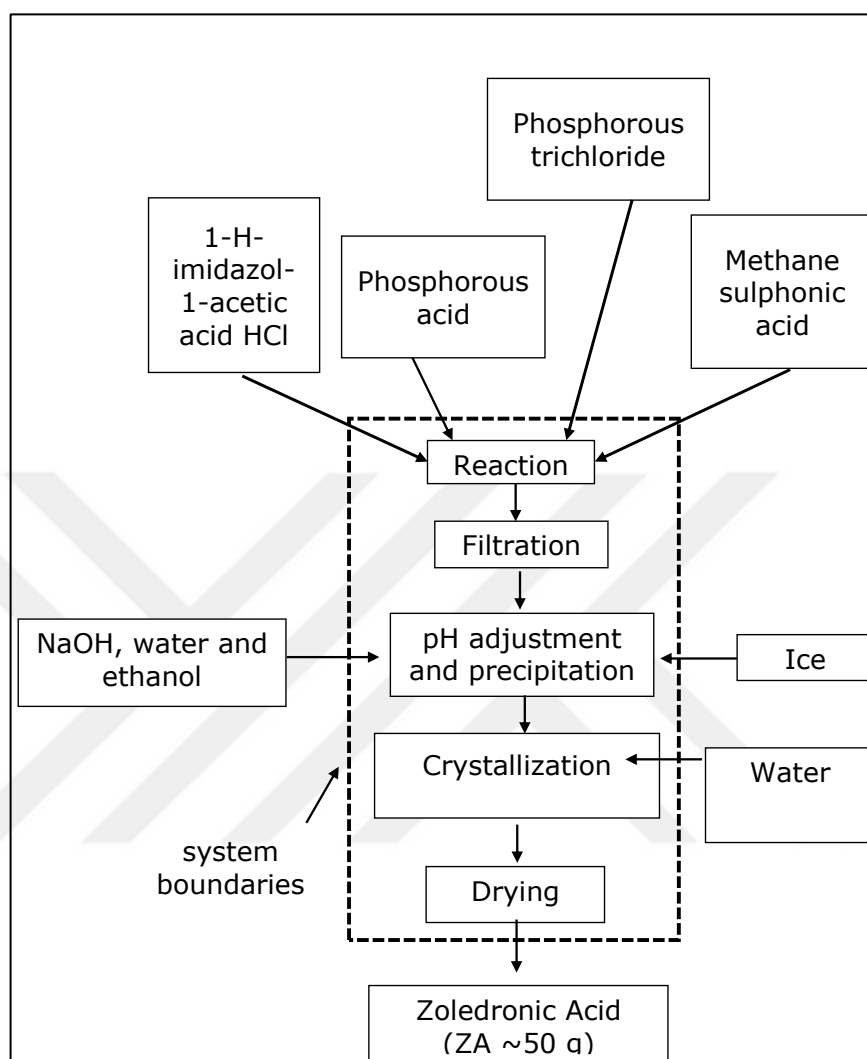


Figure B.1. Material flow in zoledronic acid synthesis.

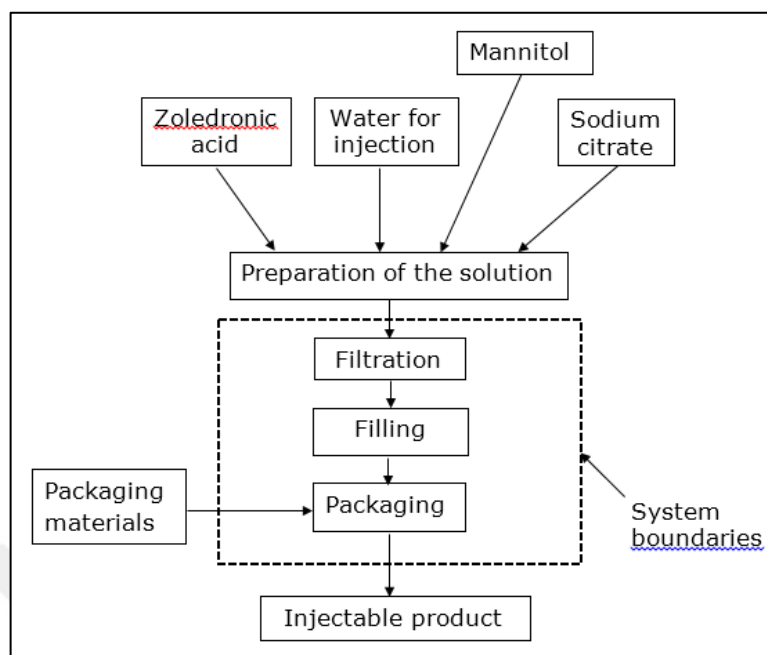


Figure B.2. Material flow in injectable zoledronic acid solution production.

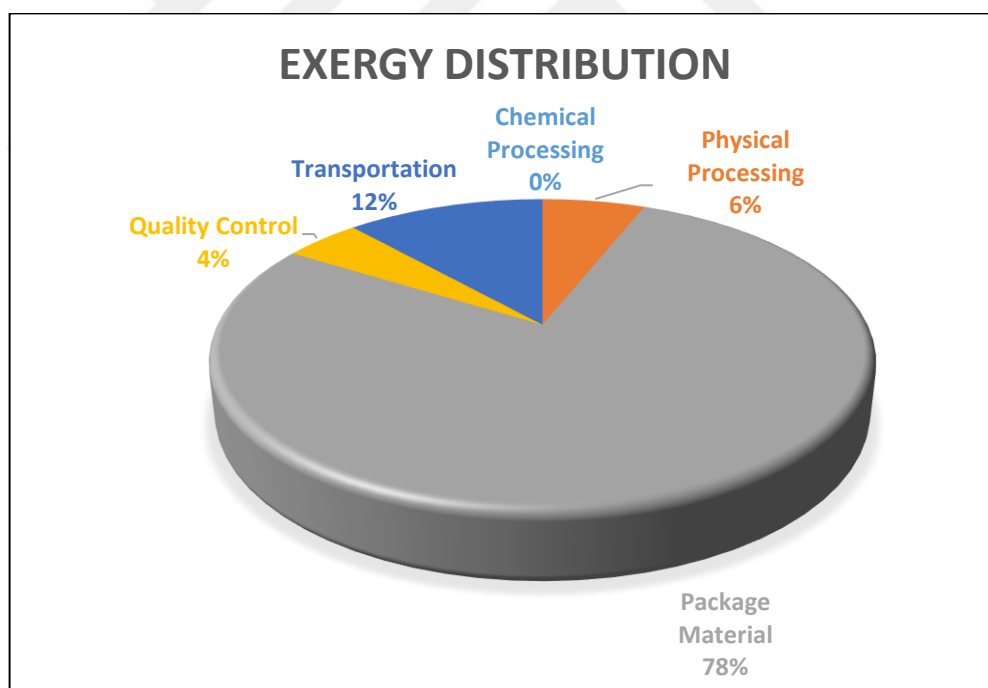


Figure B.3. Exergy allocation for each process in finished product production (Step 2)

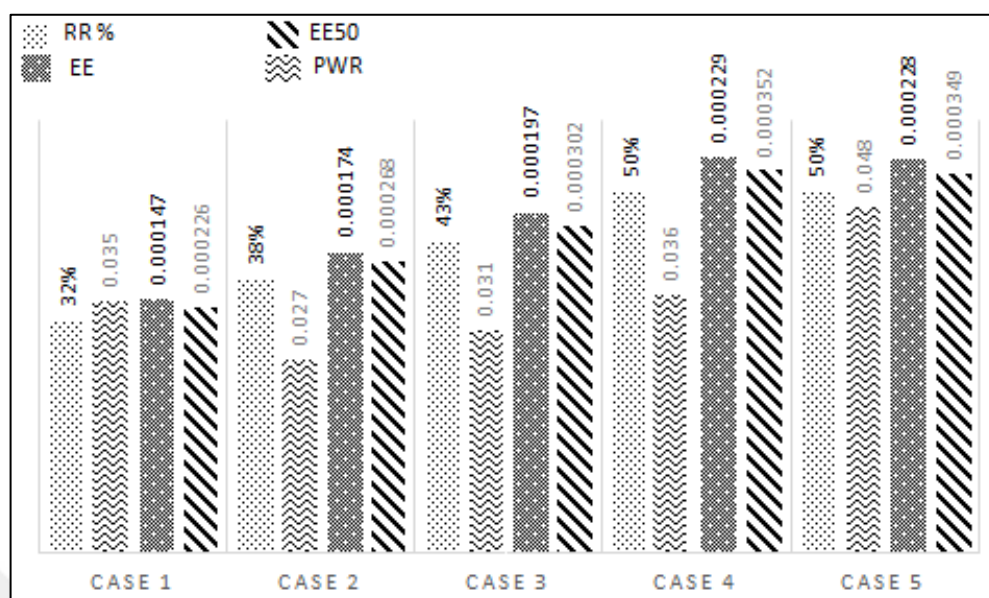


Figure B.4. Variation of the recovery ratio (RR), exergy efficiency (EE), exergy efficiency after recovery of the 50 % of the heat used in processing (EE50) and product to waste ratio (PWR) in Cases 1 through 5.

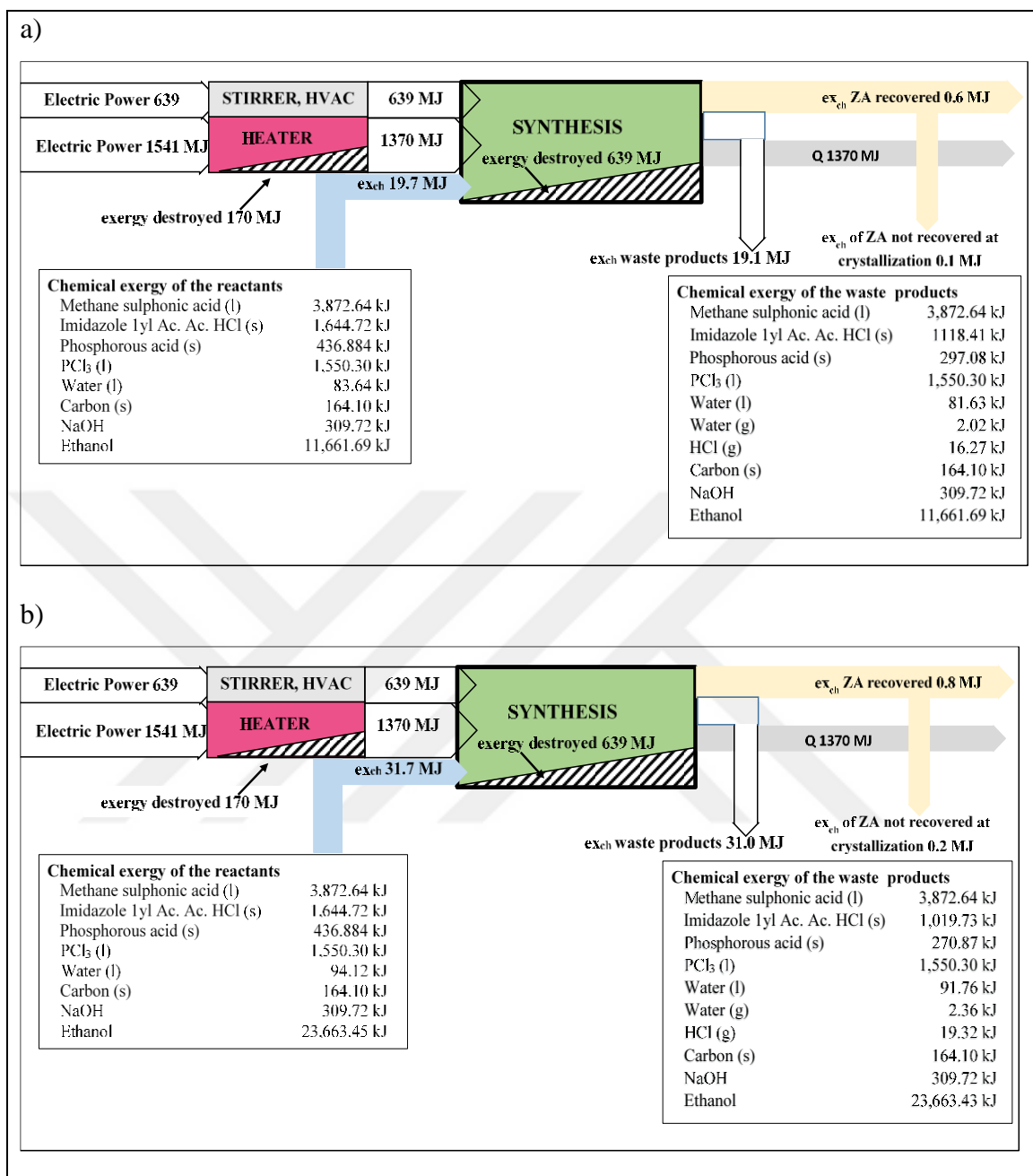


Figure B.5. Sankey Diagram of a) Case 1 and b) Case 2

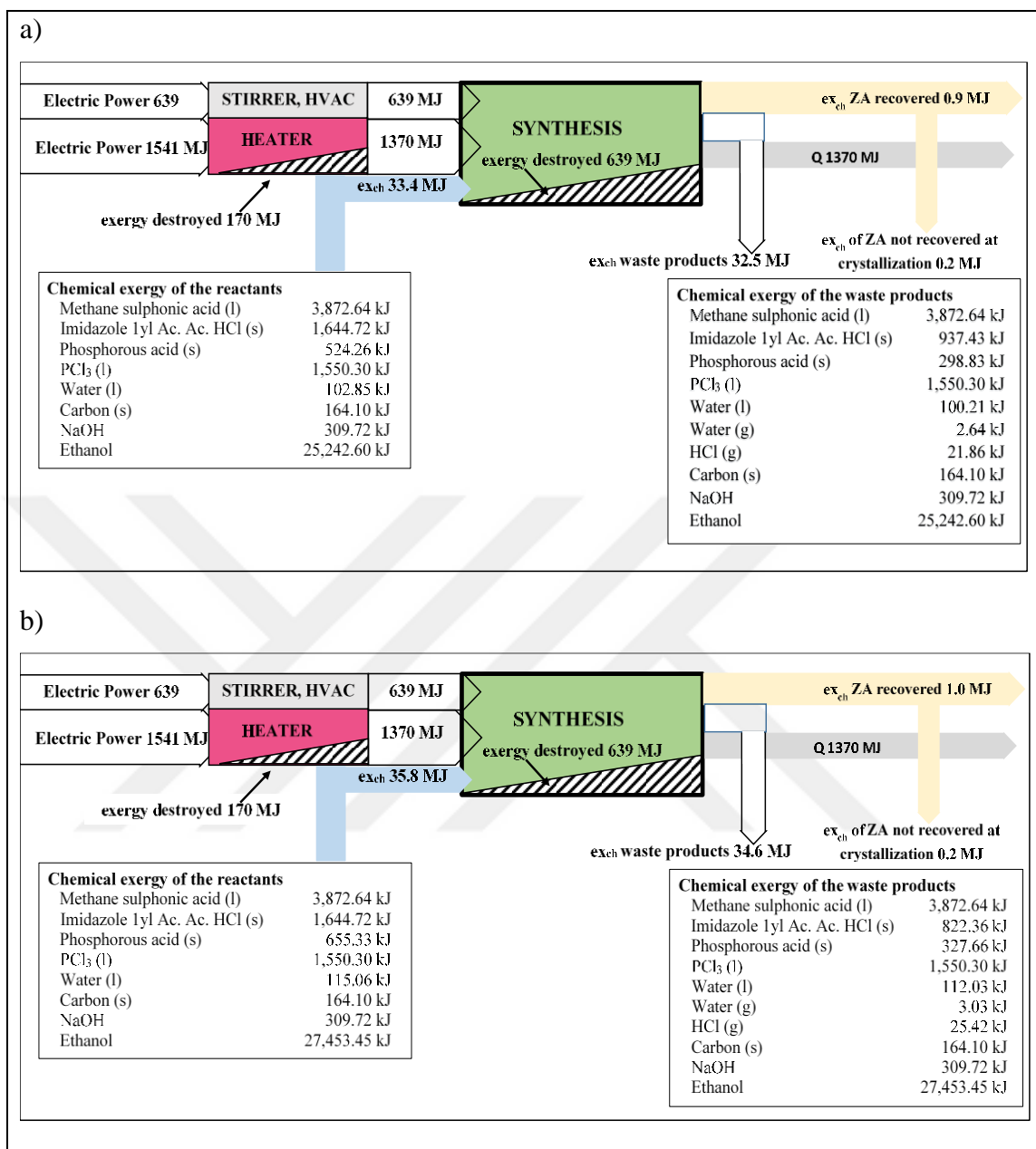


Figure B.6. Sankey Diagram of a) Case 3 and b) Case 4

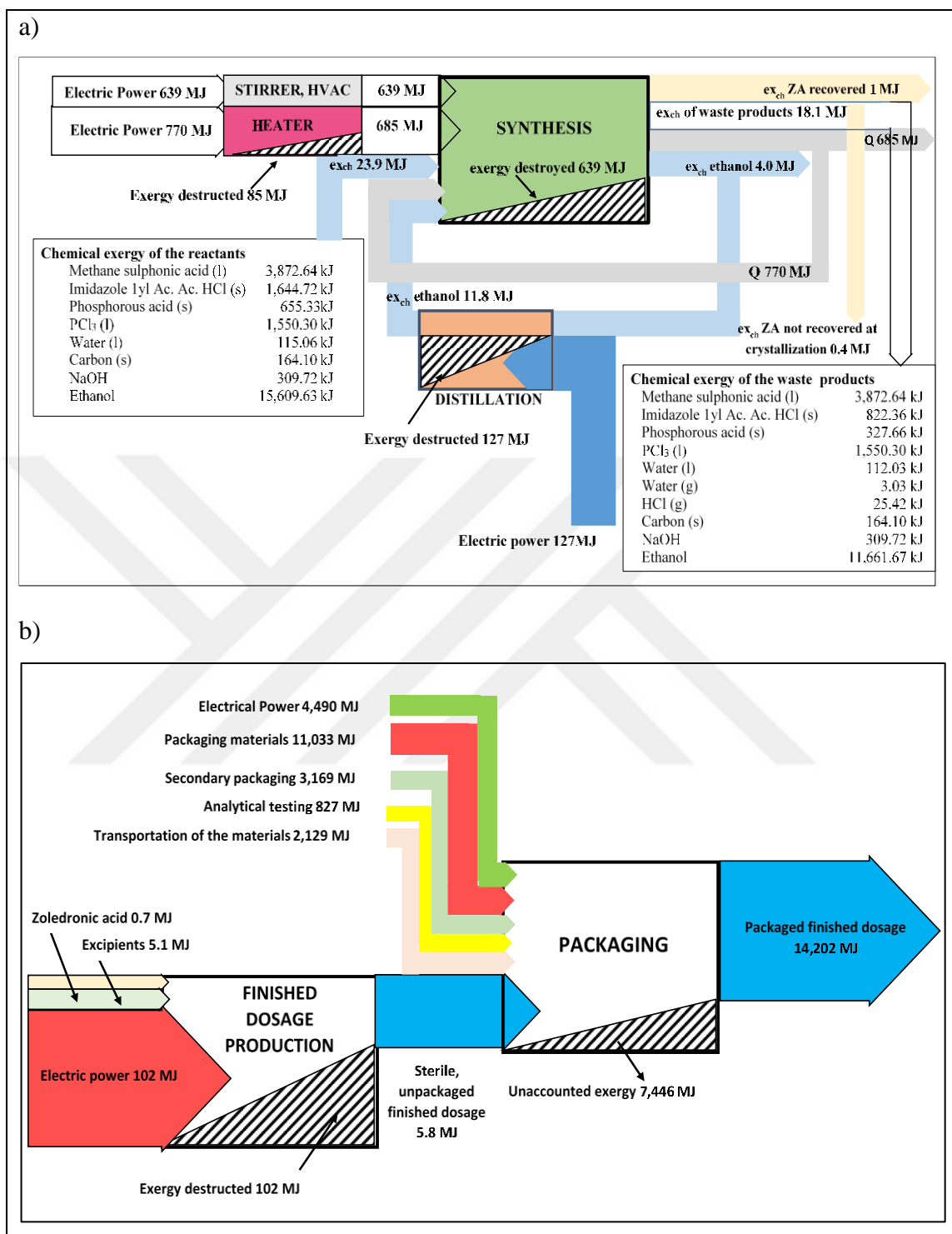


Figure B.7. Sankey Diagram of a) Case 5 and b) Step 2 injectable production

APPENDIX C: DETAILS (ADAPTED FROM THE EXCEL SHEETS) OF THE PROCESS CALCULATIONS FOR ACTIVE PHARMACEUTICAL PRODUCT SYNTHESIS

Table C.1. Mass Balance of dissolving of the reactants

Molecular Weight of each element (kg/kmol)	12.01	1.01	16.00	32.06	14.01	35.45	30.97	22.99	Molecular weight of the excipient (MW, kg/kmol)	Mole ratio of the substance x_i
Materials in the inlet stream	C	H	O	S	N	Cl	P	Na		
Methane sulphonic acid(l)	1	4	3	1	0	0	-	-	96.11	1.00
Imidazole 1yl Ac. Ac. HCl(s)	5	7	2	0	2	1	-	-	162.59	1.00
Phosphorous acid (s)	0	3	3	-	-	-	1	-	82.00	1.00
Materials in the outlet stream	C	H	O	S	N	Cl	P	Na		
Methane sulphonic acid(l)	1	4	3	1	0	0	-	-	96.11	1.00
Imidazole 1yl Ac. Ac. HCl(s)	5	7	2	0	2	1	-	-	162.59	0.15
Phosphorous acid (s)	0	3	3	-	-	-	1	-	82.00	0.30

Mass balance on elemental basis and molecular basis were evaluated. Equation (C.1) is used to calculate the data.

$$\sum(N)_{in} - \sum(N)_{out} = 0 \quad (C.1)$$

Table C.2. Thermodynamic props of dissolving of the reactants

	Heat Capacity, (C _p , kJ/mol K)	Enthalpy, (C _p ΔT, kJ/mol)	Enthalpy of formation (H _f , kJ/mol)	Total Enthalpy (H _{total} , kJ/mol) H= H _f + C _p ΔT	Entropy of formation (S°, kJ/mol K)	Entropy change (ΔS, kJ/mol K) ΔS=S°+C _p ln(T/T ₀)-Rlnx _i
Materials in the inlet stream						
Methane sulphonic acid(l)	0.190	0.000	-566.200	-566.200	-0.7370	-0.7370
Imidazole 1yl Ac. Ac. HCl(s)	0.217	0.000	-536.300	-536.300	-2.1011	-2.1011
Phosphorous acid (s)	0.103	0.000	-965.525	-965.525	-0.1638	-0.1638
Materials in the outlet stream						
Methane sulphonic acid(l)	0.190	7.600	-566.200	-558.600	-0.7370	-0.7131
Imidazole 1yl Ac. Ac. HCl(s)	0.217	8.668	-536.300	-527.632	-2.1011	-1.9183
Phosphorous acid (s)	0.103	4.112	-965.525	-961.413	-0.1638	-0.0521

The terms in Equation (C.2) calculated for Step 1.1 for dissolving of the reactants are represented in Table C.2.

$$\sum(N_i [e_i^{ch} + (h_{f,i}^0 + c_{p,i}(T - T_0) - T_0 [s_i^0 + c_{p,i} \ln \frac{T}{T_0} - R_u \ln x_i])])_{in} - \sum(N_i [e_i^{ch} + (h_{f,i}^0 + c_{p,i}(T - T_0) - T_0 [s_i^0 + c_{p,i} \ln \frac{T}{T_0} - R_u \ln x_i])])_{out} + Q \left(1 - \frac{T}{T_0}\right) - W = X_{destroyed} \quad (C.2)$$

Table C.3. Exergy and $X_{\text{destroyed}}$ calculation of dissolving of the reactants

	Physical exergy (ΔE_{ph} , kJ/mol)	Chemical Exergy (ΔE_{ph} , kJ/mol)	Total Exergy (ΔE_{tot} , kJ/mol)
Materials in the inlet stream			
Methane sulphonic acid(l)	-346.5629	968.16	621.60
Imidazole 1yl Ac. Ac. HCl(s)	89.8308	2741.20	2831.03
Phosphorous acid (s)	-916.7216	364.07	-552.65
Materials in the outlet stream			
Methane sulphonic acid(l)	-346.0943	968.16	622.07
Imidazole 1yl Ac. Ac. HCl(s)	44.0072	2741.20	2785.21
Phosphorous acid (s)	-945.8883	364.07	-581.82

Table C.4. Calculation of $X_{\text{destroyed}}$ of dissolving of the reactants

Terms used to calculate $X_{\text{destroyed}}$ (kJ)	Calculated values, kJ
Mechanical Exergy as Work (W, kJ)	938.25
Thermal exergy, (kJ) $Q(1-(T_0/T))$	1854.42
Total Exergy flow, (kJ) $(Nb)_{\text{in}}-(Nb)_{\text{out}}$	60.62
$X_{\text{destroyed}}$ (kJ)	2853.29

Each term in Equation (C.2) is calculated to find $X_{\text{destroyed}}$.

Table C.5. Mass Balance of addition of PCl_3

Molecular Weight of each element (kg/kmol)	12.01	1.01	16.00	32.06	14.01	35.45	30.97	22.99	Molecular weight of the excipient (MW, kg/kmol)	Mole ratio of the substance x_i,
Materials in the inlet stream	C	H	O	S	N	Cl	P	Na		
Methane sulphonic acid(l)	1	4	3	1	0	0	-	-	96.11	0.69
Imidazole 1yl Ac. Ac. HCl(s)	5	7	2	0	2	1	-	-	162.59	0.10
Phosphorous acid (s)	0	3	3	-	-	-	1	-	82.00	0.21
Phosphorous trichloride (s)	-	-	-	-	-	3	1	-	137.33	1.00
Materials in the outlet stream	C	H	O	S	N	Cl	P	Na		
Methane sulphonic acid(l)	1	4	3	1	0	0	-	-	96.11	0.61
Zoledronic acid(s)	5	10	7	-	2	-	2	-	272.11	0.09
HCl (g)	-	1	-	-	-	1	-	-	36.46	0.50
Water (g)	-	2	1	-	-	-	-	-	18.02	0.50
Phosphorous trichloride (s)	-	-	-	-	-	3	1	-	137.33	0.30

Mass balance on elemental basis and molecular basis were evaluated. Equation (C.1) is used to calculate the data.

Table C.6. Thermodynamic props of addition of PCl_3

	Heat Capacity, (C_p , kJ/mol K)	Enthalpy, ($C_p\Delta T$, kJ/mol)	Enthalpy of formation (H_f , kJ/mol)	Total Enthalpy (H_{total} , kJ/mol) $H = H_f + C_p\Delta T$	Entropy of formation (S° , kJ/mol K)	Entropy change (ΔS , kJ/mol K) $\Delta S = S^\circ + C_p \ln(T/T_0) - R \ln x_i$
Materials in the inlet stream						
Methane sulphonic acid(l)	0.190	7.600	-566.200	-558.600	-0.7370	-0.6826
Imidazole 1yl Ac. Ac. HCl(s)	0.217	8.668	-536.300	-527.632	-2.1011	-1.8878
Phosphorous acid (s)	0.103	4.112	-965.525	-961.413	-0.1638	-0.0216
Phosphorous trichloride (s)	0.120	0.000	-319.700	-319.700	0.5164	0.5164
Materials in the outlet stream						
Methane sulphonic acid(l)	0.190	7.600	-566.200	-558.600	-0.7370	-0.6720
Zoledronic acid(s)	0.351	14.020	-2032.960	-2018.940	-0.5705	-0.3298
HCl (g)	0.036	1.454	-92.300	-90.846	0.1868	0.2482
Water (g)	0.036	1.437	-241.820	-240.383	0.1888	0.2502
Phosphorous trichloride (s)	0.120	4.800	-319.700	-314.900	0.5164	0.6294

The terms in Equation (C.2) calculated for reaction after addition of PCl_3 are represented in Table C.6.

Table C.7. Exergy and $X_{\text{destroyed}}$ calculation of addition of PCl_3

	Physical exergy (ΔE_{ph} , kJ/mol)	Chemical Exergy (ΔE_{ch} , kJ/mol)	Total Exergy (ΔE_{tot} , kJ/mol)
Materials in the inlet stream			
Methane sulphonic acid(l)	-355.1738	968.16	612.99
Imidazole 1yl Ac. Ac. HCl(s)	34.9277	2741.20	2776.13
Phosphorous acid (s)	-954.9679	364.07	-590.90
Phosphorous trichloride (s)	-473.5724	775.15	301.58
Materials in the outlet stream			
Methane sulphonic acid(l)	-358.3312	968.16	609.83
Zoledronic acid(s)	-1920.6687	3593.91	1673.24
HCl (g)	-164.8145	84.73	-80.08
Water (g)	-314.9435	9.34	-305.60
Phosphorous trichloride (s)	-502.4512	775.15	272.70

Table C.8. Calculation of $X_{\text{destroyed}}$ of addition of PCl_3

Terms used to calculate $X_{\text{destroyed}}$ (kJ)	Calculated values, kJ
Mechanical Exergy as Work (W. kJ)	75060.00
Thermal exergy, (kJ) $Q(1-(T_0/T))$	148353.88
Total Exergy flow, (kJ) $(Nb)_{\text{in}}-(Nb)_{\text{out}}$	254.45
$X_{\text{destroyed}}$ (kJ)	223668.34

Each term in Equation (C.2) is calculated to find $X_{\text{destroyed}}$.

Table C.9. Mass Balance of cooling of the reaction products

Molecular Weight of each element (kg/kmol)	12.01	1.01	16.00	32.06	14.01	35.45	30.97	22.99	Molecular weight of the excipient (MW, kg/kmol)	Mole ratio of the substance x_i
Materials in the inlet stream	C	H	O	S	N	Cl	P	Na		
Methane sulphonic acid(l)	1	4	3	1	0	0	-	-	96.11	0.61
Zoledronic acid(s)	5	10	7	-	2	-	2	-	272.11	0.09
Phosphorous trichloride (s)	-	-	-	-	-	3	1	-	137.33	0.30
Materials in the outlet stream	C	H	O	S	N	Cl	P	Na		
Methane sulphonic acid(l)	1	4	3	1	0	0	-	-	96.11	0.61
Zoledronic acid(s)	5	10	7	-	2	-	2	-	272.11	0.09
Phosphorous trichloride (s)	-	-	-	-	-	3	1	-	137.33	0.30

Mass balance on elemental basis and molecular basis were evaluated. Equation (C.1) is used to calculate the data.

Table C.10. Thermodynamic props of cooling of the reaction products

	Heat Capacity, (C_p, kJ/mol K)	Enthalpy, (C_pΔT, kJ/mol)	Enthalpy of formation (H_f, kJ/mol)	Total Enthalpy (H_{total}, kJ/mol) H= H_f + C_pΔT	Entropy of formation (S°, kJ/mol K)	Entropy change (ΔS, kJ/mol K) ΔS= S°+C_pln(T/T₀)-Rlnx_i
Materials in the inlet stream						
Methane sulphonic acid(l)	0.19	7.60	-566.20	-558.60	-0.7370	-0.6720
Zoledronic acid(s)	0.35	14.02	-2032.96	-2018.94	-2.1011	-1.8603
Phosphorous trichloride (s)	0.12	4.80	-319.70	-314.90	0.5164	0.6294
Materials in the outlet stream						
Methane sulphonic acid(l)	0.19	4.75	-566.20	-561.45	-0.7370	-0.6807
Zoledronic acid(s)	0.35	8.76	-2032.96	-2024.20	-2.1011	-1.8762
Phosphorous trichloride (s)	0.12	3.00	-319.70	-316.70	0.5164	0.6239

The terms in Equation (C.2) calculated for cooling of the reaction products are represented in Table C.10.

Table C.11. Exergy and $X_{\text{destroyed}}$ calculation cooling of the reaction products

	Physical exergy (ΔE_{ph} , kJ/mol)	Chemical Exergy (ΔE_{ch} , kJ/mol)	Total Exergy (ΔE_{tot} , kJ/mol)
Materials in the inlet stream			
Methane sulphonic acid(l)	-358.3312	968.16	609.83
Zoledronic acid(s)	-1464.5598	3593.91	2129.35
Phosphorous trichloride (s)	-502.4512	775.15	272.70
Materials in the outlet stream			
Methane sulphonic acid(l)	-358.6110	968.16	609.55
Zoledronic acid(s)	-1465.0760	3593.91	2128.83
Phosphorous trichloride (s)	-502.6279	775.15	272.52

Table C.12. Calculation of $X_{\text{destroyed}}$ of cooling of the reaction products

Terms used to calculate $X_{\text{destroyed}}$ (kJ)	Calculated values, kJ
Mechanical Exergy as Work (W, kJ)	938.25
Thermal exergy, (kJ) $Q(1-(T_0/T))$	-0.85
Total Exergy flow, (kJ) $(Nb)_{\text{in}}-(Nb)_{\text{out}}$	1.78
$X_{\text{destroyed}}$ (kJ)	939.18

Table C.13. Calculation of $X_{\text{destroyed}}$ of heating and addition absorbent and water

Terms used to calculate $X_{\text{destroyed}}$ (kJ)	Calculated values, kJ
Mechanical Exergy as Work (W, kJ)	1563.75
Thermal exergy, (kJ) $Q(1-(T_0/T))$	2266.77
Total Exergy flow, (kJ) $(Nb)_{\text{in}}-(Nb)_{\text{out}}$	40.88
$X_{\text{destroyed}}$ (kJ)	3871.40

Table C.14. Calculation of $X_{\text{destroyed}}$ of filtration of absorbent

Terms used to calculate $X_{\text{destroyed}}$ (kJ)	Calculated values, kJ
Mechanical Exergy as Work (W, kJ)	938.25
Thermal exergy, (kJ) $Q(1-(T_0/T))$	1289.37
Total Exergy flow, (kJ) $(Nb)_{\text{in}}-(Nb)_{\text{out}}$	269.75
$X_{\text{destroyed}}$ (kJ)	2497.38

Each term in equation C.2. is calculated to find $x_{\text{destroyed}}$.

Table C.15. Mass Balance of cooling

Molecular Weight of each element (kg/kmol)	12.01	1.01	16.00	32.06	14.01	35.45	30.97	22.99	Molecular weight of the excipient (MW, kg/kmol)	Mole ratio of the substance x_i ,
Materials in the inlet stream	C	H	O	S	N	Cl	P	Na		
Methane sulphonic acid(l)	1	4	3	1	-	-	-	-	96.11	0.19
Zoledronic acid(s)	5	10	7	-	2	-	2	-	272.11	0.03
Phosphorous trichloride (s)	-	-	-	-	-	3	1	-	137.33	0.09
Water (l)	-	2	1	-	-	-	-	-	18.02	0.69
Materials in the outlet stream	C	H	O	S	N	Cl	P	Na		
Methane sulphonic acid(l)	1	4	3	1	-	-	-	-	96.11	0.19
Zoledronic acid(s)	5	10	7	-	2	-	2	-	272.11	0.03
Phosphorous trichloride (s)	-	-	-	-	-	3	1	-	137.33	0.09
Water (l)	-	2	1	-	-	-	-	-	18.02	0.69

Mass balance on elemental basis and molecular basis were evaluated. Equation (C.1) is used to calculate the data.

Table C.16. Thermodynamic props of of cooling

	Heat Capacity, (C _p , kJ/mol K)	Enthalpy, (C _p ΔT, kJ/mol)	Enthalpy of formation (H _f , kJ/mol)	Total Enthalpy (H _{total} , kJ/mol) H= H _f + C _p ΔT	Entropy of formation (S°, kJ/mol K)	Entropy change (ΔS, kJ/mol K) ΔS=S°+C _p ln(T/T ₀)-Rlnx _i
Materials in the inlet stream						
Methane sulphonic acid(l)	0.19	9.50	-566.20	-556.70	-0.7370	-0.5710
Zoledronic acid(s)	0.35	17.53	-2032.96	-2015.44	-2.1011	-1.7546
Phosphorous trichloride (s)	0.12	6.00	-319.70	-313.70	0.5164	0.7284
Water (l)	0.08	3.77	-285.83	-282.07	0.0700	0.1123
Materials in the outlet stream						
Methane sulphonic acid(l)	0.19	-3.80	-566.20	-570.00	-0.7370	-0.6136
Zoledronic acid(s)	0.35	-7.01	-2032.96	-2039.97	-2.1011	-1.8333
Phosphorous trichloride (s)	0.12	-2.40	-319.70	-322.10	0.5164	0.7014
Water (l)	0.08	-1.51	-285.83	-287.34	0.0700	0.0954

The terms in Equation (C.2) calculated for cooling are represented in Table C.16.

Table C.17. Exergy and $X_{\text{destroyed}}$ calculation of cooling

	Physical exergy (ΔE_{ph} , kJ/mol)	Chemical Exergy (ΔE_{ch} , kJ/mol)	Total Exergy (ΔE_{tot} , kJ/mol)
Materials in the inlet stream			
Methane sulphonic acid(l)	-386.5511	968.16	581.61
Zoledronic acid(s)	-1492.5691	3593.91	2101.34
Phosphorous trichloride (s)	-530.7628	775.15	244.39
Water (l)	-315.5257	0.77	-314.76
Materials in the outlet stream			
Methane sulphonic acid(l)	-387.1353	968.16	581.02
Zoledronic acid(s)	-1493.6468	3593.91	2100.26
Phosphorous trichloride (s)	-531.1318	775.15	244.02
Water (l)	-315.7572	0.77	-314.99

Table C.18. Calculation of $X_{\text{destroyed}}$ of cooling

Terms used to calculate $X_{\text{destroyed}}$ (kJ)	Calculated values, kJ
Mechanical Exergy as Work (W, kJ)	2814.75
Thermal exergy, (kJ) $Q(1-(T_0/T))$	-189.03
Total Exergy flow, (kJ) $(Nb)_{\text{in}}-(Nb)_{\text{out}}$	7.09
$X_{\text{destroyed}}$ (kJ)	2632.81

Each term in Equation (C.2) is calculated to find $x_{\text{destroyed}}$.

Table C.19. Mass Balance of of NaOH addition

Molecular Weight of each element (kg/kmol)	12.01	1.01	16.00	32.06	14.01	35.45	30.97	22.99	Molecular weight of the excipient (MW, kg/kmol)	Mole ratio of the substance x_i ,
Materials in the inlet stream	C	H	O	S	N	Cl	P	Na		
Methane sulphonic acid(l)	1	4	3	1	-	-	-	-	96.11	0.19
Zoledronic acid(s)	5	10	7	-	2	-	2	-	272.11	0.03
Phosphorous trichloride (s)	-	-	-	-	-	3	1	-	137.32	0.09
Water (l)	-	2	1	-	-	-	-	-	18.02	2.53
NaOH (l)	-	1	1	-	-	-	-	1	40.00	0.16
Materials in the outlet stream	C	H	O	S	N	Cl	P	Na		
Methane sulphonic acid(l)	1	4	3	1	-	-	-	-	96.11	0.09
Zoledronic acid(s)	5	10	7	-	2	-	2	-	272.11	0.01
Phosphorous trichloride (s)	-	-	-	-	-	3	1	-	137.32	0.04
Water (l)	-	2	1	-	-	-	-	-	18.02	0.77
NaOH (l)	-	1	1	-	-	-	-	1	40.00	0.09

Mass balance on elemental basis and molecular basis were evaluated. Equation (C.1) is used to calculate the data.

Table C.20. Thermodynamic prop's of NaOH addition

	Heat Capacity, (C _p , kJ/mol K)	Enthalpy, (C _p ΔT, kJ/mol)	Enthalpy of formation (H _f , kJ/mol)	Total Enthalpy (H _{total} , kJ/mol) H= H _f + C _p ΔT	Entropy of formation (S ^o , kJ/mol K)	Entropy change (ΔS, kJ/mol K) ΔS= S ^o +C _p ln(T/T ₀)-Rlnx _i
Materials in the inlet stream						
Methane sulphonic acid(l)	0.19	-3.80	-566.20	-570.00	-0.7370	-0.6136
Zoledronic acid(s)	0.35	-7.01	-2032.96	-2039.97	-2.1011	-1.8333
Phosphorous trichloride (s)	0.12	-2.40	-319.70	-322.10	0.5164	0.7014
Water (l)	0.08	-1.51	-285.83	-287.34	0.0700	0.0954
Water (l)	0.08	0.00	-285.83	-285.83	0.0700	0.0839
NaOH (l)	0.06	0.00	-425.61	-425.61	0.0645	0.2164
Materials in the outlet stream						
Methane sulphonic acid(l)	0.19	-3.80	-566.20	-570.00	-0.7370	-0.5488
Zoledronic acid(s)	0.35	-7.01	-2032.96	-2039.97	-2.1011	-1.7685
Phosphorous trichloride (s)	0.12	-2.40	-319.70	-322.10	0.5164	0.7663
Water (l)	0.08	-1.51	-285.83	-287.34	0.0700	0.2885
NaOH (l)	0.06	-1.19	-425.61	-426.80	0.0645	0.2618

The terms in Equation (C.2) calculated for NaOH addition are represented in Table C.20.

Table C.21. Exergy and $X_{\text{destroyed}}$ calculation of NaOH addition

	Physical exergy (ΔE_{ph} , kJ/mol)	Chemical Exergy (ΔE_{ch} , kJ/mol)	Total Exergy (ΔE_{tot} , kJ/mol)
Materials in the inlet stream			
Methane sulphonic acid(l)	-387.1353	968.16	581.02
Zoledronic acid(s)	-1493.6468	3593.91	2100.26
Phosphorous trichloride (s)	-531.1318	775.15	244.02
Water (l)	-315.7572	0.77	-314.99
Water (l)	-310.8445	0.77	-310.07
NaOH (l)	-490.0839	77.43	-412.65
Materials in the outlet stream			
Methane sulphonic acid(l)	-406.4586	968.16	561.70
Zoledronic acid(s)	-1512.9702	3593.91	2080.94
Phosphorous trichloride (s)	-550.4552	775.15	224.69
Water (l)	-335.0806	0.77	-334.31
Water (l)	-325.5560	0.77	-324.79
NaOH (l)	-504.8065	77.43	-427.38

Table C.22. Calculation of $X_{\text{destroyed}}$ of NaOH addition

Terms used to calculate $X_{\text{destroyed}}$ (kJ)	Calculated values, kJ
Mechanical Exergy as Work (W, kJ)	4691.25
Thermal exergy, (kJ) $Q(1-(T_0/T))$	-189.03
Total Exergy flow, (kJ) $(Nb)_{\text{in}}-(Nb)_{\text{out}}$	-784.07
$X_{\text{destroyed}}$ (kJ)	3718.14

Each term in Equation (C.2) is calculated to find $x_{\text{destroyed}}$.

Table C.23. Mass Balance of heating to room temperature

Molecular Weight of each element (kg/kmol)	12.01	1.01	16.00	32.06	14.01	35.45	30.97	22.99	Molecular weight of the excipient (MW, kg/kmol)	Mole ratio of the substance x_i,
Materials in the inlet stream	C	H	O	S	N	Cl	P	Na		
Methane sulphonic acid(l)	1	4	3	1	-	-	-	-	96.11	0.09
Zoledronic acid(s)	5	10	7	-	2	-	2	-	272.11	0.01
Phosphorous trichloride (s)	-	-	-	-	-	3	1	-	137.32	0.04
Water (l)	-	2	1	-	-	-	-	-	18.02	0.77
NaOH (l)	-	1	1	-	-	-	-	1	40.00	0.09
Materials in the outlet stream	C	H	O	S	N	Cl	P	Na		
Methane sulphonic acid(l)	1	4	3	1	-	-	-	-	96.11	0.09
Zoledronic acid(s)	5	10	7	-	2	-	2	-	272.11	0.01
Phosphorous trichloride (s)	-	-	-	-	-	3	1	-	137.32	0.04
Water (l)	-	2	1	-	-	-	-	-	18.02	0.77
NaOH (l)	-	1	1	-	-	-	-	1	40.00	0.09

Mass balance on elemental basis and molecular basis were evaluated. Equation (C.1) is used to calculate the data.

Table C.24. Thermodynamic props of heating to room temperature

	Heat Capacity, (C_p , kJ/mol K)	Enthalpy, ($C_p\Delta T$, kJ/mol)	Enthalpy of formation (H_f , kJ/mol)	Total Enthalpy (H_{total} , kJ/mol) $H = H_f + C_p\Delta T$	Entropy of formation (S° , kJ/mol K)	Entropy change (ΔS , kJ/mol K) $\Delta S = S^\circ + C_p \ln(T/T_0) - R \ln x_i$
Materials in the inlet stream						
Methane sulphonic acid(l)	0.19	-3.80	-566.20	-570.00	-0.7370	-0.5488
Zoledronic acid(s)	0.35	-7.01	-2032.96	-2039.97	-2.1011	-1.7685
Phosphorous trichloride (s)	0.12	-2.40	-319.70	-322.10	0.5164	0.7663
Water (l)	0.08	-1.51	-285.83	-287.34	0.0700	0.2885
NaOH (l)	0.06	-1.19	-425.61	-426.80	0.0645	0.2618
Materials in the outlet stream						
Methane sulphonic acid(l)	0.19	-0.95	-566.20	-567.15	-0.7370	-0.5388
Zoledronic acid(s)	0.35	-1.75	-2032.96	-2034.71	-2.1011	-1.7500
Phosphorous trichloride (s)	0.12	-0.60	-319.70	-320.30	0.5164	0.7726
Water (l)	0.08	-0.38	-285.83	-286.21	0.0700	0.2964
NaOH (l)	0.06	-0.30	-425.61	-425.91	0.0645	0.2649

The terms in Equation (C.2) calculated for heating to room temperature are represented in Table C.24.

Table C.25. Exergy and $X_{\text{destroyed}}$ calculation of heating to room temperature

	Physical exergy (ΔE_{ph} , kJ/mol)	Chemical Exergy (ΔE_{ch} , kJ/mol)	Total Exergy (ΔE_{tot} , kJ/mol)
Materials in the inlet stream			
Methane sulphonic acid(l)	-406.4586	968.16	561.70
Zoledronic acid(s)	-1512.9702	3593.91	2080.94
Phosphorous trichloride (s)	-550.4552	775.15	224.69
Water (l)	-335.0806	0.77	-334.31
Water (l)	-325.5560	0.77	-324.79
NaOH (l)	-504.8065	77.43	-427.38
Materials in the outlet stream			
Methane sulphonic acid(l)	-406.5841	968.16	561.58
Zoledronic acid(s)	-1513.2017	3593.91	2080.71
Phosphorous trichloride (s)	-550.5344	775.15	224.62
Water (l)	-335.1303	0.77	-334.36
Water (l)	-325.6058	0.77	-324.84
NaOH (l)	-504.8459	77.43	-427.42

Table C.26. Calculation of $X_{\text{destroyed}}$ of heating to room temperature

Terms used to calculate $X_{\text{destroyed}}$ (kJ)	Calculated values, kJ
Mechanical Exergy as Work (W, kJ)	938.25
Thermal exergy, (kJ) $Q(1-(T_0/T))$	-0.37
Total Exergy flow, (kJ) $(Nb)_{\text{in}}-(Nb)_{\text{out}}$	2.75
$X_{\text{destroyed}}$ (kJ)	940.63

Each term in Equation (C.2) is calculated to find $X_{\text{destroyed}}$.

Table C.27. Mass Balance of of addition of ethanol

Molecular Weight of each element (kg/kmol)	12.01	1.01	16.00	32.06	14.01	35.45	30.97	22.99	Molecular weight of the excipient (MW, kg/kmol)	Mole ratio of the substance x_i,
Materials in the inlet stream	C	H	O	S	N	Cl	P	Na		
Methane sulphonic acid(l)	1	4	3	1	-	-	-	-	96.11	0.09
Zoledronic acid(s)	5	10	7	-	2	-	2	-	272.11	0.01
Phosphorous trichloride (s)	-	-	-	-	-	3	1	-	137.32	0.04
Water (l)	-	2	1	-	-	-	-	-	18.02	0.77
NaOH (l)	-	1	1	-	-	-	-	1	40.00	0.09
Ethanol (l)	2	6	1	-	-	-	-	-	46.08	1.00
Materials in the outlet stream	C	H	O	S	N	Cl	P	Na		
Methane sulphonic acid(l)	1	4	3	1	-	-	-	-	96.11	0.07
Zoledronic acid(s)	5	10	7	-	2	-	2	-	272.11	0.01
Phosphorous trichloride (s)	-	-	-	-	-	3	1	-	137.32	0.04
Water (l)	-	2	1	-	-	-	-	-	18.02	0.65
NaOH (l)	-	1	1	-	-	-	-	1	40.00	0.07
Ethanol (l)	2	6	1	-	-	-	-	-	46.08	0.16

Mass balance on elemental basis and molecular basis were evaluated. Equation (C.1) is used to calculate the data.

Table C.28. Thermodynamic props of addition of ethanol

	Heat Capacity, (C_p , kJ/mol K)	Enthalpy, ($C_p\Delta T$, kJ/mol)	Enthalpy of formation (H_f , kJ/mol)	Total Enthalpy (H_{total} , kJ/mol) $H = H_f + C_p\Delta T$	Entropy of formation (S° , kJ/mol K)	Entropy change (ΔS , kJ/mol K) $\Delta S = S^\circ + C_p \ln(T/T_0) - R \ln x_i$
Materials in the inlet stream						
Methane sulphonic acid(l)	0.19	-0.95	-566.20	-567.15	-0.7370	-0.5388
Zoledronic acid(s)	0.35	-1.75	-2032.96	-2034.71	-2.1011	-1.7500
Phosphorous trichloride (s)	0.12	-0.60	-319.70	-320.30	0.5164	0.7726
Water (l)	0.08	-0.38	-285.83	-286.21	0.0700	0.2964
NaOH (l)	0.06	-0.30	-425.61	-425.91	0.0645	0.2649
Ethanol (l)	0.11	0.00	-277.69	-277.69	0.1607	0.1607
Materials in the outlet stream						
Methane sulphonic acid(l)	0.19	-0.95	-566.20	-567.15	-0.7370	-0.5249
Zoledronic acid(s)	0.35	-1.75	-2032.96	-2034.71	-2.1011	-1.7362
Phosphorous trichloride (s)	0.12	-0.60	-319.70	-320.30	0.5164	0.7865
Water (l)	0.08	-0.38	-285.83	-286.21	0.0700	0.3241
NaOH (l)	0.06	-0.30	-425.61	-425.91	0.0645	0.2788
Ethanol (l)	0.11	-0.56	-277.69	-278.25	0.1607	0.3114

The terms in Equation (C.2) calculated for addition of ethanol are represented in Table C.28.

Table C.29. Exergy and $X_{\text{destroyed}}$ calculation of addition of ethanol

	Physical exergy (ΔE_{ph} , kJ/mol)	Chemical Exergy (ΔE_{ch} , kJ/mol)	Total Exergy (ΔE_{tot} , kJ/mol)
Materials in the inlet stream			
Methane sulphonic acid(l)	-406.5841	968.16	561.58
Zoledronic acid(s)	-1513.2017	3593.91	2080.71
Phosphorous trichloride (s)	-550.5344	775.15	224.62
Water (l)	-335.1303	0.77	-334.36
Water (l)	-325.6058	0.77	-324.84
NaOH (l)	-504.8459	77.43	-427.42
Ethanol (l)	-325.5786	1356.01	1030.43
Materials in the outlet stream			
Methane sulphonic acid(l)	-410.7177	968.16	557.44
Zoledronic acid(s)	-1517.3353	3593.91	2076.57
Phosphorous trichloride (s)	-554.6680	775.15	220.48
Water (l)	-339.2639	0.77	-338.49
Water (l)	-329.7394	0.77	-328.97
NaOH (l)	-508.9795	77.43	-431.55
Ethanol (l)	-371.0318	1356.01	984.98

Table C.30. Calculation of $X_{\text{destroyed}}$ of addition of ethanol

Terms used to calculate $X_{\text{destroyed}}$ (kJ)	Calculated values, kJ
Mechanical Exergy as Work (W, kJ)	625.50
Thermal exergy, (kJ) $Q(1-(T_0/T))$	-12.82
Total Exergy flow, (kJ) $(Nb)_{\text{in}}-(Nb)_{\text{out}}$	583.77
$X_{\text{destroyed}}$ (kJ)	1196.45

Each term in Equation (C.2) is calculated to find $x_{\text{destroyed}}$.

Table C.31. Mass Balance of stirring

Molecular Weight of each element (kg/kmol)	12.01	1.01	16.00	32.06	14.01	35.45	30.97	22.99	Molecular weight of the excipient (MW, kg/kmol)	Mole ratio of the substance x_i ,
Materials in the inlet stream	C	H	O	S	N	Cl	P	Na		
Methane sulphonic acid(l)	1	4	3	1	-	-	-	-	96.11	0.07
Zoledronic acid(s)	5	10	7	-	2	-	2	-	272.11	0.01
Phosphorous trichloride (s)	-	-	-	-	-	3	1	-	137.32	0.04
Water (l)	-	2	1	-	-	-	-	-	18.02	0.61
NaOH (l)	-	1	1	-	-	-	-	1	40.00	0.07
Ethanol (l)	2	6	1	-	-	-	-	-	46.08	0.16
Materials in the inlet stream	C	H	O	S	N	Cl	P	Na		
Methane sulphonic acid(l)	1	4	3	1	-	-	-	-	96.11	0.07
Zoledronic acid(s)	5	10	7	-	2	-	2	-	272.11	0.01
Phosphorous trichloride (s)	-	-	-	-	-	3	1	-	137.32	0.04
Water (l)	-	2	1	-	-	-	-	-	18.02	0.61
NaOH (l)	-	1	1	-	-	-	-	1	40.00	0.07
Ethanol (l)	2	6	1	-	-	-	-	-	46.08	0.16

Mass balance on elemental basis and molecular basis were evaluated. Equation (C.1) is used to calculate the data.

Table C.32. Thermodynamic props of stirring

	Heat Capacity, (C _p , kJ/mol K)	Enthalpy, (C _p ΔT, kJ/mol)	Enthalpy of formation (H _f , kJ/mol)	Total Enthalpy (H _{total} , kJ/mol) H= H _f + C _p ΔT	Entropy of formation (S°, kJ/mol K)	Entropy change (ΔS, kJ/mol K) ΔS= S°+C _p ln(T/T ₀)-Rlnx _i
Materials in the inlet stream						
Methane sulphonic acid(l)	0.19	-0.95	-566.20	-567.15	-0.7370	-0.5249
Zoledronic acid(s)	0.35	-1.75	-2032.96	-2034.71	-2.1011	-1.7362
Phosphorous trichloride (s)	0.12	-0.60	-319.70	-320.30	0.5164	0.7865
Water (l)	0.08	-0.38	-285.83	-286.21	0.0700	0.3242
NaOH (l)	0.06	-0.30	-425.61	-425.91	0.0645	0.2788
Ethanol (l)	0.11	-0.56	-277.69	-278.25	0.1607	0.3114
Materials in the outlet stream						
Methane sulphonic acid(l)	0.19	-0.95	-566.20	-567.15	-0.7370	-0.5249
Zoledronic acid(s)	0.35	-1.75	-2032.96	-2034.71	-2.1011	-1.7362
Phosphorous trichloride (s)	0.12	-0.60	-319.70	-320.30	0.5164	0.7865
Water (l)	0.08	-0.38	-285.83	-286.21	0.0700	0.3242
NaOH (l)	0.06	-0.30	-425.61	-425.91	0.0645	0.2788
Ethanol (l)	0.11	-0.56	-277.69	-278.25	0.1607	0.3114

The terms in Equation (C.2) calculated for stirring are represented in Table C.32.

Table C.33. Exergy and $X_{\text{destroyed}}$ calculation of stirring

	Physical exergy (ΔE_{ph} , kJ/mol)	Chemical Exergy (ΔE_{ch} , kJ/mol)	Total Exergy (ΔE_{tot} , kJ/mol)
Materials in the inlet stream			
Methane sulphonic acid(l)	-410.7177	968.16	557.44
Zoledronic acid(s)	-1517.3353	3593.91	2076.57
Phosphorous trichloride (s)	-554.6680	775.15	220.48
Water (l)	-339.2639	0.77	-338.49
Water (l)	-329.7394	0.77	-328.97
NaOH (l)	-508.9795	77.43	-431.55
Ethanol (l)	-371.0318	1356.01	984.98
Materials in the outlet stream			
Methane sulphonic acid(l)	-410.7177	968.16	557.44
Zoledronic acid(s)	-1517.3353	3593.91	2076.57
Phosphorous trichloride (s)	-554.6680	775.15	220.48
Water (l)	-339.2639	0.77	-338.49
Water (l)	-329.7394	0.77	-328.97
NaOH (l)	-508.9795	77.43	-431.55
Ethanol (l)	-371.0318	1356.01	984.98

Table C.34. Calculation of $X_{\text{destroyed}}$ of stirring

Terms used to calculate $X_{\text{destroyed}}$ (kJ)	Calculated values, kJ
Mechanical Exergy as Work (W, kJ)	11259.00
Thermal exergy, (kJ) $Q(1-(T_0/T))$	-12.82
Total Exergy flow, (kJ) $(Nb)_{\text{in}}-(Nb)_{\text{out}}$	0.00
$X_{\text{destroyed}}$ (kJ)	11246.18

Each term in Equation (C.2) is calculated to find $X_{\text{destroyed}}$.

Table C.35. Mass Balance of cooling to a temperature lower than 0 °C

Molecular Weight of each element (kg/kmol)	12.01	1.01	16.00	32.06	14.01	35.45	30.97	22.99	Molecular weight of the excipient (MW, kg/kmol)	Mole ratio of the substance x_i
Materials in the inlet stream	C	H	O	S	N	Cl	P	Na		
Methane sulphonic acid(l)	1	4	3	1	-	-	-	-	96.11	0.07
Zoledronic acid(s)	5	10	7	-	2	-	2	-	272.11	0.01
Phosphorous trichloride (s)	-	-	-	-	-	3	1	-	137.32	0.04
Water (l)	-	2	1	-	-	-	-	-	18.02	0.65
NaOH (l)	-	1	1	-	-	-	-	1	40.00	0.07
Ethanol (l)	2	6	1	-	-	-	-	-	46.08	0.16
Materials in the outlet stream	C	H	O	S	N	Cl	P	Na		
Methane sulphonic acid(l)	1	4	3	1	-	-	-	-	96.11	0.07
Zoledronic acid(s)	5	10	7	-	2	-	2	-	272.11	0.01
Phosphorous trichloride (s)	-	-	-	-	-	3	1	-	137.32	0.04
Water (l)	-	2	1	-	-	-	-	-	18.02	0.65
NaOH (l)	-	1	1	-	-	-	-	1	40.00	0.07
Ethanol (l)	2	6	1	-	-	-	-	-	46.08	0.16

Mass balance on elemental basis and molecular basis were evaluated. Equation (C.1) is used to calculate the data.

Table C.36. Thermodynamic props of cooling to a temperature lower than 0 °C

	Heat Capacity, (C _p , kJ/mol K)	Enthalpy, (C _p ΔT, kJ/mol)	Enthalpy of formation (H _f , kJ/mol)	Total Enthalpy (H _{total} , kJ/mol) H= H _f + C _p ΔT	Entropy of formation (S°, kJ/mol K)	Entropy change (ΔS, kJ/mol K) ΔS= S°+C _p ln(T/T ₀)-Rlnx _i
Materials in the inlet stream						
Methane sulphonic acid(l)	0.19	-0.95	-566.20	-567.15	-0.7370	-0.5249
Zoledronic acid(s)	0.35	-1.75	-2032.96	-2034.71	-2.1011	-1.7362
Phosphorous trichloride (s)	0.12	-0.60	-319.70	-320.30	0.5164	0.7865
Water (l)	0.08	-0.38	-285.83	-286.21	0.0700	0.3241
NaOH (l)	0.06	-0.30	-425.61	-425.91	0.0645	0.2788
Ethanol (l)	0.11	-0.56	-277.69	-278.25	0.1607	0.3114
Materials in the outlet stream						
Methane sulphonic acid(l)	0.19	-5.70	-566.20	-571.90	-0.7370	-0.5419
Zoledronic acid(s)	0.35	-10.52	-2032.96	-2043.48	-2.1011	-1.7674
Phosphorous trichloride (s)	0.12	-3.60	-319.70	-323.30	0.5164	0.7758
Water (l)	0.08	-2.26	-285.83	-288.09	0.0700	0.3107
NaOH (l)	0.06	-1.79	-425.61	-427.40	0.0645	0.2735
Ethanol (l)	0.11	-3.34	-277.69	-281.03	0.1607	0.3014

The terms in Equation (C.2) calculated for cooling to a temperature lower than 0 °C are represented in Table C.36.

Table C.37. Exergy and $X_{\text{destroyed}}$ calculation of cooling to a temperature lower than 0 °C

	Physical exergy (ΔE_{ph} , kJ/mol)	Chemical Exergy (ΔE_{ch} , kJ/mol)	Total Exergy (ΔE_{tot} , kJ/mol)
Materials in the inlet stream			
Methane sulphonic acid(l)	-410.7177	968.16	557.44
Zoledronic acid(s)	-1517.3353	3593.91	2076.57
Phosphorous trichloride (s)	-554.6680	775.15	220.48
Water (l)	-339.2639	0.77	-338.49
Water (l)	-329.7394	0.77	-328.97
NaOH (l)	-508.9795	77.43	-431.55
Ethanol (l)	-371.0318	1356.01	984.98
Materials in the outlet stream			
Methane sulphonic acid(l)	-410.4180	968.16	557.74
Zoledronic acid(s)	-1516.7825	3593.91	2077.13
Phosphorous trichloride (s)	-554.4788	775.15	220.67
Water (l)	-339.1452	0.77	-338.38
Water (l)	-329.6206	0.77	-328.85
NaOH (l)	-508.8856	77.43	-431.46
Ethanol (l)	-370.8560	1356.01	985.15

Table C.38. Calculation of $X_{\text{destroyed}}$ of cooling to a temperature lower than 0 °C

Terms used to calculate $X_{\text{destroyed}}$ (kJ)	Calculated values, kJ
Mechanical Exergy as Work (W, kJ)	938.25
Thermal exergy, (kJ) $Q(1-(T_0/T))$	-726.90
Total Exergy flow, (kJ) $(N_b)_{\text{in}}-(N_b)_{\text{out}}$	-8.08
$X_{\text{destroyed}}$ (kJ)	203.27

Each term in Equation (C.2) is calculated to find $X_{\text{destroyed}}$.

Table C.39. Mass Balance of filtration and collecting of the product

Molecular Weight of each element (kg/kmol)	12.01	1.01	16.00	32.06	14.01	35.45	30.97	22.99	Molecular weight of the excipient (MW, kg/kmol)	Mole ratio of the substance x_i
Materials in the inlet stream	C	H	O	S	N	Cl	P	Na		
Methane sulphonic acid(l)	1	4	3	1	-	-	-	-	96.11	0.07
Zoledronic acid(s)	5	10	7	-	2	-	2	-	272.11	0.01
Phosphorous trichloride (s)	-	-	-	-	-	3	1	-	137.32	0.04
Water (l)	-	2	1	-	-	-	-	-	18.02	0.65
NaOH (l)	-	1	1	-	-	-	-	1	40.00	0.07
Ethanol (l)	2	6	1	-	-	-	-	-	46.08	0.16
Materials in the outlet stream	C	H	O	S	N	Cl	P	Na		
Methane sulphonic acid(l)	1	4	3	1	-	-	-	-	96.11	0.07
Zoledronic acid(s)	5	10	7	-	2	-	2	-	272.11	1.00
Phosphorous trichloride (s)	-	-	-	-	-	3	1	-	137.32	0.04
Water (l)	-	2	1	-	-	-	-	-	18.02	0.65
NaOH (l)	-	1	1	-	-	-	-	1	40.00	0.07
Ethanol (l)	2	6	1	-	-	-	-	-	46.08	0.16

Mass balance on elemental basis and molecular basis were evaluated. Equation (C.1) is used to calculate the data.

Table C.40. Thermodynamic props of filtration and collecting of the product

	Heat Capacity, (C_p , kJ/mol K)	Enthalpy, ($C_p\Delta T$, kJ/mol)	Enthalpy of formation (H_f , kJ/mol)	Total Enthalpy (H_{total} , kJ/mol) $H = H_f + C_p\Delta T$	Entropy of formation (S° , kJ/mol K)	Entropy change (ΔS , kJ/mol K) $\Delta S = S^\circ + C_p \ln(T/T_0) - R \ln x_i$
Materials in the inlet stream						
Methane sulphonic acid(l)	0.19	-5.70	-566.20	-571.90	-0.7370	-0.5419
Zoledronic acid(s)	0.35	-10.52	-2032.96	-2043.48	-2.1011	-1.7674
Phosphorous trichloride (s)	0.12	-3.60	-319.70	-323.30	0.5164	0.7758
Water (l)	0.08	-2.26	-285.83	-288.09	0.0700	0.3107
NaOH (l)	0.06	-1.79	-425.61	-427.40	0.0645	0.2735
Ethanol (l)	0.11	-3.34	-277.69	-281.03	0.1607	0.3014
Materials in the outlet stream						
Methane sulphonic acid(l)	0.19	-3.80	-566.20	-570.00	-0.7370	-0.5358
Zoledronic acid(s)	0.35	-7.01	-2032.96	-2039.97	-2.1011	-2.1255
Phosphorous trichloride (s)	0.12	-2.40	-319.70	-322.10	0.5164	0.7793
Water (l)	0.08	-1.51	-285.83	-287.34	0.0700	0.3144
NaOH (l)	0.06	-1.19	-425.61	-426.80	0.0645	0.2747
Ethanol (l)	0.11	-2.23	-277.69	-279.92	0.1607	0.3046

The terms in Equation (C.2) calculated for filtration and collecting of the product are represented in Table C.40.

Table C.41. Exergy and $X_{\text{destroyed}}$ calculation of filtration and collecting of the product

	Physical exergy (ΔE_{ph} , kJ/mol)	Chemical Exergy (ΔE_{ch} , kJ/mol)	Total Exergy (ΔE_{tot} , kJ/mol)
Materials in the inlet stream			
Methane sulphonic acid(l)	-410.4180	968.16	557.74
Zoledronic acid(s)	-1516.7825	3593.91	2077.13
Phosphorous trichloride (s)	-554.4788	775.15	220.67
Water (l)	-339.1452	0.77	-338.38
Water (l)	-329.6206	0.77	-328.85
NaOH (l)	-508.8856	77.43	-431.46
Ethanol (l)	-370.8560	1356.01	985.15
Materials in the outlet stream			
Methane sulphonic acid(l)	-410.3255	968.16	557.83
Zoledronic acid(s)	-1406.5829	3593.91	2187.33
Phosphorous trichloride (s)	-554.3220	775.15	220.83
Water (l)	-338.9474	0.77	-338.18
Water (l)	-329.4229	0.77	-328.65
NaOH (l)	-508.6734	77.43	-431.24
Ethanol (l)	-370.6915	1356.01	985.32

Table C.42. Calculation of $X_{\text{destroyed}}$ of filtration and collecting of the product

Terms used to calculate $X_{\text{destroyed}}$ (kJ)	Calculated values, kJ
Mechanical Exergy as Work (W, kJ)	625.50
Thermal exergy, (kJ) $Q(1-(T_0/T))$	0.00
Total Exergy flow, (kJ) $(Nb)_{\text{in}}-(Nb)_{\text{out}}$	-76.20
$X_{\text{destroyed}}$ (kJ)	549.23

Each term in Equation (C.2) is calculated to find $x_{\text{destroyed}}$.

Table C.43. Mass Balance of crystallization at a temperature lower than 0 °C

Molecular Weight of each element (kg/kmol)	12.01	1.01	16.00	32.06	14.01	35.45	30.97	Molecular weight of the excipient (MW, kg/kmol)	Mole ratio of the substance x_i
Materials in the inlet stream	C	H	O	S	N	Cl	P		
Zoledronic acid(s)	5	10	7	-	2	-	2	272.11	1.00
Water (l)	-	2	1	-	-	-	-	18.02	1.00
Materials in the outlet stream	C	H	O	S	N	Cl	P		
Zoledronic acid(s)	5	10	7	-	2	-	2	272.11	0.00
Water (l)	-	2	1	-	-	-	-	18.02	1.00

Mass balance on elemental basis and molecular basis were evaluated. Equation (C.1) is used to calculate the data.

Table C.44. Thermodynamic props of crystallization at a temperature lower than 0 °C

	Heat Capacity, (C_p , kJ/mol K)	Enthalpy, ($C_p\Delta T$, kJ/mol)	Enthalpy of formation (H_f , kJ/mol)	Total Enthalpy (H_{total} , kJ/mol) $H = H_f + C_p\Delta T$	Entropy of formation (S° , kJ/mol K)	Entropy change (ΔS , kJ/mol K) $\Delta S = S^\circ + C_p \ln(T/T_0) - R \ln x_i$
Materials in the inlet stream						
Zoledronic acid(s)	0.35	0.00	-2032.96	-2032.96	-0.5705	-0.5705
Water (l)	0.08	0.00	-285.83	-285.83	0.0700	0.0700
Materials in the outlet stream						
Zoledronic acid(s)	0.35	22.78	-2032.96	-2010.18	-0.5705	-0.1403
Water (l)	0.08	4.89	-285.83	-280.94	0.0700	0.0705

The terms in Equation (C.2) calculated for crystallization at a temperature lower than 0 °C are represented in Table C.44.

Table C.45. Exergy and $X_{\text{destroyed}}$ calculation of crystallization at a temperature lower than 0 °C

	Physical exergy (ΔE_{ph} , kJ/mol)	Chemical Exergy (ΔE_{ch} , kJ/mol)	Total Exergy (ΔE_{tot} , kJ/mol)
Materials in the inlet stream			
Zoledronic acid(s)	-1862.9382	3593.91	1730.97
Water (l)	-306.6751	0.77	-305.91
Materials in the outlet stream			
Zoledronic acid(s)	-2000.4027	3593.91	1593.51
Water (l)	-306.2888	0.77	-305.52

Table C.46. Calculation of $X_{\text{destroyed}}$ of crystallization at a temperature lower than 0 °C

Terms used to calculate $X_{\text{destroyed}}$ (kJ)	Calculated values, kJ
Mechanical Exergy as Work (W, kJ)	22518.00
Thermal exergy, (kJ) $Q(1-(T_0/T))$	7790.01
Total Exergy flow, (kJ) $(Nb)_{\text{in}}-(Nb)_{\text{out}}$	12.44
$X_{\text{destroyed}}$ (kJ)	30320.45

Each term in Equation (C.2) is calculated to find $x_{\text{destroyed}}$.

Table C.47. Mass Balance of stirring the raw material and heating up

Molecular Weight of each element (kg/kmol)	12.01	1.01	16.00	32.06	14.01	35.45	30.97	Molecular weight of the excipient (MW, kg/kmol)	Mole ratio of the substance x_i
Materials in the inlet stream	C	H	O	S	N	Cl	P		
Zoledronic acid(s)	5	10	7	-	2	-	2	272.11	0.00
Water (l)	-	2	1	-	-	-	-	18.02	1.00
Materials in the outlet stream	C	H	O	S	N	Cl	P		
Zoledronic acid(s)	5	10	7	-	2	-	2	272.11	0.00
Water (l)	-	2	1	-	-	-	-	18.02	1.00

Mass balance on elemental basis and molecular basis were evaluated. Equation (C.1) is used to calculate the data.

Table C.48. Thermodynamic props of stirring the raw material and heating up

	Heat Capacity, (C_p , kJ/mol K)	Enthalpy, ($C_p\Delta T$, kJ/mol)	Enthalpy of formation (H_f , kJ/mol)	Total Enthalpy (H_{total} , kJ/mol) $H = H_f + C_p\Delta T$	Entropy of formation (S° , kJ/mol K)	Entropy change (ΔS , kJ/mol K) $\Delta S = S^\circ + C_p \ln(T/T_0) - R \ln x_i$
Materials in the inlet stream						
Zoledronic acid(s)	0.35	22.78	-2032.96	-2010.18	-0.5705	-0.0328
Water (l)	0.08	4.89	-285.83	-280.94	0.0700	0.0851
Materials in the outlet stream						
Zoledronic acid(s)	0.35	22.78	-2032.96	-2010.18	-0.5705	-0.0328
Water (l)	0.08	4.89	-285.83	-280.94	0.0700	0.0851

The terms in Equation (C.2) calculated for stirring the raw material and heating up are represented in Table C.48.

Table C.49. Exergy and $X_{\text{destroyed}}$ calculation of stirring the raw material and heating up

	Physical exergy (ΔE_{ph} , kJ/mol)	Chemical Exergy (ΔE_{ch} , kJ/mol)	Total Exergy (ΔE_{tot} , kJ/mol)
Materials in the inlet stream			
Zoledronic acid(s)	-2000.4027	3593.91	1593.51
Water (l)	-306.2888	0.77	-305.52
Materials in the outlet stream			
Zoledronic acid(s)	-2000.4027	3593.91	1593.51
Water (l)	-306.2888	0.77	-305.52

Table C.50. Calculation of $X_{\text{destroyed}}$ of stirring the raw material and heating up

Terms used to calculate $X_{\text{destroyed}}$ (kJ)	Calculated values, kJ
Mechanical Exergy as Work (W, kJ)	67554.00
Thermal exergy, (kJ) $Q(1-(T_0/T))$	23370.03
Total Exergy flow, (kJ) $(Nb)_{\text{in}}-(Nb)_{\text{out}}$	0.00
$X_{\text{destroyed}}$ (kJ)	90924.03

Each term in Equation (C.2) is calculated to find $x_{\text{destroyed}}$.

Table C.51. Mass Balance of cooling

Molecular Weight of each element (kg/kmol)	12.01	1.01	16.00	32.06	14.01	35.45	30.97	Molecular weight of the excipient (MW, kg/kmol)	Mole ratio of the substance x_i
Materials in the inlet stream	C	H	O	S	N	Cl	P		
Zoledronic acid(s)	5	10	7	-	2	-	2	272.11	0.00
Water (l)	-	2	1	-	-	-	-	18.02	1.00
Materials in the outlet stream	C	H	O	S	N	Cl	P		
Zoledronic acid(s)	5	10	7	-	2	-	2	272.11	0.00
Water (l)	-	2	1	-	-	-	-	18.02	1.00

Mass balance on elemental basis and molecular basis were evaluated. Equation (C.1) is used to calculate the data.

Table C.52. Thermodynamic props of cooling

	Heat Capacity, (C_p , kJ/mol K)	Enthalpy, ($C_p\Delta T$, kJ/mol)	Enthalpy of formation (H_f , kJ/mol)	Total Enthalpy (H_{total} , kJ/mol) $H = H_f + C_p\Delta T$	Entropy of formation (S° , kJ/mol K)	Entropy change (ΔS , kJ/mol K) $\Delta S = S^\circ + C_p \ln(T/T_0) - R \ln x_i$
Materials in the inlet stream						
Zoledronic acid(s)	0.35	24.54	-2032.96	-2008.43	-0.5705	-0.0280
Water (l)	0.08	5.27	-285.83	-280.56	0.0700	0.0861
Materials in the outlet stream						
Zoledronic acid(s)	0.35	-8.76	-2032.96	-2041.72	-0.5705	-0.1327
Water (l)	0.08	-1.88	-285.83	-287.71	0.0700	0.0636

The terms in Equation (C.2) calculated for cooling are represented in Table C.52.

Table C.53. Exergy and $X_{\text{destroyed}}$ calculation of cooling

	Physical exergy (ΔE_{ph} , kJ/mol)	Chemical Exergy (ΔE_{ch} , kJ/mol)	Total Exergy (ΔE_{tot} , kJ/mol)
Materials in the inlet stream			
Zoledronic acid(s)	-2000.0790	3593.91	1593.83
Water (l)	-306.2193	0.77	-305.45
Materials in the outlet stream			
Zoledronic acid(s)	-2002.1869	3593.91	1591.72
Water (l)	-306.6721	0.77	-305.90

Table C.54. Calculation of $X_{\text{destroyed}}$ of cooling

Terms used to calculate $X_{\text{destroyed}}$ (kJ)	Calculated values, kJ
Mechanical Exergy as Work (W, kJ)	33777.00
Thermal exergy, (kJ) $Q(1-(T_0/T))$	-2408.01
Total Exergy flow, (kJ) $(Nb)_{\text{in}}-(Nb)_{\text{out}}$	83.38
$X_{\text{destroyed}}$ (kJ)	31452.37

Each term in Equation (C.2) is calculated to find $x_{\text{destroyed}}$.

Table C.55. Mass Balance of stirring

Molecular Weight of each element (kg/kmol)	12.01	1.01	16.00	32.06	14.01	35.45	30.97	Molecular weight of the excipient (MW, kg/kmol)	Mole ratio of the substance x_i ,
Materials in the inlet stream	C	H	O	S	N	Cl	P		
Zoledronic acid(s)	5	10	7	-	2	-	2	272.11	0.00
Water (l)	-	2	1	-	-	-	-	18.02	1.00
Materials in the outlet stream	C	H	O	S	N	Cl	P		
Zoledronic acid(s)	5	10	7	-	2	-	2	272.11	0.00
Water (l)	-	2	1	-	-	-	-	18.02	1.00

Mass balance on elemental basis and molecular basis were evaluated. Equation (C.1) is used to calculate the data.

Table C.56. Thermodynamic props of stirring

	Heat Capacity, (C_p , kJ/mol K)	Enthalpy, ($C_p\Delta T$, kJ/mol)	Enthalpy of formation (H_f , kJ/mol)	Total Enthalpy (H_{total} , kJ/mol) $H = H_f + C_p\Delta T$	Entropy of formation (S° , kJ/mol K)	Entropy change (ΔS , kJ/mol K) $\Delta S = S^\circ + C_p \ln(T/T_0) - R \ln x_i$
Materials in the inlet stream						
Zoledronic acid(s)	0.35	-8.76	-2032.96	-2041.72	-0.5705	-0.1327
Water (l)	0.08	-1.88	-285.83	-287.71	0.0700	0.0636
Materials in the outlet stream						
Zoledronic acid(s)	0.35	-8.76	-2032.96	-2041.72	-0.5705	-0.1327
Water (l)	0.08	-1.88	-285.83	-287.71	0.0700	0.0636

The terms in Equation (C.2) calculated for stirring are represented in Table C.56.

Table C.57. Exergy and $X_{\text{destroyed}}$ calculation of stirring

	Physical exergy (ΔE_{ph} , kJ/mol)	Chemical Exergy (ΔE_{ch} , kJ/mol)	Total Exergy (ΔE_{tot} , kJ/mol)
Materials in the inlet stream			
Zoledronic acid(s)	-2002.1869	3593.91	1591.72
Water (l)	-306.6721	0.77	-305.90
Materials in the outlet stream			
Zoledronic acid(s)	-2002.1869	3593.91	1591.72
Water (l)	-306.6721	0.77	-305.90

Table C.58. Calculation of $X_{\text{destroyed}}$ of stirring

Terms used to calculate $X_{\text{destroyed}}$ (kJ)	Calculated values, kJ
Mechanical Exergy as Work (W, kJ)	33777.00
Thermal exergy, (kJ) $Q(1-(T_0/T))$	-2408.01
Total Exergy flow, (kJ) $(Nb)_{\text{in}}-(Nb)_{\text{out}}$	0.00
$X_{\text{destroyed}}$ (kJ)	31368.99

Each term in Equation (C.2) is calculated to find $x_{\text{destroyed}}$.

Table C.59. Mass Balance of filtration

Molecular Weight of each element (kg/kmol)	12.01	1.01	16.00	32.06	14.01	35.45	30.97	Molecular weight of the excipient (MW, kg/kmol)	Mole ratio of the substance x_i ,
Materials in the inlet stream	C	H	O	S	N	Cl	P		
Zoledronic acid(s)	5	10	7	-	2	-	2	272.11	0.00
Water (l)	-	2	1	-	-	-	-	18.02	1.00
Materials in the outlet stream	C	H	O	S	N	Cl	P		
Zoledronic acid(s)	5	10	7	-	2	-	2	272.11	1.00
Water (l)	-	2	1	-	-	-	-	18.02	1.00

Mass balance on elemental basis and molecular basis were evaluated. Equation (C.1) is used to calculate the data.

Table C.60. Thermodynamic props of filtration

	Heat Capacity. (C_p , kJ/mol K)	Enthalpy, ($C_p\Delta T$, kJ/mol)	Enthalpy of formation (H_f , kJ/mol)	Total Enthalpy (H_{total} , kJ/mol) $H = H_f + C_p\Delta T$	Entropy of formation (S° , kJ/mol K)	Entropy change (ΔS , kJ/mol K) $\Delta S = S^\circ + C_p \ln(T/T_0) - R \ln x_i$
Materials in the inlet stream						
Zoledronic acid(s)	0.35	-8.76	-2032.96	-2041.72	-0.5705	-0.1327
Water (l)	0.08	-1.88	-285.83	-287.71	0.0700	0.0636
Materials in the outlet stream						
Zoledronic acid(s)	0.35	-7.01	-2032.96	-2039.97	-0.5705	-0.1263
Water (l)	0.08	-1.51	-285.83	-287.34	0.0700	0.0650

The terms in Equation (C.2) calculated for filtration are represented in Table C.60.

Table C.61. Exergy and $X_{\text{destroyed}}$ calculation of filtration

	Physical exergy (ΔE_{ph} , kJ/mol)	Chemical Exergy (ΔE_{ch} , kJ/mol)	Total Exergy (ΔE_{tot} , kJ/mol)
Materials in the inlet stream			
Zoledronic acid(s)	-2002.1869	3593.91	1591.72
Water (l)	-306.6721	0.77	-305.90
Materials in the outlet stream			
Zoledronic acid(s)	-2002.3301	3593.91	1591.58
Water (l)	-306.7029	0.77	-305.93

Table C.62. Calculation of $X_{\text{destroyed}}$ of filtration

Terms used to calculate $X_{\text{destroyed}}$ (kJ)	Calculated values, kJ
Mechanical Exergy as Work (W, kJ)	8131.50
Thermal exergy, (kJ) $Q(1-(T_0/T))$	0.00
Total Exergy flow, (kJ) $(Nb)_{\text{in}}-(Nb)_{\text{out}}$	5.66
$X_{\text{destroyed}}$ (kJ)	8137.16

Each term in Equation (C.2) is calculated to find $x_{\text{destroyed}}$.

Table C.63. Mass Balance of drying

Molecular Weight of each element (kg/kmol)	12.01	1.01	16.00	32.06	14.01	35.45	30.97	Molecular weight of the excipient (MW, kg/kmol)	Mole ratio of the substance x_i
Materials in the inlet stream	C	H	O	S	N	Cl	P		
Zoledronic acid(s)	5	10	7	-	2	-	2	272.11	0.89
Water (l)	-	2	1	-	-	-	-	18.02	0.11
Materials in the outlet stream	C	H	O	S	N	Cl	P		
Zoledronic acid(s)	5	10	7	-	2	-	2	272.11	0.94
Water (l)	-	2	1	-	-	-	-	18.02	0.06
Water (g)	-	2	1	-	-	-	-	18.02	1.00

Mass balance on elemental basis and molecular basis were evaluated. Equation (C.1) is used to calculate the data.

Table C.64. Thermodynamic props of drying

	Heat Capacity, (C_p , kJ/mol K)	Enthalpy, ($C_p\Delta T$, kJ/mol)	Enthalpy of formation (H_f , kJ/mol)	Total Enthalpy (H_{total} , kJ/mol) $H = H_f + C_p\Delta T$	Entropy of formation (S° , kJ/mol K)	Entropy change (ΔS , kJ/mol K) $\Delta S = S^\circ + C_p \ln(T/T_0) - R \ln x_i$
Materials in the inlet stream						
Zoledronic acid(s)	0.35	-8.76	-2032.96	-2041.72	-0.5705	-0.5920
Water (l)	0.08	-1.88	-285.83	-287.71	0.0700	0.2465
Materials in the outlet stream						
Zoledronic acid(s)	0.35	-7.01	-2032.96	-2039.97	-0.5705	-0.5901
Water (l)	0.08	-1.51	-285.83	-287.34	0.0700	0.3002
Water (g)	0.04	-0.72	-241.82	-242.54	0.1888	0.1863

The terms in Equation (C.2) calculated for drying are represented in Table C.64.

Table C.65. Exergy and $X_{\text{destroyed}}$ calculation of drying

	Physical exergy (ΔE_{ph} , kJ/mol)	Chemical Exergy (ΔE_{ch} , kJ/mol)	Total Exergy (ΔE_{tot} , kJ/mol)
Materials in the inlet stream			
Zoledronic acid(s)	-1865.32	3593.91	1728.59
Water (l)	-361.17	0.77	-360.40
Materials in the outlet stream			
Zoledronic acid(s)	-1864.12	3593.91	1729.79
Water (l)	-376.79	0.77	-376.02
Water (g)	-298.07	9.34	-288.73

Table C.66. Calculation of $X_{\text{destroyed}}$ of drying

Terms used to calculate $X_{\text{destroyed}}$ (kJ)	Calculated values, kJ
Mechanical Exergy as Work (W, kJ)	360288.00
Thermal exergy, (kJ) $Q(1-(T_0/T))$	0.00
Total Exergy flow, (kJ) $(Nb)_{\text{in}}-(Nb)_{\text{out}}$	-2.83
$X_{\text{destroyed}}$ (kJ)	360285.17

Each term in Equation (C.2) is calculated to find $X_{\text{destroyed}}$.

Table C.67. Exergy difference, work and heat terms for each stage and $X_{\text{destroyed}}$

Step No	Total Exergy flow, (kJ) (N_b) _{in} -(N_b) _{out}	Mechanical Exergy as Work (W, kJ)	Thermal exergy, (kJ) $Q(1-(T_0/T))$	$X_{\text{destroyed}}$ (kJ)	$X_{\text{destroyed}}$ (kJ) For each stage
1.1.1	60.620	938.250	1,854.424	2,853.293	227,460.812
1.1.2	5,891.974	75,060.000	148,353.882	223,668.337	
1.1.3	1.782	938.250	-0.851	939.181	
1.2.1	40.883	1,563.750	2,266.769	3,871.402	6,368.780
1.2.2	269.754	938.250	1,289.374	2,497.378	
1.3.1	7.092	2,814.750	-189.035	2,632.808	6,350.952
1.3.2	-784.071	4,691.250	-189.035	3,718.144	
1.4.1	2.750	938.250	-0.368	940.632	16,672.008
1.4.2	583.774	625.500	-12.820	1,196.454	
1.4.3	0.000	11,259.000	-12.820	1,1246.180	
1.4.4	-8.080	938.250	-726.897	203.274	
1.4.5	0.000	11,259.000	-8,722.762	2,536.238	
1.4.6	-76.197	625.500	0.000	549.231	
1.5.1	12.436	22,518.000	7,790.011	30,320.446	552,488.166
1.5.2	0.000	67,554.000	23,370.032	90,924.032	
1.5.3	83.380	33,777.000	-2,408.013	31,452.366	
1.5.4	0.000	33,777.000	-2,408.013	31,368.987	
1.5.5	-5.666	8,131.500	0.000	8,137.164	
1.5.6	-2.828	360,288.000	0.000	360,285.172	

Table C.68. Step 1 Synthesis of Zoledronic acid Process Step Details

Step and sub-steps of the process
<p>Step 1.1 Reaction</p> <p>1.1.1. dissolving of the reactants</p> <p>1.1.2. reaction after addition of PCl_3</p> <p>1.1.3. cooling of the reaction products</p>
<p>Step 1.2 Filtration</p> <p>1.2.1. Addition absorbent and water</p> <p>1.2.2. Filtration of absorbent</p>
<p>Step 1.3 pH adjustment a temperature lower than $0\text{ }^\circ\text{C}$</p> <p>1.3.1. Cooling</p> <p>1.3.2. NaOH addition</p>
<p>Step 1.4 Precipitation</p> <p>1.4.1. Heating to room temperature</p> <p>1.4.2. Addition of ethanol</p> <p>1.4.3. Stirring</p> <p>1.4.4. Cooling to a temperature lower than $0\text{ }^\circ\text{C}$</p> <p>1.4.5. Filtration and collecting of the product</p>
<p>Step 1.5 Product recovery</p> <p>1.5.1. Addition of raw material</p> <p>1.5.2. Stirring the raw material and heating up</p> <p>1.5.3. Cooling</p> <p>1.5.4. Stirring</p> <p>1.5.5. Filtration</p> <p>1.5.6. Drying</p>

Table C.72. Chemical properties of substances

Material	Enthalpy of formation (ΔH_f , kJ/mol)	Gibbs Energy (ΔG , kJ/mol)	Exergy of species (ΔE , KJ/mol)	Heat Capacity (C_p , kJ/mol K)	Standard molar Entropy (ΔS° , kJ/mol K)
Methane sulphonic acid(l)	-566.200	-527.30	968.16	0.190	-0.737
Imidazole 1yl Ac. Ac. HCl(s)	-536.300	-203.10	2741.20	0.217	-2.101
Phosphorous acid (s)	-965.525	-857.46	364.07	0.103	-0.164
Zoledronic Acid	-2032.960	-1375.30	3593.91	0.351	-0.571
Phosphorous trichloride (l)	-319.700	-272.30	775.15	0.120	0.516
Phosphorous trichloride (g)	-287.000	-267.80	779.65	0.072	0.422
Hydrochloric acid (g)	-92.300	-95.33	84.73	0.036	0.187
Water (g)	-241.820	-228.57	9.34	0.036	0.189
Water (l)	-285.830	-237.13	0.77	0.075	0.070
Sodium hydroxide (l)	-425.610	-379.49	77.43	0.060	0.065
Ethanol (l)	-277.690	-174.78	1356.01	0.112	0.161

APPENDIX D: DETAILS (ADAPTED FROM THE EXCEL SHEETS) OF THE PROCESS CALCULATIONS FOR FINISHED DOSAGE FORM

Table D.1. Thermodynamic props of dissolving of reactants

	Heat Capacity, (C_p , kJ/mol K)	Enthalpy, ($C_p\Delta T$, kJ/mol)	Enthalpy of formation (H_f , kJ/mol)	Total Enthalpy (H_{total} , kJ/mol) $H = H_f + C_p\Delta T$	Entropy of formation (S° , kJ/mol K)	Entropy change (ΔS , kJ/mol K) $\Delta S = S^\circ + C_p \ln(T/T_0) - R \ln y_i$
Materials in the inlet stream						
Mannitol	0.2390	0.00	-1337.5	-1337.5	0.2385	0.6657
Water	0.0753	0.00	-285.83	-285.83	0.0700	0.1404
ZA	0.3505	0.00	-2032.96	-2032.96	-0.5705	-0.5705
Sodium citrate	0.3657	0.00	-2269.64	-2269.64	0.4291	0.4291
Materials in the outlet stream						
Mannitol	0.2390	0.00	-1337.5	-1337.5	0.2385	0.6743
Water	0.0753	0.00	-285.83	-285.83	0.0700	0.0704
ZA	0.3505	0.00	-2032.96	-2032.96	-0.5705	0.4593
Sodium citrate	0.3657	0.00	-2269.64	-2269.64	0.4291	1.2874

Table D.2. Exergy and $X_{destroyed}$ calculation of dissolving of reactants

	Physical exergy (ΔE_{ph} , kJ/mol)	Chemical Exergy (ΔE_{ch} , kJ/mol)
Materials in the inlet stream		
Mannitol	-1535.8722	3183.51
Water	-306.8095	0.77
ZA	-1862.9382	3593.91
Sodium citrate	-2397.5118	2170.95
Water	-306.6751	0.77
Materials in the outlet stream		
Mannitol	-1538.4337	3183.51
Water	-306.7964	0.77
ZA	-2169.8363	3593.91
Sodium citrate	-2653.2966	2170.95

Table D.3. Calculation of $X_{destroyed}$ of dissolving of reactants

Terms used to calculate $X_{destroyed}$ (kJ)	Calculated values, kJ
Mechanical Exergy as Work (W, kJ)	9,000.00
Thermal exergy, (kJ) $Q(1-(T_0/T))$	0.00
Total Exergy flow, (kJ) $(Nb)_{in}-(Nb)_{out}$	1.19
$X_{destroyed}$ (kJ)	9,001.19

Table D.4. Thermodynamic props of filtering

	Heat Capacity, $(C_p, \text{kJ/mol K})$	Enthalpy, $(C_p\Delta T, \text{kJ/mol})$	Enthalpy of formation $(H_f, \text{kJ/mol})$	Total Enthalpy $(H_{total}, \text{kJ/mol})$ $H = H_f + C_p\Delta T$	Entropy of formation $(S^0, \text{kJ/mol K})$	Entropy change $(\Delta S, \text{kJ/mol K})$ $\Delta S = S^0 + C_p \ln(T/T_0) - R \ln y_i$
Materials in the inlet stream						
Mannitol	0.2390	0.00	-1337.5	-1337.5	0.2385	0.6743
Water	0.0753	0.00	-285.83	-285.83	0.0700	0.0704
ZA	0.3505	0.00	-2032.96	-2032.96	-0.5705	0.4593
Sodium citrate	0.3657	0.00	-2269.64	-2269.64	0.4291	1.2874
Materials in the outlet stream						
Mannitol	0.2390	0.00	-1337.5	-1337.5	0.2385	0.6743
Water	0.0753	0.00	-285.83	-285.83	0.0700	0.0704
ZA	0.3505	0.00	-2032.96	-2032.96	-0.5705	0.4593
Sodium citrate	0.3657	0.00	-2269.64	-2269.64	0.4291	1.2874

$$\sum(N_i [e_i^{ch} + (h_{f,i}^0 + c_{p,i}(T - T_0) - T_0 [s_i^0 + c_{p,i} \ln \frac{T}{T_0} - R_u \ln x_i])])_{in} - \sum(N_i [e_i^{ch} + (h_{f,i}^0 + c_{p,i}(T - T_0) - T_0 [s_i^0 + c_{p,i} \ln \frac{T}{T_0} - R_u \ln x_i])])_{out} + Q \left(1 - \frac{T}{T_0}\right) - W = X_{destroyed}$$

(D.1)

Table D.5. Exergy and $X_{\text{destroyed}}$ calculation of filtering

	Physical exergy (ΔE_{ph} , kJ/mol)	Chemical Exergy (ΔE_{ch} , kJ/mol)
Materials in the inlet stream		
Mannitol	-1538.4337	3183.51
Water	-306.7964	0.77
ZA	-2169.8363	3593.91
Sodium citrate	-2653.2966	2170.95
Materials in the outlet stream		
Mannitol	-1538.4337	3183.51
Water	-306.7964	0.77
ZA	-2169.8363	3593.91
Sodium citrate	-2653.2966	2170.95

Table D.6. Calculation of $X_{\text{destroyed}}$ of filtering

Terms used to calculate $X_{\text{destroyed}}$ (kJ)	Calculated values, kJ
Mechanical Exergy as Work (W, kJ)	1,890.00
Thermal exergy, (kJ) $Q(1-(T_0/T))$	0.00
Filter used,(kJ)	3,878.10
Total Exergy flow, (kJ) $(Nb)_{\text{in}}-(Nb)_{\text{out}}$	0.00
$X_{\text{destroyed}}$ (kJ)	5,768.10

Each term in Equation (D.2) is calculated to find $x_{\text{destroyed}}$. Additional materials used during filtration is added to the calculations as part of work. Filter material production energy and production energy of filter is considered.

Table D.7. Thermodynamic props of sterilization and filling

	Heat Capacity, (C_p , kJ/mol K)	Enthalpy, ($C_p\Delta T$, kJ/mol)	Enthalpy of formation (H_f , kJ/mol)	Total Enthalpy (H_{total} , kJ/mol) $H = H_f + C_p\Delta T$	Entropy of formation (S° , kJ/mol K)	Entropy change (ΔS , kJ/mol K) $\Delta S = S^\circ + C_p \ln(T/T_0) - R \ln y_i$
Materials in the inlet stream						
Mannitol	0.2390	0.00	-1337.5	-1337.5	0.2385	0.6743
Water	0.0753	0.00	-285.83	-285.83	0.0700	0.0704
ZA	0.3505	0.00	-2032.96	-2032.96	-0.5705	0.4593
Sodium citrate	0.3657	0.00	-2269.64	-2269.64	0.4291	1.2874
Materials in the outlet stream						
Mannitol	0.2390	0.00	-1337.5	-1337.5	0.2385	0.6743
Water	0.0753	0.00	-285.83	-285.83	0.0700	0.0704
ZA	0.3505	0.00	-2032.96	-2032.96	-0.5705	0.4593
Sodium citrate	0.3657	0.00	-2269.64	-2269.64	0.4291	1.2874

Table D.8. Exergy and $X_{destroyed}$ calculation of sterilization and filling

	Physical exergy (ΔE_{ph} , kJ/mol)	Chemical Exergy (ΔE_{ch} , kJ/mol)
Materials in the inlet stream		
Mannitol	-1538.4337	3183.51
Water	-306.7964	0.77
ZA	-2169.8363	3593.91
Sodium citrate	-2653.2966	2170.95
Materials in the outlet stream		
Mannitol	-1538.4337	3183.51
Water	-306.7964	0.77
ZA	-2169.8363	3593.91
Sodium citrate	-2653.2966	2170.95

Table D.9. Calculation of $X_{\text{destroyed}}$ of sterilization and filling

Terms used to calculate $X_{\text{destroyed}}$ (kJ)	Calculated values, kJ
Mechanical Exergy as Work (W, kJ)	1,156.752
Packaging Materials, as Work (W, kJ) Bottles and stoppers	7,748.193
Thermal exergy, (kJ) $Q(1-(T_0/T))$	0
Total Exergy flow, (kJ) $(Nb)_{\text{in}}-(Nb)_{\text{out}}$	0
$X_{\text{destroyed}}$ (kJ)	8,904.945

Each term in Equation (D.1) is calculated to find $x_{\text{destroyed}}$. Additional materials used during filtration is added to the calculations as part of work. Bottle and stopper material production energy and production energy of each material are considered in the calculations. (See Table B.8)

Table D.10. Calculation of $X_{\text{destroyed}}$ of capping

Terms used to calculate $X_{\text{destroyed}}$ (kJ)	Calculated values, kJ
Mechanical Exergy as Work (W, kJ)	225.216
Packaging Materials, as Work (W, kJ) caps	3285.540
Thermal exergy, (kJ) $Q(1-(T_0/T))$	0.000
Total Exergy flow, (kJ) $(Nb)_{\text{in}}-(Nb)_{\text{out}}$	0.000
$X_{\text{destroyed}}$ (kJ)	4225.694

Each term in Equation (D.2) is calculated to find $x_{\text{destroyed}}$. Additional materials used during filtration is added to the calculations as part of work. Cap material and production energy are considered in the calculations (See Table B.6). Capping operation is added to the mechanical exergy term. (See Table B.8).

Table D.11. Calculation of $X_{\text{destroyed}}$ of secondary packaging

Terms used to calculate $X_{\text{destroyed}}$ (kJ)	Calculated values, kJ
Mechanical Exergy as Work (W, kJ)	118.080
Packaging Materials, as Work (W, kJ) labels, leaflets, carton boxes	3,167.445
Thermal exergy, (kJ) $Q(1-(T_0/T))$	0.000
Total Exergy flow, (kJ) $(Nb)_{\text{in}}-(Nb)_{\text{out}}$	0.000
$X_{\text{destroyed}}$ (kJ)	3,285.526

Mechanical term includes, pump work, mixer work, HVAC system and machine operations. Mechanical Exergy for secondary packaging includes, HVAC work D class during the operation time. Each material used during packaging are considered, as their material and production energy (Table B.6).